SENSITIZATION OF LANTHANIDE AND ORGANIC-BASED PHOSPHORESCENCE VIA ENERGY TRANSFER AND HEAVY-ATOM EFFECTS

Ravi K. Arvapally, B.S., B.Ed., M.S.

Dissertation Prepared for the Degree of

DOCTOR OF PHILOSOPHY

UNIVERSITY OF NORTH TEXAS

May 2010

APPROVED:

Mohammad A. Omary, Major Professor
Thomas R. Cundari, Committee Member
Teresa D. Golden, Committee Member
Angela K. Wilson, Committee Member and Co-Director, Center for Advanced Scientific Computing and Modeling
William E. Acree Jr., Chair of the Department of Chemistry
Michael Monticino, Dean of the Robert B. Toulouse School of Graduate Studies

Arvapally, Ravi K. *Sensitization of Lanthanides and Organic-Based Phosphorescence via Energy Transfer and Heavy-Atom Effects*. Doctor of Philosophy (Chemistry), May 2010, 213 pp., 14 tables, 83 illustrations, references, 343 titles.

The major topics discussed are the phosphorescence sensitization in the lanthanides via energy transfer and in the organics by heavy atom effects. The f-f transitions in lanthanides are parity forbidden and have weak molar extinction coefficients. Upon complexation with the ligand, ttrpy (4'-p-Tolyl-[2,2':6',2"]-terpyridine) the absorption takes place through the ligand and the excitation is transferred to the lanthanides, which in turn emit. This process is known as "sensitized luminescence." Bright red emission from europium and bright green emission from terbium complexes were observed. There is ongoing work on the making of OLEDs with neutral complexes of lanthanide hexafluoroacetyl acetonate/ttrpy, studied in this dissertation. Attempts to observe analogous energy transfer from the inorganic donor complexes of Au(I) thiocyanates were unsuccessful due to poor overlap of the emissions of these systems with the absorptions of Eu(III) and Tb(III).

Photophysics of silver-aromatic complexes deals with the enhancement of phosphorescence in the aromatics. The heavy atom effect of the silver is responsible for this enhancement in phosphorescence. Aromatics such as naphthalene, perylene, anthracene and pyrene were involved in this study. Stern Volmer plots were studied by performing the quenching studies. The quenchers employed were both heavy metals such as silver and thallium and lighter metal like potassium. Dynamic quenching as the predominant phenomenon was noticed.

ACKNOWLEDGEMENTS

My special thanks to Department of Chemistry, University of North Texas for giving me the opportunity to study and to finish my Ph.D. At first, I thank Prof. Mohammad A. Omary for giving me the guidance, advice and support in scientific research as a graduate student in his group. I would not forget the great help from Dr. Omary for raising my confidence during times of hardship in my personal life too. I thank all the Omary group members for their cooperation in the lab and for their valuable friendship which helped me finish the projects assigned to me.

My sincere thanks to our collaborators, Professors. Angela K. Wilson (UNT), Howard H. Patterson (U. of Maine), and the late. R. C. Elder (U. of Cincinnati) for their assistance in one of my projects which is included in Chapter 4 of this dissertation. My special thanks to Dr. Xiaoping Wang and Dr. Nesterov Vladimir for determining several of my X-ray crystal structures of lanthanide complexes. I would like to thank Dr. Charles Campana at Bruker AXS Inc. for solving the crystal structure of $[Eu(ttrpy)_2Cl_2]Cl$. I would like to thank to Dr. K. Veera Reddy from Nizam College, Hyderabad, India, whose teaching has motivated me to continue my career in chemistry. I wish to thank my professor, the late Dr. K. L. Omprakash from Nizam College, Hyderabad, India, who inspired me to pursue research in chemistry.

My heartful thanks to my parents, Rajesham Arvapally and Sujatha Arvapally, whose love and encouragement were critical for allowing me to finish my Ph.D. program. I am also thankful to my brothers, Kiran Arvapally and Hari Arvapally for their constant stimulation. Last but not least, I am grateful to my wife, Archana Donthula for

whose companionship, patience and love advanced me to reach so far. I am very much thankful to our kids, Ritvik Arvapally and Satvik Arvapally whose love and smiles allowed me to overcome the difficult times during my late Ph.D. period.

TABLE OF CONTENTS

Page

LIST OF TABLES

Page

LIST OF ILLUSTRATIONS

Pages

CHAPTER 1

INTRODUCTION

1.1 Overview of Dissertation

There has been continuous research interest in the field of organic light emitting diodes (OLEDs) for the past decade.[1] For all OLED device applications based on organic materials, the first excited triplet energy level is of great importance.[2] The charge recombination takes place in the triplet energy level due to electrical recombination. To measure the triplet energy level, phosphorescent measurements have to be carried out. The radiative lifetime decay of this phosphorescence is very slow because of the spin forbidden nature of the $T_1 \rightarrow S_o$ transition. According to spin statistics, the electron-hole combination in electroluminescence yields singlet:triplet excitons in a 1:3 ratio.[3] If the emitter is a fluorescent molecule, only singlet excitons can emit light and the electroluminescence quantum yield will have an upper limit of 25%. It is better to take advantage of both fluorescence and phosphorescence. As phosphorescence is spin-forbidden, introduction of heavy atoms will cause spin-orbit coupling, which enhances the intersystem crossing of singlet to triplet. This way, enhancement in phosphorescence can be observed. This dissertation discusses two means for phosphorescence sensitization in lanthanide and transition metal complexes.

The spin-orbit perturbations of electronic states play an important role in the photophysics of molecular systems. The incorporation of a heavy atom into the molecular systems leads to changes in photophysical properties by enhancing the

intercombination transitions which is known as heavy atom effect.[4] This heavy atom effect can be internal when the heavy atom is directly coordinated to the fluorophore and external when it is in its vicinity. The internal heavy atom effect can be employed to study the electronic structure of molecules.[4] Another difference between internal and external heavy atom effect can be visualized in terms of symmetry. There will be loss in symmetry in internal heavy atom effect as the heavy metal is directly bonded to the molecule (e.g., an aromatic molecule) which is not the case with the external heavy atom effect.[5] Heavy atoms take an important role in studying the relation between the luminescence properties and the electronic structure. The heavy atom effect in the luminescence of polyatomic systems was first studied by McClure in 1949.[6] Intersystem crossing from singlet to triplet is forbidden which can be explained due to the spin selection rule. But in complexes of heavy atoms, intersystem crossing is induced due to enhanced spin-orbit coupling. This heavy atom facilitates the population of triplet from singlet excited states, which in turn enhances the phosphorescence and reduces the radiative lifetime of the molecule. The heavy atom effect can only be observed when the emitting triplet electronically couples with the heavy metal.[7] There are several publications reported on heavy atom effect by Omary et al.[8] Heavy atom effects cause quenching of fluorescence, enhancement of phosphorescence and reduction in radiative lifetime of the fluorophore to which it is complexed. This is seen in both the examples given below. The Omary group has found that π complexation of naphthalene with $\{[3,5\text{-}(CF_3)_2Pz]Ag_3\}$ resulted in the quenching of fluorescence and enhancement in the phosphorescence along with a three order magnitude reduction in the lifetime of

naphthalene.[8a] Gabbaï, Omary and coworkers have found a similar situation with π complexation of polycylic aromatic molecules to the trimeric perfluoro-*o*-phenylenemercury(II) complex $[Hg(o\text{-}C_6F_4)]_3$, where intense $T_1 \rightarrow S_o$ enhancement of arene phosphorescence and reduction in lifetime by 5 orders of magnitude were observed.[8g]

This dissertation partly deals with the spectroscopic studies of lanthanides with the organic sensitizer, 4′-*p*-Tolyl-[2,2′;6′,2″] terpyridine (ttrpy) and also the complexes of silver perchlorate with aromatics in chapters 2 and 3, respectively. Chapter 2 is about the complexes of ttrpy with lanthanides such as europium, terbium, neodymium and erbium. This chapter explains the heavy atom effect of lanthanides on the heteroaromatic ligand by enhancement of the phosphorescence of lanthanides and quenching of fluorescence of the ttrpy. This occurs by the sensitization of lanthanide luminescence. Neutral complexes of lanthanides can be used in organic light emitting diodes (OLEDs). Chapter 3 deals with the synthesis and characterization of complexes of polyhydrocarbons with silver perchlorate. Crystal structures of silver-aromatic complexes are well known, but not their electronic properties. This chapter explains the electronic properties of silver-aromatic compounds. The heavy atom effect of silver on the aromatics will be observed by how the fluorescence quenching occurs, enhancement in the phosphorescence of aromatics and reduction in the phosphorescence lifetimes. Stern-Volmer studies are done to see what kind of quenching occurs in these kinds of complexes. Chapter 4 discusses the structure-luminescence relationship of $Au(SCN)_2^-$ species with various counterions. This chapter

explains how the luminescence properties are varied with changing the counterions from lighter to bulkier. Chapter 5 has the conclusions and the research expansion on these topics. The following discussion explains some of the properties of these complexes studied.

1.2 Electronic Structure and Optical Properties of the Lanthanides

The lanthanides, cerium to lutetium (atomic number 58-71) are 14 elements that follow lanthanum in the periodic table, in which the 14 4f electrons are progressively added to the lanthanum configuration. The 4f electrons are shielded from the external environment by an outer core of 5s and 5p electrons. As a result the absorption and emission spectra consist of narrow bands. Therefore, the atomic properties of lanthanides are retained even after formation of complexes with different ligands or chelates. Most metal ion complexes absorb visible and/or UV radiation but only a few re-emit the absorption energy in the form of visible or UV photons. However, the trivalent lanthanide ions and their complexes are known to luminesce, giving sharp atomic bands corresponding to f-f transition localized on the central metal atom. The +3 oxidation state is the most stable oxidation state even in aqueous solutions.[9] Most lanthanide (III) ions are known to luminesce but the presence of water molecules in the inner coordination sphere deactivate the Ln(III) luminescence nonradiatively and quench the luminescence.[9b]

Transitions between f orbitals of lanthanide (III) ions are strictly parity forbidden. Many f-f transitions are also spin forbidden; however, spin-orbit coupling makes the transitions more observable. Nevertheless, both restrictions have important

consequences. The bands have very low absorption coefficients and the radiative lifetimes of f-f states are rather long. The absorption and emission spectra of lanthanide (III) ions give sharp, spectrally narrow bands compared to other inorganic systems. The positions of these sharp bands are little affected by the nature of the ligand coordinated to lanthanide (III) ions. This is because the inner 4f electrons are shielded from the ligand field and other external stimuli by the outer 5s and 5p electrons. The variety and complex nature of these bands are due to the large number of electronic levels. (Figure 1.1)

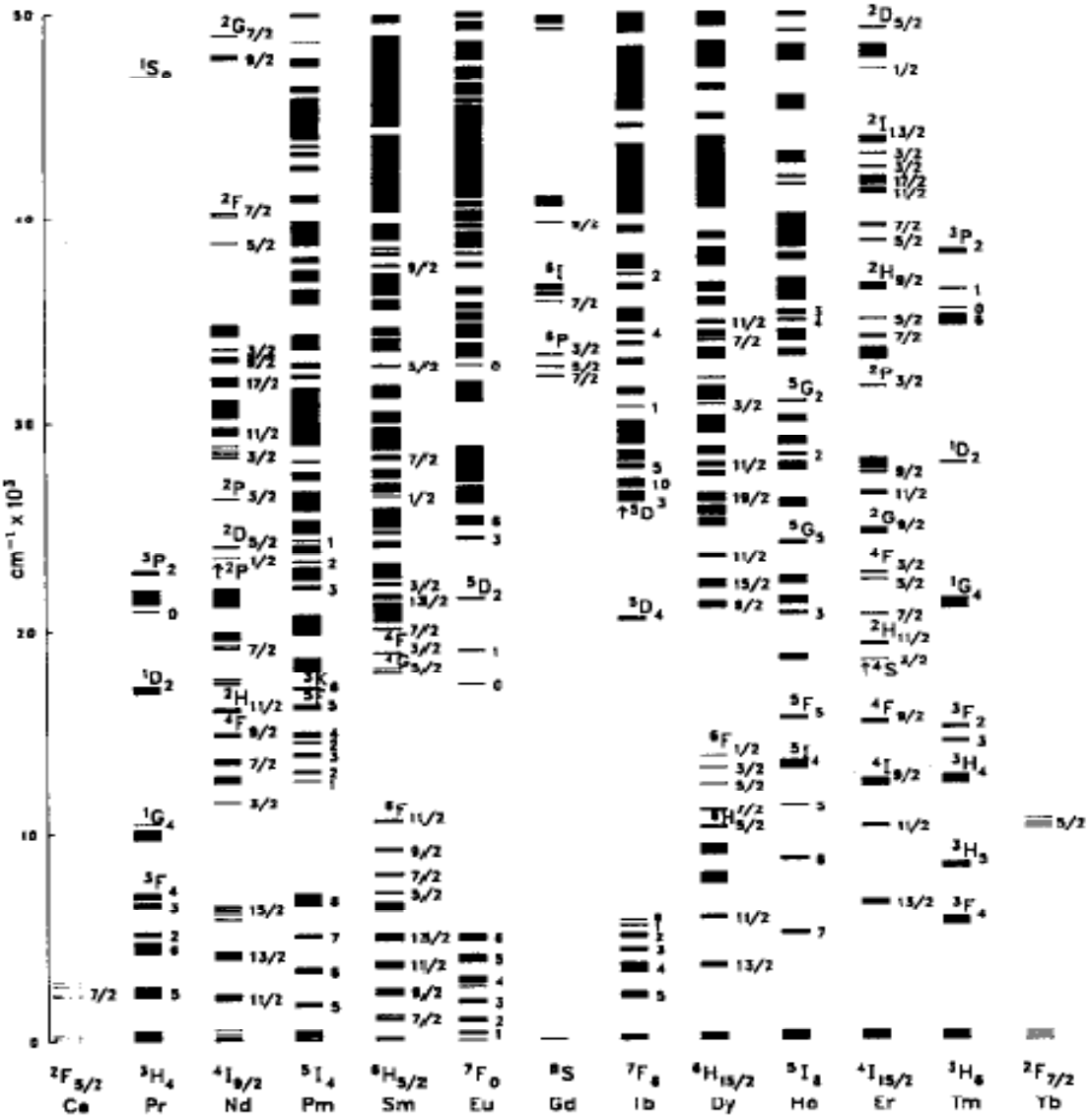

Figure 1.1 Energy level diagram for Ln (III) ions. The term symbols follow Russel-Saunders notation ($^{2S+1}L_J$). Reproduced with permission from Carnall, W. T.; Goodman, G. L.; Rajnak, K.; Rana, R. S. *J. Chem. Phys.* **1989,** *90,* 3443-3457. Copyright [2009], American Institute of Physics.

The energy states in Ln(III) ions derive from the splitting of the $4f^n$ electronic configuration because of electrostatic interaction and spin-orbit coupling. The large spin-orbit coupling due to their large atomic numbers cause the individual J levels to be

well separated. These electronic states are non-degenerate and, therefore, only the total angular momentum (J) is a good quantum number to describe a non-degenerate electronic state. The first excited state energy is several thousand wave numbers above the ground state.[9b] As a result the first excited state is essentially unpopulated by electrons except at very high temperatures. Splittings of f^n configuration by external fields such as ligand fields are very small and in the range of a few 100 cm^{-1}.[9b] This situation is in contrast to the coordination compounds of d-block transition compounds in which ligand-field splittings of 5000-30,000 cm^{-1} are known.[9b,10] The nonradiative processes are relatively inefficient in Ln(III) systems because of shielding of f-electrons. Eu(III), Tb(III) and Gd(III) have large energy gaps between the ground electronic state and first excited state. The presence of large energy gap reduces the possibility of quenching of luminescence of the Ln(III) luminescence according to energy gap law.[11] However, quenching of luminescence of Ln(III) by solvent molecules especially by water is a major disadvantage for their use in practical applications.

1.2.1 Tb(III), Eu(III), Nd(III) and Er(III) Luminescence

Terbium and europium trivalent ions are the two commonly used lanthanides as they emit in the visible region. For near-infrared (NIR) emission applications, on the other hand, neodymium (III) and erbium (III) are typically used.

1.2.1.1 Terbium(III)

$^5D_4$ is the lowest excited state in the case of terbium. The emission transitions are $^5D_4 \rightarrow {}^7F_J$, the most common of which have J=6, 5, 4, 3, 2, 1 and 0. Among these transitions, the intense transition is being the $^5D_4 \rightarrow {}^7F_5$, which occurs around 542 nm.[12]

This transition remains remarkably intense under various solution and pH conditions. As a result, Tb(III) emission is considered superior when compared to Eu(III) emission for either direct or indirect excitation in the blue and near-ultraviolet spectral ranges for luminescence titrations.[13] The Tb(III) luminescence shows some sensitivity to the nature of the bonded ligands, particularly the $^5D_4 \rightarrow {}^7F_{6,4,2}$ transitions, but it cannot be used to probe the structure of the complexes due to the degeneracy of $^5D_4$ level. The $^5D_4 \rightarrow {}^7F_{3,5}$ transitions have strong magnetic dipole character.

1.2.1.2 Europium(III)

In Eu(III), the lowest excited state is $^5D_0$. The emission occurs from this state. The transitions are $^5D_0 \rightarrow {}^7F_J$, the most common of which have J=0, 1, 2, 3 and 4. The intense transitions are being $^5D_0 \rightarrow {}^7F_{1,2,4}$. The $^5D_0 \rightarrow {}^7F_2$ peak is highly sensitive to the structure change and environment effects. As a result this $^5D_0 \rightarrow {}^7F_2$ line is known as hypersensitive peak.[14] The intensity of electric dipole transitions strongly depend on the site symmetry whereas the magnetic dipole transitions do not depend on the site symmetry as they are parity allowed.[15] If Eu^{3+} occupies an inversion symmetry site in the crystal site, the orange red emission, magnetic dipole transition $^5D_0 \rightarrow {}^7F_1$ which is about 590 nm is dominant. If the Eu^{3+} does not occupy the inversion symmetry site, the red emission, electric dipole transition $^5D_0 \rightarrow {}^7F_2$ (around 613 nm) is the dominant peak.[14] In solution, emission from $^5D_1$ excited state is usually weak while the luminescence from the upper $^5D_2$ and $^5D_3$ is often efficiently quenched.[13]

The important transitions of Eu^{3+} are generally $^5D_0 \rightarrow {}^7F_1$ and $^5D_0 \rightarrow {}^7F_2$. For systems in which there is only one type of Eu^{3+} site or else only one type of Eu^{3+}, the

$^5D_0 \rightarrow {}^7F_1$ emission peak will split into at most 3 components and $^5D_0 \rightarrow {}^7F_2$ will have 5 components. The relative intensities, number and the energy spacings give the detailed information about structure and symmetry around the Eu^{3+} center.[16] The $^5D_0 \rightarrow {}^7F_2$ peak is very useful in identification of organic compounds such as tetracycline (TC) and its homologues such as chorotetracycline, doxycycline and oxytetracycline. The intensity of this peak increased as pH increased with the maximum reaching when the concentration ratio of Eu^{3+}/[TC]=1.[17] Wolfson et al. have demonstrated the use of $^5D_0 \rightarrow {}^7F_2$ peak in the detection of E. *C*oli tRNA. They found an increase in Eu^{3+} luminescence intensity as the Eu^{3+} is titrated with tRNA until the ratio between Eu^{3+}/tRNA reached 1:3.[18]

1.2.1.3 Erbium(III)

The lowest excited state is $^4I_{13/2}$. The emission occurs from this state to the ground state $^4I_{15/2}$. There is only one transition from $^4I_{13/2} \rightarrow {}^4I_{15/2}$. This emission line occurs in the NIR region at 1540 nm. This 1540 nm peak is useful in laser and optical fiber communications systems because it is coincident with the signal wavelength used in glass fiber system.[19] Enrichi used silica doped with erbium for biosensing and bioimaging applications.[20] Erbium doped nanocrystals of $NaYF_4$ were used as up-conversion phosphors for sensitive detection of bio molecules.[21] Phosphors that emit higher energy photons after absorbing lower energy excitation photons are called as up-conversion phosphors.

1.2.1.4 Neodymium(III)

The lowest excited state is $^4F_{3/2}$. The transitions will be from $^4F_{3/2} \rightarrow {}^4I_{J,}$ where J=15/2, 13/2, 11/2, 9/2. $^4F_{3/2} \rightarrow {}^4I_{9/2}$ occurs at 880 nm, $^4F_{3/2} \rightarrow {}^4I_{11/2}$ occur at 1064 nm and $^4F_{3/2} \rightarrow {}^4I_{13/2}$ emission observed at 1345 nm.[22] Nd-YAG laser whose emission at 1064 nm is used in biological applications such as coagulation of the vascular malformation of the different kind and localization, as well as chemodectoma removal.[23] Optical fibers doped with neodymium and erbium can serve as in line lasers and optical amplifiers in fiber optic telecommunication systems.[24] Hasegawa et al. have fabricated organic electroluminescence device using a Nd(III) complex as the emitting layer.[25]

There is a great interest in frequency upconversion materials mainly because a visible source can be pumped by a near infrared (NIR) laser would be useful in high capacity data storage, barcode scanning, submarine communications, laser printing, biotechnology, biomedical instruments and diagnostics and three dimensional display.[26] Nd^{3+} is one of the most important lanthanide ion which is used for upconversion process because of its favorable energy levels. When pumped with 1064 nm peak of Nd:YAG laser, a thulium (Tm^{3+}) doped ZBLAN fiber demonstrated a 4 step upconversion in which UV peaks at 284 nm, 365 nm and visible peaks at 453 nm and 480 nm were observed.[27] This was the first shortest UV laser emission ever obtained for thulium doped fiber.

As f-f transitions are weak due to low molar extinction coefficients, population of excited states of the Ln(III) by direct excitation will be inefficient. As a result a highly absorbing chromophore containing ligand (donor) when coordinated to Ln(III)

(acceptor) will be useful. This complex when excited the chromophore absorbs the energy and transfers it to the lanthanide to promote it to its excited state, by which lanthanide based emission is observed. This phenomenon is known as "sensitized luminescence." As the chromophore acts as antennae in absorbing the excitation energy, it is also called as an "antennae effect." This energy transfer from antennae to the Ln(III) can takes place via either the singlet excited state S_1 or triplet excited state T_1 of the chromophore. However, it is believed that it occurs from S_1 to the lanthanide, in most common examples.

Energy transfer from the ligand to the Ln(III) can be explained by two phenomena, Dexter exchange[28] and Förster resonance.[29,30] In both processes, the energy transfer occurs by a radiationless mechanism. In the Dexter exchange mechanism, the donor and acceptor must collide with each other. It depends on the good spectral overlap between the donor emission and acceptor absorption. In Förster resonance process, on the other hand, energy from the donor is transferred to the acceptor through a long range interaction. This interaction is a coulombic interaction, typically a dipole-dipole interaction or, more generally, multipole interaction. In this phenomenon, there is no need of short contact between the donor and acceptor. It occurs over distances as long as 50-100 Å.

Dexter and Förster mechanisms can be distinguished from each other by measurements of the rate constants for energy transfer (k_{ET}), comparing them to the rate constant for diffusion (k_{DIF}), and then measuring the rate constant for energy transfer as a function of solvent viscosity. If k_{ET} is significantly greater than k_{DIF} and if

k_{ET} is insensitive to solvent viscosity, then the dipole-dipole (Förster) interaction is dominant. On the other hand, if k_{ET} is comparable to, or less than, k_{DIF} and k_{ET} is sensitive to viscosity, then close contact between donor and acceptor is needed (Dexter process).[31]

The donors can be inorganic or organic chromophores in nature. Assefa et al. have studied the lanthanide complexes of gold(I) and silver(I) dicyanides.[32] The inorganic donors overviewed herein are cyano d^{10} and d^8 complexes. In both complexes the luminescence from the $[Au(CN)_2]^-$ and $[Ag(CN)_2]^-$ cluster donors were quenched, and sensitized luminescence was observed from europium. In $Eu[Au(CN)_2]_3$, as temperature increased from 10 K to 150 K, the luminescence intensity of various europium peaks was quenched. But in the case of $Eu[Ag(CN)_2]_3$, the luminescence intensity was enhanced. On the other hand, Yersin and co-workers studied energy transfer from $[Pt(CN)_4]^{2-}$ donor species to various lanthanides.[33] In $M_2[[Pt(CN)_4]_3.nH_2O$ (M= Eu, Tb, Sm], efficient energy transfer was observed from $[Pt(CN)_4]^{2-}$ stacks to the lanthanides, Eu and Sm.[33] Polarized emission measurements at high pressure were performed on $Sm_2[Pt(CN)_4]_3$.[34] At low pressure, sensitized luminescence from Sm^{3+} was observed. But at high pressure, 25 kbar emission from $[Pt(CN)_4]^{2-}$ clusters was observed. Similar results were noticed in the case of $Eu[Au(CN)_2]_3$ at high pressure. Emission from $[Au(CN)_2]^-$ species was observed at high pressures. This is due to structural arrangement in $[Au(CN)_2]^-$. Because of the two dimensional clustering arrangements of $[Au(CN)_2]^-$ complexes, electronic energy bands are formed as opposed to discrete molecular orbitals. A relatively small decrease of the Au-Au separations leads

to a significant reduction of the band gap energy and thus also to a large red shift of the lowest electronic transition. As a result, the spectral overlap between $[Au(CN)_2]^-$ emission and Eu^{3+} absorption diminishes and only $[Au(CN)_2]^-$ emission was observed at high pressure. In contrast, samarium doped calcium tungstate crystals exhibited efficient quenching of tungstate emission by sensitizing the Sm^{3+} emission.[35]

Rawashdeh-Omary et al. have studied tunable energy transfer in pure crystals of $Tb[Au(CN)_2]_3$ and $Tb[Ag(CN)_2]_3$.[36] Efficient energy transfer was observed in $Tb[Ag(CN)_2]_3$ when compared to $Tb[Au(CN)_2]_3$. This is due to good match of energy levels in $Tb[Ag(CN)_2]_3$ between the donor $[Ag(CN)_2]^-$ clusters and the acceptor Tb^{3+} ion. The spectral overlap between $[Au(CN)_2]^-$ cluster emission and Tb^{3+} acceptor is poor, leading to observance of blue donor emission in place of green acceptor luminescence in $Tb[Au(CN)_2]_3$.

Organic donors such as terpyridine and terpyridine-like compounds are known in the literature.[37] The terpyridine and terpyridine-like chromophores not only form photo- and redox-active complexes with transition metal ions as catalysts[37b,c] but also lanthanide complexes with intense emission as probes in biology and medicine.[37e,38] Lanthanides complexes exhibit diverse and unpredictable structural variations in both coordination number and also coordination geometry. The design and development of lanthanide complexes are of increasing interest. The ligands with suitable chromophores may coordinate to lanthanides and energy is efficiently transferred to lanthanides whereby sensitized luminescence is observed from lanthanides. The terpyridine like

ligand, 4′-*p*-Tolyl-[2,2′;6′,2″] terpyridine (ttrpy) with extensive conjugation can form such complexes.

In chapter 2, photophysical studies of ttrpy with the lanthanides such as europium, terbium, neodymium and erbium complexes were discussed. The lanthanides have low molar extinction coefficients as the f-f transitions are laporte forbidden. Direct excitation of these lanthanides results in low quantum yield. To circumvent this problem, a chromophore which has high extinction coefficient can be coordinated to the lanthanide. This way, the chromophore absorbs the excitation energy and sensitizes the emission of lanthanide. Terpyridine like ligand, 4′-*p*-Tolyl-[2,2′;6′,2″] terpyridine (ttrpy) which has extended conjugation acts as a good antennae in harvesting the absorbed energy and then sensitizing the lanthanide emission. Neutral complexes of the lanthanide with this ttrpy can be useful in organic light emitting diode (OLED) fabrication.

1.3 Photophysics of Silver-Aromatic Systems

Synthesis of paracyclophane[39] and the discovery of ferrocene,[40] instigated the study of metal sandwich systems in organometallic chemistry and remained a favorite subject for several decades. Paracyclophane has two benzene rings which are held face-to-face linked by methylene bridges. Paracyclophane and ferrocene along with arenes, carboranes, polycylic aromatics and even porphyrins have resulted in the synthesis of several organotransition metal sandwiches. Different double-, triple-, tetra-, penta-, hexa-, and multilayered compounds are known in the literature. More recently, Omary, Fackler and Burini described other interesting classes of sandwich complexes in

which large cations are sandwiched between macrocyclic (9-membered ring) trinuclear Au(I) complexes acting as metalloaromatic π systems.[41]

Metallocenes[42] and cyclophanes[43] are the most commonly known double layer molecules in organometallic and organic chemistry. Triple-layer complexes form special classes of sandwich compounds involving Lewis acid ligands in the bridging position to hold the metal complex fragments together.[42,44] On the basis of mass spectrometric studies for $M_2Cp_3^+$ type complexes (M= Ni or Fe), the possible existence of a triple decker complex was first suggested in 1964.[45] But it was first isolated by Werner and Salzer for a Ni complex, $Cp_3Ni_2^+BF_4^-$.[46] Triple-decker porphyrin compounds were also known in the literature.[47] Other metal sandwich complexes like tetra-decker,[39,40a] penta-decker,[40b] hexa-decker[48] and staircase oligomeric sandwich complexes are also known.[49] A great focus is now given to multilayer lanthanide metal complexes.[50] For example, these organometallic lanthanide complexes of cyclooctatetraene have been prepared by a combination of laser vaporization and molecular beam methods.[50 b] These complexes are shown to be multilayer sandwich structures with Ln atoms and the C_8H_8 molecules are alternately stacked up by mass spectrometry, photoionization spectroscopy and photoelectron spectroscopy.

Single ring aromatics were first studied in 1920 where they are known to form 1:1 complexes with silver ions.[51] Theoretical calculations were done on benzene-$AgClO_4$ systems for their bonding by Mulliken.[52] In 1958, a crystal structure for the benzene-$AgClO_4$ was published.[53] The crystal structure showed -C_6H_6-Ag-C_6H_6-Ag- chains with perchlorate ions. At the same time solution equilibrium studies on metal-π interactions

were reviewed by Andrews.[54] A molecular orbital theoretical treatment of the electronic requirements of silver-aromatic hydrocarbon complexes indicated that coordination of silver cations may take place at more than one position in a molecule which has more than one position of equal or nearly equal reactivity. There will be no electronic perturbation on the hydrocarbon as long as the second silver ion coordinates far from the first one in the same hydrocarbon.[55] Further studies on the theory of cation-π interactions have been studied by Dougherty for organic-π systems,[56] whereas Omary and Cundari carried out analogous studies for inorganic analogues.[57]

The five coordinate $C_6H_6.AgAlCl_4$ complex was synthesized and its crystal structure was established.[58] It has infinite planar chains composed of $AlCl_4^-$ tetrahedra connected by Ag-Cl bonds with π type Ag(I)-aromatic interactions perpendicular to the sheet. Amma and his co-workers have synthesized several of silver-aromatic complexes and their crystal structures were determined. For example, complexes of silver perchlorate with naphthalene,[59] anthracene,[60] indene,[61] *m*-xylene,[62] cyclohexylbenzene,[63] and acenapthene and acenaphthyl[64] have been described. Complexes of pyrene and perylene with silver perchlorate were also known.[65] In all these silver perchlorate-aromatic complexes, crystal structures are well known. Silver acts as a Lewis acid in these compounds, which may enhance or quench the fluorescence and phosphorescence properties of pure aromatics upon coordination.

Surprisingly, despite the long history of structural and theoretical studies of such cation-π systems, photophysical studies accompanied with this interaction remain

largely lacking. Chapter 3 studies the electronic properties of complexes of silver perchlorate with naphthalene, pyrene, anthracene and perylene.

1.4 Structural and Photophysical Studies of Thiocyanate Complexes

The linear thiocyanate ion can coordinate through either sulfur or nitrogen, or both in metal ion compounds.[66] Although several examples containing each type of bonded thiocyanates are known, N-bonded thiocyanate complexes are generally formed by first row transition metal complexes.[67] N- bonded thiocyanate complexes for lanthanides such as praseodymium and neodymium are also known in the literature.[68] Many compounds of S-bonded thiocyanates are known.[69,70] Recently mixed metal complex of thiocyanate was synthesized in which sulfur was coordinated to mercury and nitrogen was bonded to manganese.[71]

Nockemann et al. have synthesized anionic rare earth thiocyanate complexes which can be used as building blocks for low-melting metal containing ionic liquids.[72] Nonlinear optical materials capable of frequency conversion are of great importance for several applications like optical computing, laser sensing, photonic devices, optical memories, and optical switches.[73] Organic materials can be used in these processes but they may have high nonlinearity, wide transparency range but low mechanical and thermal stability. On the other hand, inorganic materials were found to possess high mechanical and thermal stabilities. Hence semi-organic compounds having the combined properties of organic and inorganic materials will be useful.[74] Some of the bimetallic thiocyanates having the chemical formula $AB(SCN)_4$ are zinc mercury

thiocyanate (ZMTC), cadmium mercury thiocyanate (CMTC), manganese mercury thiocyanate (MMTC) and zinc cadmium mercury thiocyanate (ZCTC).

Gold(I) cyanides are the important intermediates for recovery and recycling of gold,[75] gold surface technology[76] and gold plating.[77] Gold extraction process generally employs cyanide as the leaching agent. Thiocyanates as the leaching agent have technological and environmental advantages over cyanide.[78] Gold(I) thiocyanate complexes have been investigated for their use as antitumor and anti-HIV activity.[79] There are other gold complexes such as gold(I) phosphine complexes,[80] which exhibit antitumor activity.

Luminescence in $M[Au(CN)_2]$ and $M[Ag(CN)_2]$ has been attributed to their intermolecular association via Au-Au and Ag-Ag interaction to form extended 2-dimensional sheets. Rawashdeh-Omary et al. have showed the excited-state interactions of dicyanoaurates(I) and dicyanoargentates(I) in solution.[81] Linear two coordinate gold(I) complexes of the type L-Au-X (L=neutral, X=anionic ligand) form monomers in solution and also in gas phase. Because of their simple molecular structure, these molecules can act as model building blocks for supramolecular structures. There is growing structural evidence for them to readily associate as dimers, oligomers and polymers as a result of intermolecular Au-Au interactions. The Schmidbaur group has synthesized linear two coordinate gold(I) thiocyanate complexes of the type L-Au-SCN (L=tetrahydrothiophene, trimethylphosphine and xylyl or mesityl isocyanide).[82] The tetrahydrothiophene gold(I) thiocyanate complex exhibits aurophilic contacts within a chain polymer (Au-Au= 3.006 Å), whereas the $(Me_3P)Au(SCN)$ forms

dimers with short Au-Au contacts (Au-Au= 3.099 Å). The xylyl and mesityl complexes exhibit weak intermolecular Au-Au contacts with Au-Au distance of 3.983 Å and 3.397 Å respectively, because of the relative bulkiness of the phosphine. Elbjeirami et al. have studied neutral isonitrile gold(I) complexes.[83] They have shown that the emission energies are based on the association mode instead of Au-Au distances in RNCAuX compounds. They found that the linear-chain compounds with long but extended Au-Au separations exhibit lower emission energies than those in dimer compounds with much shorter Au-Au distances.

Establishing a clear structure-luminescence relationship remains an elusive goal in this area. It is clearly known that intramolecular or intermolecular aurophilic bonding is necessary to observe Au-centered luminescence in two-coordinate complexes while three coordinate complexes do not require such interactions.[84] The difficulty lies in trying to relate the luminescence energy to the crystallographic Au-Au ground state distances as situations wherein direct correlation,[85] inverse correlation,[83,86] and even absence of correlation[87] were reported to exist between the luminescence energy and the Au-Au distance. This is in contrast to the luminescent systems of other metals such as tetracyanoplatinates(II) wherein clear correlation has long been established between the luminescence energy and the Pt-Pt distance;[88] other recent reports reinforce this trend for other types of Pt(II) complexes that exhibit Pt-Pt interactions.[89] In chapter 4, the structure-luminescence relationship in Au(I) complexes, $[Au(SCN)_2]^-$, in which the effect of varying the counterion on both supramolecular structure and the luminescence energy are investigated. These studies are virtuous in their own rights toward the

aforementioned goal of clarifying structure luminescence relationships in Au(I) systems. Moreover, insights into possible future studies that utilize $[Au(SCN)_2]^-$ and $[Ag(SCN)_2]^-$ donor clusters to lanthanide acceptor are established.

Chapter 5 discusses the conclusion of chapters 2, 3 and 4 along with future expansion for the studied chapters.

1.5 References

[1] So, F.; Krummacher, B.; Mathai, M. K.; Poplavskyy, D.; Choulis, S. A.; Choong, V, -A. *J. Appl. Phys.* **2007**, *102*, 091101(1)- 091101(21).

[2] Monkman, A.; Rothe, C.; King, S.; Dias, F. *Adv Polym Sci.* **2008**, *212*, 187-225.

[3] Yanagi, H.; Shibutani, T. *Thin solid films* **2003**, *438-439*, 33-38.

[4] Solovyov, K. N.; Borisevich, E. A. *Phys. Usp.* **2005**, *48*, 231-253.

[5] Weinzierl, G.; Friedrich, J. *Chem. Phys. Lett.* **1981**, *80*, 55-59.

[6] McClure, D. S. *J. Chem. Phys.* **1949**, *17*, 905-913.

[7] Kunkely, H.; Vogler, A. *Inorg. Chem. Comm.* **2008**, *11*, 669-671.

[8] (a) Omary, M. A.; Elbjeirami, O.; Gamage, C. S. P.; Sherman, K. M.; Dias, H. V. R. *Inorg. Chem.* **2009**, *48*, 1784-1786. (b) Taylor, T. J.; Elbjeirami, O.; Burress, C. N.; Tsunoda, M.; Bodine, M, I.; Omary, M. A. *J. Inorg. Organomet. Polym Mater.* **2008**, *18*, 175-179. (c) Elbjeirami, O.; Burress, C. N.; Gabbaie, F. P.; Omary, M. A. *J. Phys. Chem. C* **2007**, *111*, 9522-9529. (d) Burress, C. N.; Bodine, M, I.; Elbjeirami, O.; Reibenspies, J. H.; Omary, M. A.; Gabbaie, F. P. *Inorg. Chem.* **2007**, *46*, 1388-1395. (e) Omary, M. A.; Mohamed, A. A.; Rawashdeh-Omary, M. A.; Fackler, J. P. *Coord. Chem. Rev.* **2005**, *249*, 1372-1381. (f) Mohamed, A. A.; Rawashdeh-Omary, M. A.; Omary, M. A.; Fackler, J. P., Jr. *Dalton Trans.* **2005**, *15*, 2597-2602. (g) Omary, M. A.; Kassab, R. M.; Haneline, M. R.; Elbjeirami, O.; Gabbaie, F. P. *Inorg. Chem.* **2003**, *42*, 2176-2178.

[9] (a) Piguet, C.; Bünzli, J. –C. G.; Donnio, B.; Guillon, D. *Chem. Commun.* **2006**, 3755-3768. (b) Bünzli, J. –C. G. *Acc. Chem. Res.* **2006**, *39*, 53-61.

[10] Horrocks, W. D., Jr.; Albin, M. *Prog. Inorg. Chem.* **1984**, *31*, 1-104.

[11] Freed, K. F.; Jortner, J. *J. Chem. Phys.* **1970**, *52*, 6272-6291.

[12] Leonard, J. P.; Gunnlaugsson, T. *J Fluoresc.* **2005**, *15*, *585-595.*

[13] Bunzli, J. –C. G.; Choppin, G. R. *Lanthanide Probes in Life, Chemical and Earth Sciences.* **1989** Elsevier, PP 237.

[14] Chen, L.; Liu, Y.; Li, Y. *J. Alloys Compd.* **2004**, *381*, 266-271.

[15] Wang, C.; Yan, B. *J. Non-Cryst. Solids* **2008**, *354*, 962-969.

[16] Richardson, F. S. *Chem. Rev.* **1982**, *82*, 541-552.

[17] Georges, J. *Analyst* **1993**, *118*, 1481-1486.

[18] Wolfson, J. M.; Kearns, D. R. *Biochemistry* **1436**, *14*, 1436-1444.

[19] Kuriki, K.; Koike, Y. *Chem*. *Rev*. **2002**, *102*, 2347-2356.

[20] Enrichi, F. *Ann*. *N*. *Y*. *Acad*. *Sci*. **2008**, *1130*, 262-266.

[21] Yi, G.; Lu, H.; Zhao, S.; Ge, Y.; Yang, W.; Chen, D.; Guo, L. –H. *Nano Lett*. **2004**, *4*, 2191-2196.

[22] Hasegawa, Y.; Wada, Y.; Yanagida, S. *J*. *Photochem*. *Photobiol., C* **2004**, *5*, 183-202.

[23] Tomaszewska, M.; Kukwa, A.; Tulibacki, M.; Wojtowicz, P.; Oledzka, I.; Jezewska, E. *Proc*. *SPIE Int*. *Soc*. *Opt*. *Eng*. **2007**, *6598*, 659802/1-689802/5.

[24] Weber, R. J. K.; Felten, J. J.; Cho, B.; Nordine, P. C. *Nature* **1998**, *393*, 769-771.

[25] Hasegawa, Y.; Wada, Y.; Yanagida, S. *J*. *Photochem*. *Photobiol*., C **2004**, *5*, 183-202.

[26] Som, T.; Karmakar, B. *J*. *Alloys Compd*. **2009**, *476*, 383-389.

[27] El-Agmy, R. M. *Laser Phys*. **2008**, *18*, 803-806.

[28] Dexter, D. L. *J*. *Chem*. *Phys*. **1953**, *21*, 836-850.

[29] Förster, T. *Naturwissenschaften*. **1946**, *33*, 166-175.

[30] Förster, T. *T. Ann*. *Phys*. **1948**, *2*, 55-73.

[31] Turro, N. J. In *Modern Molecular Photochemistry.* University science books. CA.**1991.** Chapter 9.

[32] Assefa, Z.; Shankle, G.; Patterson, H. H.; Reynolds, R. *Inorg*. *Chem*. **1994**, *33*, 2187-2195.

[33] Yersin, H. *J*. *Chem*. *Phys*. **1978**, *68*, 4707-4713.

[34] Yersin, H.; Stock, M. *J*. *Chem*. *Phys*. **1982**, *76*, 2136-2138.

[35] Treadway, M. J.; Powell, R. C. *Phys*. *Rev*. *B*. **1975**, *11*, 862-874.

[36] Rawashdeh-Omary, M. A.; Larochelle, C. L.; Patterson, H. H. *Inorg*. *Chem*. **2000**, *39*, 4527-4534.

[37] (a) Holland, J. M.; Liu, X.; Zhao, J. P.; Mabbs, F. E.; Kilner, C. A.; Thornton-Pett, M.; Halcrow, M. A. *J*. *Chem*. *Soc*., *Dalton Trans*. **2000**, *19*, 3316-3324. (b) Shuangxi, W.; Ying, Z.; Fangjie, Z.; Qiuying, W.; Liufang, W. *Polyhedron* **1992**, *11*, 1909-1915. (C) Collin, J. -P.; Guillerez, S.; Sauvage, J. -P. *J*. *Chem*. *Soc*., *Chem*. *Commun*. **1989**, 776-778. (d) Kirchhoff, J. R.; McMillin, D. R.; Marnot, P. A.; Sauvage, J. -P. *J*. *Am*. *Chem*.

Soc. **1985**, *107*, 1138-1141. (e) Elhabiri, M.; Scopelliti, R.; Bünzli, J-C G.; Piguet, C. *J*. *Am*. *Chem*. *Soc*. **1999**, *121*, 10747-10762.

[38] Mürner, H. -R.; Chassat, E.; Thummel, R. P.; Bünzli, J- C. G. *J*. *Chem*. *Soc*., *Dalton Trans*. **2000**, 2809-2816.

[39] Cram, D. J.; Steinberg, H. *J*. *Am*. *Chem*. *Soc*. **1951**, *73*, 5691-5704.

[40] (a) Kealy, T. J.; Pauson, P. L. *Nature* **1951**, *168*, 1039-1040. (b) Miller, S. A.; Tebboth, J. A.; Tremaine, J. F. *J*. *Chem*. *Soc*. **1952**, 632-635.

[41] (a) Omary, M. A.; Mohamed, A. A.; Rawashdeh-Omary, M. A.; Fackler, J. P., Jr. *Coord*. *Chem*. *Rev*. **2005**, *249*, 1372-1381. (b) Burini, A.; Bravi, R.; Fackler, J. P., Jr.; Galassi, R.; Grant, T. A.; Omary, M. A.; Pietroni, B. R.; Staples, R. J. *Inorg*. *Chem*. **2000**, *39*, 3158-3165. (c) Burini, A.; Mohamed, A. A.; Fackler, J. P., Jr. *Comments Inorg*. *Chem*. **2003**, *24*, 253-280. (d) Elbjeirami,O.; McDougald, R.; Omary, M. A. From Abstracts of Papers, 237th ACS National Meeting, Salt Lake city, UT, March 22-26. (e) McDougald, R. N., Jr.; Firas, A.; Elbjeirami, O.; Omary, M. A. Abstracts, 64th Southwest Regional Meeting of the American Chemical Society, Little Rock, AR. October 1-4.

[42] Werner, H. *Angew*. *Chem*. *Int*. *Ed*. **1977**, *16*, 1-9.

[43] Diederich, F, in: Stoddart, J. F (Ed.), *Cyclophanes, Monographs in Supramolecular Chemistry 2*, Royal Society of Chemistry, Cambridge, **1991**, 6-18.

[44] (a) Siebert, W. *Angew*. *Chem*. *Int*. *Ed*. **1985**, *24*, 943-958. (b) Grimes, R. N. *Chem*. *Rev*. **1992**, *92*, 251-268.

[45] Schumacher, E.; Taubenest, R. *Helv*. *Chim*. *Acta*. **1964**, *47*, 1525-1529.

[46] Werner, H.; Salzer, A. *Synth*. *React*. *Inorg*. *Met*. *Org*. *Chem*. **1972**, *2*, 239-248.

[47] Dubowchik, G. M.; Hamilton, A. D. *J*. *Chem*. *Soc*., *Chem*. *Commun*. **1986**, 665-666.

[48] Pauson, P. L. *Pure Appl*. *Chem*. **1977**, *49*, 839-855.

[49] Warren, K. D. *Struct*. *Bond*. **1976**, *27*, 45-159.

[50] (a) Bochkarev, M. N.; Fedushkin, I. L.; Cherkasov, V. K.; Nevodchikov, V. I.; Schumann, H.; Görlitz. *Inorg*. *Chim*. *Acta*. **1992**, *201*, 69-74. (b) Kurikawa, T.; Negishi, Y.; Hayakawa, F, Nagao, S.; Miyajima, K.; Nakajima, A.; Kaya, K. *J*. *Am*. *Chem*. *Soc*. **1998**, *120*, 11766-11772.

[51] (a) Hill, A. E. *J*. *Am*. *Chem*. *Soc*. **1921**, *43*, 254-268. (b) Hill, A. E. *J*. *Am*. *Chem*. *Soc*. **1922**, *44*, 1163-1193 (c) Hill, A. E.; Miller, F. W., Jr. *J*. *Am*. *Chem*. *Soc*. **1925**, *47*, 2702-2712.

[52] Mulliken, R. S. *J*. *Am*. *Chem*. *Soc*. **1952**, *74*, 811-824.

[53] Smith, H. G.; Rundle, R. E. *J. Am. Chem. Soc.* **1958**, *80*, 5075-5080.

[54] Andrew, L. J. *Chem. Rev.* **1954**, *54*, 713-776.

[55] Fukui, K.; Imamura, A.; Yonezawa, T.; Nagata, C. *Bull. Chem. Soc. Jpn.* **1961**, *34*, 1076-1080.

[56] (a) Dougherty, D. A. *Science* **1996**, *271*, 163-168. (b) Gallivan, J. P.; Dougherty, D. A. *J. Am. Chem. Soc.* **2000**, *122*, 870-874. (c) Zacharias, N.; Dougherty, D. A. *Trends Pharmacol. Sci.* **2002**, *23*, 281-287. (d) Gallivan, J. P.; Dougherty, D. A. *Proc. Natl. Acad. Sci. U.S.A.* **1999**, *96*, 9459-9464. (e) Mecozzi, S.; West, A. P., Jr.; Dougherty, D. A. *J. Am. Chem. Soc.* **1996**, *118*, 2307-2308. (f) Ngola, S. M.; Dougherty, D. A. *J. Org. Chem.* **1998**, *63*, 4566-4567. (g) Ma, J. C.; Dougherty, D. A. *Chem. Rev.* **1997**, *97*, 1303-1324. (h) Mecozzi, S.; West, A. P., Jr.; Dougherty, D. A. *Proc. Natl. Acad. Sci. U.S.A.* **1996**, *93*, 10566-10571.

[57] Tekarli, S. M.; Cundari, T. R.; Omary, M. A. *J. Am. Chem. Soc.* **2008**, *130*, 1669-1675.

[58] Turner, R. W.; Amma, E. L. *J. Am. Chem. Soc.* **1966**, *88*, 3243-3247.

[59] Hall Griffith, E. A.; Amma, E. L. *J. Am. Chem. Soc.* **1974**, *96*, 743-749.

[60] Hall Griffith, E. A.; Amma, E. L. *J. Am. Chem. Soc.* **1974**, *96*, 5407-5413.

[61] Rodesiler, P. F.; Hall Griffith, E. A.; Amma, B. L. *J. Am. Chem. Soc.* **1972**, *94*, 761-766.

[62] Taylor, I. F., Jr.; Hall Griffith, E. A.; Amma, E. L. *J. Am. Chem. Soc.* **1969**, *91*, 5745-5749.

[63] Amma, E. L.; Hall Griffith, E. A. *J. Am. Chem. Soc.* **1971**, *93*, 3167-3172.

[64] Rodesiler, P. F.; Amma, E. L. *Inorg. Chem.* **1972**, *11*, 388-395.

[65] Munakata, M.; Wu, L, P.; Kuroda-Sawa, T.; Maekawa, M.; Suenaga, Y.; Sugimoto, K. *Inorg. Chem.* **1997**, *36*, 4903-4905.

[66] Livingstone, S. E. *Quart. Rev.* (London), **1965**, *19*, 386-425.

[67] (a) Brown, B. W.; Lingafelter, E. C. *Acta Cryst.* **1963**, *16(8)*, 735-738. (b) Vaira, M. D.; Mani, F. *J. Chem. Soc. Dalton Trans.* **1985**, *11*, 2327-2332.

[68] Cotton, S. A.; Franckevicius, V.; How, R. E.; Ahrens, B.; Ooi, L. L.; Mahon, M. F.; Raithby, P. R.; Teat, S. J. *Polyhedron* **2003**, *22*, 1489-1497.

[69] Pyrka, G. J.; Fernando, Q.; Inoue, M. B.; Inoue, M. *Inorg. Chim. Acta.* **1989**, *156*, 257-264.

[70] Chiswell, B.; Livingstone, S. E. *J. Chem. Soc.* **1959**, 2931-2936.

[71] Li, C. –S.; Xue, L.; Che, Y. –X.; Luo, F.; Zheng, J. –M.; Mak, T. C.W. *Inorg. Chim. Acta*. **2007**, *360*, 3569-3579.

[72] Nockemann, P.; Thijs, B.; Postelmans, N.; Hecke, K. V.; Meerveit, L. V.; Binnemans, K. *J. Am. Chem. Soc.* **2006**, *128*, 13658-13659.

[73] Wang, X.; Xu, D.; Lu, M.; Yuan, D.; Zhang, G.; Xu, S.; Guo, S.; Jiang, X.; Liu, J.; Song, C.; Ren, Q.; Huang, J.; Tian, Y. *Mater. Res. Bull.* **2003**, *38*, 1269-1280.

[74] Kumari, P. N. S.; Kalainathan, S.; Raj, N. A. N. *Mater. Lett.* **2007**, *61*, 4423-4425.

[75] Adams, M. D.; Jones, M. W.; Dew, D. W, in: Schmidbaur, H (Ed.), *Gold, Progress in Chemistry, Biochemistry and Technology*, Wiley, Chichester, **1999**, p. 65.

[76] Puddephatt, R. J, in: Schmidbaur, H. (Ed.), *Gold, Progress in Chemistry, Biochemistry and Technology,* Wiley, Chichester, **1999**, p.237.

[77] Grossmann, H.; Saenger, K. E.; Vinarickey, E, in: Schmidbaur, H (Ed.), *Gold, Progress in Chemistry, Biochemistry and Technology,* Wiley, Chichester, **1999**, p.199.

[78] Adams, M. D.; Jones, M. W.; Dew, D. W, in: Schmidbaur, H (Ed.), *Gold, Progress in Chemistry, Biochemistry and Technology*, Wiley, Chichester, **1999**, p. 82.

[79] Mirabelli, C. K.; Johnson, R. K.; Hill, D. T.; Faucette, L. F.; Girard, G. R.; Kuo, G. Y.; Sung, C. M.; Crooke, S. T. *J. Med. Chem.* **1986**, *29*, 218-223.

[80] (a) Shaw, C. F.; Beery, A. *Inorg. Chim. Acta*. **1986**, *123*, 213-216 (b) Berners-Price, S. J.; Mirabelli, C. K.; Johnson, R. K.; Mattern, M. R.; McCabe, F. L.; Faucette, L. F.; Sung, C. M.; Mong, S. -M.; Sadler, P. J.; Crooke, S. T. *Cancer Research* **1986**, *46*, 5486-5493.

[81] Rawashdeh-Omary, M. A.; Omary, M. A.; Patterson, H. H.; Fackler, J. P. Jr. *J. Am. Chem. Soc.* **2001**, *123*, 11237-11247.

[82] Mathieson, T.; Schier, A.; Schmidbaur, H. *J. Chem. Soc., Dalton Trans.* **2001**, 1196-1200.

[83] (a) Elbjeirami, O.; Omary, M. A.; Stender, M.; Balch, A. L. *Dalton Trans.* **2004**, *20*, 3173-3175. (b) Elbjeirami, O.; Gonser, M. W. A.; Stewart, B. N.; Bruce, A. E.; Bruce, M. R. M.; Cundari, T. R.; Omary, M. A. *Dalton Trans.* **2009**, 1522-1533.

[84] For a review, see: Forward, J. M.; Fackler, J. P., Jr.; Assefa, Z. Photophysical and Photochemical Properties of Gold(I) complexes. In O*ptoelectronic Properties of Inorganic Compounds;* Roundhill, D. M.; Fackler, J. P., Jr., Eds.; plenum: New York **1999**; Chapter 6.

[85] Assefa, Z.; McBrunnett, B. G.; Staples, R. J.; Fackler, J. P., Jr.; Assmann, B.; Angermaier, K.; Schmidbaur, H. *Inorg*. *Chem*. **1995**, *34*, 75-83.

[86] (a) Coker, N. L.; Krause Bauer, J. A.; Elder, R. C. *J*. *Am*. *Chem*. *Soc*. **2004**, *126*, 12-13. (b) Coker, N. L.; Bedel, C. E.; Krause, J. A.; Elder, R. C. *Acta Crystallogr*. **2006**, *E62*, m319-m321.

[87] Morris, R. L. W.; Olmstead, M. M.; Balch, A. L.; Omary, M. A.; Elbjeirami, O. *Inorg*. *Chem*. **2003**, *42*, 6741-6748.

[88] (a) Gliemann, G.; Yersin, H. *Struc*. *Bonding*. **1985**, *62*, 87-153. (b) Yersin, H.; Gliemann, G. *Ann*. *N*. *Y*. *Acad*. *Sci*. **1978**, *313*, 539-559.

[89] (a) Ma, B.; Li, J.; Djurovich, P. I.; Yousuffuddin, M.; Bau, R.; Thompson, M. E. *J*. *Am*. *Chem*. *Soc*. **2005**, *127*, 28-29. (b) Lu, W.; Chan, M. C. W.; Zhu, N.; Che, C. –M.; Li, C.; Hui, Z. *J*. *Am*. *Chem*. *Soc*. **2004**, *126*, 7639-7651.

CHAPTER 2

PHOTOPHYSICS OF LANTHANIDE- 4′-*P*-TOLYL-[2,2′;6′,2″]-TERPYRIDINE COMPLEXES

2.1 Introduction

Sensitized luminescence is an emission by energy transfer. There will be two principal components in this phenomenon, a donor and an acceptor. The donor can be an inorganic or organic chromophore such as organic ligands whereas the acceptor can be a lanthanide (Ln) metal. Ln(III) ions are typically chelated with ligands that have broad intense absorption bands that may sensitize Ln(III) luminescence. Intense luminescence will be observed from the Ln(III) ion when the intramolecular energy transfer from the excited state of the ligand to the emitting level of Ln(III) ion occurs. Lehn named this phenomenon as "antennae effect."[1]

Lanthanide ions and their complexes are used in a large number of applications. This is mainly due to their optical properties and efficient emission in the UV/Vis to near IR regions. Sensitized luminescence is involved in most of the lanthanide complex applications. For example lanthanide ions and complexes are used as spectroscopic structural probes in biological systems,[2] in selective hydrolysis of DNA and RNA,[3] in chiral recognition of biological substrates,[2c] as scavengers of free radicals,[2d] in time-resolved microscopy,[4] as solid-state porous material,[5] in luminescence lighting or display devices,[5a,5b,6,7] and in luminescence sensors.[8] They are also used in the study of mechanisms of several biological processes, energy and electron transfer, lanthanide induced perforation of cell membranes[2d,9] use in medicine, in radioimmunotherapy,[10]

and magnetic resonance imaging.[11] In these applications knowledge of structure and spectroscopy of single crystals is essential in order to understand the mechanism of interaction of lanthanide complexes with biological specimens.

Lanthanide metal ions exhibit sharp absorption and emission bands. This is due to their 4f electrons which are responsible for rendering atomic transition type for molecular species. The 4f orbitals are effectively shielded by the outer 5s and 5p orbitals. Because of this shielding, various states arising from the f^n configurations due to interactions with external forces are split only to the extent of 100 cm^{-1}.[12] As a result, the absorption and emission bands are sharp due to f-f transitions, which arise from a transition of one J state of an f^n configuration to another J state of the same Russell- Saunders transition. Because of their long lifetimes, large Stokes' shifts[†] and narrow emission bands, they are very useful in the biomedical analysis. But to observe favorable luminescence properties from the lanthanide metal cations, it is required to have efficient shielding of the metal center from the radiationless deactivation that occurrs from vibronic oscillations of for example OH, NH and CH bands upon interaction with the environment such as solvent molecules.[13] The most common oxidation state of Ln species is +3 in the aqueous media. Coordination numbers of 8 and 9 are the most common and the simplest way to fulfill this is by coordinating to four bidentate[14] or three tridentate ligands, respectively. Complexes of lanthanides with tridentate ligands are mostly studied and these include terpyridines,[15] pyridine 2, 6- dicarboxylates,[16] and

[†] This is deemed "apparent" Stokes shift because it refers to the practical definition of the term that measures the energy difference between the donor chromophore absorption and acceptor (Ln (III)) emission, whereas the near zero Stokes shift is necessary via the strict definition of the concept by which the same pair of states are invoked in the absorption and emission.

several C_3-symmetric podands.[17] Saturation of first coordination sphere is not enough to obtain efficient emission from lanthanide complexes. High thermodynamic stability and chemical inertness in solution are also necessary to avoid decomplexation.

Several compounds of lanthanides containing chelating anionic ligands with oxygen donors are known.[18] Prior to 1964, nitrogen coordinating compounds are well characterized in association with oxygen donors as observed in polyaminepolycarboxylates[19] and 8-quinolates.[20] The assumption that Ln^{3+}-N interactions are weaker than Ln^{3+}-O interactions is based on the observation that the cationic complexes derived from N- donors could not be isolated. This indicates that there is significant difference in the bonding characteristics of lanthanide ions to the d-type transition metal ions. This is particularly attributed to the effective shielding of the lanthanide 4f orbitals by the outer $5s^2 5p^6$ orbitals. The metal-ligand bonding in lanthanide complexes is mostly electrostatic as supported by the magnetic, spectral and kinetic data.[18a] Complexes of lanthanides with neutral N donors could not be isolated in aqueous media indicated that the Ln^{3+}-N interactions are weaker.[21] Since 1964, a number of cationic and neutral complexes of lanthanides with N-donors are synthesized based on the fact that these compounds can be stable in non-aqueous media of moderate polarity. Calorimetric measurements of stepwise enthalpies of formation of these N-donor lanthanide compounds supported the fact that these complexes are thermodynamically stable species in non-aqueous media.[21,22] The fact that most of these N-donor complexes with lanthanides have coordination numbers of 8 or 9 strongly suggests that the Ln^{3+}-N interactions are stronger than previously assumed.

Coordination numbers greater than 6 are more favored in these lanthanide compounds.[18a] The coordination number is varied which is usually between 6 to 12 is attributed to the factors such as steric factors and electrostatic forces of attraction and repulsion. And also the relatively large size of lanthanide ions (La^{3+}= 1.061 Å, Lu^{3+}= 0.848 Å) make the coordination number greater than 6 allowable.

In 1963, 1,10-phenanthroline and 2,2′-bipyridyl complexes of lanthanides were the first isolated with weakly basic nitrogen donor compounds.[23] The number of neutral ligands coordinated to the lanthanide ions depends on the coordinating ability of the anion present. Only monosubstitued complexes are obtained when the anion is a strongly coordinating chelate such as diketonate or acetate. This indicates that the weakly basic amine is not strong enough to displace a strong coordinating species. However, when a bidentate ligand such as 1,10-phenanthroline or the bipyridyl group is coordinated to the tris-diketonate complex, the lanthanide coordination sphere is expanded indicating a significant Ln^{3+}- N interaction.[24] Bis-phenonthroline and bipyridyl complexes were obtained when the anion is chloride, nitrate or salicylate.[25] Addition of the excess ligand did not result into tris species. In all of these complexes, a coordination number greater than six is found by coordinating to anions and solvent molecules. The coordination number decreases from 9 to 8 across the lanthanide (III) series.[26] Table 2.1 shows the different complexes of lanthanides with varied coordination numbers.

Table 2.1. Coordination numbers and lanthanide complexes showing those numbers.

Coordination number	Examples
8	$[Sc_2(N0_3)_2(\mu\text{-}OH)_2(bpce)_2][N0_3].2MeCN$,[27] Q[Eu(RCOCHCOR']],[28] $[RCOCHCOR']_3Ln[phen]$,[29] $[Ln(tta)_3(Fc_2Phen)]$ and $[Ln(fta)_3(phen)$[30]
9	$[Sc(terpy)(NO_3)_3]$,[27] $Pt(terpy)Cl_3(H_2O)_8$,[31] $[Eu(terpy)_3](ClO_4)_3$,[32] $Pr(terpy)(acac)(NO_3)_2.H_2O$,[33] $M(terpy)(acac)(NO_3)_2$[33] M= Nd to Lu, $Eu(DPM)_3Terpy$,[34] $[Eu(DBM)_3(TPTZ)]$[35]
10	$[Eu(bipy)_2(NO_3)_3]$,[25b] $[Eu(terpy)(NO_3)_3.(H_2O)]$,[25b] $[Tb(terpy)(NO_3)_3.(H_2O)]$,[25b] $La(NO_3)_3(terpy)(CH_3CN)$,[25a] $La(Phen)_2(NO_3)_3$,[36] $La(bipy)_2(NO_3)_3$,[37] $La(terpy)(acac)(NO_3)_2.H_2O$,[33]
11	$[Ce(NO_3)_4(H_2O).$ 4,4'-bipy][4,4'-bipyH][38]

A seven-coordinate complex of europium was discovered in 2007.[39] It is a complex of $EuCl_3$ with 2,2'-bipyridine-N,N-dioxide. Several complexes of lanthanides with simple molecules such as phenonthroline and bipyridine are known, as shown in Table 2.1. and their structural and photophysical properties were established. Melby et al. have synthesized several lanthanide compounds with β-diketonates and

phenonthroline as ligands and shown some preliminary photophysical measurements.[28] Piguet et al. have synthesized a large number of lanthanide complexes with tridentate nitrogen ligands (Figure 2.1).[40]

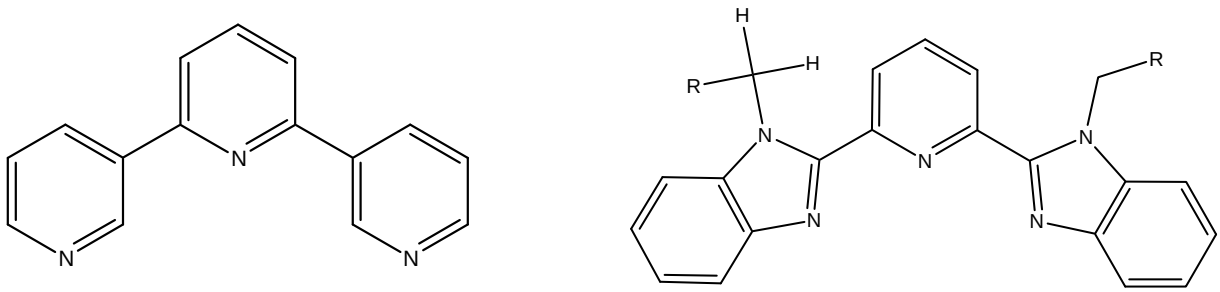

(a) (b) R=H, CH_2CH_3, $(CH_3O)_2C_6H_3$, $(CH_2)_6CH_3$

Figure 2.1 Structures of terpy (a) and benzimidazole pyridine (b)

The distal pyridine rings on the terpy ligand were replaced by benzimidazole rings with various substituents. Several triple-helical structures containing lanthanide metals with the terpy ligand modifications were reported in the same work along with the structural and photophysical properties. Assefa and his coworkers have studied the structural and photophysical properties of europium tetracyanoplatinates along with terpy.[41] They found that dual donors i.e, tetracyanoplatinate and terpy were sensitizing the emission of the Eu^{3+}. They took the advantage of both organic donor, terpy and the inorganic sensitizer, $[Pt(CN)_4]^{2-}$ as the antennae. Michael et al. have synthesized some tridentate heterocyclic nitrogen ligands and their complexes with several lanthanides,[42] toward utilization in the separation of actinides-lanthanides extraction mixtures. This group utilized the same ligand used in the present work but they have not reported any photophysical properties. The ligand 4'-*p*-Tolyl-[2,2';6',2"]-terpyridine which is

abbreviated as "ttrpy" is a terpyridine ligand with tolyl group substituted on the central pyridine ring of the terpyridine. The methyl group, which is electron-donating, in conjunction with the benzene ring attached to the terpyridine makes it strongly bonded to the lanthanides. Bellusci et al. have found that the substitution of neutral ligands with electron-donating groups such as methyl or methoxy enhances the coordinating ability of the ligands over their unsubstituted analogues.[43] The ttrpy ligand which is tridentate and is superior to bidentate ligands such as bipyridine and 1,10-phenonthroline in terms of coordination to lanthanides. Compared to the ligands synthesized by Claude et al., ttrpy is a simpler ligand with fewer substitutions.

We are interested in the structural aspects and photophysical properties of this ttrpy ligand and its analogues with various lanthanides, both such as the visible emitters europium and terbium and the near IR-emitters neodymium and erbium. We have also studied the variations in the structural behavior and photophysical properties by changing the counterions including more strongly-coordinating anions chlorides and nitrates to the more poorly coordinating perchlorate ions. The effect of the number of the ttrpy ligands on the quantum yield was studied. The effect of phonon energies due to the counterions such as perchlorates and solvent on the quantum yield and lifetimes were measured. Neutral complexes of ttrpy in combination with β-diketonate, i.e. hexafluoroacetylacetonato (hfa) with europium and terbium are also presented. The hfa ligand has relatively low vibrational coupling to lanthanides.[44] This is important to avoid the luminescence-quenching vibrational coupling to the lanthanide.[45] The hfa ligand has minimal number of hydrogens and is replaced by fluorines which are heavier compared

to hydrogen and aids in enhancement of emission by reducing thermal quenching.[46] The C-H oscillators vibrate at higher energy than the C-F. The complexes of hfa with lanthanides have enhanced thermal stability and volatility when compared with its non-fluorinated analogs.[47] These neutral lanthanide complexes can be employed in OLED devices. Also, the mechanism of the efficient way of sensitization of the lanthanides by the ttrpy ligand was studied.

2.2 Experimental Section

2.2.1 Materials

Europium chloride, terbium chloride, erbium chloride, europium nitrate, terbium nitrate, erbium nitrate, erbium perchlorate and neodymium perchlorate were obtained from Alfa Aesar. Europium perchlorate, terbium perchlorate, neodymium nitrate and neodymium chloride were obtained from strem chemicals. The lanthanide salts of chlorides and nitrates were used as received. The perchlorate salts were containing water, which was evaporated under sulfuric acid atmosphere and dried off completely before use in the reaction. 4'-*p*-Tolyl-[2,2';6',2"]-terpyridine (abbreviated as "ttrpy" or "L") was obtained from Aldrich and used as received. The solvents methanol and acetonitrile were obtained from Mallinckrodt and distilled using standard procedures prior to use. Pentane was obtained from Mallinckrodt and used as received. Diethylether was obtained from J.T. Baker and was used as received.

2.2.2 Synthesis

2.2.2.1 Synthesis of $[Eu(L)_2Cl_2]Cl.2CH_3OH$

A solution of 0.014 g ($3.8x10^{-5}$ moles) europium chloride dissolved in minimum minimum amount of distilled methanol was prepared. To this, 0.0247 g ($7.64x10^{-5}$ moles) of ttrpy dissolved previously in a minimum amount of distilled methanol was added. Later, the solution mixture was stirred and refluxed at 70 °C for 30 minutes. After that, the solution was concentrated by rotary evaporator and then vapor diffused by ether and left at room temperature. A week later, single crystals were obtained. Anal. Calcd (found) for $C_{44}H_{34}Cl_3EuN_6$. $2CH_3OH$: C 57.01 (56.32), H 4.37 (3.83), N 8.67 (8.37).

2.2.2.2 Synthesis of $[Tb(L)_2Cl_2]Cl.\ 2CH_3OH$

A solution of 0.0196 g ($5.24x10^{-5}$ moles) terbium chloride dissolved in minimum amount of distilled methanol was prepared. To this, 0.034 g ($1.04x10^{-4}$ moles) of ttrpy dissolved previously in a minimum amount of distilled methanol was added. Later, the solution mixture was stirred and refluxed at 70 °C for 30 minutes. After that, the solution was concentrated by rotary evaporator and then vapor diffused by ether and left at room temperature. A week later, single crystals were obtained. Anal. Calcd (found) for $C_{44}H_{34}Cl_3TbN_6$. $2CH_3OH$: C 56.60 (56.44), H 4.34 (4.00), N 8.61 (8.58).

2.2.2.3 Synthesis of $[Er(L)_2Cl_2]Cl.\ 2CH_3OH$

A solution of 0.02 g ($5.23x10^{-5}$ moles) erbium chloride dissolved in minimum amount of distilled methanol was prepared. To this, 0.0339 g ($1.04x10^{-5}$ moles) of ttrpy

dissolved previously in a minimum amount of distilled methanol was added. Later, the solution mixture was stirred and refluxed at 70 °C for 30 minutes. After that, the solution was concentrated by rotary evaporator and then vapor diffused by ether and left at room temperature. A week later, single crystals were obtained. Anal. Calcd (found) for $C_{44}H_{34}Cl_3ErN_6$. $2CH_3OH$. H_2O: C 55.11 (55.13), H 4.42 (4.23), N 8.38 (8.43).

2.2.2.4 Synthesis of $[CH_3OH.Nd(L)Cl_2(\mu\text{-}Cl)_2Cl_2(L)Nd.CH_3OH]$

A solution of 0.03 g ($8.36x10^{-5}$ moles) neodymium chloride dissolved in minimum amount of distilled methanol was prepared. To this, 0.0541 g ($1.67x10^{-4}$ moles) of ttrpy previously dissolved in a minimum amount of distilled methanol was added. Later, the solution mixture was refluxed at 70 °C for 30 minutes. After that, it is vapor diffused by ether and left at RT. Nice single crystals were obtained after 2 months. Anal. Calcd (found) for $C_{44}H_{34}Cl_6Nd_2N_6$. $2CH_3OH$: C 45.58 (45.45), H 3.49 (3.31), N 6.93 (6.87).

2.2.2.5 Synthesis of $2[Eu(L)(NO_3)_2(MeOH)(H_2O)](NO_3)\cdot 2[Eu(L)(NO_3)_3(MeOH)]\cdot [Eu(L)(NO_3)_2(MeOH)_2](NO_3)\cdot 4MeOH$

A solution of 0.01 g ($2.24x10^{-5}$ moles) of europium nitrate dissolved in minimum amount of distilled methanol was prepared. To this, 0.0145 g ($4.48x10^{-5}$ moles) of ttrpy previously dissolved in a minimum amount of distilled methanol was added. Later, the solution mixture was refluxed at 70 °C for 30 minutes. After that, the solution mixture was vapor diffused by ether and left at RT. Few weeks later, single crystals were obtained. Anal. Calcd (found) for $C_{66}H_{51}Eu_3N_{18}O_{27}$. $2H_2O$: C 39.24 (38.95), H 2.74 (2.7), N 12.48 (12.05).

2.2.2.6 Synthesis of $2[Tb(L)(NO_3)_2(MeOH)(H_2O)](NO_3)\cdot 2[Tb(L)(NO_3)_3(MeOH)]\cdot [Tb(L)(NO_3)_2(MeOH)_2](NO_3)\cdot 4MeOH$

A solution of 0.0114 g ($2.51x10^{-5}$ moles) terbium nitrate dissolved in minimum amount of distilled methanol was prepared. To this, 0.0163 g ($5.03x10^{-5}$ moles) of ttrpy previously dissolved in a minimum amount of distilled methanol was added. Later, the solution mixture was refluxed at 70 °C for 30 minutes. After that, the solution mixture was vapor diffused by pentane and left at RT. Few weeks later, single crystals were obtained. Anal. Calcd (found) for $C_{66}H_{51}Tb_3N_{18}O_{27}$: C 39.54 (38.86), H 2.56 (2.56), N 12.57 (11.92).

2.2.2.7 Synthesis of $Er(L)(NO_3)_3MeOH\cdot MeOH$

A solution of 0.01 g ($2.256x10^{-5}$ moles) erbium nitrate dissolved in minimum amount of distilled methanol was prepared. To this, 0.0146 g ($4.51x10^{-4}$ moles) of ttrpy previously dissolved in a minimum amount of distilled methanol was added. Later, the solution mixture was refluxed at 70 °C for 30 minutes. After that, the solution mixture was vapor diffused by ether and left at RT. Pure powder was obtained. Anal. Calcd (found) for $C_{22}H_{17}ErN_6O_{9.}\ CH_3OH.\ 4\ H_2O$: C 35.38 (35.38), H 3.74 (3.22), N 10.76 (10.98).

2.2.2.8 Synthesis of $Nd(L)(NO_3)_3MeOH\cdot MeOH$

A solution of 0.0215 g ($4.9x10^{-5}$ moles) neodymium nitrate dissolved in minimum amount of distilled methanol was prepared. To this, 0.0317 g ($9.8x10^{-4}$ moles) of ttrpy previously dissolved in a minimum amount of distilled methanol was added. Later, the

solution mixture was refluxed at 70 °C for 30 minutes. After that, the solution mixture was vapor diffused by ether and left at RT. Few weeks later, single crystals were obtained. Anal. Calcd (found) for $C_{22}H_{17}N_6NdO_9$. CH_3OH: C 40.29 (39.61), H 3.09 (2.87), N 12.26 (12.05).

2.2.2.9 Synthesis of $[Eu(L)_3](ClO_4)_3 \cdot 2MeCN$

A solution of 0.052 g ($1.15x10^{-4}$ moles) europium perchlorate dissolved in minimum amount of distilled acetonitrile was prepared. To this europium perchlorate solution, 0.0748 g ($2.3x10^{-4}$ moles) of ttrpy dissolved in a minimum amount of distilled acetonitrile was added. Later, the solution mixture was refluxed for 30 minutes at 85 °C. The solution turned to brown. After 30 minutes, the solution mixture was vapor diffused by ether for crystal growth. Few weeks later, single crystals were obtained. Anal. Calcd (found) for $C_{66}H_{51}Cl_3EuN_9O_{12}$: C 55.81 (55.09), H 3.62 (3.68), N 8.87 (9.47).

2.2.2.10 Synthesis of $[Tb(L)_2(ClO_4)_2(H_2O)](ClO_4) \cdot MeOH \cdot 0.5Et_2O$

A solution of 0.0126 g ($2.75x10^{-5}$ moles) terbium perchlorate dissolved in minimum amount of distilled methanol was prepared. To this, 0.0089 g ($2.75X10^{-5}$ moles) of ttrpy was added. The solution mixture was refluxed at 70 °C for 30 minutes. Later, the solution was subjected to vapor diffusion by ether for crystal growth and left at RT. Several weeks later, single crystals were obtained. Anal. Calcd (found) for $C_{66}H_{51}Cl_3N_9O_{12}Tb$. H_2O: C 54.84 (54.27), H 3.70 (3.46), N 8.72 (8.36).

2.2.2.11 Synthesis of $[Er(L)_2(ClO_4)(MeOH)](ClO_4)_2 \cdot 2MeOH$

A solution of 0.015 g ($2.61x10^{-5}$ moles) erbium perchlorate dissolved in minimum amount of distilled methanol was prepared. To this, 0.0084 g ($2.61x10^{-5}$ moles) of ttrpy previously dissolved in a minimum amount of distilled methanol was added. Later, the solution mixture was refluxed at 70 °C for 30 minutes. After that, it is vapor diffused by ether and left at room temperature. Few weeks later, single crystals were obtained. Anal. Calcd (found) for $C_{45}H_{37}Cl_3ErN_6O_{12}$: C 47.94 (47.28), H 3.31 (3.05), N 7.45 (7.47).

2.2.2.12 Synthesis of $[Nd(L)_2(ClO_4)_2(H_2O)](ClO_4) \cdot MeOH \cdot 0.5Et_2O$

A solution of 0.0157 g ($3.54x10^{-5}$ moles) neodymium perchlorate dissolved in minimum amount of distilled methanol was prepared. To this, 0.01149 g ($3.54x10^{-5}$ moles) of ttrpy previously dissolved in a minimum amount of distilled methanol was added. Later the solution mixture was refluxed at 70 °C for 30 minutes. After that, it is vapor diffused by ether and left at room temperature. Few weeks later, single crystals were obtained. Anal. Calcd (found) for $C_{44}H_{34}Cl_3N_6NdO_{12}$, CH_3OH. H_2O: C 47.43 (47.42), H 3.54 (3.52), N 7.38 (7.02).

2.2.3 X-ray Crystallography

Single crystal X-ray diffraction data for all the lanthanide complexes were collected by Dr. Xiaoping Wang on a Bruker SMART APEX II CCD-based diffractometer and a Mo Kα fine focus sealed tube (λ = 0.71073 Å) with a graphite monochromator operated at 50 kV, 30 mA at 100 K. The data frames for each compound were integrated with the available APEX2 software[48] using a narrow-frame algorithm. The

structures were solved and refined using the SHELXTL™ program package.[49] All nonhydrogen atoms are refined anisotropically. Hydrogen atoms were assigned calculated positions and allowed to ride on the attached carbon atoms in final structure refinements. The pertinent X-ray data is summarized in Tables 2.2-2.5. X-ray crystallography for $[Eu(ttrpy)_2Cl_2]Cl$ was performed at Bruker AXS Inc. by Dr. Charles Campana. The X-ray intensity data were measured at 100(2) K on a Bruker SMART APEX II CCD area detector system equipped with a graphite monochromator and a Mo Kα fine-focus sealed tube (λ = 0.71073 Å) operated at 1.5 kW power (50 kV, 30 mA). The detector was placed at a distance of 4.921 cm. from the crystal. The structure was solved and refined using the Bruker SHELXTL™ (Version 6.1) Software Package. The structure was solved and refined using the Bruker SHELXTL (Version 6.1) Software Package, using the space group P-1, with Z = 2 for the formula unit, $C_{45}H_{40}N_6O_2Cl_3Eu$. Hydrogen atoms are displayed with an arbitrarily small radius.

2.2.4 Quantum Yield Measurements

Quantum yield measurements were made by using the integrating sphere attached to the spectrophotometer instrument.

2.3 Results and Discussion

2.3.1 Crystal Structures

2.3.1.1 Crystal Structure of $[Eu(L)_2Cl_2]Cl \cdot 2\ (CH_3OH)$

This complex crystallizes in the triclinic system with a P-1 space group. It is coordinated to nitrogens of two molecules of ttrpy and two chlorides, given rise to a

coordination number of 8. The average distance between Eu-N is 2.56 Å. The chloride atoms are *cis-* to each other with an angle of 100.03° (Cl1-Eu-Cl2). The two ttrpy molecules are almost orthogonally coordinated to the europium through the nitrogens. The central pyridine and two pyridine sidearms of the ligand adopt a *cis- cis-* conformation, resulting in an approximately planar coordination of the metal. The arrangement of two ttrpy molecules orthogonally reduces the steric hindrance around the europium and makes the coordination of 8 feasible. The average distance between Eu-N is 2.562 Å. Eu-N bonds to co-ordinated terpyridyl molecules average 2.575 Å in the nine-coordinate $[Eu(terpy)_3](ClO_4)_3$.[50] The Eu-N distance in the 10-coordinate complex, $[Eu(spy)(NO_3)_2]NO_3$ (spy= 2,2′: 6′,2″: 6″,2‴: 6‴,2⁗: 6⁗,2⁗′-sexipyridine) lies in the range of 2.536 to 2.389 Å.[51] The Eu-Cl distances in the cation $[Eu(ttrpy)_2Cl_2]^+$ are 2.668 and 2.684 Å, overall longer than those observed in $EuPy_4Cl_3$ (Eu-Cl, 2.674, 2.641, 2.648 Å)[52] and in analogous $[LnCl_3(pybox)_2]$ (2.633 Å),[53] but in the range observed for $Eu(tpy)Cl_3(H_2O)_4$ (tpy= 2,2′:6′,2″-terpyridine) complexes (Eu-Cl, 2.747 Å),[54] with Cl ligands occupying both axial and the equatorial sites. Figure 2.2 is the crystal structure of this complex.

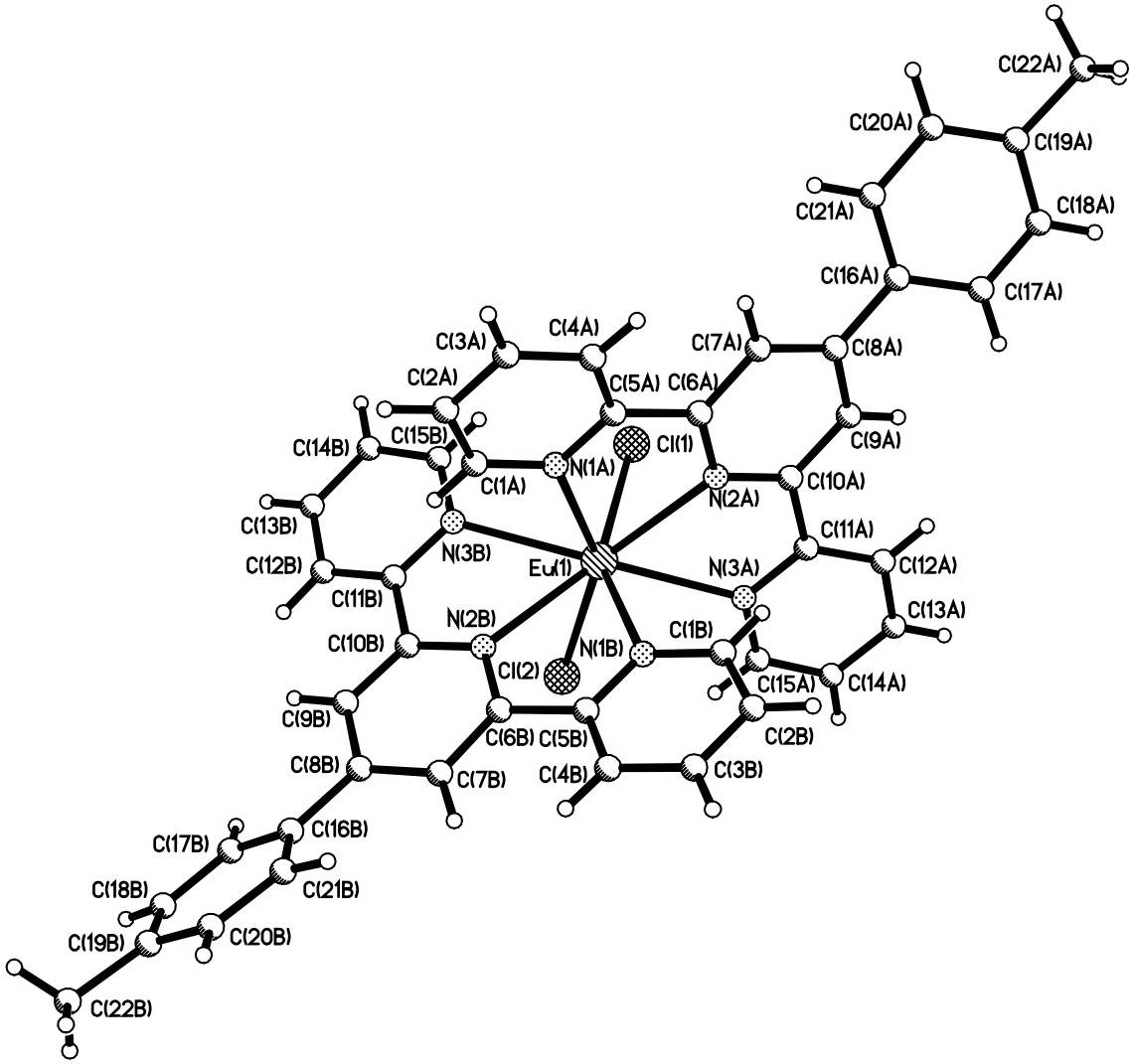

Figure 2.2. Crystal structure of $[Eu(L)_2Cl_2]Cl$.

2.3.1.2 Crystal Structure of $[Tb(L)_2Cl_2]Cl.\ 2CH_3OH$

This complex crystallizes in the P-1 space group. There are two molecules of ttrpy coordinated to the terbium metal center with 8 as coordination number, 6 heterocyclic nitrogen atoms from two tridentate ttrpy molecules and 2 chloride ions. The distance between two nearest terbium atoms is 9.80 Å. The average Tb-N distance is 2.54 Å. This lies is in the range of 2.536 to 2.564 Å of $[Tb(terpy)]NO_3)_3.\ H_2O]$.[25b] The angle between the Cl1-Tb-Cl2 is 99.15° slightly less than that in the $[Eu(L)_2Cl_2]Cl$. Figure 2.3 is the crystal structure of $[Tb(L)_2Cl_2]Cl$.

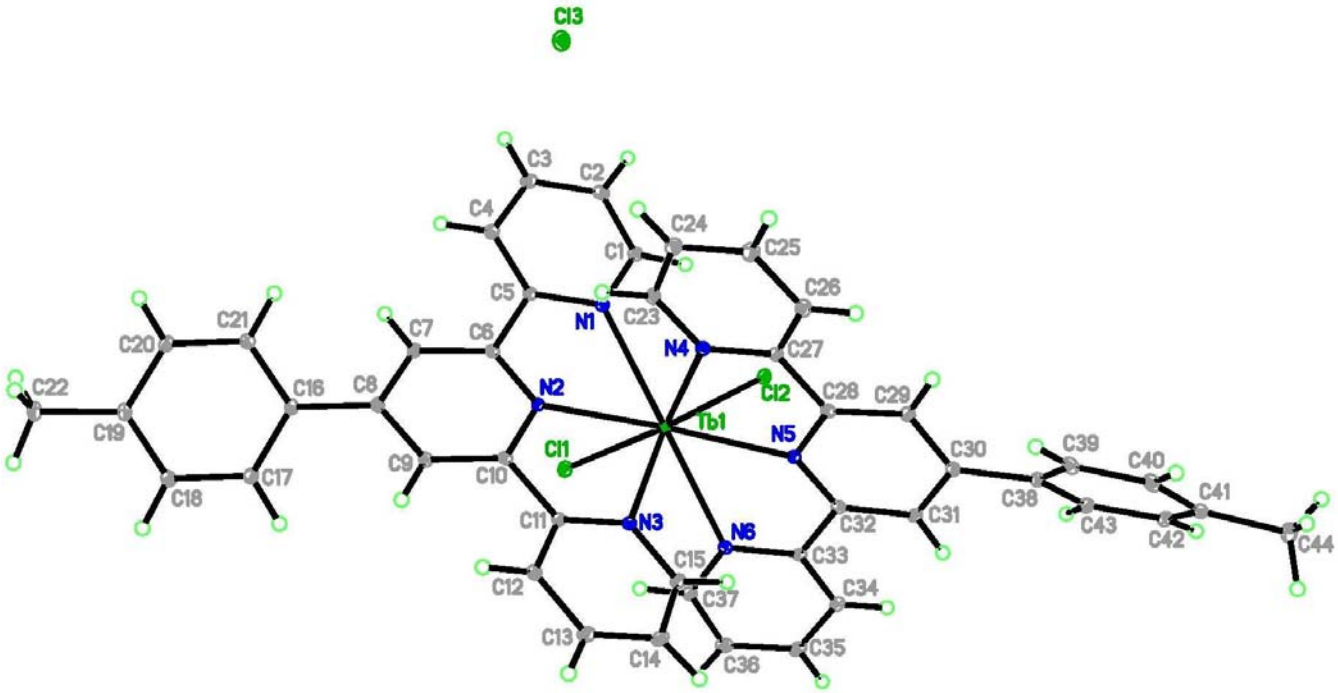

Figure 2.3 Crystal structure of $[Tb(L)_2Cl_2]Cl$.

2.3.1.3 Crystal Structure of $[Er(L)_2Cl_2]Cl.\ 2CH_3OH$

This complex crystallizes in the P-1 space group as in the case of $[Tb(ttrpy)Cl_2]Cl$. The coordination of the ttrpy molecules and chlorides are also the same as in $[Tb(ttrpy)Cl_2]Cl$. The distance between the two nearest erbium atoms is 13.02 Å. The nitrogens of the ttrpy molecules are asymmetrically attached to the erbium center as can be seen from the bond distances between Er-N are different (Er-N1= 2.545 Å, Er-N2= 2.495 Å, Er-N3= 2.505 Å, Er-N4= 2.505 Å, Er-N5= 2.488 Å and Er-N6= 2.530 Å). The Cl1-Er-Cl2 angle is 97.84°, which is lower than the corresponding angle in both the europium and terbium chloride complexes. The average Er-N distance is 2.51 Å. Figure 2.4 is the crystal structure of $[Er(L)_2Cl_2]Cl$.

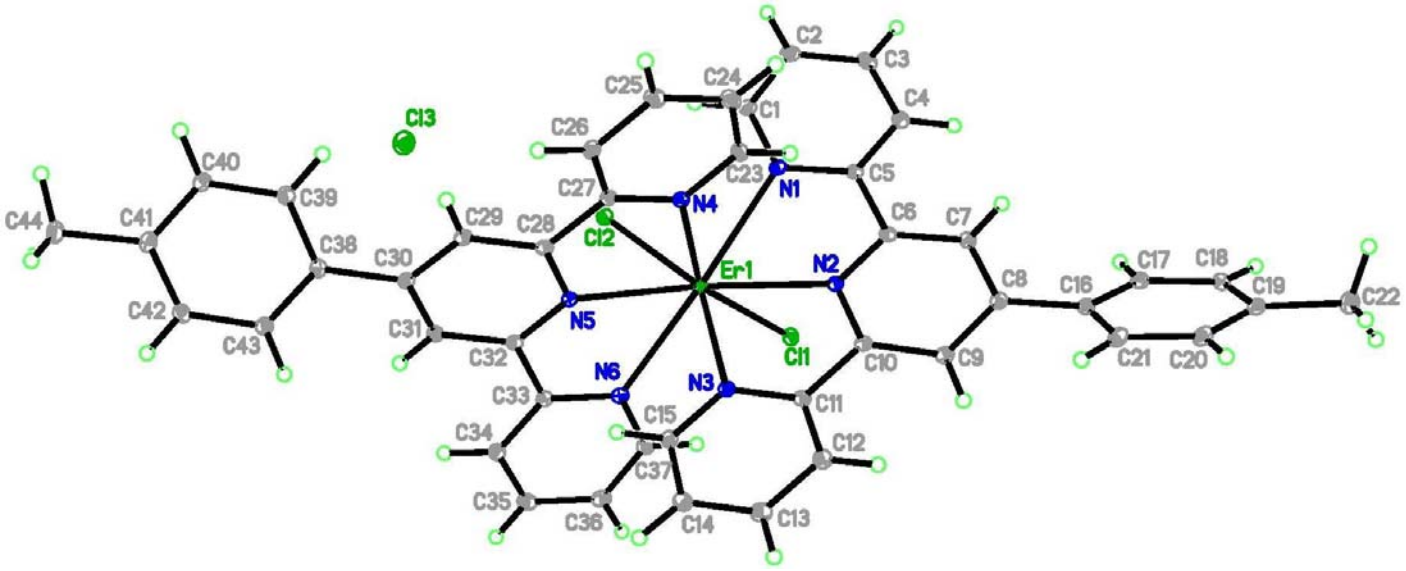

Figure 2.4. Crystal structure of $[Er(L)_2Cl_2]Cl$.

2.3.1.4 Crystal Structure of $[CH_3OH.Nd(L)Cl_2(\mu\text{-}Cl)_2Cl_2(L)Nd.CH_3OH]$

This is a neutral complex that crystallizes differently from the rest of the lanthanide chloride complexes even though it belongs to the same P-1 space group. It crystallizes as a dimer with chloro bridging ligands. Each neodymium is bounded to 3 nitrogens of the ttrpy ligand, two chlorides, two bridging chlorides and a methanol molecule making the coordination number as 8. The distance between the two neodymium atoms in the dimer is 4.62 Å. The average Nd-N distance is 2.565 Å. It lies in the range of average value of 2.61 Å for the cationic and the average value of 2.62 Å for the neutral complex of Nd with the terpy molecule, $[Nd(OTf)_2(terpy)_2(Py)]^+$ and $[Nd(OTf)_3(terpy)_2]$. MeCN, respectively.[55] It is comparable to the mean value of 2.60 Å for the eight-coordinate complex of $[NdI_2(terpy)_2]I$[56] and 2.617 Å for the nine-coordinate compound, $[NdCl(terpy)(H_2O)_5]Cl_2$.[54] The angle along Nd-Cl-Nd is 74.32°. This is comparable to the Cl-Nd-Cl' angle, 73.44°, of the $[\{((Me_3Si)_2N)_2Nd(\mu'\text{-}Cl)Li(THF)_3\}(\mu\text{-}Cl)]_2$.[57] In the Nd_2Cl_2 rhomb, the two chlorine atoms are symmetrically located between the two neodymium atoms with a bond length of 2.816 Å and 2.986 Å. Nd-O bond distance of coordinated methanol is 2.507 Å, which is in good agreement with the reported value for lanthanide complexes where methanol is coordinated to complete the coordination polyhedron.[58] Figure 2.5 shows the crystal structure.

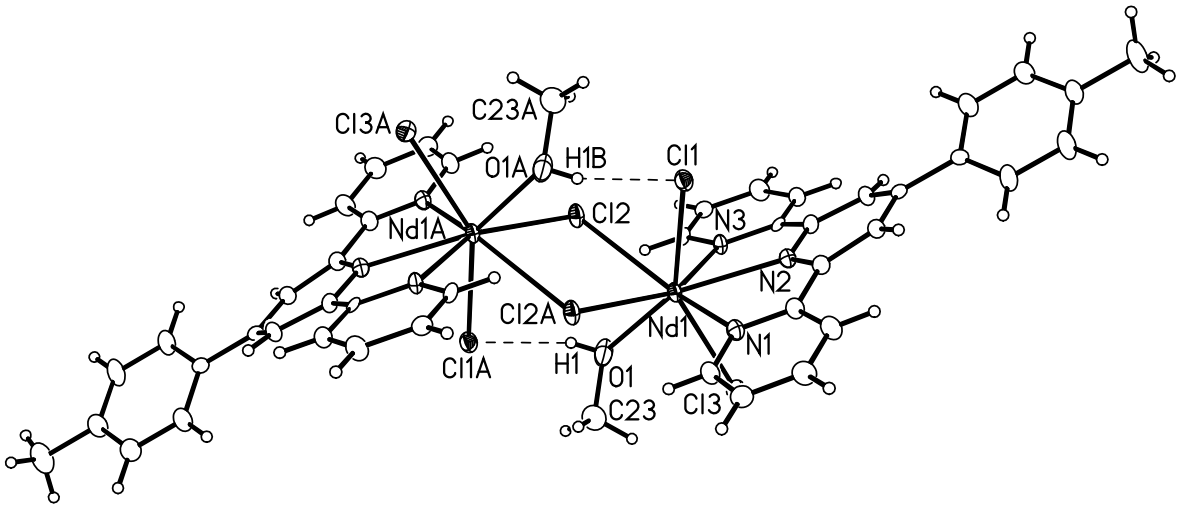

Figure 2.5. Crystal structure of $[CH_3OH.Nd(L)Cl_2(\mu\text{-}Cl)_2Cl_2(L)Nd.CH_3OH]$.

X-ray data information of the lanthanide chloride-ttrpy complexes is given in Table 2.2.

2.3.1.5 Crystal Structure of $2[Eu(L)(NO_3)_2(MeOH)(H_2O)](NO_3)\cdot 2[Eu(L)(NO_3)_3(MeOH)]\cdot [Eu(L)(NO_3)_2(MeOH)_2](NO_3)\cdot 4MeOH$

This compound belongs to *Pnna* space group. IR spectra shows 35-40 cm^{-1} blue shifts for the C=C and C=N pyridyl stretching frequencies upon complexation, which is characteristic of meridional tricoordination of the terpyridine units to the metal.[59] Vibrational spectroscopy is also well-suited for investigating the binding mode of the nitrate anions.[60] The large separations detected between the antisymmetric (ν_a) and the symmetric (ν_s) stretching vibrations of the NO_3 group ($\Delta\nu = \nu_a - \nu_s$ = 178-225 cm^{-1}) point to bidentate coordination with local C_{2v} symmetry.[60b,61] Figure 2.6 shows the crystal of this compound. The asymmetric unit consists of three independent

monomeric metal species, two uncoordinated nitrate anions and two methanol molecules. The metal coordination species includes two cations of $[Eu(ttrpy)(NO_3)_2(MeOH)(H_2O)]^+$ (**Eu1**) and $[Eu(ttrpy)(NO_3)_2(MeOH)_2]^+$ (**Eu3**), and one neutral molecule $[Eu(ttrpy)(NO_3)_3(MeOH)]$ (**Eu2**), each of which being coordinated by three nitrogen atoms from one tridentate ligand, ttrpy and two bidentate nitrato groups. The 9, 10, 10-coordination sphere of Eu1, Eu2 and Eu3 site is then completed by O-atoms from coordinated solvent molecules or another nitrate group, respectively. The nitrate groups are essentially planar, and the ttrpy ligand is coordinated in the usual meridional planar way, as was observed for $[Eu(L)_2Cl_2]Cl$ and also in $[Eu(NO_3)_3(bpt)(MeOH)]$ and other ttrpy complexes.[61,62] The average distance between the Eu and the 9 nitrogens from the 3 ttrpy ligands is 2.55 Å. This mean distance between Eu-N can be comparable to average Eu-N bond length of 2.544 Å in $[Eu(terpy)(NO_3)_3.\ H_2O]$.[25b]

The successful characterization of three metal coordination species in the crystal structure of $Eu(L)_2(NO_3)_3$ and the terbium nitrate complex indicate that there exists a dynamic equilibrium between these species in solution (Chart 1), probably via the stereoselective solvolysis of the equatorial nitrate group in Eu1 to two methanol molecules in Eu2 or one water and one methanol molecule in Eu3.[63]

Cation (**a**) $[Eu(L)(NO_3)_2(MeOH)(H_2O)]^+$

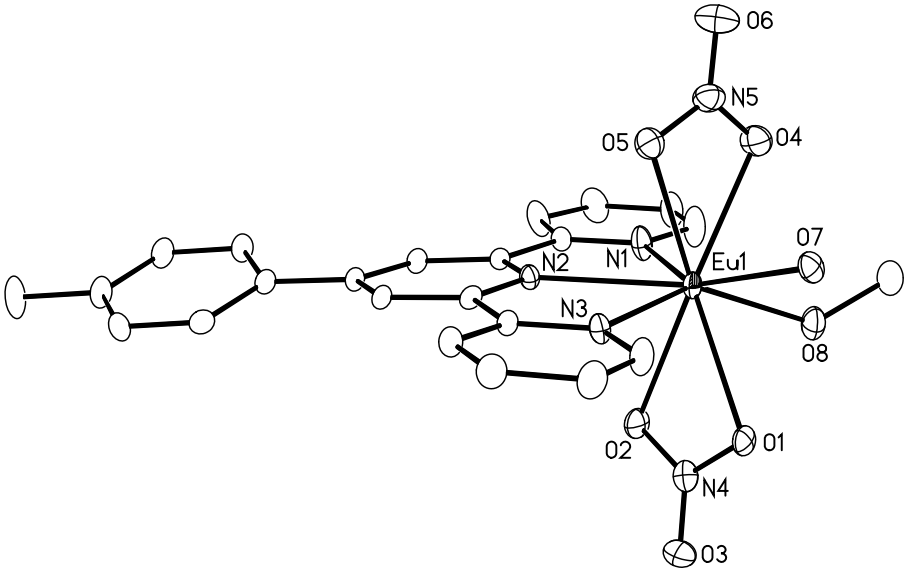

Molecule (**b**) $[Eu(L)(NO_3)_3(MeOH)]$

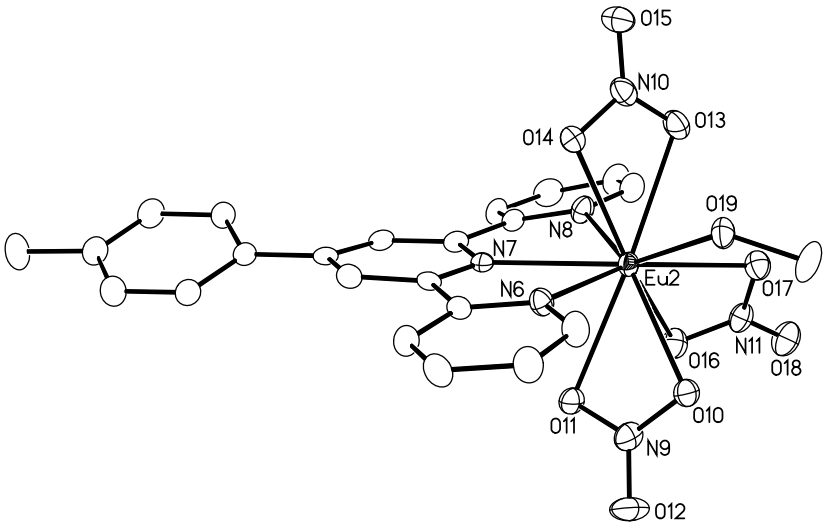

Cation (**c**) $[Eu(L)(NO_3)_2(MeOH)_2]^+$

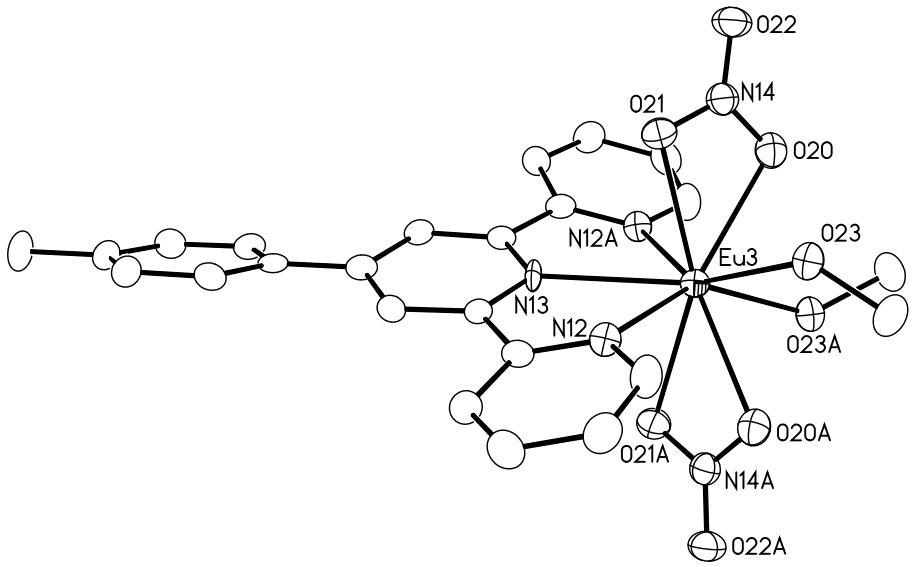

Figure 2.6. Crystal structure of $2[Eu(L)(NO_3)_2(MeOH)(H_2O)](NO_3)\cdot 2[Eu(L)(NO_3)_3(MeOH)]\cdot[Eu(L)(NO_3)_2(MeOH)_2](NO_3)\cdot 4MeOH$.

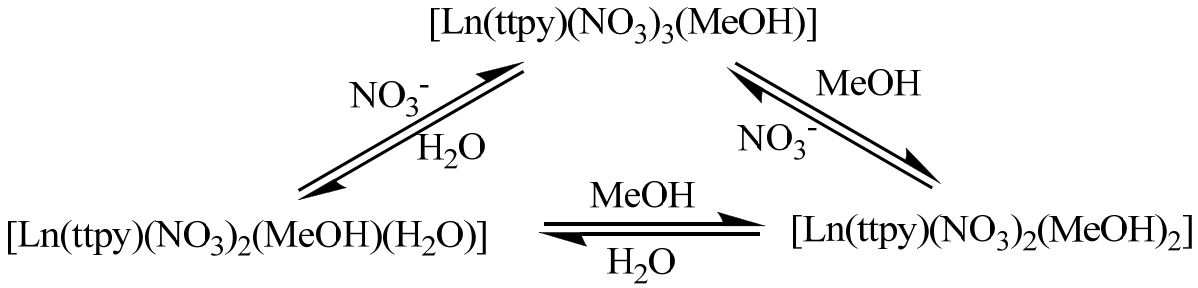

Chart 1 showing the dissociation pattern of europium nitrate ttrpy complex.

2.3.1.6 Crystal Structure of $2[Tb(L)(NO_3)_2(MeOH)(H_2O)](NO_3)\cdot 2[Tb(L)(NO_3)_3(MeOH)]\cdot [Tb(L)(NO_3)_2(MeOH)_2](NO_3)\cdot 4MeOH$

This compound crystallizes in the same way as the europium nitrate complex. It belongs to the *Pnna* space group. It is isostructural to the europium nitrate complex. The average distance between the Tb and 9 nitrogen atoms of the 3 ttrpy ligands is 2.52 Å. This mean distance of 2.52 Å is approximately 0.03 Å shorter compared to the europium analogue (2.55 Å). Figure 2.7 shows the crystal structure for this compound.

Cation (**a**) $[Tb(L)(NO_3)_2(MeOH)(H_2O)]^+$

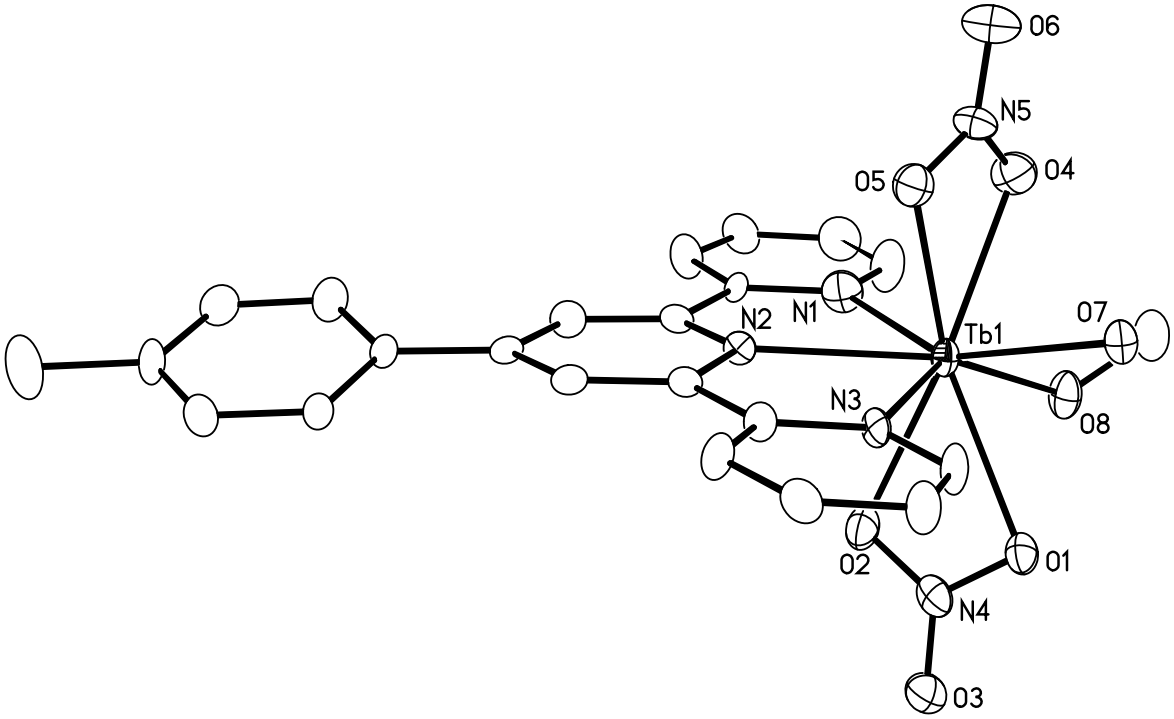

Molecule (**b**) $[Tb(L)(NO_3)_3(MeOH)]$

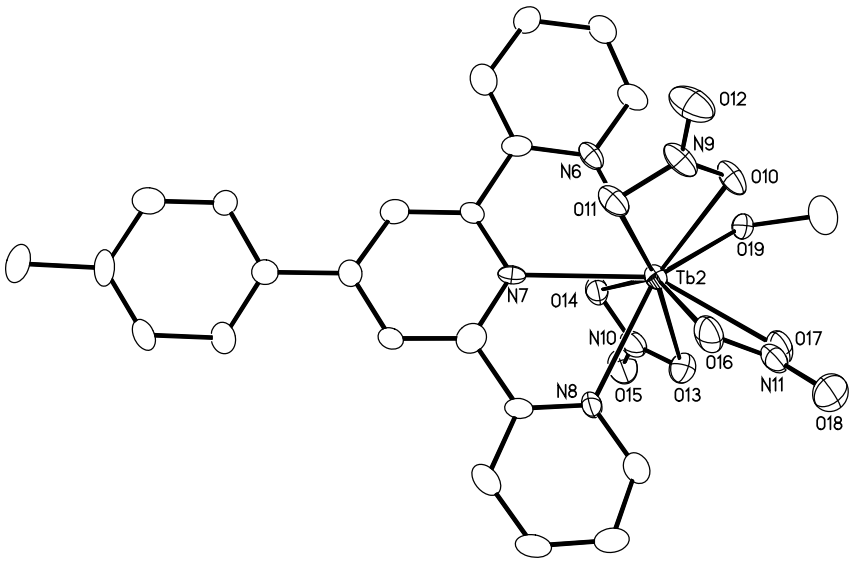

Cation (**c**) $[Tb(L)(NO_3)_2(MeOH)_2]^+$

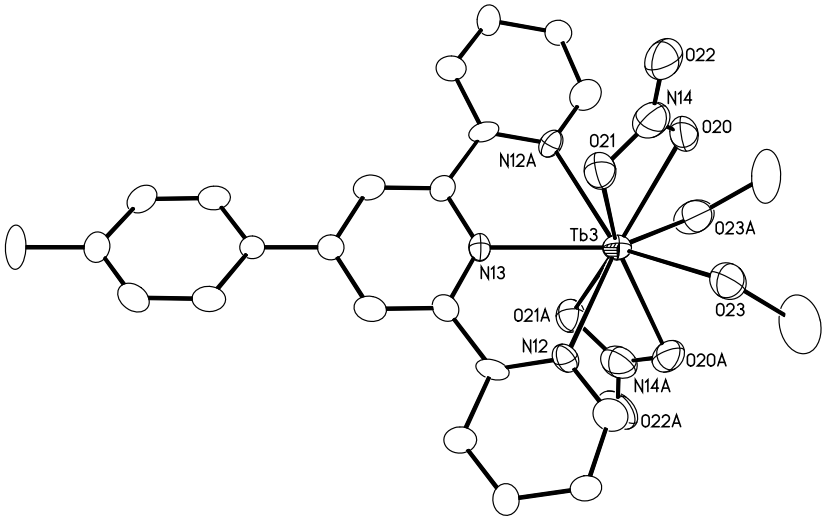

Figure 2.7. Crystal structure of $2[Tb(L)(NO_3)_2(MeOH)(H_2O)](NO_3)\cdot 2[Tb(L)(NO_3)_3(MeOH)]\cdot[Tb(L)(NO_3)_2(MeOH)_2](NO_3)\cdot 4MeOH$.

2.3.1.7 Crystal Structure of $Nd(L)(NO_3)_3MeOH{\cdot}MeOH$

This compound is completely different when compared to the europium and terbium analogues. It belongs to the triclinic system with a P-1 space group. It is a neutral compound with the coordination environment around neodymium being ten. Neodymium is bound to three nitrogens coming from one ttrpy and six oxygen atoms coming from three nitrates. The neodymium and the nitrogens from the ttrpy are almost in the same plane. It is also bounded to one molecule of methanol. The crystal structure of this compound is similar to that of the $[Ln(terpy)(NO_3)_3(EtOH)]$[63d] where Ln= Yb, Lu. The average distance of Yb-N is 2.455 Å and in Lu-N is 2.458 Å. The average distance between Nd-N in this complex is 2.590 Å, which is longer than the Ln-N distances in the $[Ln(terpy)(NO_3)_3(EtOH)]$. The distance between two neodymium atoms in adjacent molecules is 9.00 Å. Figure 2.8 is the crystal structure for this compound.

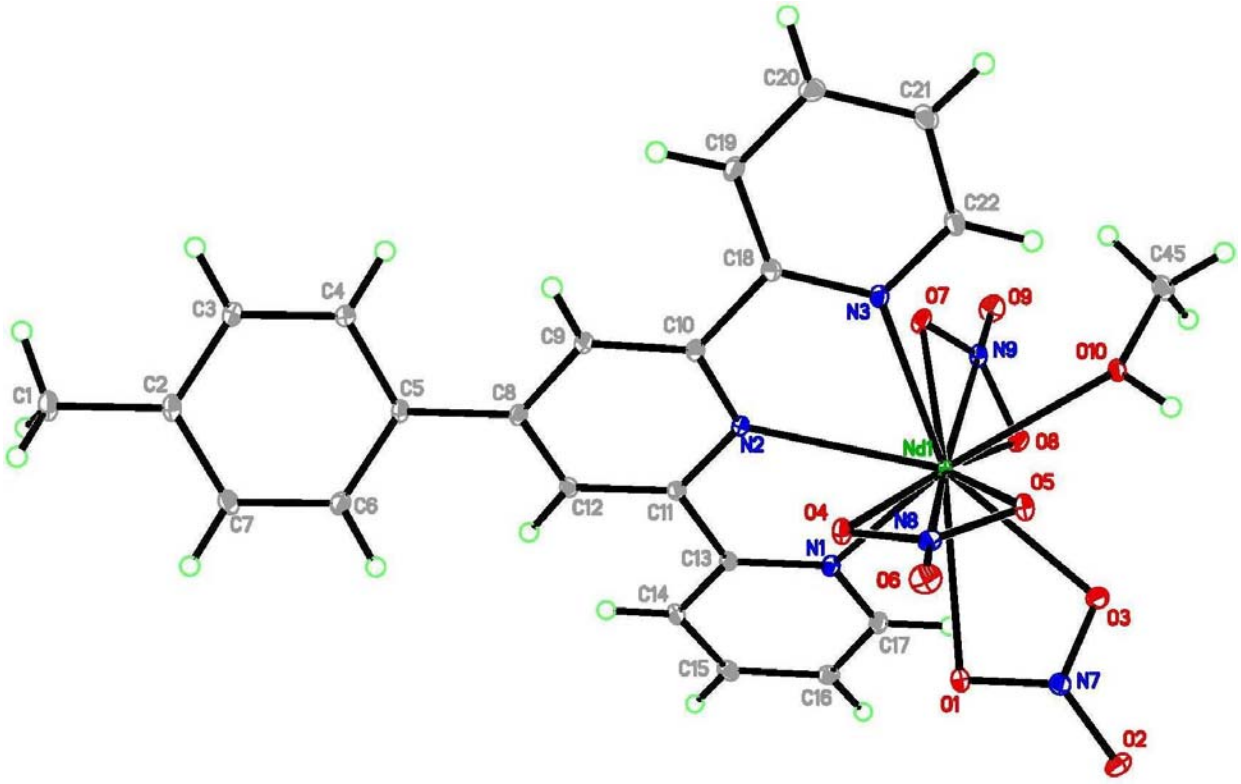

Figure 2.8. Crystal structure of $Nd(L)(NO_3)_3MeOH$.

X-ray data information for the lanthanide-ttrpy nitrate complexes is given in Table 2.3.

2.3.1.8 Crystal Structure of $[Eu(L)_3][ClO_4]_3.2MeCN$

When starting from a lanthanide salt with a weakly coordinating anion such as perchlorate, hygroscopic 1:2 and 1:3 complexes are isolated while the syntheses of the 1:1 complexes require the presence of a strongly coordinating anion such as nitrate, as observed for other terpyridine-like ligands.[50,54,61,64] Good elemental analysis results could not obtained for the complexes, as the solvation is difficult to control and depends on the drying conditions. We noted that the 1:3 complex is particularly difficult to isolate, even in the presence of a large excess of ligand because the 1:2 species is more

stable and less soluble and therefore crystallizes more easily than the 1:3 adduct. Upon complexation, changes in vibrational spectra are evident; in particular, the two ring vibrations of the pyridine moieties (1602 and 1566 cm^{-1} in the free ligand) are blue-shifted in the complexes by 11−14 and 3−5 cm^{-1} in both 1:2 and 1:3 complexes, respectively.[62] Although perchlorate is very weakly coordinating anion, examples are reported for both monodentate and bidentate modes of perchlorate in their metal complexes.[65] Vibrations for ionic perchlorate could be identified in the spectrum of the 1:3 complex, i.e. the two expected symmetrical vibrations at ~1110 and 625 cm^{-1}, while spectra of the 1:2 complexes reveal vibrational modes of monodentate perchlorate (622, 658, 924−929, 1007, 1094 cm^{-1}).[60,65]

In agreement with IR spectra results, the crystal structure in Figure 2.9 shows the compound to be composed of a cation, $[[Eu(ttrpy)_3]^{3+}$, three uncoordinated perchlorate anions and two solvent molecules. Each ligand adopts a *cis- cis-* conformation leading to a tridentate meridional coordination to the europium atom, which lies approximately in the plane defined by the three coordinating nitrogen atoms of each ligand (deviation: 0.05(3) Å). The individual aromatic rings are planar within experimental error and the main torsion of the ttrpy ligands is achieved by twisting about the interannular C-C bonds between the pyridine rings (9.63°, 57.27°; 26.28°, 50.73°; 20.91°, 25.35° for three ttrpy ligands, respectively), leading to helical twist of the tridentate ligands as found in the structures of $[Eu(terpy)_3]^{3+}$ (12°, 26°)[15b,32] and $[Eu_2(bismbzimpy)]^{6+}$ (average value: 23.3°).[66] The Eu(III) atom in $[Eu(ttrpy)_3]^{3+}$ is coordinated by nine heterocyclic nitrogen atoms giving a slightly distorted tricapped trigonal prismatic

coordination around the metal ion with six side pyridyl nitrogen atoms occupying the vertices of the prism and the three central pyridine nitrogen atoms occupying the capping positions and forming an equatorial plane containing the Eu(III) (deviation from the plane: 0.021(5) Å. As a result of the non-symmetric coordination of the three independent tridentate ligands to Eu(III), we observe three noncrystallographic pseudo-C_2 axes along the Eu-N(central pyridine) directions leading to a pseudo-D_3 symmetry for the cation $[Eu(ttrpy)_3]^{3+}$ as previously proposed for $[Eu(terpy)_3]^{3+}$ which also displays some distortions from pure D_3-symmetry.[32] The helical wrapping of the three ttrpy ligands around the C_3 axis in $[Eu(ttrpy)_3]^{3+}$ leads to the observation of the closely packed cylindrical pseudo-D_3 $[Eu(ttrpy)_3]^{3+}$ cations columns along the a direction; the resulting interstitial channels being occupied by ClO_4^- and MeCN molecules lying close to a 3-fold screw axis along the c direction. The geometries of the individual pyridine rings are quite normal and the Eu-N bond lengths, which lie in the range 2.55-2.62 Å (e.s.d. 0.002), are typical of those already observed for lanthanide complexes.[15,32,50,54,61,66] Yongjun et al. also found the perchlorate complex of europium with 2,6-bis(1,2,3-triazol-4-yl)pyridines as 9 cooridinate.[67]

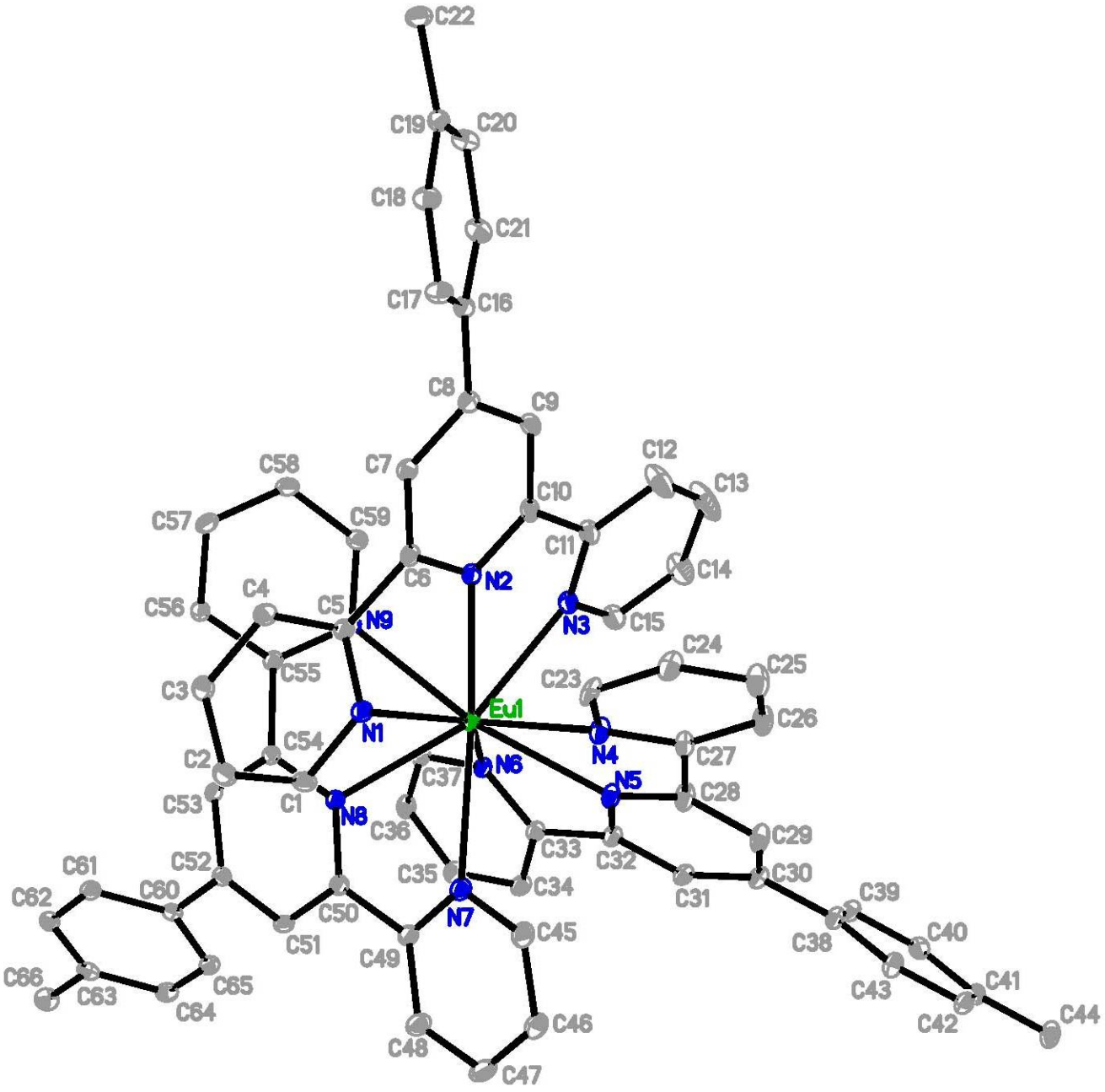

Figure 2.9. Crystal structure of $[Eu(L)_3](ClO_4)_3$.

2.3.1.9 Crystal Structure of $[Tb(L)_2(ClO_4)_2(H_2O)](ClO_4)\cdot MeOH\cdot 0.5Et_2O$

The structure of this compound (Figure 2.10) is composed of a cation, $[Tb(ttrpy)_2(ClO_4)_2(H_2O)]^+$, one uncoordinated perchlorate anion, one molecule of methanol and half a molecule of Et_2O per formula unit. The uncoordinated diethyl ether molecule is disordered in two positions with occupancy of ~50%. The Tb^{III} atom in the cation $[Tb(ttrpy)_2(ClO_4)_2(H_2O)]^+$ is nine-coordinated by two meridional tridentate ttrpy ligands, one molecule of water, and two perchlorate anions, leading to a low-symmetry coordination site around the metal ion. The two ligands are wrapped around the metal ion in a helical way, as was observed for $[Lu(L^1)_2(MeOH)(H_2O)]^{3+}$.[68] The cations were held together by multiple weak C-H···O interactions between ttrpy and ClO_4 anions.

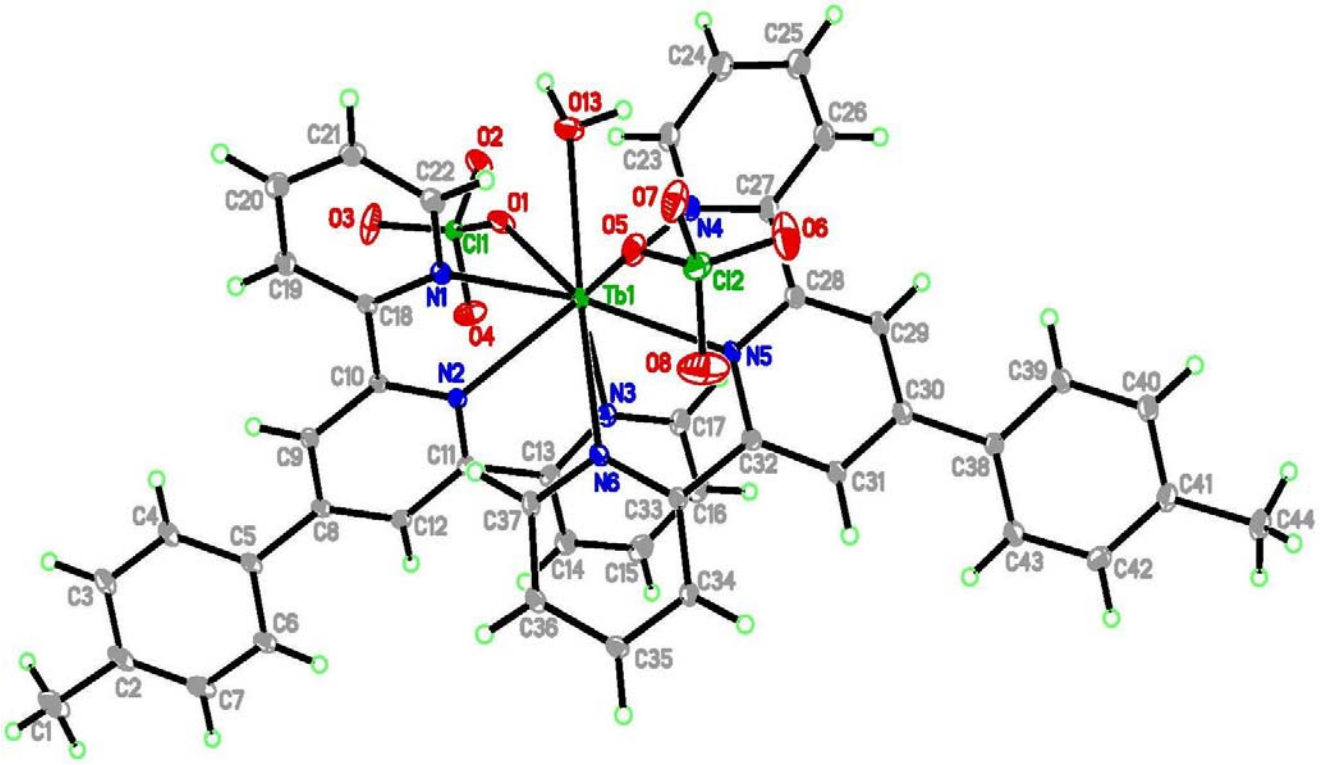

Figure 2.10. Crystal structure of $[Tb(L)_2(ClO_4)_2(H_2O)](ClO_4)\cdot MeOH\cdot 0.5Et_2O$.

2.3.1.10 Crystal Structure of $[Er(L)_2(ClO_4)(MeOH)](ClO_4)_2\cdot 2MeOH$

This is a monoclinic system with P2(1)/ C space group. Erbium is coordinated to six nitrogen atoms, three from each ttrpy molecule and to the oxygen atom of the perchlorate ion. The perchlorate ion was coordinated in a tetrahedral manner with one oxygen atom to the Er metal. There is one molecule of methanol solvent in the inner coordination sphere. The average distance between Er and the six nitrogens from the two ttrpy ligands is 2.46 Å. Figure 2.11 shows the crystal structure.

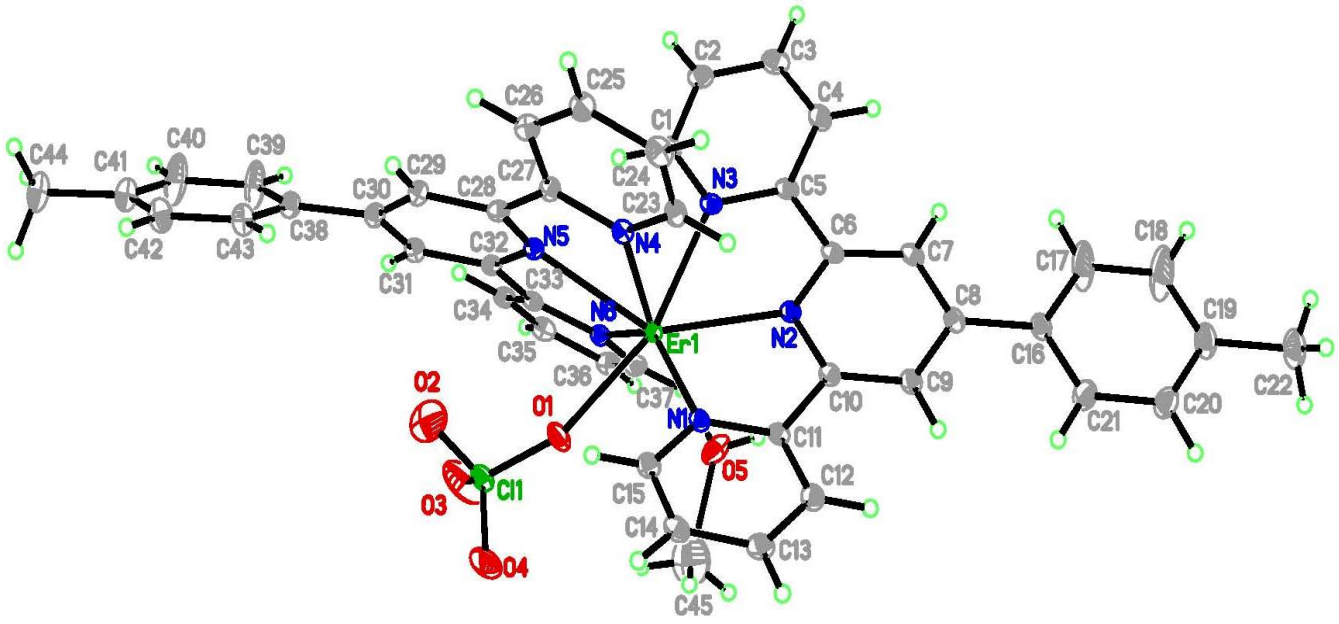

Figure 2.11 Crystal structure of $[Er(L)_2(ClO_4)(MeOH)](ClO_4)_2 \cdot 2MeOH$.

2.3.1.11 Crystal Structure of $[Nd(L)_2(ClO_4)_2(H_2O)](ClO_4) \cdot MeOH \cdot 0.5Et_2O$

This structure is the same as in the analogous europium and terbium perchlorate complexes. It belongs to the triclinic system with a P-1 space group. Neodymium is coordinated to six nitrogens from the two molecules of ttrpy and two oxygen atoms from two perchlorate ions making the coordination number 8. The perchlorate ions are coordinated to the central neodymium metal in tetrahedral fashion with one oxygen atom. The average Nd-N distance is 2.59 Å. Figure 2.12 shows the crystal structure.

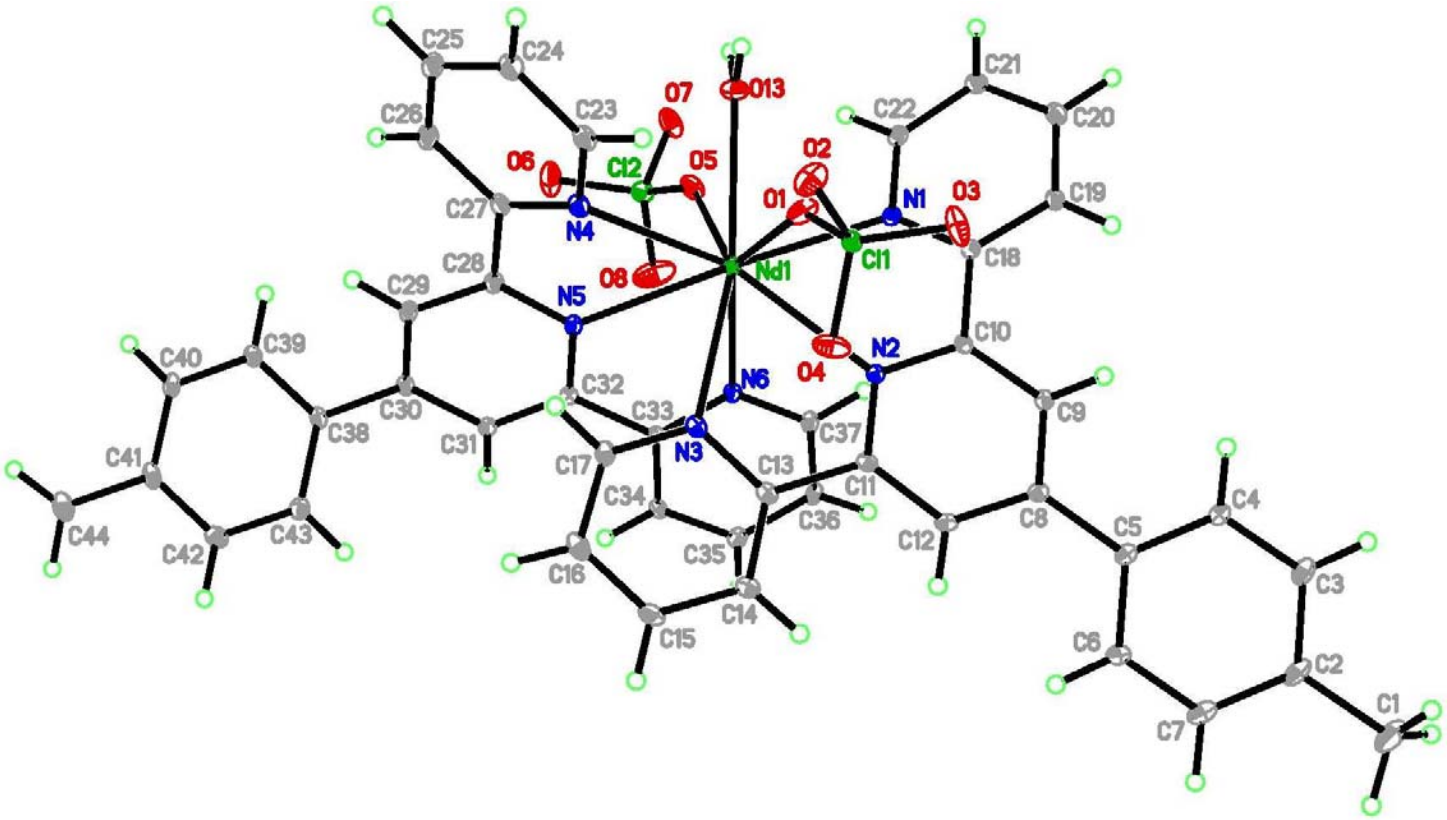

Figure 2.12. Crystal structure of $[Nd(L)_2(ClO_4)_2(H_2O)](ClO_4)\cdot MeOH\cdot 0.5Et_2O$.

X-ray data for the lanthanide-ttrpy perchlorate complexes is given in Table 2.4.

2.3.1.12 Crystal Structure of $Eu(hfa)_3(L).(THF)$

Most of the ternary lanthanide-β-diketonates-terpyridine complexes, Ln(β-diketonate)$_3$(tpy), reported were synthesized by one-pot reaction from the lanthanide salt, β-diketone, and the terpyridine-like ligand in the presence of a suitable base.[28,44] However, adventitious hydrolysis may result in unexpected lanthanide oxo/hydroxo complexes.[69] Another procedure is using the reaction of neutral Ln(β-diketonate)$_3$ with the terpyridine analogues in a dried organic solvent,[70] which has successfully produced a number of organic base adducts with various lanthanide β-diketonates. Thus, the reaction of $Eu(hfa)_3$ with ttrpy in dry THF affords $Eu(hfa)_3(ttpy)(THF)$ in high yield. The

coordination of $Eu(hfa)_3(ttpy)(THF)$ features three hfa and one ttrpy ligand. The coordination polyhedron may be best described as a distorted square antiprism monocapped by the central pyridine N atom [N(2)]. The Eu–O(hfa) distances of $Eu(hfa)_3(ttrpy)(THF)$ range from 2.3747(19) Å to 2.4707(19) Å. These distances are within the range reported for similar complexes.[28,44] The ttrpy ligand is nearly coplanar. The mean Eu–N bond distance is 2.574 Å, consistent with previously reported lanthanide- terpyridine complexes.[50,54,61] Figure 2.13 shows the crystal structure.

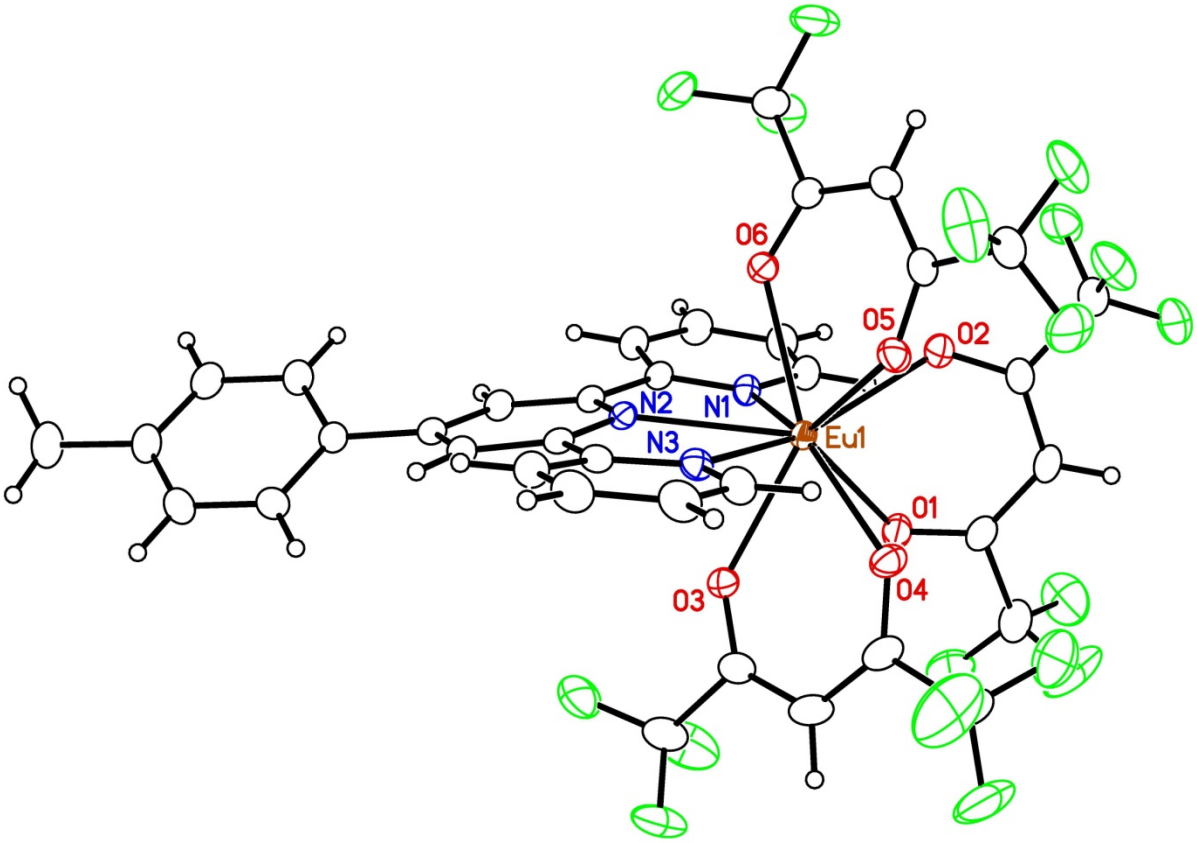

Figure 2.13. Crystal structure of $Eu(hfa)_3(L).(THF)$.

2.3.1.13 Crystal Structure of $Tb(hfa)_3(ttrpy).(THF)$

This structure is similar to that of $Eu(hfa)_3(L)$. The average Tb-N and Tb-O distances are 2.54 Å is 2.40 Å, respectively. The average distance of Tb-N and Tb-O distances are smaller when compared to Eu-N and Eu-O distances in $Eu(hfa)_3(L)$. Figure 2.14 shows the crystal structure.

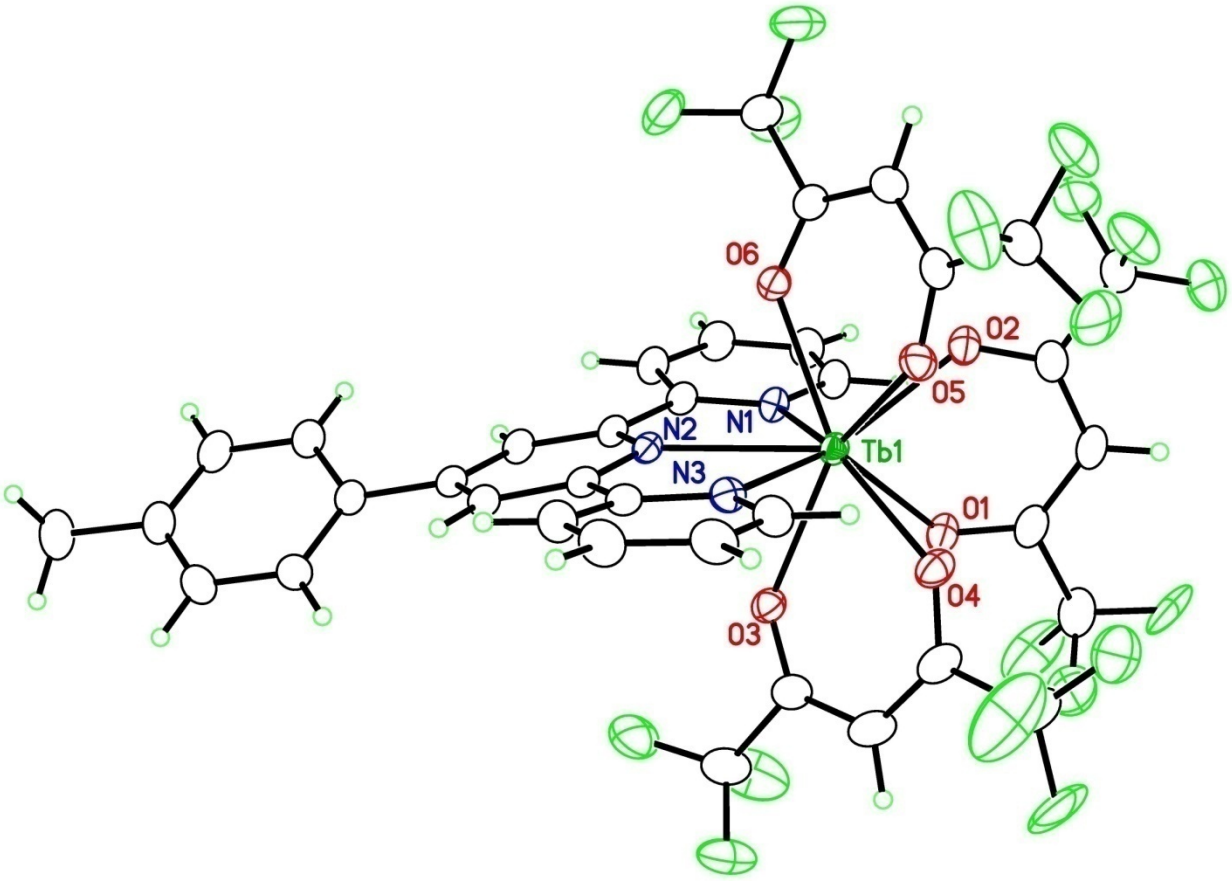

Figure 2.14. Crystal structure of $Tb(hfa)_3(L)$.

X-ray data for the $Ln(hfa)_3(ttrpy)$ complexes is given in Table 2.5.

Table 2.2 X-ray crystal structure information of lanthanide-ttrpy chloride complexes.

	$[Eu(ttrpy)_2Cl_2]Cl$	$[Tb(ttrpy)_2Cl_2]Cl$	$[Er(ttrpy)_2Cl_2]Cl$	$[Nd(ttrpy)_2Cl_2]Cl$
Formula	$[Eu(C_{22}H_{17}N_3)_2Cl_2]Cl\cdot 2(CH_3OH)$	C46 H42 Cl3 N6 O2 Tb	C44 H36 Cl3 Er N6, 2(C H3 O H)	C48 H48 Cl6 N6 Nd2 O4
FW	955.14	976.13	984.47	1274.10
Color	clear prism	Colorless rectangle	Pale pink	White block
Crystal system	triclinic	Triclinic	Triclinic	Triclinic
space group	P-1	P-1	P -1	P -1
a (Å)	12.0702(2)	12.0682(6)	12.0515(5)	8.8071(4)
b (Å)	12.5308(2)	12.5461(6)	12.5263(5)	12.0066(5)
c (Å)	13.6326(2)	13.6523(7)	13.6389(6)	13.0628(6)
α (deg)	85.0630(10)	84.9800(10)	84.9370(10)	104.4180(10)
β (deg)	87.0820(10)	87.4840(10)	87.8050(10)	97.5540(10)
γ (deg)	87.8400(10)	87.8200(10)°.	87.8210(10)	107.4280(10)°.
V (Å^3)	2050.46(6)	2055.95(18)	2048.16(15)	1244.25(10)
Z	2	2	2	1
ρ (g·cm^{-3})	1.547	1.577	1.596	1.700
T	100(2) K	100(2) K	100(2) K	100(2) K
λ(Å)	0.71073	0.71073	0.71073	0.71073
F(000)	964	984	990	632
θ (deg)	2.63-30.54	1.50 - 27.56	1.5- 26.77	1.65 - 26.37
Index ranges	-17 ≤*h* ≤17	-15≤h≤15	-15≤h≤15	-11≤h≤11
	-17 ≤*k* ≤17	-16≤k≤16	-15≤k≤15	-15≤k≤15
	-19 ≤ l≤19	-17≤l≤17	-17≤l≤17	-16≤l≤16
Data / restraints / parameters	12426 / 0 / 558	9427 / 4 / 653	8736 / 3 / 535	5079 / 86 / 329
GOF on F^2	1.066	1.115	1.022	1.102
R_1, ωR_2 [*I>2□ (I)*]	0.0333, 0.0900	0.0171, 0.0451	0.0186, 0.0482	0.0256, 0.0699
R_1, ωR_2 (all data)	0.0379, 0.0935	0.0179, 0.0456	0.0202, 0.0491	0.0279, 0.0716
Largest diff. peak and hole (eÅ^3)	4.525 and -1.213	1.041 and -0.645	1.135 and -0.658	1.805 and -0.587

Table 2.3 X-ray crystal structure information of lanthanide-ttrpy nitrate complexes.

	$[Eu(ttrpy)_2NO_3)_2]NO_3$	$[Tb(ttrpy)_2(NO_3)_3]NO_3$	$Nd(ttrpy)(NO_3)_3$
Formula	$C_{120}\ H_{129}\ Eu_5\ N_{30}\ O_{57}$	$C_{60}\ H_{64.50}\ N_{15}\ O_{28.50}\ Tb_{2.50}$	$C_{24}\ H_{25}\ N_6\ Nd\ O_{11}$
FW	3663.33	1849.07	717.74
Color	Colorless block	Colorless block	Colorless block
Crystal system	Orthorhombic	Orthorhombic	Triclinic
space group	P n n a	P n n a	P -1
a (Å)	26.8605(8)	26.8036(14)	9.6286(4)
b (Å)	34.8748(10)	34.5998(18)	11.8820(5)
c (Å)	14.8630(5)	14.8443(8)	24.0264(11)
α (deg)	90	90	87.2140(10)
β (deg)	90	90	89.3950(10
γ (deg)	90	90	89.0600(10)
V (Å^3)	13923.0(7)	13766.6(13)	2745.0(2)
Z	4	8	4
ρ (g·cm^{-3})	1.748	1.784	1.737
T	100(2) K	100(2) K	100(2) K
λ(Å)	0.71073	0.71073	0.71073
F(000)	7320	7360	1436
θ (deg)	1.49- 25.30	1.18 - 25.35	1.70 -26.94
Index ranges	-31≤h≤32	-32≤h≤32	-12≤h≤12
	-28≤k≤41	-41≤k≤41	-15≤k≤15
	-17≤l≤17	-17≤l≤17	-30≤l≤30
Data / restraints / parameters	12674 / 4 / 989	12602 / 1 / 967	11879 / 0 / 783
GOF on F^2	1.042	1.347	1.046
R_1, ωR_2 [$I>2\sigma(I)$]	0.0322, 0.1139	0.0613, 0.1708	0.0190, 0.0479
R_1, ωR_2 (all data)	0.0365, 0.1186	0.0801, 0.1797	0.0226, 0.0501
Largest diff. peak and hole (eÅ^3)	4.103 and -2.642	3.208 and -2.584	0.753 and -0.440

Table 2.4. X-ray crystal structure information of the lanthanide-ttrpy perchlorate complexes.

	$[Eu(ttrpy)_3](ClO_4)_3$	$[Tb(ttrpy)_2(ClO_4)]ClO_4$	$[Er(L)_2(ClO_4)_2]ClO_4$	$[Nd(ttrpy)_2(ClO_4)_2]ClO_4$
Formula	$C_{140}\ H_{114}\ C_{l6}\ Eu_2\ N_{22}\ O_{24}$	$C_{47}\ H_{45}\ Cl_3\ N_6\ O_{14.50}\ Tb$	$C_{47}\ H_{46}\ Cl_3\ Er\ N_6\ O_{15}$	$C_{47}\ H_{45}\ Cl_3\ N_6\ Nd\ O_{14.50}$
FW	3005.15	1191.16	1208.51	1176.48
Color	Colorless block	Colorless block	Pink plate	colorless block
Crystal system	Triclinic	Triclinic	Monoclinic	Triclinic
space group	P-1	P -1	P 2(1)/c	P -1
a (Å)	9.4663(5)	11.7062(8)	16.1343(11)	11.8056(5)
b (Å)	18.6476(10)	14.7549(10)	14.4805(10)	14.7399(7)
c (Å)	19.4888(10)	15.2993(10)	21.0575(14)	15.2695(7)
α (deg)	104.1340(10)	89.6170(10)	90	89.5490(10)
β (deg)	92.4600(10)	74.8130(10)	96.5920(10)	74.6770(10)
γ (deg)	98.5220(10)	69.2280(10)	90	69.4720(10)
V (Å^3)	3288.0(3)	2373.6(3)	4887.2(6)	2389.32(19)
Z	1	2	4	2
ρ (g·cm^{-3})	1.518	1.667	1.642	1.635
T	100(2) K	100(2) K	100(2) K	100(2) K
λ(Å)	0.71073	0.71073	0.71073	0.71073
F(000)	1528	1202	2436	1192
θ (deg)	1.08 - 26.74	1.39 -26.53	1.27 -26.00	1.39 - 26.81°.
Index ranges	-11≤h≤11	-14≤h≤14	-19≤h≤19	-14≤h≤14
	-23≤k≤23	-18≤k≤18	-17≤k≤17	-18≤k≤18
	-24≤l≤24	-19≤l≤19	-25≤l≤25	-19≤l≤19
Data / restraints / parameters	13926 / 59 / 899	9857 / 8 / 679	9587 / 27 / 653	10207 / 8 / 680
GOF on F^2	1.084	1.073	1.026	1.017
R_1, ωR_2 [$I>2\sigma(I)$]	0.0319, 0.0751	0.0411, 0.1045	0.0440, 0.1178	0.0339, 0.0733
R_1, ωR_2 (all data)	0.0348, 0.0763	0.0459, 0.1082	0.0501, 0.1243	0.0450, 0.0779
Largest diff. peak and hole (eÅ^3)	1.561 and -1.029	2.448 and -1.751	2.564 and -1.264	1.362 and -0.877

Table 2.5. X- ray crystal data for $Ln(hfa)_3(ttrpy)$ complexes.

	$Eu(hfa)_3(ttrpy)\cdot THF$	$Tb(hfa)_3(ttrpy)\cdot THF$
Formula	C41 H28 Eu F18 N3 O7	C41 H28 F18 N3 O7 Tb
FW	1168.62	1175.58
Color	Colorless block	Colorless block
Crystal system	Triclinic	Triclinic
space group	P -1	P -1
a (Å)	8.8276(6)	8.8588(11)
b (Å)	16.0224(10)	15.963(2)
c (Å)	16.3177(10)	16.247(2)
α (deg)	74.7380(10)	104.9540(10)
β (deg)	80.3840(10)	99.841(2)
γ (deg)	89.8010(10)	90.023(2)
V ($Å^3$)	2193.3(2)	2184.7(5)
Z	2	2
ρ ($g\cdot cm^{-3}$)	1.770	1.787
T	100(2) K	100(2) K
λ(Å)	0.71073	0.71073
F(000)	1152	1156
θ (deg)	1.31- 27.62	1.60 - 27.16
Index ranges	-11≤h≤11	-11≤h≤11
	-20≤k≤20	-20≤k≤20
	-20≤l≤21	-20≤l≤20
Data / restraints / parameters	10165 / 83 / 662	9673 / 60 / 663
GOF on F^2	1.025	1.064
R_1, ωR_2 [$I>2\sigma(I)$]	0.0270, 0.0660	0.0262, 0.0668
R_1, ωR_2 (all data)	0.0294, 0.0675	0.0266, 0.0671
Largest diff. peak and hole ($eÅ^3$)	1.275 and -1.000	2.245 and -0.864

2.3.2 Infrared Spectra

The Infrared spectra values are given in Table 2.6 and the spectra are in Figures. 2.15-2.18. In the free ttrpy ligand (L), the $\upsilon_{C=C}$ and $\upsilon_{C=N}$ values occurred at 1566 cm^{-1} and 1602 cm^{-1}, respectively. In the lanthanide-ttrpy complexes the $\upsilon_{C=C}$ stretching frequencies range from 1565-1580 cm^{-1}. This indicates that the complexes are formed between the ligand and the lanthanides. The C=N stretch occurred at 1602 cm^{-1} in the free ligand whereas in the complexes this C=N stretch varied from 1600-1618 cm^{-1}. The C=N stretch is increased in almost all the complexes except in the $[Cl_2Nd(L)(\mu\text{-}Cl)_2Nd(L)Cl_2]$, wherein it was decreased by 1 cm^{-1}. A similar situation was observed in the complex of cerium with bipyrimidine.[71] The general rise in this frequency is due to complexation.[72] Sigma bonding (as in protonation) causes a rise in the frequency while π-bonding causes a decrease.[73] The small rise in C=N stretching frequency in these complexes compared to those of Pt, Pd, Os and Rh can be attributed to weaker sigma bonding.[74] In all the nitrate complexes except $Er(L)(NO_3)_3$ there were peaks around 842 cm^{-1} and a broad peak within 1400-1550 cm^{-1} apart from peaks within 1700-1800 cm^{-1}. In all the nitrate complexes except erbium complex, the peaks between 1700-1800 cm^{-1} are doubly split by more than 25 cm^{-1} apart within the doublet, which can be ascribed to bidentate coordination.[33] If the peaks in this region of nitrate complexes were a single peak, that would indicate that the coordination of the nitrate is monodentate. In erbium nitrate complex, no splitting of peaks in the 1700-1800 cm^{-1} region was observed. This indicates monodentate coordination of the nitrate. There is also a narrow peak at 1384 cm^{-1}, which indicates that nitrate could be ionic in nature.[75]

The perchlorate ion can coordinate in bidentate or monodentate, or does not coordinate and instead exists as a counter ion. It is very hard to distinguish between purely bidentate, and a mixture of ionic and monodentate species, because same number of bands would be observed in IR spectra.[76] If the peak at 930 cm^{-1} is absent or very weak, the coordinated perchlorate peaks may be ruled out.[76] This situation is observed in the case of $[Eu(L)_3](ClO_4)_3$. There is no 930 cm^{-1} peak in this compound. It is also confirmed by the X-ray structure for this compound. It shows that all three perchlorate ions act as counterions. In $[Tb(L_2)(ClO_4)_2]ClO_4$, there was a weak peak at 930 cm^{-1}, which indicates that there were no perchlorate ions coordinated to terbium. But the peak at 1094 was split into two. This shows that it has coordinated perchlorate ions. This is confirmed by the presence of two perchlorates coordinated through oxygen in the X-ray crystal structure. In erbium and neodymium perchlorate compounds of the ttrpy ligand, there is a clear peak at 930 cm^{-1}, clearly indicating ionic perchlorates. They also show a peak splitting at about 1100 cm^{-1}, which can be ascribed to coordinated perchlorate.[15b] The υ_{Ln-Cl} usually occur around 240-220 cm^{-1} which is beyond the detection of our instrument.[77,78] But the C=N and C=C stretch clearly indicates that the complexes of lanthanides with chlorides are formed. A broad peak is observed in some of the complexes between 3000-3500 cm^{-1}, which indicates the presence of moisture or solvent molecules coordinated to the lanthanide.[79]

Table 2.6 IR spectral data for all the lanthanide complexes studied.

Compound's name	$\upsilon_{C=C}$, cm^{-1}	$\upsilon_{C=N}$, cm^{-1}	$\upsilon_{Cl-O(ClO4)}$, cm^{-1}	$\upsilon_{N-O(NO3)}$, cm^{-1}	$\upsilon_{C-F,}$ cm^{-1}	$\upsilon_{C=O}$, cm^{-1}
ttrpy	1566	1602				
$[Eu(L)_2Cl_2]Cl$	1572	1611				
$[Tb(L)_2Cl_2]Cl$	1572	1613				
$[Er(L)_2Cl_2]Cl$	1572	1615				
$[Nd(L)_2Cl_2]Cl$	1570	1600				
$[Eu(L)_2(NO_3)_2]NO_3$	1571	1606		1740, 1781		
$[Tb(L)_2(NO_3)_2]NO_3$	1572	1607		1744, 1784		
$Er(L)(NO_3)_3$	1575	1618		1769		
$Nd(L)(NO_3)_3$	1570	1605		1736, 1777		
$[Eu(L)_3](ClO_4)_3$	1565	1611	1092, 622			
$[Tb(L)_2(ClO_4)_2]ClO_4$	1570	1616	1094, 622			
$[Er(L)_2(ClO_4)](ClO_4)_2$	1574	1615	1111, 930, 626			
$[Nd(L)_2(ClO_4)_2]ClO_4$	1574	1609	1094, 931, 624			
$Eu(hfa)_3$					1258-1145	1650
$Eu(hfa)_3(L)$	1575	1612			1255-1142	1654
$Tb(hfa)_3$					1260-1133	1651
$Tb(hfa)_3(L)$	1580	1613			1263-1139	1656

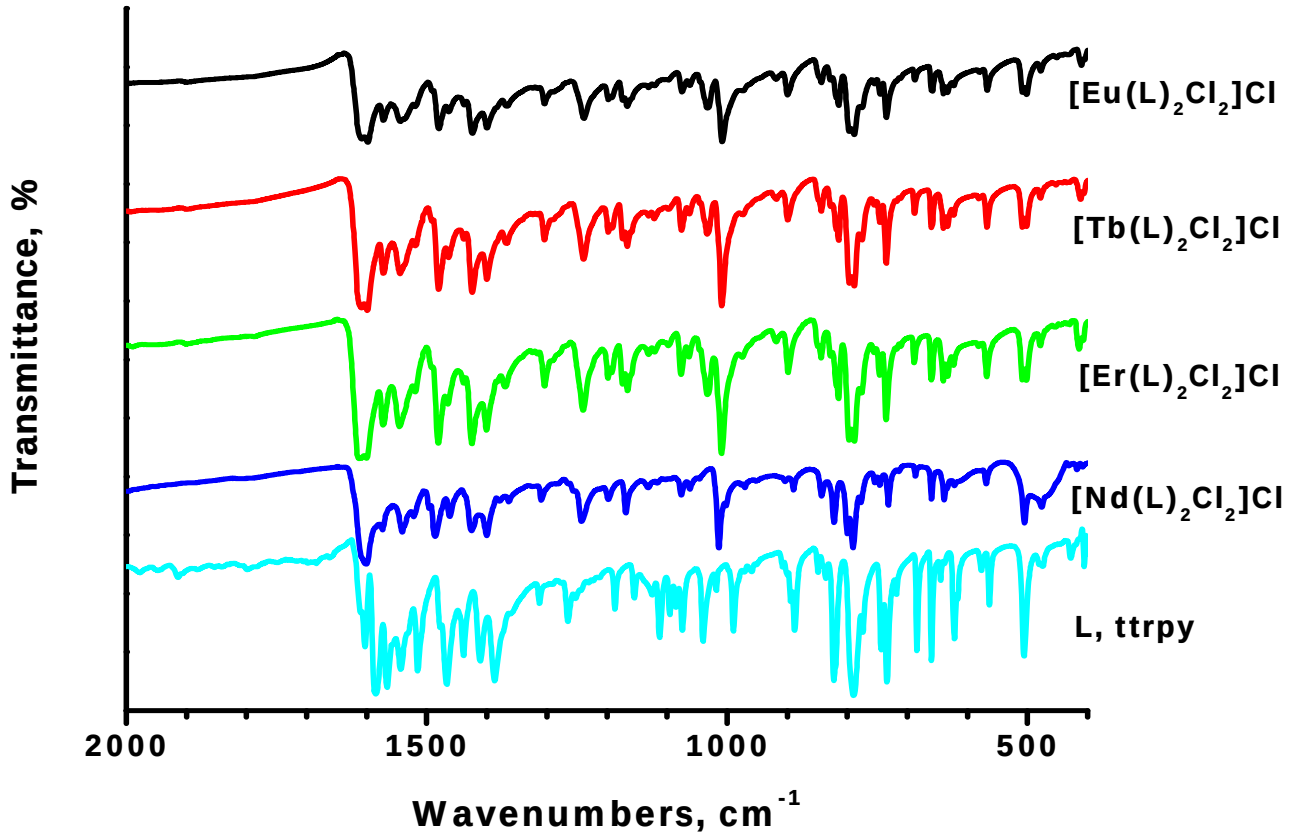

Figure 2.15. IR spectra of the ligand, ttrpy and its complexes with lanthanide chlorides.

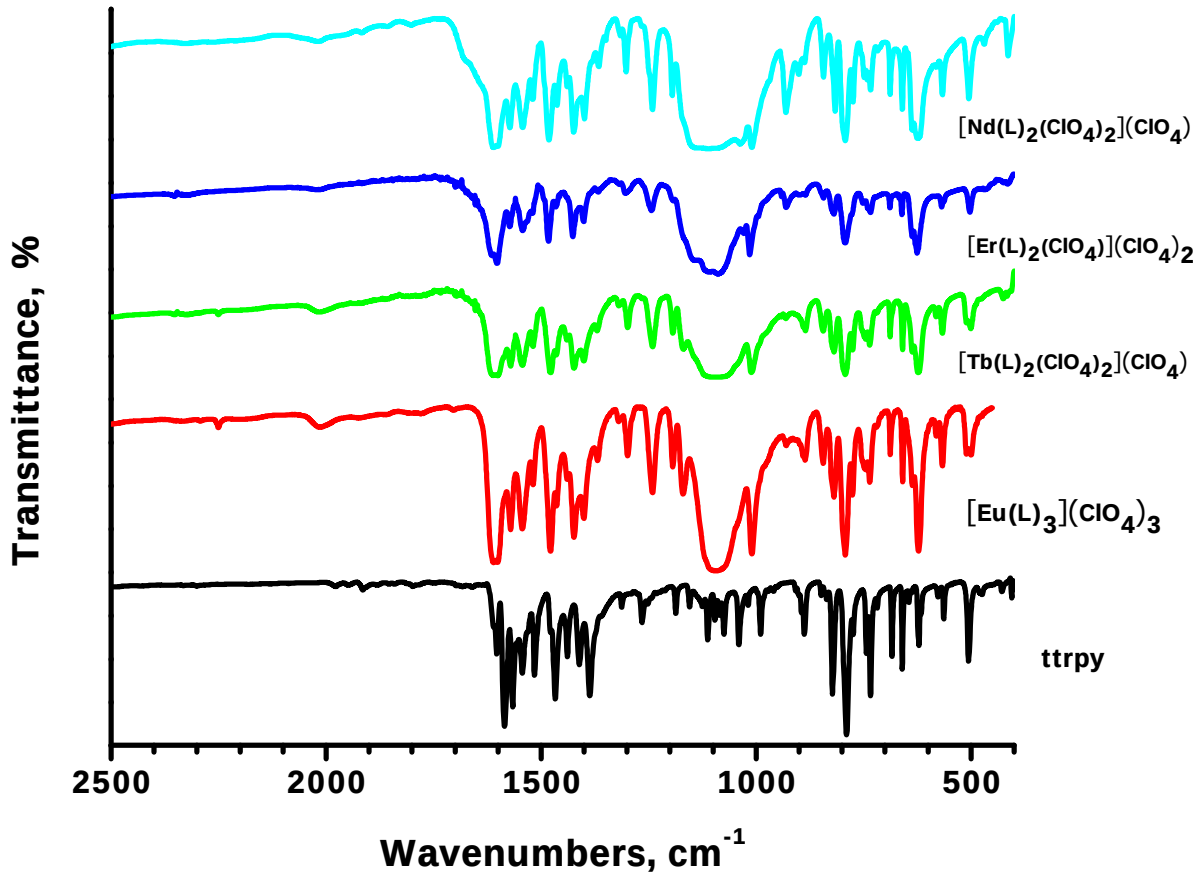

Figure 2.16. IR spectra of the ligand, ttrpy and its complexes with lanthanide perchlorates.

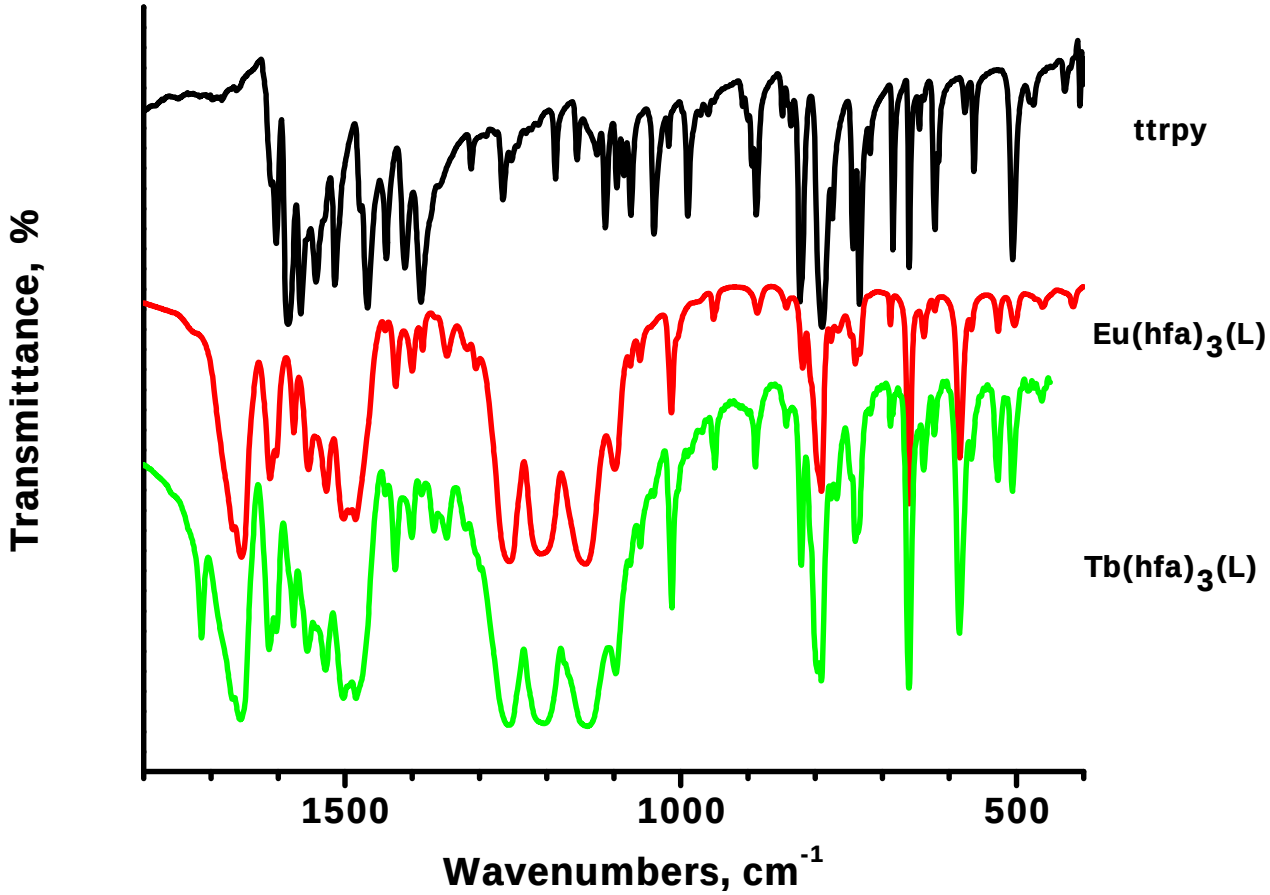

Figure 2.17. IR spectra of the ligand, ttrpy and its complexes with $Eu(hfa)_3$ and $Tb(hfa)_3$.

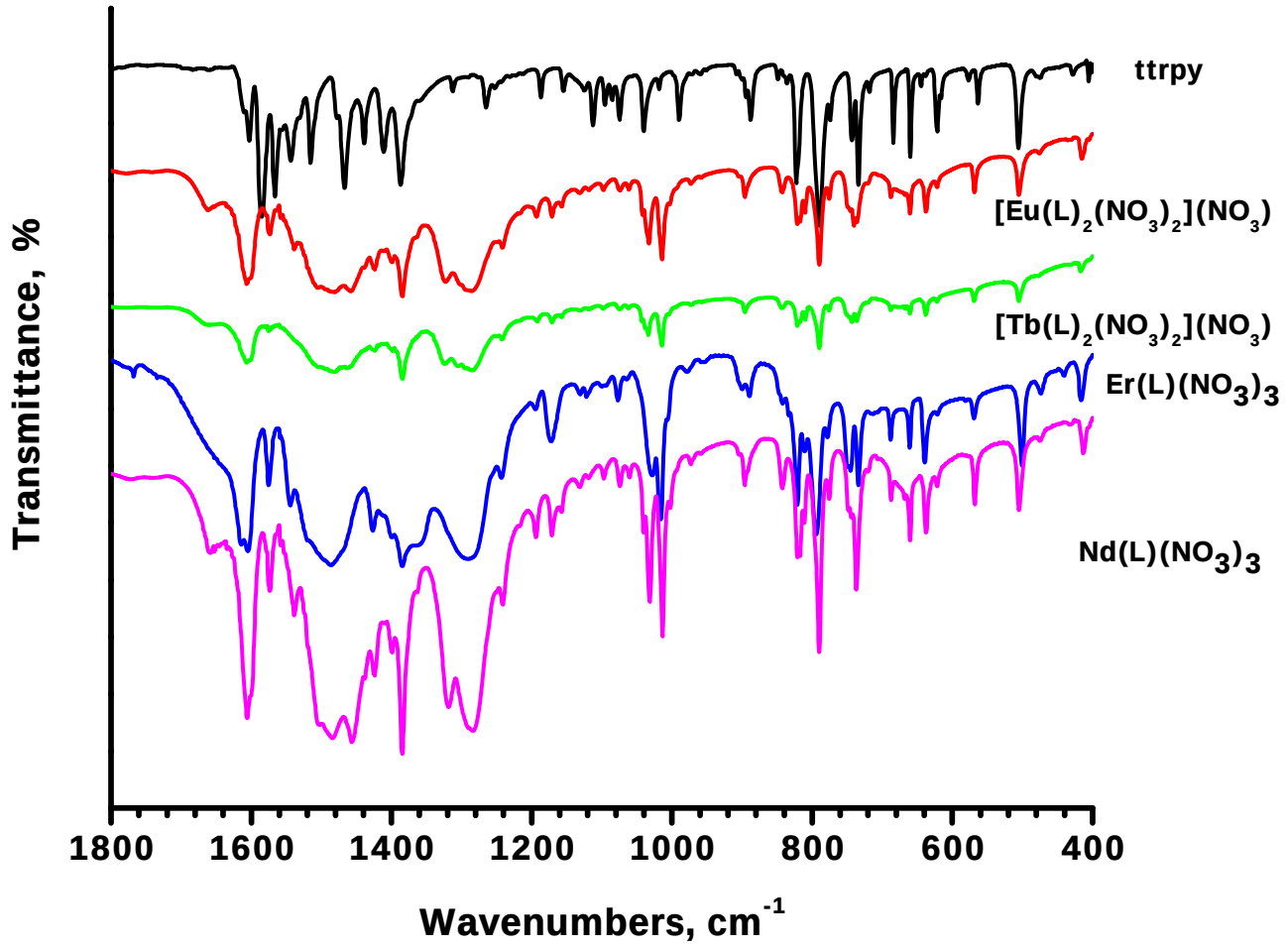

Figure 2.18. IR spectra of the ligand, ttrpy and its complexes with lanthanide nitrate.

2.3.3 UV-Vis Studies

The ligand, ttrpy shows the π-π^* transitions occurring in the UV region. All the complexes in solution of methanol show the same transitions (Figures 2.19-2.22). No f-f transitions due to the lanthanides are observed except at higher concentration very weak transitions in the $[Er(L)_2(NO_3)_2]NO_3$. The f-f transitions are forbidden due to Laporte selection rule. Their molar extinction coefficients will be less than 10 $M^{-1}cm^{-1}$.[80] Zhang et al. have studied the pyridine-2,6-dicarboxamide compounds of several lanthanides.[81] They found that the UV absorption peaks of the free ligand did not change upon complexation, implying that the conjugation of the planar ligand did not change significantly. Similar observations are seen in all of the complexes herein. The spectral shapes of the lanthanide complexes in methanol are similar to that of free ligand in methanol, suggesting the coordination of the Ln^{3+} ions does not have significant influence on the π-π^* state energy.[79] The λ_{max} values are almost equal to the free ligand values except in few cases where they are slightly shifted by 395 cm^{-1} to 1250 cm^{-1}. This indicates that the conjugate of the planar ligand did not undergo drastic changes. These λ_{max} and the corresponding ε values are given in Table 2.7. The molar absorption coefficients values of the lanthanide complexes with the ttrpy ligand are higher than that of the free ligand. For example, ε value of all the lanthanide chloride complexes of ttrpy are almost twice to that of the ttrpy itself. This is because the complexes have two molecules of ttrpy coordinated to them. This is also resulted in highest quantum yield in $[Eu(ttrpy)_3](ClO_4)_3$ which has three molecules of ttrpy coordinated to Eu^{3+}. In case of bis(benzmidazolyl) pyridines with lanthanides, the π-π^*

absorption shifts to slightly lower energy upon complexation.[40c] Bis(bipyridine) anionic complexes of lanthanides showed that the π-π^* transitions of the bipyridine unit undergo bathochromic (red) shift upon coordination to europium and terbium.[82]

The anions in the lanthanide complexes herein do not have any significant effect on the UV-Vis absorption spectral wavelengths. Chen et al. have synthesized several platinum triimine, [Pt(tbtrpy)X]Y compounds with varying counterions.[83] By varying the X and Y in the complexes, they have finely tuned the absorption spectra into the red wavelength region. The planar conjugate system of the ttrpy ligand unchanged upon coordination with the lanthanides, which will be useful for the sensitization of the Ln (III) ion luminescence.

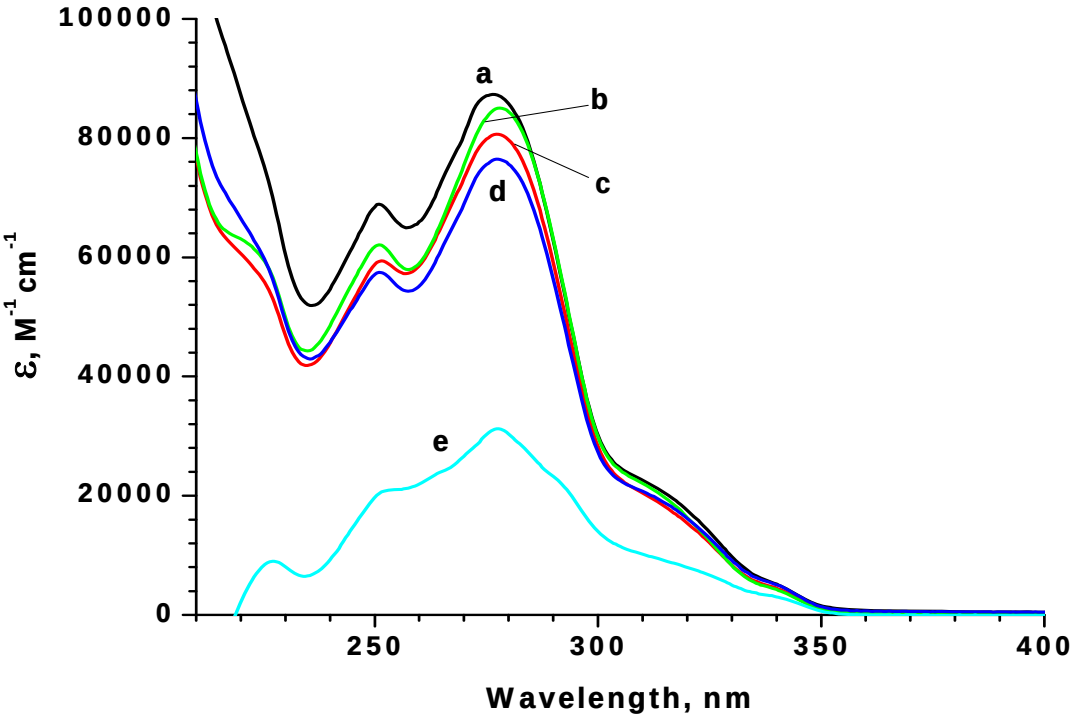

Figure 2.19. UV-Vis absorption spectra of the ttrpy ligand and its lanthanide chloride complexes in methanol. (a) 10^{-5} M $[Eu(L)_2Cl_2]Cl$ (b) 10^{-5} M $[Er(L)_2Cl_2]Cl$ (c) 10^{-5} M $[Tb(L)_2Cl_2]Cl$ (d) 10^{-5} M $[Nd(L)Cl_2(\mu\text{-}Cl)_2Nd(L)Cl_2$ (e) 10^{-5} M ttrpy, L.

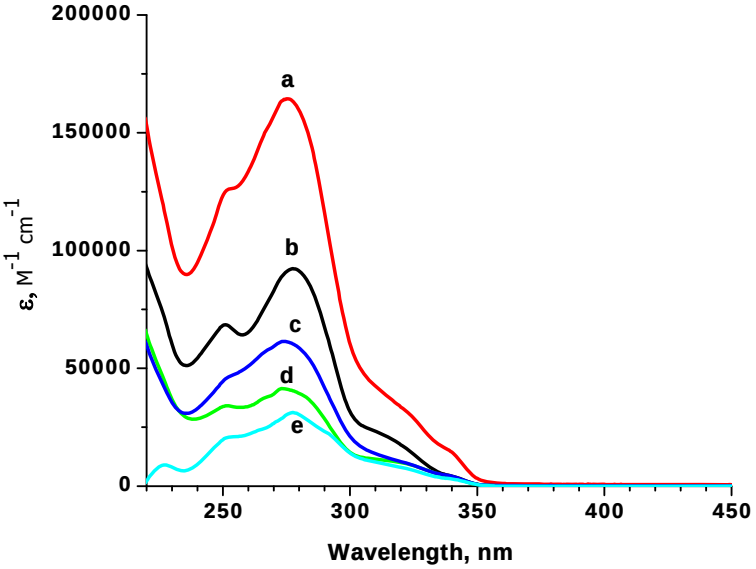

Figure 2.20. UV-Vis absorption spectra of the ttrpy ligand and its lanthanide nitrate complexes in methanol. (a) 10^{-5} M $[Tb(L)_2(NO_3)_2]NO_3$ (b) 10^{-5} M $[Eu(L)_2(NO_3)_2]NO_3$ (c) 10^{-5} M $Nd(L)(NO_3)_3$ (d) 10^{-5} M $Er(L)(NO_3)_3$ (e) 10^{-5} M ttrpy, L.

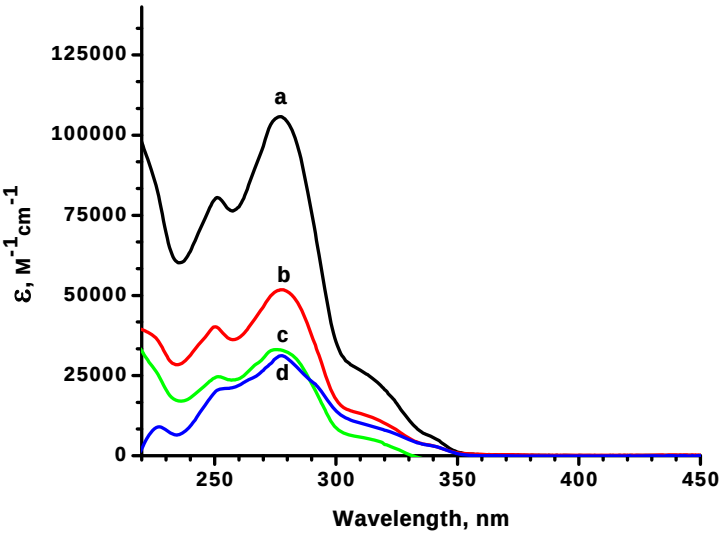

Figure 2.21. UV-Vis absorption spectra of the ttrpy ligand and its lanthanide perchlorate complexes in methanol. (a) 5 x 10^{-6} M $[Eu(L)_3](ClO_4)_3$ (b) 10^{-5} M $[Tb(L)_2(ClO_4)_2](ClO_4)$ (c) 10^{-5} M $[Nd(L)_2(ClO_4)_2](ClO_4)$ (d) 10^{-5} M ttrpy, L.

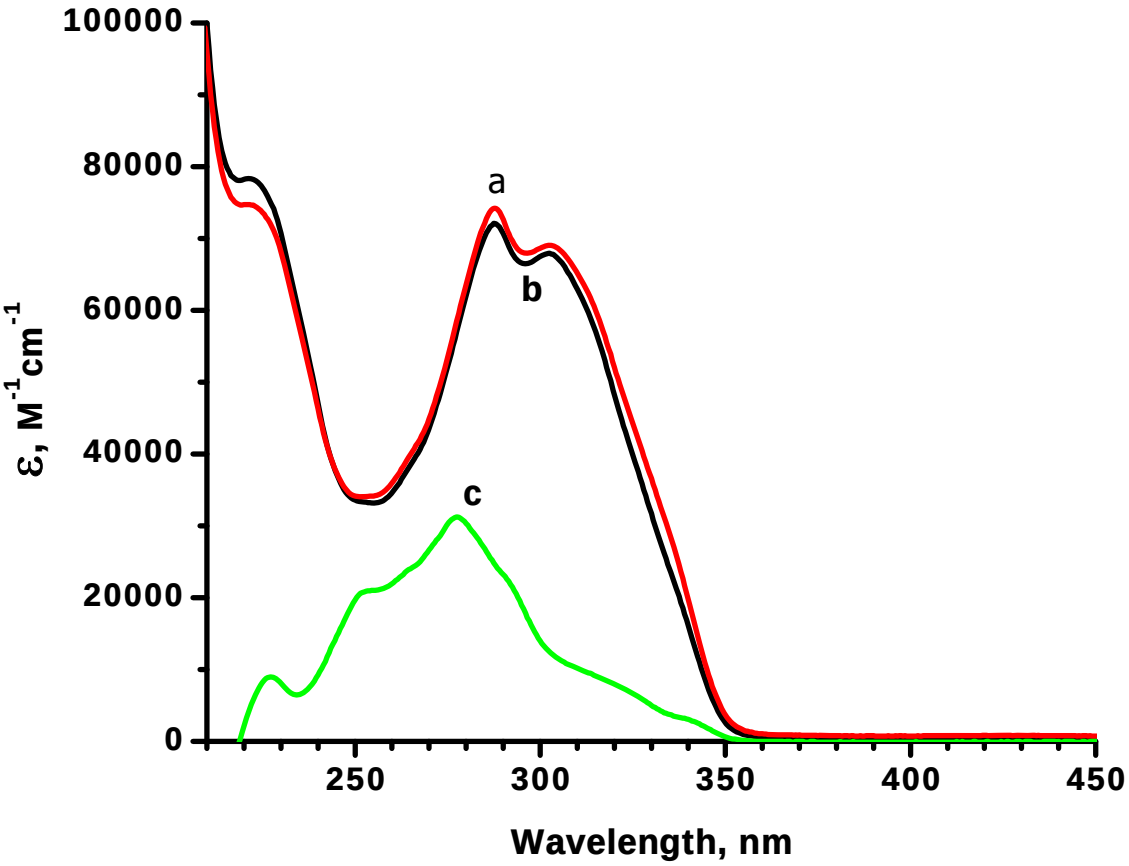

Figure 2.22. UV-Vis absorption spectra of the ttrpy ligand and its complexes with $Eu(hfa)_3$ and $Tb(hfa)_3$ in methanol. (a) 10^{-5} M $[Eu(hfa)_3(L)$ (b) 10^{-5} M $[Tb(hfa)_3(L)$ (c) 10^{-5} M ttrpy, L.

Table 2.7. λ_{max} and ε values for the free ligand and the lanthanide-ttrpy complexes.

Compound	λ_{max}, nm		$\varepsilon/10^3$, M^{-1} cm^{-1}	
ttrpy (L)	277	322	31	7.6
$[Eu(L)_2Cl_2]Cl$	277	322	87	15.9
$[Tb(L)_2Cl_2]Cl$	277	322	79.9	13.9
$[Er(L)_2Cl_2]Cl$	277	322	84	15.3
$[Cl_2(L)Nd(\mu\text{-}Cl)_2Nd(L)Cl_2]Cl$	277	322	76	15.3
$[Eu(L)_2(NO_3)_2]NO_3$	277	322	92	15.9
$[Tb(L)_2(NO_3)_2]NO_3$	274	322	162.6	30.9
$[Er(L)_2(NO_3)_2]NO_3$	277	322	41.5	9.7
$Nd(L)(NO_3)_3$	274	322	61.3	9.8
$[Eu(L)_3](ClO_4)_3$	277	322	105.6	18.8
$[Tb(L)_2(ClO_4)_2]ClO_4$	277	322	51.6	9.3
$[Er(L)_2(ClO_4)](ClO_4)_2$	277	322	76.4	13.4
$[Nd(L)_2(ClO_4)_2]ClO_4$	274	317	66.2	8.8
$Eu(hfa)_3(L)$	274	318	168.2	46
$Tb(hfa)_3(L)$	287	315	58.8	41.6

2.3.4 Luminescence Studies

At room temperature in methanol solution excitation of the ligand in one of its two absorption bands at *ca.* 250 and 280 nm yields one broad fluorescence band centered around 350 nm. No emission from the triplet state is observable at room temperature. Solid ttrpy displays two fluorescence bands centered around 363 and 560 nm, with lifetime of 1.44 and 5.15 ns, respectively. The latter band is broad and structured whose intensity is strongly dependent on the excitation energy, decreasing with increasing λ_{exc}, suggesting an excimer fluorescence origin, a situation observed in pyrene systems.[84] The quantum yields of the ligand-centered fluorescence are low and complexation to Gd(III) does not significantly alter these values. Both structured fluorescence and phosphorescence bands of the free ligand are seen at 77 K in methanol solutions, centered around 350 and 470 nm with lifetime of 3.7 ns and 1.8 s, respectively (Figure. 2.23). Upon complexation to Gd(III), both the fluorescence and phosphorescence bands shift to low energy (Figure. 2.23). The maximum of the ligand singlet state is lowered significantly by *ca*. 1500 cm^{-1} and the ligand triplet state undergoes only a small shift to lower energy, by approx. 1200 cm^{-1}. A phenomenon generally observed with the gadolinium complexes.[85] Upon complexation of substituted 4-Hydroxypyridine- 2,6-dicarboxylic acid diethyl ester with gadolinium, the energy of the ligand singlet state is lowered by 600 cm^{-1} and the triplet state by 1250 cm^{-1}.[85a]

Lifetimes for the fluorescence and phosphorescence of free ligand and gadolinium (III) complexes are reported in Table 2.8. The singlet state of the free ligand ttrpy has a characteristic lifetime of 1.3 and 3.1 ns in methanol at 298 K and 77

K, respectively. Complexation to Gd(III) does not significantly change the fluorescence lifetime of the ligand attaining 4.1 ns for the Gd-ttrpy complex in solution. Contrary to the fluorescence, complexation to Gd(III) leads to an approx. 250-fold shorter lifetime of the ligand-centered phosphorescence concomitant with a noticeable sensitization of the phosphorescence/fluorescence intensity ratio (vide infra), a consequence of the heavy atom effect, as observed for instance in d^{10} metal complexes.[70,86] Similar phenomenon was observed by Deiters et al. who found that the ligand phosphorescence lifetime is shortened by 40 times.[85a] The large spin–orbit coupling of the lanthanide center facilitates intersystem crossing from singlet state S_1 to triplet state T_1.

The phosphorescence due to the Gd(III) can be ruled out as its emission occurs in the UV region at about 310 nm.[87] So the emission observed in the Gd(III) complex with the ttrpy ligand is assigned to phosphorescence of the ligand. The energy level of the Gd(III) (32,231 cm^{-1}) is too high compared to the triplet energy level (22,800 cm^{-1}) of the ligand for the intramolecular energy transfer to take place from the ligand to the Gd(III). As a result, no sensitization of Gd(III) luminescence was observed. For the efficient energy transfer, there should be a better overlap between the donor (the organic ligand) emission and the acceptor (Ln^{3+}) absorption. Figure 2.23 shows the spectra of the ttrpy ligand emission and the acceptor (Eu^{3+}, Tb^{3+}) absorption. Both Tb^{3+} and Eu^{3+} absorption overlaps with the ligand singlet and triplet emission. The energy transfer due to the singlet or the triplet pathway is discussed in the section 2.3.4.1.

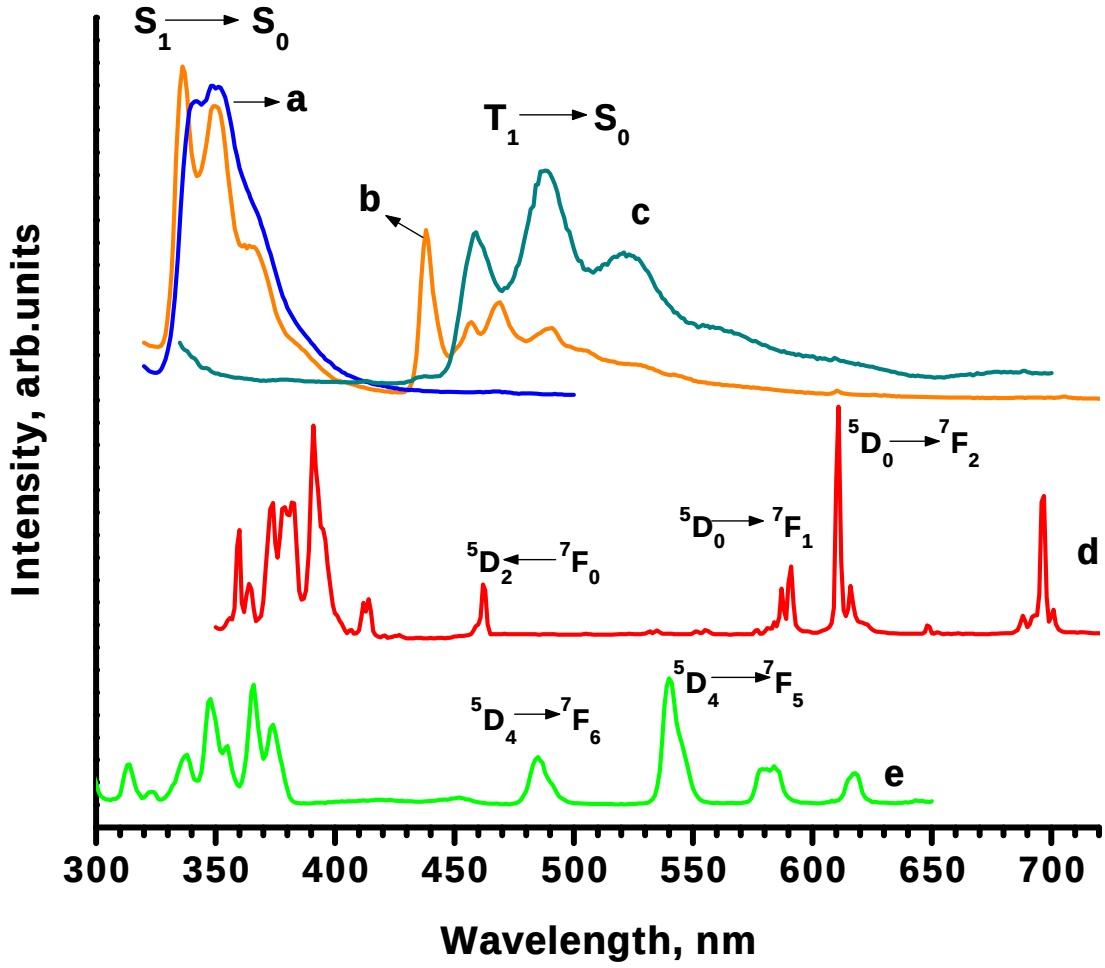

Figure 2.23. Emission spectra of ttrpy, $Gd(ttrpy)(NO_3)_3$, $TbCl_3$ and $EuCl_3$ in methanol (a) 10^{-3} M ttrpy in methanol at RT, λ_{exc} = 290 nm (b) 10^{-3} M ttrpy in methanol at 77 K, λ_{exc} = 290 nm (c) 3.3 X 10^{-3} M $Gd(ttrpy)(NO_3)_3$ in methanol at 77 K, λ_{exc} = 320 nm. (d) 10^{-3} M $EuCl_3$ in methanol at RT. (e) 10^{-3} M $TbCl_3$ in methanol at RT.

Table 2.8 Energy of the singlet and triplet states and lifetimes for the free ligand and the Gd^{III} complexes.

Compound	c / M	T /K	$E(S_1)$ / cm^{-1}	$E(T_1)$ / cm^{-1}	τ_F / ns	τ_p / ms
ttrpy	Solid	298	27500		1.24	
ttrpy	Solid	77	28900		3.74	
ttrpy	1.0×10^{-3}	298	29800	/	1.26	/
ttrpy	1.0×10^{-3}	77	29800	22800	3.14	1930
$Gd(ttrpy)(NO_3)_3$	3.3×10^{-3}	77	/	21800	/	7.83
$Gd(ttrpy)(NO_3)_3$	solid	77	26110	22800	4.63	13.7

The intensity ratio between the triplet and singlet state emissions for the ligand is enhanced upon decreasing temperature or upon coordination to Gd. For free ttrpy, the phosphorescence at 298 K is negligible and it accounts for 50% at 77 K; in contrast the ratio $P(^3\pi\pi^*) / [F(^1\pi\pi^*) + P(^3\pi\pi^*)]$ for the Gd complex reaches almost 100% in methanol solution at 77 K. The remarkable enhancement of the ligand phosphorescence upon cooling and upon complexation to Gd could be arising from the relatively electron-rich tolyl substitution at the 4-positions of terpyridine, which imparts the ttrpy ligand polar character. This effect can result in a larger intersystem crossing (isc) population rate k_{isc} or/and less effective deactivation processes. The latter argument is sustained by the lifetime data: τ ($^3\pi\pi^*$) for the Gd complex represents

about 250-fold decrease vs the free ligand. Therefore, the large enhancement observed in the $P\,(^3\pi\pi^*)$ / $[(F\,(^1\pi\pi^*)+\ P\,(^3\pi\pi^*)]$ ratio reflects both an increased k_{isc} and a decreased deactivation of triplet state in the substituted terpyridine-like ligand ttrpy and its Gd complexes. Sinha et al. has shown that substitution at the 4'-position of terpyridine-like ligand, significantly affects the photophysical properties of the ligand and its complexes,[88] resulting from the presence of relatively close-lying $n\pi^*$ and $\pi\pi^*$ states in terpyridine-like ligands which can be coupled vibronically (proximity effect).[89] Both the lowest singlet state (S_1) and the lowest triplet state (T_1) are of mixed character of strongly coupled $n\pi^*$ and $\pi\pi^*$ states. The coupling of energetically close lying $n\pi^*$ and $\pi\pi^*$ states result in very efficient intersystem crossing processes, which is enhanced by coordination to Gd(III) ions. The profound influence of coordination on the photophysical properties of the oligopyridines also resulted from the conformational changes (*e.g.* ttrpy from *trans-trans* to *cis-cis*) and the change of the overall charge.

2.3.4.1 Metal Centered Emission

Upon UV irradiation, solid and solutions of Eu(III) and Tb(III) complexes strongly emit light in the characteristic red for Eu(III) and green region for Tb(III), respectively (Figures. 2.24-2.31). The excitation spectra of all the lanthanide complexes are similar to that of the ligand excitation. It is known in the literature that the excitation and the absorption spectra of strongly absorbing samples will be different as the excitation is effective in the tail of the absorption band.[90] The excitation spectra in all the complexes have shown similar features. The excitation spectra of the complexes does not show any sharp peaks due to the lanthanide f-f transitions except in few complexes such as

$[Eu(L)_2Cl_2]Cl$ in the solid state at 77K (Figure 2.29) and $Eu(hfa)_3L$ at RT and 77K (Figures 2.28 and 2.29). Monitoring the lanthanide emission peaks, ligand absorption was dominant compared to the weak f-f transitions thus indicating an efficient sensitization of lanthanide emission through ligand triplet levels. The excitation is red shifted compared to absorption in all of the solution and solid state spectra. The excitation spectra of 10^{-4} M solutions of both Eu and Tb ttrpy complexes show a major peak at about 345 nm with a shoulder at 310 nm (Figures 2.24 and 2.25). The excitation spectra of europium complexes with chlorides, nitrates and perchlorates as counterions in solid state were showing peak maximum between 360-385 nm and extending upto 450 nm at RT (Figure 2.28). The peak maximum at 77 K was between 350-375 nm extending upto 440 nm (Figure 2.29). Terbium complexes with chlorides, nitrates and perchlorates as counterions were showing the excitation maximum between 360-380 nm with a tail upto 440 nm at RT in the solid state (Figure 2.30). All the terbium complexes have the excitation maximum at about 360 nm with a tail extending upto 400 nm at 77 K (Figure 2.31). $Eu(hfa)_3L$ at RT was exhibiting a broad peak with maximum at 365 nm extending upto 475 nm along with a line like peak at 466 nm ($^5D_2 \leftarrow {}^7F_0$) corresponding to the europium absorption (Figure 2.28). But at 77 K the peak maximum was 350 nm extending upto 440 nm along with faint 466 nm peak (Figure 2.29). In case of $Tb(hfa)_3L$ both at RT and 77K, the excitation peak maximum was at about 365 nm extending upto 460 nm with shoulders at 403 and 438 nm were observed (Figures 2.30-2.31). The $Ln(hfa)_3L$ complexes studied here have similar excitation spectra features as reported by Eliseeva et al.[91]

The photoluminescence spectra in the solution of both europium and terbium complexes were exhibiting features of both ligand and the lanthanide emission upon ttrpy ligand excitation (Figures 2.24-2.25). The ligand emission was exhibiting a broad peak at 400 nm in all the solution emission spectra. This broad peak is not due to the dissociated ttrpy ligand in the solution because the ligand singlet emission is at 330 nm and the triplet emission is at 440 nm. This peak at 400 nm is also not from impurity as the solvent alone did not show any emission. The emission from the lanthanides is less intense in the solution compared to the solid state. This is because the vibronic interaction of the O-H oscillators from the methanol with the emitting states of the lanthanides. The lanthanide line like emission spectra in the solution of all the europium complexes is similar likewise terbium emission in all the terbium complexes.

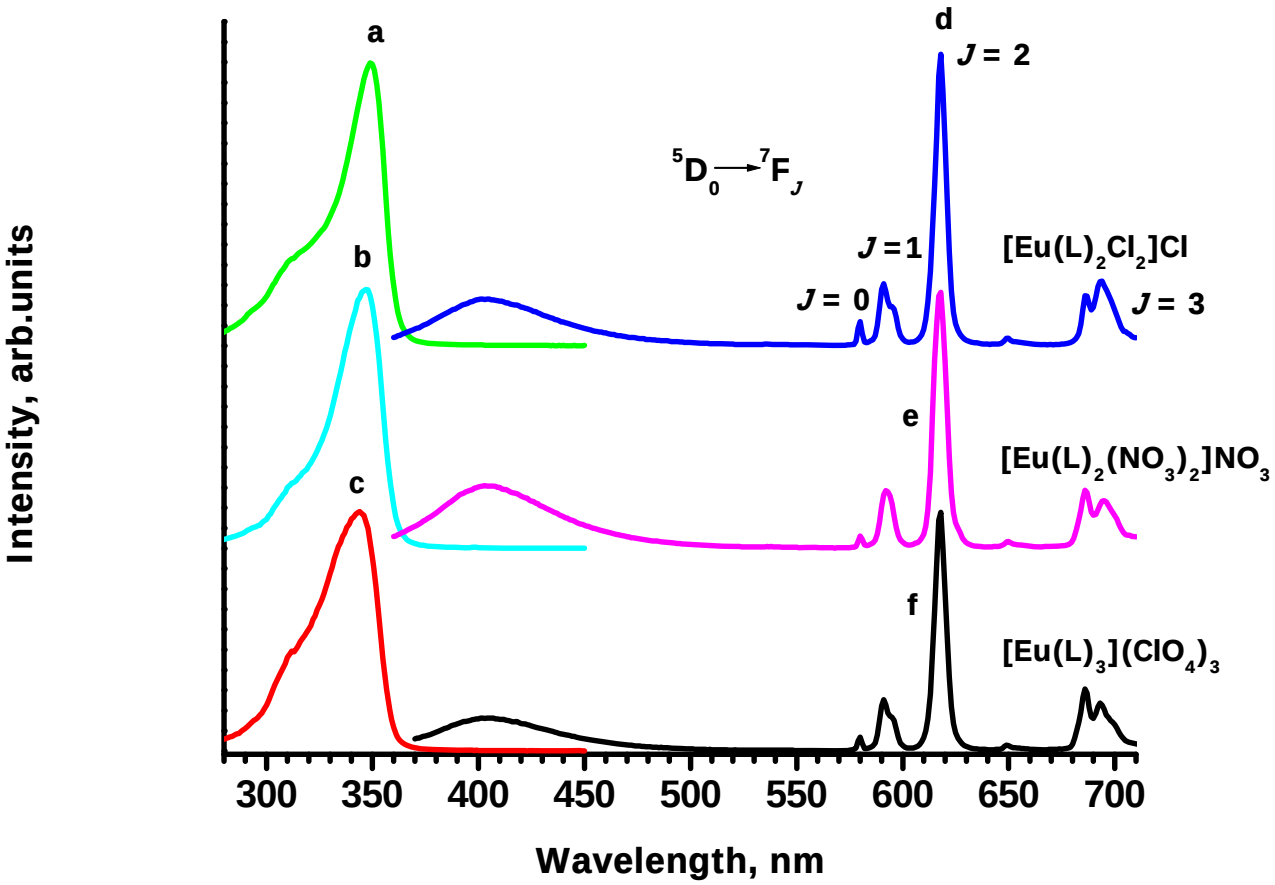

Figure 2.24. Luminescence excitation (a-c), λ_{emi} = 617 nm and emission (d-f), λ_{exc} = 345 nm for 10^{-4} M solutions of Eu-ttrpy complexes in methanol.

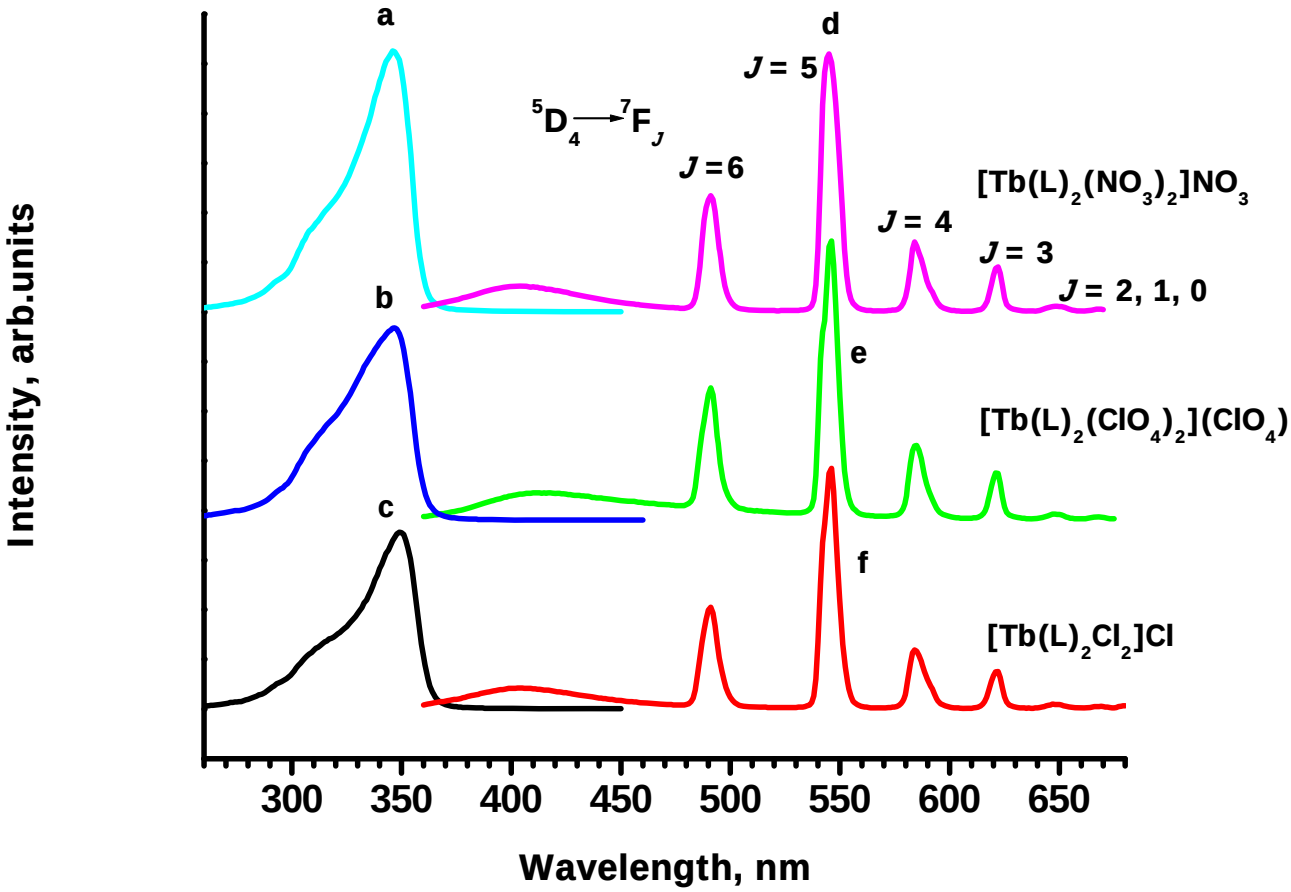

Figure.2.25. Luminescence excitation (a-c), λ_{emi} = 545 nm and emission (d-f), λ_{exc} = 345 nm for 10^{-4} M solutions of Tb-ttrpy complexes in methanol.

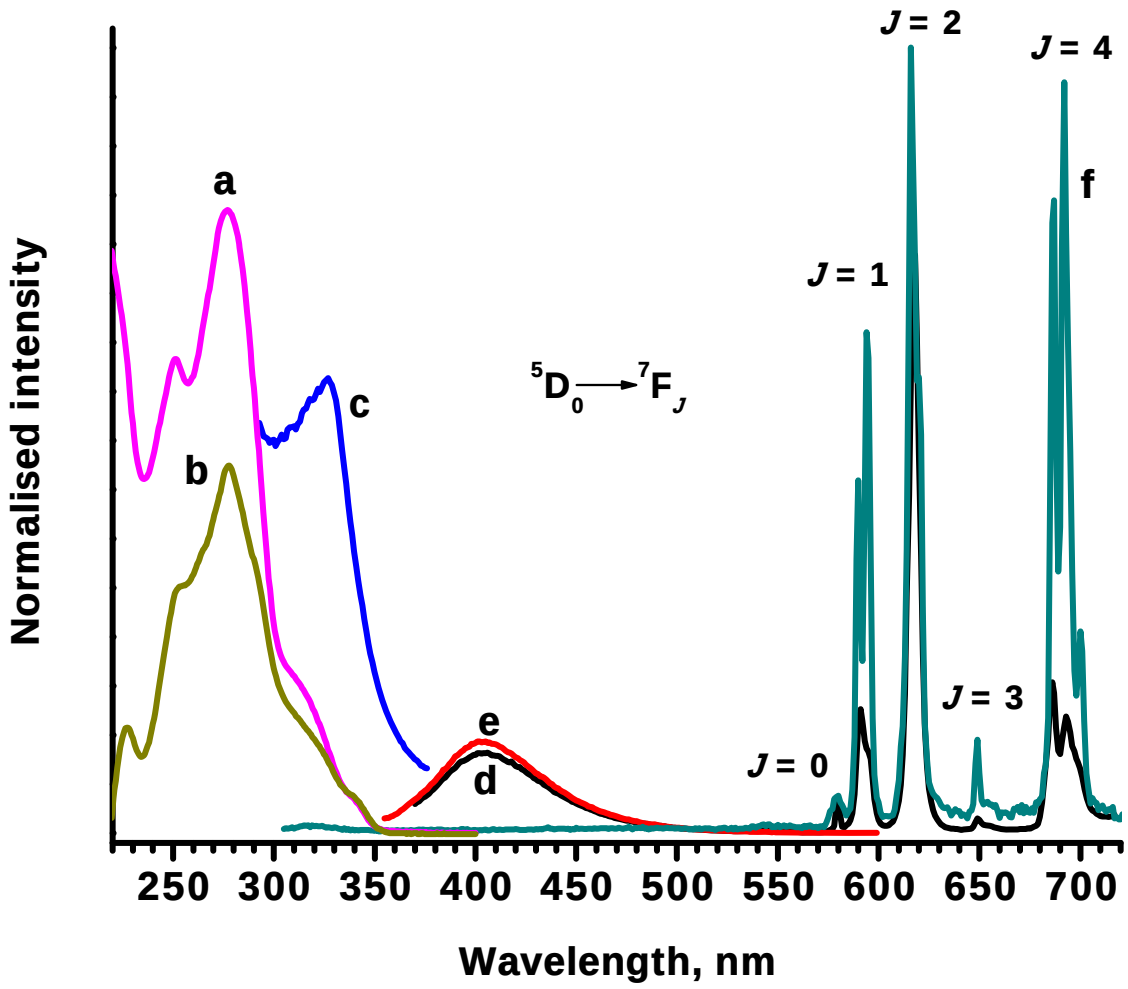

Figure 2.26. Absorption (a-b), luminescence excitation (c) and luminescence emission (d-f) for $Eu(ttrpy)_3(ClO_4)_3$ in solution and the solid state. (a) $Eu(ttrpy)_3(ClO_4)_3$ in methanol, c = 1.0×10^{-5} M; (b) ttrpy in MeOH, c = 1.0×10^{-5} M; (c) 10^{-5} M ttrpy in methanol, λ_{emi} = 470 nm (d) $Eu(ttrpy)_3(ClO_4)_3$ in MeOH, c = 1.0×10^{-5} M; λ_{exc} = 345 nm (e) $Eu(ttrpy)_3(ClO_4)_3$ in MeOH, c = 1.0×10^{-6} M, λ_{exc} = 345 nm; (f) $Eu(ttrpy)_3(ClO_4)_3$ crystalline solid at 298 K, λ_{exc} = 290 nm.

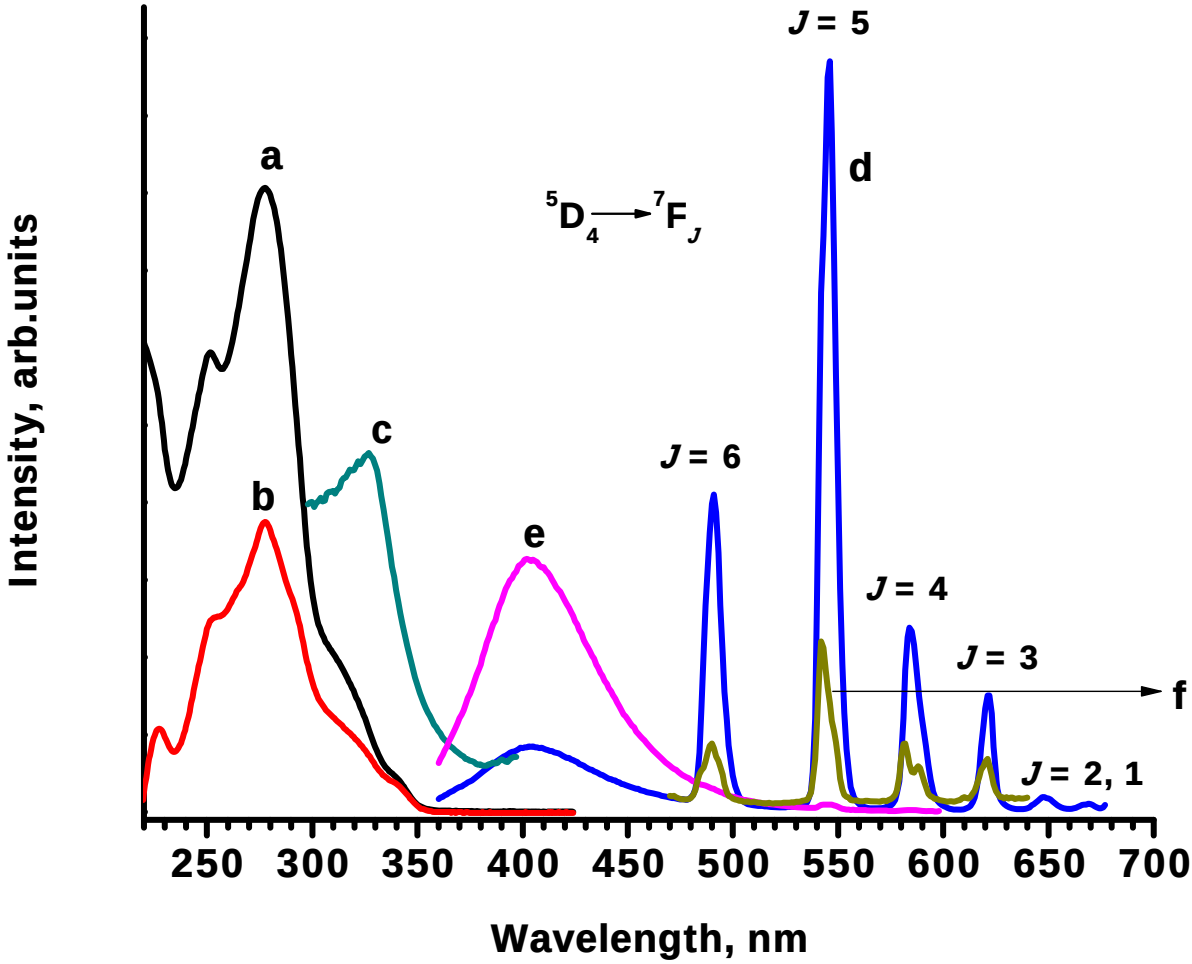

Figure 2.27. Absorption (a-b), luminescence excitation (c) and luminescence emission (d-f) for $[Tb(ttrpy)_2Cl_2]Cl$ in solution and in solid state. (a) 10^{-5} M $[Tb(ttrpy)_2Cl_2]Cl$ in methanol (b) 10^{-5} M ttrpy in methanol (c) 10^{-5} M ttrpy in methanol, λ_{emi} = 470 nm (d) 10^{-4} M $[Tb(ttrpy)_2Cl_2]Cl$ in methanol (e) 10^{-5} M $[Tb(ttrpy)_2Cl_2]Cl$ in MeOH, λ_{exc} = 350 nm (f) $[Tb(ttrpy)_2Cl_2]Cl$ crystalline solid at 298 K, λ_{exc} = 375 nm.

In the solid state, under ligand excitation of all the europium and terbium complexes, the characteristic bright red and green luminescence due to $^5D_0 \longrightarrow {}^7F_J$ (J = 0-4) and $^5D_4 \longrightarrow {}^7F_J$ (J = 6-0) transitions were observed, respectively. No emission from the ligand was observed. The presence of ligand absorption in the excitation spectra and absence of any emission due to the ligand clearly indicates that the lanthanide emission is sensitized both in europium and terbium complexes. The emission spectra of crystalline Eu(III) complexes at ambient temperature are depicted in Figure. 2.26. The overall band shape and intensity of the individual transitions are very similar in all the europium complexes. The phosphorescence intensity ratio of P ($^5D_0 \rightarrow {}^7F_2$) / P ($^5D_0 \rightarrow {}^7F_1$) is 1.62, 3.10 and 3.39 at 298 K vs 1.28, 2.44 and 3.69 at 77 K for complexes of $[Eu(ttrpy)_2(NO_3)_3]NO_3$, $[Eu(ttrpy)_2Cl_2]Cl$ and $[Eu(ttrpy)_3](ClO_4)_3$, respectively. The number of components observed for the $^5D_0 \longrightarrow {}^7F_J$ (J = 1–4) transitions point to low symmetries of the emitting Eu(III) sites. For the nitrate complex of $[Eu(ttrpy)_2(NO_3)_3]NO_3$ the asymmetry and broadness of the weak $^5D_0 \rightarrow {}^7F_0$ transition is indicative of more than one emitting site (Figure 2.29),[‡] as confirmed by the crystal structure of $[Eu(ttrpy)_2(NO_3)_2]NO_3$ that three species involving various coordinated MeOH or H_2O solvent in the first coordination sphere co-exist in equilibrium.

The $^5D_0 \rightarrow {}^7F_2$ peak in the $Eu(hfa)_3(L)$ was the most intense when compared to other peaks (Figures 2.28-2.29). The hypersensitive peak $^5D_0 \rightarrow {}^7F_2$ is most intense in $Eu(hfa)_3(L)$ indicates highly polarizable[92] and a low symmetry around Eu^{3+} site.[70a] If the

[‡] Lack of resolution of the fluorimeter, a qualitative description is given.

Eu^{3+} does not occupy site of inversion symmetry, then the $^5D_0 \rightarrow {}^7F_2$ is dominant.[93] Similar observation was found for the complexes of europium with β diketonates and substituted bipyridine and phenonthrolines.[94] The phosphorescence intensity ratio, *P* ($^5D_0 \rightarrow {}^7F_2$)/*P* ($^5D_0 \rightarrow {}^7F_1$) is 18. Such a large intensity ratio is a typical for europium β diketonate complexes.[30] This large intensity ratio also indicates that the Eu^{3+} does not occupy a site with high symmetry.[95] Complexes with a centrosymmetric coordination sphere have *P* ($^5D_0 \rightarrow {}^7F_2$)/*P* ($^5D_0 \rightarrow {}^7F_1$) values that are lower than 0.7.[96] The β diketonate ligands, when coordinated to Eu^{3+}, usually lead to stronger luminescence than that in the parent compound, especially when the β diketonate has aromatic or fluorinated substituents.[92] Complexes of europium with the β diketonate have high radiative rate and hence are the better luminescent complexes.[97] The β diketonates with trifluoromethyl groups, such as hfa, have an effect which is two fold. First, the trifluoromethyl group acts as electron withdrawing groups which make the bond ionic; weaker interactions lead to longer Ln-O bonds in fluorinated species compared to non-fluorinated analogues.[94] Second, this longer Ln-O bond eases the steric congestion around the metal making it available for coordination with the neutral ligand such as ttrpy here. As a result both in $Eu(hfa)_3(L)$ and $Tb(hfa)_3(L)$, the coordination around the central metal is 9. Among the europium compounds, the $[Eu(ttrpy)_3](ClO_4)_3$ has the highest quantum yield with 21.0 % in the solid state. The highest quantum yield for the europium complexes reported in the literature was 75%.[98]

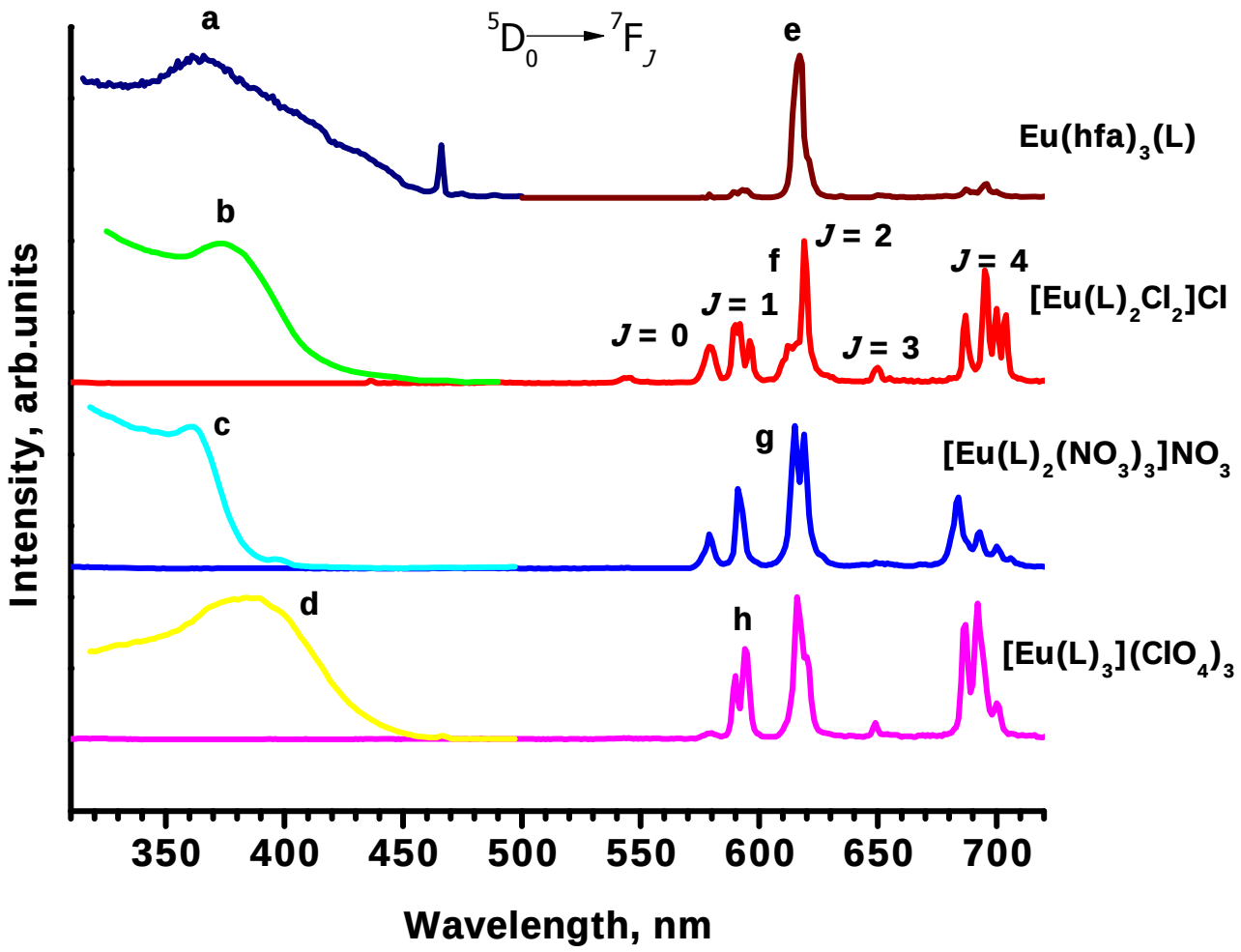

Figure 2.28. Photoluminescence spectra of europium-ttrpy complexes at room temperature. Excitation spectra (a-d) and Emission spectra (e-f). (a) $Eu(hfa)_3L$, λ_{emi} = 617 nm (b) $[Eu(L)_2Cl_2]Cl$, λ_{emi} = 619 nm (c) $[Eu(L)_2(NO_3)_2]NO_3]$, λ_{emi} = 615 nm (d) $[Eu(L)_3](ClO_4)_3$, λ_{emi} = 615 nm (e) $Eu(hfa)_3L$, λ_{exc} = 365 nm (f) $[Eu(L)_2Cl_2]Cl$, λ_{exc} = 290 nm (g) $[Eu(L)_2(NO_3)_2]NO_3]$, λ_{exc} = 290 nm (h) $[Eu(L)_3](ClO_4)_3$, λ_{exc} = 290 nm.

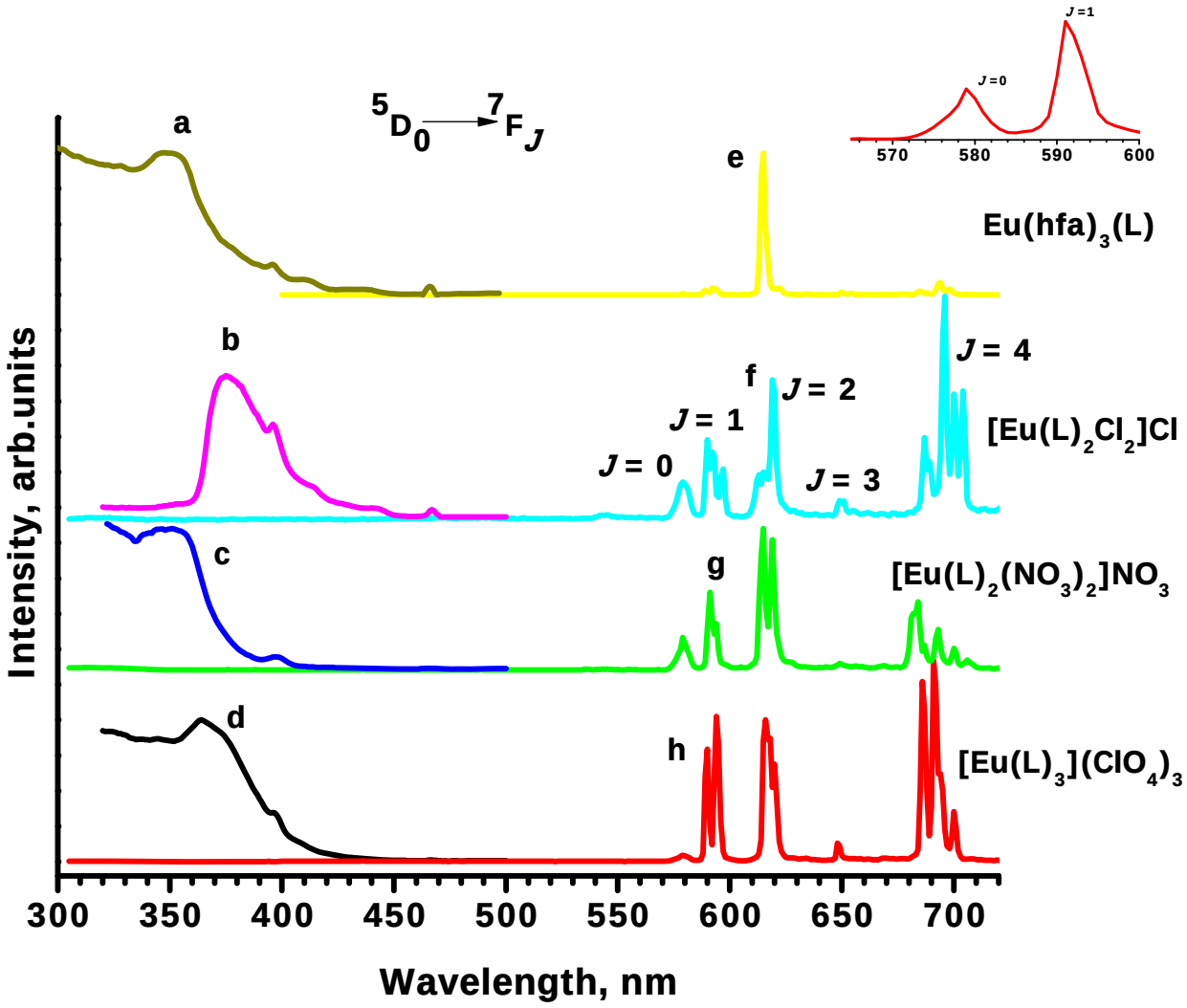

Figure 2.29. Photoluminescence spectra of europium-ttrpy complexes at 77 K. Excitation spectra (a-d) and Emission spectra (e-f). (a) $Eu(hfa)_3L$, λ_{emi} = 617 nm (b) $[Eu(L)_2Cl_2]Cl$, λ_{emi} = 619 nm (c) $[Eu(L)_2(NO_3)_2]NO_3]$, λ_{emi} = 615 nm (d) $[Eu(L)_3](ClO_4)_3$, λ_{emi} = 615 nm (e) $Eu(hfa)_3L$, λ_{exc} = 315 nm (f) $[Eu(L)_2Cl_2]Cl$, λ_{exc} = 290 nm (g) $[Eu(L)_2(NO_3)_2]NO_3]$, λ_{exc} = 290 nm (h) $[Eu(L)_3](ClO_4)_3$, λ_{exc} = 290 nm. Inset. $^5D_0 \longrightarrow {}^7F_J$ J = 0, 1 for $[Eu(L)_2(NO_3)_2]NO_3$.

The $^5D_4 \longrightarrow {}^7F_6$ (around 490 nm), $^5D_4 \longrightarrow {}^7F_5$ (around 545 nm) transitions are generally most populated transitions appeared in all the terbium compounds (Figures. 2.30 and 2.31). The $^5D_4 \longrightarrow {}^7F_5$ transition is the hypersensitive transition in the case of terbium complexes. The $^5D_4 \longrightarrow {}^7F_4$ (around 585 nm) and $^5D_4 \longrightarrow {}^7F_3$ (around 620 nm) though weak compared to the prominent ones still appeared in all the terbium ttrpy compounds. $Tb(hfa)_3(ttrpy)$ was not as bright as the $Tb(hfa)_3$ precursor compound itself. This could be due to two reasons. 1) It may be due to poor overlap between ligand triplet energy states to terbium $^5D_4$ level. But Figure 2.22 suggests that the overlap between the donor triplet state and the Tb acceptor level is very good. So this is ruled out. 2) Back energy transfer from terbium energy level to the ligand triplet energy level occurs because of close energy levels.[95] The energy gap between the ligand triplet level and the terbium $^5D_4$ level is 2400 cm^{-1} which is below the threshold i.e 3500 cm^{-1}. As a result $Tb(hfa)_3(ttrpy)$ is very inefficient compared to its precursor. The back energy transfer is a well-known phenomenon in the case of terbium complexes. It is observed in several reports both in the solid state and solution samples.[99] The quantum yield values for europium compounds are higher than those of terbium compounds in the solid state. For all the compounds, the lifetime at 77 K is longer when compared to room temperature. It is very common that at low temperatures, the non-radiative decay is minimized and longer life time is expected.

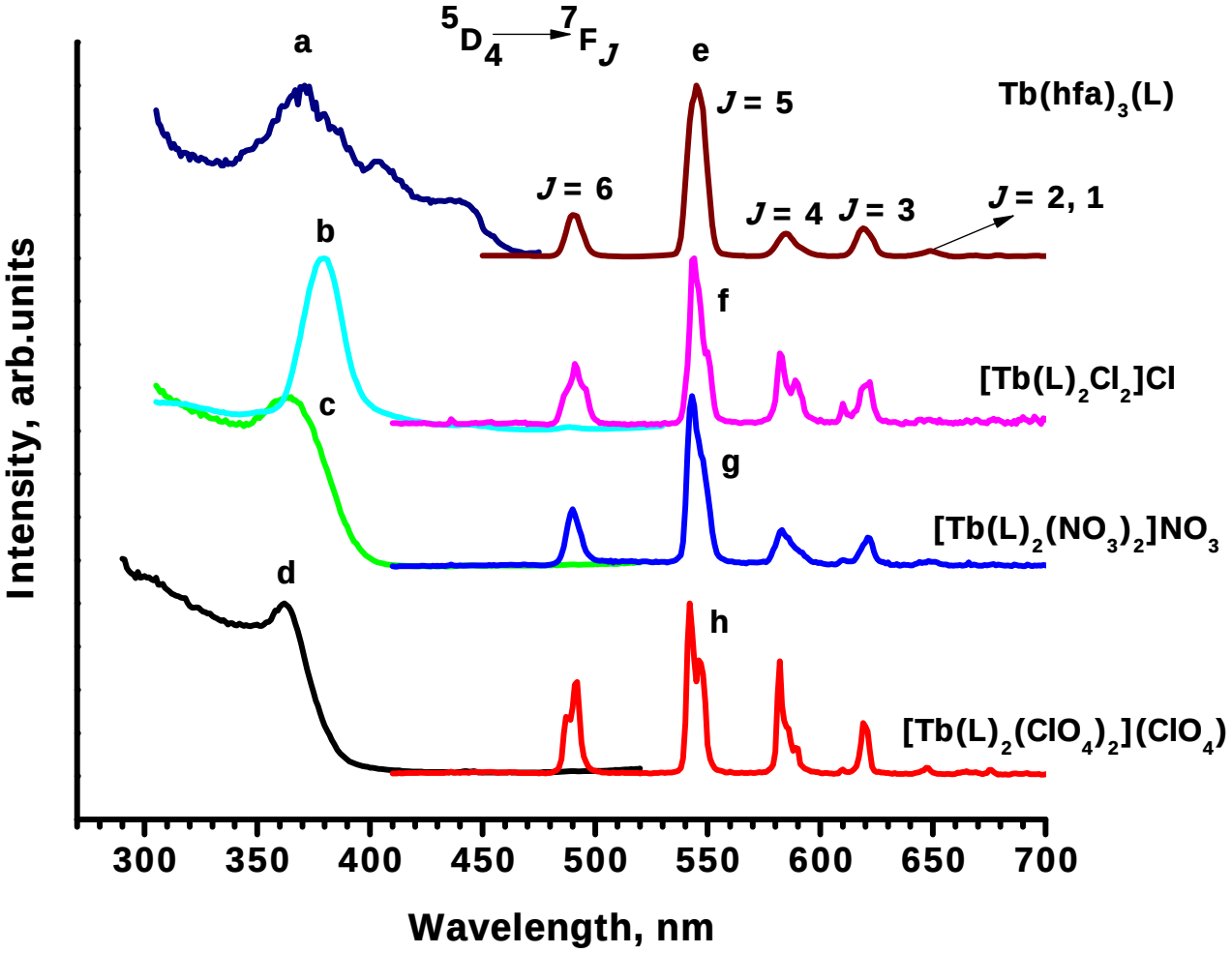

Figure 2.30. Photoluminescence spectra of terbium-ttrpy complexes at room temperature. Excitation spectra (a-d) and Emission spectra (e-f). (a) $Tb(hfa)_3L$, λ_{emi} = 545 nm (b) $[Tb(L)_2Cl_2]Cl$, λ_{emi} = 544 nm (c) $[Tb(L)_2(NO_3)_2]NO_3$, λ_{emi} = 542 nm (d) $[Tb(L)_2(ClO_4)_2]ClO_4$, λ_{emi} = 543 nm (e) $Tb(hfa)_3L$, λ_{exc} = 360 nm (f) $[Tb(L)_2Cl_2]Cl$, λ_{exc} = 290 nm (g) $[Tb(L)_2(NO_3)_2]NO_3$, λ_{exc} = 290 nm (h) $[Tb(L)_2(ClO_4)_2]ClO_4$, λ_{exc} = 290 nm.

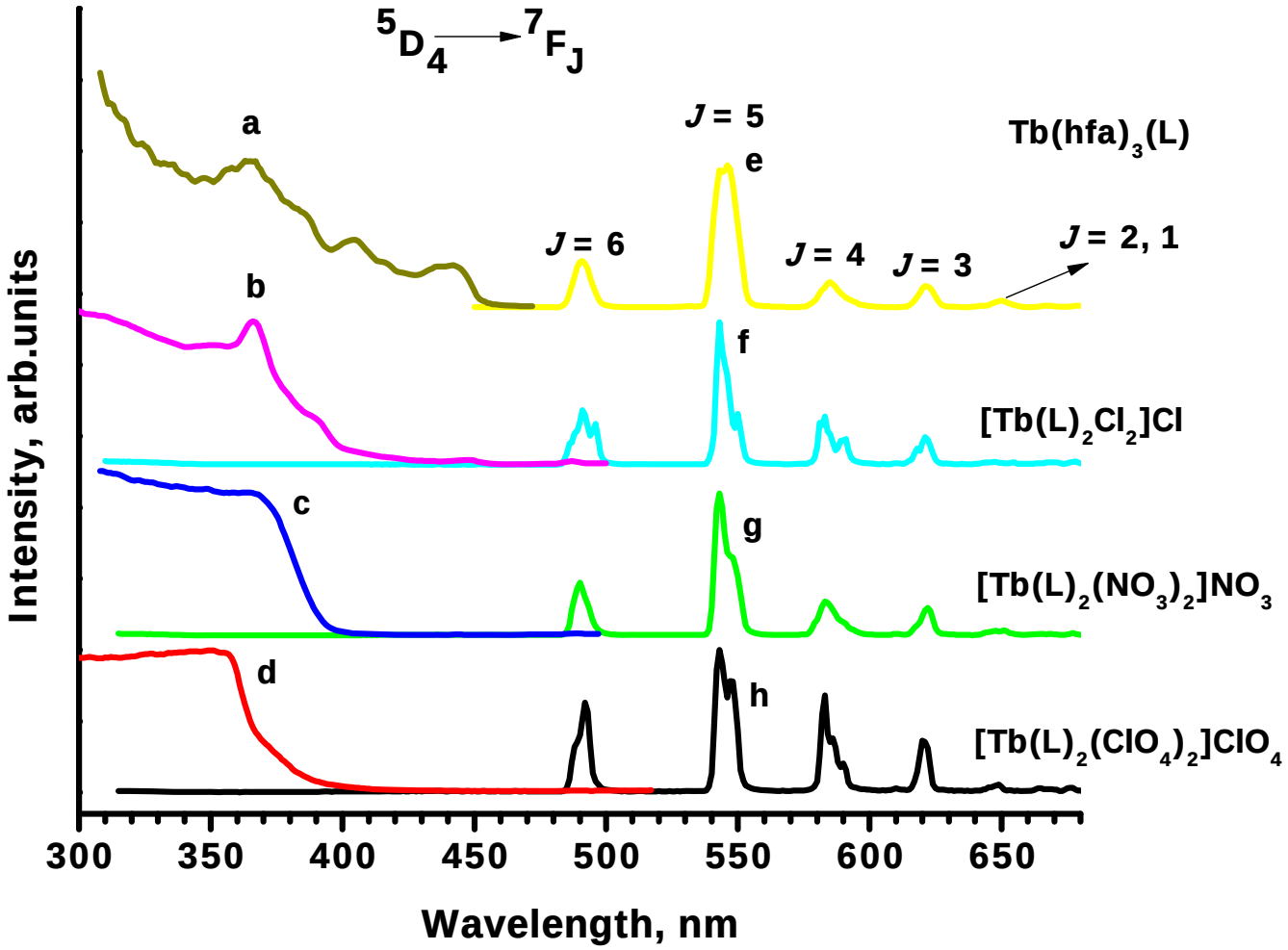

Figure 2.31. Photoluminescence spectra of terbium-ttrpy complexes at 77 K. Excitation spectra (a-d) and Emission spectra (e-f). (a) $Tb(hfa)_3L$, λ_{emi} = 545 nm (b) $[Tb(L)_2Cl_2]Cl$, λ_{emi} = 543 nm (c) $[Tb(L)_2(NO_3)_2]NO_3$, λ_{emi} = 543 nm (d) $[Tb(L)_2(ClO_4)_2]ClO_4$, λ_{emi} = 543 nm (e) $Tb(hfa)_3L$, λ_{exc} = 360 nm (f) $[Tb(L)_2Cl_2]Cl$, λ_{exc} = 290 nm (g) $[Tb(L)_2(NO_3)_2]NO_3$, λ_{exc} = 290 nm (h) $[Tb(L)_2(ClO_4)_2]ClO_4$, λ_{exc} = 290 nm.

The quantum yields of the metal centered emission of the complexes upon ligand excitation are listed in Table 2.9. Absolute quantum yield measurements were done using the equation 1 and 2.[100]

$$\phi_{PL} = E_i(\lambda)-(1-A)E_0(\lambda) / L_e(\lambda)(A) \quad (1)$$

$$\text{Where } A = L_o(\lambda)-L_i(\lambda) / L_0(\lambda) \quad (2)$$

$E_i(\lambda)$ and $E_0(\lambda)$ are the integrated luminescence as a result of direct excitation of sample and indirect excitation, respectively. Emission from indirect excitation is due to the reflected light from sphere walls hitting the walls.

A is the absorbance which is measured by integrating the excitation profiles.

$L_i(\lambda)$ = integration of excitation profile when the sample is directly excited.

$L_0(\lambda)$ = integration of excitation profile when the sample is indirectly excited.

$L_e(\lambda)$ = integration of excitation profile for an empty sphere.

The complexes of ttrpy with Eu(III) are approximately 4-9 times stronger emitters than the corresponding Tb(III) complexes, indicating that ttrpy sensitize Eu(III) better than Tb(III), a case consistent with other classes of sensitizer molecules where energy transfer is efficient towards only Eu^{3+} or Tb^{3+} but not both cations due to the energy gap constrains between the antenna donor triplet state and the cations. Both solid Eu^{3+} and Tb^{3+} complexes show much less intensity as compared to their solution, resulting from the self quenching effect. However, we noted that the quantum yield of solid $[Eu(ttrpy)_3][ClO_4]_3$ is more than two times compared to its methanol solution. Generally in solution, the efficient quenching of lanthanide luminescence occurs by energy loss to high frequency vibrational modes of the solvent. Even in case

of $[Eu(ttrpy)_3][ClO_4]_3$ in methanol, the O-H vibrations from methanol are responsible for lower quantum yield than in the solid state.

The intense red emission observed for $[Eu(ttrpy)_3]^{3+}$ in the solid state can also be attributed to the well protected and well-separated Eu cations in crystals of $[Eu(ttpy)_3](ClO_4)_3$, where the shortest Eu-Eu distance is 9.466 Å and the intermolecular interaction between the ligands is weak without observable π-π stacking interactions, which prevents self-quenching in crystal of $[Eu(ttrpy)_3](ClO_4)_3$. This does not mean that other compounds have stronger Ln-Ln interactions or else π-π stacking interactions.

Table 2.9. Lifetime and quantum yield data for Eu^{III} and Tb^{III} complexes.

Compound	λ_{max} / nm	ε / M^{-1} cm^{-1}	τ / ms RT	τ / ms 77 K	τ / ms in MeOH	ϕ / % solid	ϕ / % soln
ttrpy	277	31130					
$[Eu(L)_2Cl_2]Cl$	277	87310	1.51	1.54	0.394	12.3	6.0
$Eu(L)(NO_3)_3$	277	92160	0.526	0.595	0.531	8.97	8.0
$[Eu(L)_3](ClO_4)_3$	277	105800	1.656	1.95	0.433	21.1	9.5
$Eu(hfa)_3(L)$	287	74208	0.739	0.888	0.596	10.2	21.0
$[Tb(L)_2Cl_2]Cl$	277	80610	0.266	1.34	0.874	2.24	12.9
$Tb(L)(NO_3)_3$	275	164368	0.167	1.29	0.654	0.96	13.5
$[Tb(L)_2(ClO_4)_2]ClO_4$	277	51770	0. 362	1.160	0.682	6.2	10.0
$Tb(hfa)_3(L)$	287	72080	0.089	0.819	0.005	4.32	0.45

Yang et al. has shown that the most efficient energy transfer mechanism for sensitized lanthanide ion emission is a direct and fast singlet pathway, which has achieved the highest quantum yield for Eu^{3+} ion emission via visible light excitation (the

excitation window extends up to 515 nm).[70a] However, most lanthanide complexes follow the triplet energy transfer pathway, as induced by the efficient intersystem crossing resulted from the heavy-atom effect of lanthanides.[70,101,102] Figure 2.32 explains the energy transfer pathway taking place in the lanthanide complexes studied herein. Both singlet and triplet energy levels of the ligand are suitable to transfer their energy to europium and terbium energy levels as seen in Figure 2.32. However, the intersystem crossing from the ttrpy ligand singlet to triplet was efficient as evidenced in the emission spectra of Gd(ttrpy)$(NO_3)_3$ complex. In Figure 2.23, upon ligand excitation, Gd(ttrpy)$(NO_3)_3$ at 77K shows only phosphorescence due to the ligand and no emission due to the fluorescence was observed. This indicates that the triplet energy level of the ligand is responsible for the sensitization of the europium and terbium emission. Qualitatively this confirms that the triplet energy transfer pathway is the efficient route here.

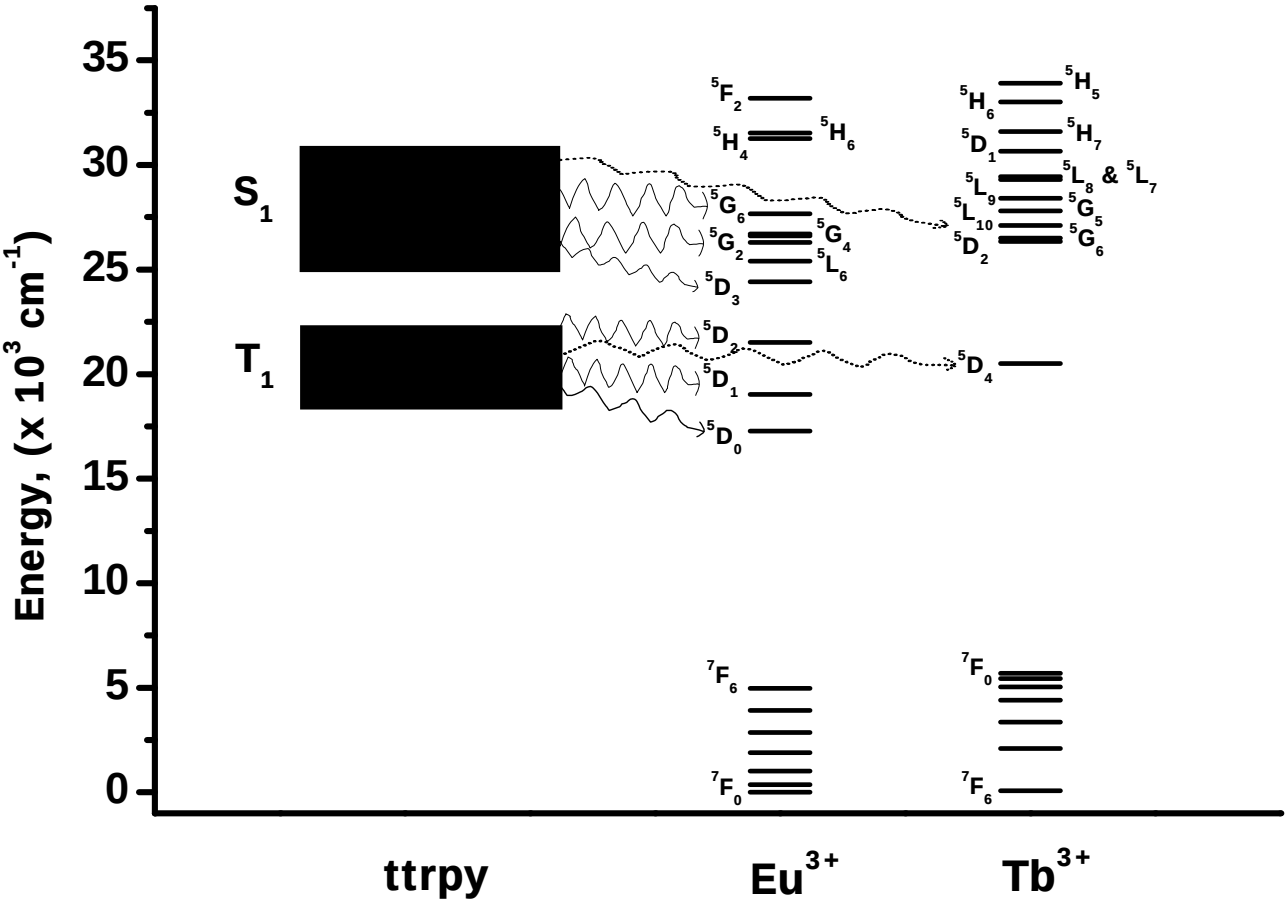

Figure 2.32 Energy level diagram for the ttrpy ligand with the Eu(III)[103] and Tb(III)[104] levels.

For a triplet ET mechanism, the absolute quantum yield of lanthanide-centered luminescence can be expressed by equation 3: [105]

$$Q^{Ln} = \eta_{isc}\, \eta_{et} k_r^0 / k_{obs} \qquad \textbf{(3)}$$

where η_{isc} stands for the intersystem crossing efficiency of the antenna, η_{et} for that of the energy transfer step, while k_r^0 and $k_{obs} = 1/\tau_{obs}$ are the radiative and observed rate constants, respectively. The energy gap constrains for efficient antenna ligand

sensitized lanthanide-centered emission has been described by Verhoeven et al.[106] The energy gap between the lowest singlet and triplet state of the ligand should be at least 5000 cm^{-1} to generate efficient intersystem crossing with sizable η_{isc}. For efficient energy transfer from ligand triplet state (T_1) to the luminescent excited state of the lanthanide ion (η_{et}), the ligand optimum T_1 state should be ~ 3500 cm^{-1} more energetic. This is based on the empirical rules defined for an optimal ligand-to-metal energy transfer: 2500 < ΔE ($^3\pi\pi^*$ - $^5D_0$) < 3500 cm^{-1} for Eu(III) ions and 2500 < ΔE ($^3\pi\pi^*$ - $^5D_4$) < 4000 cm^{-1} for Tb(III) ions.[85c,91] Otherwise, back energy transfer from lanthanide to the ligand occurs, a temperature-dependent non-radiative deactivation mode affecting k_{obs}. Latva et al. has observed the back energy transfer process in the terbium complexes, where the energy difference between the ligand T_1 state and $^5D_4$ level for Tb^{3+} is less than 1850 cm^{-1}.[99d] The ligand singlet–triplet gap, taken as the difference between the most energetic fluorescence and phosphorescence features identified in the emission spectra of the Gd-ttrpy complexes studied here (Table 2.8), amounts to 6900 cm^{-1}. These values are over the lower limit of 5000 cm^{-1} as defined above and thus on favorable grounds for a large η_{isc}. Looking at the energy of the ligand triplet states in the Gd^{3+} complexes, one can conclude that an energy transfer to the lanthanide metal ions is feasible to the ^5D_J (J = 0–2) levels of Eu(III) (17500 cm^{-1}) and the $^5D_4$ level of Tb(III) (20400 cm^{-1}). For the energy transfer to Eu(III), the energy gaps between the triplet and the $^5D_0$ and $^5D_1$ levels are in the range of the optimum value of 3500 cm^{-1} proposed by Verhoeven et al.[106] For energy transfer to Tb^{III} the energy gap (2400 cm^{-1}) is below the threshold value, which induces the thermal energy

back transfer, as confirmed by the large increase of the lifetime of the terbium-centered emission in Tb^{3+}-complexes observed when the temperature is lowered from 298 K to 77 K. The longest lifetime observed in $[Eu(ttrpy)_3](ClO_4)_3$ (~2 ms) indicates that the Eu(III) ion is well protected from solvent access and free of deactivating water molecules in the first coordination sphere, consistent with the crystal structure and vibrational data, where three tridentate ttrpy ligands completely saturate the europium coordination sphere.

2.3.4.2 Near Infra Red (NIR) Luminescence from Neodymium

The solutions of $[Nd(ttrpy)_2Cl_2]Cl$ and $Nd(ttrpy)(NO_3)_3$, when excited with ligand absorption at about 350 nm, exhibit NIR luminescence due to the neodymium center observed (Figures 2.33-2.34). No luminescence in the visible region due to the ttrpy ligand was observed. Also the excitation spectrum corresponds to the absorption of the ligand. This indicates that the energy transfer from the ligand to the neodymium has occurred efficiently.[107] The ligand excitation results in narrow metal based emission peaks of neodymium which are due to transitions from $^4F_{3/2} \longrightarrow {}^4I_J$ (where J= 9/2, 11/2 and 13/2). The emission transition $^4F_{3/2} \longrightarrow {}^4I_{9/2}$ at about 880 nm is not observable due to instrument limitations.[§] The other two transitions at around 1064 nm ($^4F_{3/2} \longrightarrow {}^4I_{11/2}$) and 1330 nm ($^4F_{3/2} \longrightarrow {}^4I_{13/2}$) are observed. The emission peak of neodymium at 1064 nm can be used in potential laser systems such as Nd-YAG laser. The 1330 nm peak of the neodymium can be utilized as optical amplifier in telecommunications window.[108]

[§] The NIR scan region for the instrument is from 900 nm to 1400 nm. As the peak at 880 nm is out of this region, it was not observed.

There is direct absorption due to the neodymium observed at 585 nm but it is very weak compared to the ligand absorption at about 350 nm. The transitions are phosphorescent with lifetimes of less than 10 microseconds. The lifetime decays are monoexponential. The lifetimes obtained for these complexes are comparable to the literature values for the neodymium complexes.[109] The lifetimes of the chloride complex are shorter than those for the nitrate complex. The Nd(ttrpy)$(NO_3)_3$ complex has 3 υ_{N-O}(1650 cm^{-1}) peaks from the nitrate groups along with one υ_{O-H} (3300 cm^{-1}) from methanol, whereas the chloride complex of neodymium has one υ_{O-H} (3300 cm^{-1}) from methanol. Just considering the vibrational frequencies, the Nd(ttrpy)$(NO_3)_3$ should have shorter lifetimes because of quenching of its luminescence by multiphonon relaxation due to N-O and O-H vibrations. Apparently this is not the case. The chloride complex is most effectively quenched by the O-H vibrations of the methanol molecule with lower lifetimes than the Nd(ttrpy)$(NO_3)_3$ complex. As the measurements were done in methanol solvent, solvation effect may be the reason. The Nd(ttrpy)$(NO_3)_3$ is already 10 coordinated whereas the [Nd(ttrpy)$_2Cl_2$]Cl is only 8 coordinated. Additional methanol molecules, therefore, would have a higher chance to be coordinated to the [Nd(ttrpy)$_2Cl_2$]Cl complex, which makes it decay nonradiatively more easily than Nd(ttrpy$(NO_3)_3$.

The lifetimes of these neodymium complexes in different concentrations is given in table 2.10. An estimated quantum yield (QY) of the Nd(III) luminescence can be calculated for a complex by comparison of the complexed neodymium with the natural lifetime (the luminescence lifetime in the absence of quenching processes) of Nd, τ_0. By

using the equation 4, a QY of 0.35 % for the $[Nd(ttrpy)_2Cl_2]Cl$ and 3 % for the $Nd(ttrpy)(NO_3)_3$ was obtained with natural lifetime (τ_0) of Nd taken as 270 μs.[110] These quantum yield values are also comparable to the literature values.[109d]

$$\phi=\tau/\tau_0 \qquad (4)$$

Table 2.10 Lifetimes of neodymium complexes in methanol

Compound	τ, in μs		
	10^{-3} M	10^{-4} M	10^{-5} M
$[Nd(ttrpy)_2Cl_2]Cl$	0.789	0.957	1.189
$Nd(ttrpy)(NO_3)_3$	6.83	8.3	-

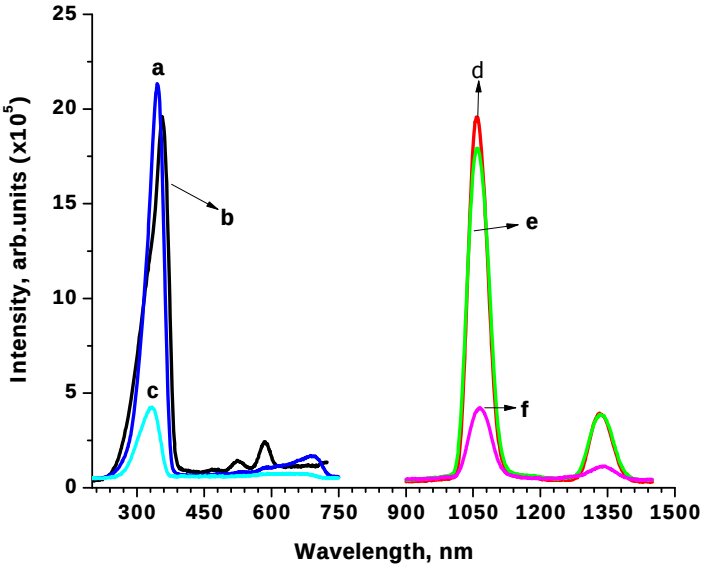

Figure 2.33. Excitation and emission spectra of $[Nd(ttrpy)_2Cl_2]Cl$ in methanol. Excitation spectra (a-c) and Emission spectra (d-f). (a) 10^{-4} M, λ_{emi} = 1060 nm (b) 10^{-3} M, λ_{emi} = 1060 nm (c) 10^{-5} M, λ_{emi} = 1060 nm (d) 10^{-3} M λ_{exc} = 355 nm (e) 10^{-4} λ_{exc} = 355 nm (f) 10^{-3} M λ_{exc} = 330 nm.

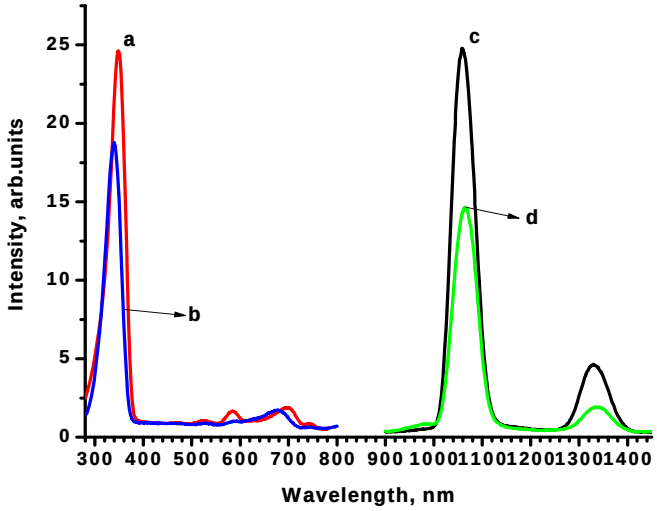

Figure 2.34. Excitation and emission spectra of $Nd(ttrpy)(NO_3)_3$ in methanol. Excitation spectra (a,b) and Emission spectra (c,d). (a) 10^{-3} M, λ_{emi} = 1060 nm (b) 10^{-4} M, λ_{emi} = 1060 nm (c) 10^{-3} M, λ_{exi} = 350 nm (d) 10^{-4} M, λ_{exi} = 350 nm.

2.4 Conclusions

Several lanthanide complexes of the ttrpy ligand, were synthesized and characterized. The crystal structures of all the compounds were obtained. UV-Vis absorption and IR spectra clearly indicated the formation of the compounds. The excitation spectra of the europium and terbium ttrpy compounds have shown ligand based absorption as dominant and no direct absorption due to europium or else terbium was observed when monitored with the lanthanide emission. This indicates the sensitization of lanthanide luminescence and confirms transfer of energy occurred in the excited state. As a result sensitized luminescence was observed in europium and terbium ttrpy compounds. The sensitized luminescence was very weak in the case of $Tb(hfa)_3(L)$. This is due to the back energy transfer from the terbium emitting level to the ligand triplet level. $Eu(hfa)_3L$ being a neutral complex used for OLED fabrication.

Triplet excitation pathway was effective in the sensitization of the lanthanides as the singlet pathway was not observed. The effect of the number of ttrpy ligands on the luminescence intensity and quantum yield was seen. The $[Eu(L)_3][(ClO_4)_3]$ has highest quantum yield among all the europium compounds in the solid state because of europium coordinating to three ttrpy ligands whereas. The phononic effect of counterions such as perchlorates and solvent was seen on the quantum yield. NIR emission from the Nd complexes was observed too.

2.5 References

[1] Lehn, J. -M. *Angew. Chem. Int. Ed. Engl.* **1990**, *29*, 1304-1319.

[2] (a) Horrocks, W. D., Jr.; Bolender, J. P.; Smith, W. D.; Supkowski, R. M. *J. Am. Chem. Soc*. **1997**, *119*, 5972-5973. (b) Bunzli, J. –C. G.; Piguet, C. *Chem*. *Rev*. **2002**, *102*, 1897-1928. (C) Tsukube, H.; Shinoda, S. *Chem. Rev*. **2002**, *102*, 2389-2403. (d) Wang, K.; Li, R.; Cheng, Y.; Zhu, B. *Coord*. *Chem*. *Rev*. **1999**, *190-192*, 297-308.

[3] (a) Zheng, Z. *Chem*. *Commun*. **2001**, *24*, 2521-2529. (b) Roigk, A.; Hettich, R.; Schneider, H. -J. *Inorg*. *Chem*. **1998**, *37*, 751-756.

[4] Mikola, H.; Takalo, H.; Hemmila, I. *Bioconjugate Chem*. **1995**, *6*, 235-241.

[5] (a) Bunzli, J.–C. G, in: Bunzli, J.-C. G.; Choppin, G. R. (Eds)., *Lanthanide Probes in Life, Chemical and Earth Science, Elsevier.* **1989**, *p 219*. (b) de Sa, G. F.; Malta, O. L.; de Mello Donega, C.; Simas, A. M.; Longo, R. L.; Santa-Cruz, P. A.; da Silva, E. F. Jr. *Coord*. *Chem*. *Rev*. **2000**, *196*, 165-195. (c) Krupa, J. C.; Queffelec, M. *J. Alloys*. *Compd*. **1997**, *250*, 287-292. (d) Wegh, R. T.; Meijerink, A. *Phys*. *Rev*. *B* **1999**, *60*, 10820-10830. (d) Hill, R. J.; Long, D. –L.; Hubberstey, P.; Schröder, M.; Champness, N. R. *J. Solid State Chem*. **2005**, *178*, 2414-2419.

[6] Ronda, C. R. *J. Alloys Compd*. **1995**, *225*, 534-538.

[7] Kido, J. *Chem*. *Rev*. **2002**, *102*, 2357-2368.

[8] (a) Parker, D.; Senanayake, P. K.; Williams, J. A. G. *J. Chem*. *Soc., Perkin Trans*. **1998**, *10*, 2129-2139. (b) Sokolnicki, J.; Wiglusz, R.; Radzki, S.; Graczyk, A.; Legendziewicz. *Opt*. *Mater*. **2005**, *249*, 2489-2509.

[9] Wang, K.; Rongchang, L.; Cheng, Y.; Zhu, B. *Coord*. *Chem*. *Rev*. **1999**, *190-192*, 297-308.

[10] Li, W. P.; Ma, D. S.; Higginbotham, C.; Hoffman, T.; Ketring, A. R.; Cutler, C. S.; Jurisson, S. S. *Nucl*. *Med*. *Bio*. **2001**, *28*, 145-154.

[11] Reichert, D. E.; Lewis, J. S.; Anderson, C. J. *Coord*. *Chem*. *Rev*. **1999**, *184*, 3-66.

[12] Bünzli, J. –C. G. *Acc*. *Chem*. *Res*. **2006**, *39*, 53-61.

[13] (a) Horrocks, W. D., Jr.; Sudnick, D. R. *J. Am*. *Chem*. *Soc*. **1979**, *101*, 334-340. (b) Horrocks, W. D., Jr.; Sudnick, D. R. *Acc*. *Chem*. *Res*. **1981**, *14*, 384-392. (c) Supkowski, R. M.; Horrocks, W. D., Jr. *Inorg*. *Chim*. *Acta* **2002**, *340*, 44-48. (d) Yanagida, S.; Hasegawa, Y.; Murakoshi, K.; Wada, Y.; Nakashima, N.; Yamanaka, T. *Coord*. *Chem*. *Rev*. **1998**, *171*, 461-480.

[14] (a) Binnemans, K.; Lenarts, P.; Driesen, K.; Gröller-Walrand, C. *J. Mater. Chem.* **2004**, *14*, 191-195. (b) Shavaleev, N. M.; Pope, S. J. A.; Bell, Z. R.; Faulkner, S.; Ward, M. D. *J. Chem. Soc., Dalton Trans.* **2003**, 808-814. (c) de Mello Donega´, C.; Junior, S. A.; de Sa´, G. F. *Chem. Commun.* **1996**, 1199-1200.

[15] (a) Chapman, R. D.; Loda, R. T.; Riehl, J. P.; Schwartz, R. W. *Inorg. Chem.* **1984**, *23*, 1652-1657. (b) Durham, D. A.; Frost, G. H.; Hart, F. A. *J. Inorg. Nucl. Chem.* **1969**, *31*, 833-838.

[16] (a) Brayshaw, P. A.; Bünzli, J.-C. G.; Froidevaux, P.; Harrowfield, J. M.; Kim, Y.; Sobolev, A. N. *Inorg. Chem.* **1995**, *34*, 2068-2076. (b) Harrowfield, J. M.; Kim, Y.; Skelton, B. W.; White, A. H. *Aust. J. Chem.* **1995**, *48*, 807-823.

[17] (a) Bretonnie`re, Y.; Wietzke, R.; Lebrun, C.; Mazzanti, M.; Pe´caut, J. *Inorg. Chem.* **2000**, *39*, 3499-3505. (b) Senegas, J.-M.; Bernardinelli, G.; Imbert, D.; Bünzli, J.-C. G.; Morgantini, P.-Y.; Weber, J.; Piguet, C. *Inorg. Chem.* **2003**, *42*, 4680-4695. (c) Koeller, S.; Bernardinelli, G.; Bocquet, B.; Piguet, C. *Chem. Eur. J.* **2003**, *9*, 1062-1074. (d) Koeller, S.; Bernardinelli, G.; Piguet, C. *J. Chem. Soc., Dalton Trans.* **2003**, 2395-2404. (e) Renaud, F.; Piguet, C.; Bernardinelli, G.; Bünzli, J.-C. G.; Hopfgartner, G. *J. Am. Chem. Soc.* **1999**, *121*, 9326-9342.

[18] (a) Moeller, T. *MTP International Review of Science, Series one:* Bagnall, K.W., Ed.; Butterworths: London, **1972**, Vol 7, pp 275-298. (b) Moeller, T.; Birnbaum, E. R.; Forsberg, J. H.; Gayhart, R. B. in *Progress in the Science and Technology of the Rare Earths.* Pergamon press*,* New York, **1968**, *Vol.* 3, pp 66-128. (c) Moeller, T.; Martin, D. F.; Thompson, L. C.; Ferrus, R.; Feistel.; Randall, W. J. *Chem. Rev.* **1965**, *65*, 1-50.

[19] Moeller, T.; Horwitz, E. P. *J. Inorg. Nucl. Chem.* **1959**, *12*, 49-59.

[20] Moeller, T.; Jackson, D. E. *Anal. Chem.* **1950**, *22*, 1393-1397.

[21] Forsberg, J. H.; Wathen, C. A. *Inorg. Chem.* **1971**, *10*, 1379-1383.

[22] Forsberg, J. H.; Moeller, T. *Inorg. Chem.* **1969**, *8*, 889-892.

[23] (a) Hart, F. A.; Laming, F. P. *Proc. Chem. Soc.* **1963**, 107-108. (b) Lobanov, N. I.; Smirnova, V. A. *Zh. Neorg. Khim.* **1963**, *8*, 2206-2207 (c) Lobanov, N. I.; Smirnova, V. A. *Zh. Neorg. Khim.* **1963**, *8*, 2208-2210.

[24] Selbin, J.; Ahmad, N.; Bhacca, N. *Inorg. Chem.* **1971**, *10*, 1383-1387.

[25] (a) Frechette, M.; Bensimon, C. *Inorg. Chem.* **1995**, *34*, 3520-3527. (b) Cotton, S. A.; Noy, O. E.; Liesener, F.; Raithby, P. R. *Inorg. Chim. Acta.* **2003**, *344*, 37-42. (c) Sinha, S. P. *Spectrochim. Acta.* **1964**, *20*, 879-886. (d) Moss, D. S.; Sinha, S. P. *Z. Phys. Chem.* **1969**, *63*, 190-192. (e) Hart, F. A.; Laming, F. P. *J. Inorg. Nucl. Chem.*

1964, *26*, 579-585. (f) Hart, F. A.; Laming, F. P. *J. Inorg. Nucl. Chem.* **1965**, *27*, 1605-1610. (g) Rohatgi, K. K.; Sen Gupta, S. K. *J. Inorg. Nucl. Chem.* **1970**, *32*, 2247-2253. (h) Sinha, S. P.; Butter, E. *Mol. Phys.* **1969**, *16*, 285-298.

[26] Peters, J. A.; Huskens, J.; Raber, D. J. *Prog. Nucl. Magn. Res. Spectrosco.* **1996**, *28*, 283-350.

[27] Arif, A. M.; Hart, F.A.; Hursthouse, M. B.; Pett, M. T.; Zhu, W. *J. Chem. Soc., Dalton Trans.* **1984**, 2449-2454.

[28] Melby, L. R.; Rose, N. J.; Abramson, E.; Caris, J. C. *J. Am. Chem. Soc.* **1964**, *86*, 5117-5125.

[29] Bauer, H.; Blanc, J.; Ross, D. L. *J. Am. Chem. Soc.* **1964**, *86*, 5125-5131.

[30] Yuan, Y. –F.; Cardinaels, T.; Lunstroot, K.; Hecke, K. V.; Meervelt, L. V.; Walrand, C. G.; Binnemans, K.; Nockemann, P. *Inorg. Chem.* **2007**, *46*, 5302-5309.

[31] Radanovich, L. J.; Glick, M. D. *Inorg. Chem.* **1971**, *10*, 1463-1468.

[32] Frost, G. H.; Hart, F. A.; Heath, C.; Hursthouse, M .B. *Chem. Comm.* **1969**, 1421-1422.

[33] Fukuda, Y.; Nakao, A.; Hayashi, K. *J. Chem. Soc., Dalton Trans.* **2002**, 527-533

[34] Holz, R. C.; Thompson, L. C. *Inorg. Chem.* **1988**, *27*, 4640-4644.

[35] De Silva, C. R.; Wang, J.; Carducci, M. D.; Rajapakshe, S. A.; Zheng, Z. *Inorg. Chim. Acta.* **2004**, *357*, 630-634.

[36] Frechette, M.; Butler, I. R.; Hynes, R.; Detellier, C. *Inorg. Chem.* **1992**, *31*, 1650-1656.

[37] Frechette, M. *Can. J. Chem.* **1993**, *71*, 377-383.

[38] Strzyzewska, M. B.; Tosik, A. *Inorg. Chim. Acta.* **1978**, *30*, 189-196.

[39] Tedmann, O. M.; Madan, S. K.; Zavalij, P. Y.; Oliver, S. R. J. *Inorg. Chim. Acta.* **2007**, *360*, 3408-3413.

[40] (a) Piguet, C.; Williams, A. F.; Bernardinelli, G.; Bünzli, J. –C. G. *Inorg. Chem.* **1993**, *32*, 4139-4149. (b) Piguet, C.; Bünzli, J. –C. G.; Bernardinelli, G.; Bochet, C. G.; Froidevaux, P. *J. Chem. Soc. Dalton. Trans.* **1995**, 83-97. (c) Petoud, S.; Bünzli, J. –C. G.; Schenk, K. J.; Piguet, C. *Inorg. Chem.* **1997**, *36*, 1345-1353.

[41] Maynard, B. A.; Smith, P. A.; Ladner, L.; Jaleel, A.; Beedoe, N.; Crawford, C.; Assefa, Z.; Sykora, R. E. *Inorg. Chem.* **2009**, *48*, 6425-6435

[42] Drew, M. G. B.; Iveson, P. B.; Hudson, M. J.; Liljenzin, J. L.; Spjuth, Lena.; Cordier, P. -Y.; Enarsson, A.; Hill, C.; Madic, C. *J. Chem. Soc., Dalton. Trans.* **2000**, 821-830.

[43] Bellusci, A.; Barberio, G.; Crispini, A.; Ghedini, M.; Deda, M. L; Pucci, D. *Inorg. Chem.* **2005**, *44*, 1818-1825.

[44] De Silva, C. R.; Wang, R.; Zheng, Z. *Polyhedron* **2006**, *25*, 3449-3455.

[45] Quici, S.; Cavazzini, M.; Marzanni, G.; Accorsi, G.; Armaroli, N.; Ventura, B.; Barigelletti, F. *Inorg. Chem.* **2005**, *44*, 529-537.

[46] Nugent, L. J.; Burnett, J. L.; Baybarz, R. D.; Werner, G. K.; Tanner, S. P.; Tarrant, J. R.; Keller, O. L., Jr. *J.* Phys. *Chem.* **1969**, *73*, 1540-1549.

[47] Yu, J.; Zhou, L.; Zhang, H. Z.; Zheng, Y.; Li, H.; Deng, R.; Peng, Z.; Li, Z. *Inorg. Chem.* **2005**, *44*, 1611-1618.

[48] APEX2 Version 2.1-0, Bruker Advanced X-ray Solutions Inc. (**2006**), Madison, WI.

[49] SHELXTL™ Version 6.14, Bruker Advanced X-ray Solutions Inc. (**2003**), Madison, WI

[50] Semenova, L. I.; Sobolev, A. N.; Skelton, B. W.; White, A. H. *Aust. J. Chem.* **1999**, *52*, 519-529.

[51] Constable, E.C.; Chotalia, R.; Tocher, D. A. *J. Chem. Soc., Chem. Commun.* **1992**, 771-773.

[52] Hu, N. –H.; Lin, Y. –H.; Shen, Q.; Xing, Y.; Shi, E. –D. *Acta Chim. Sinica.* **1986**, *44*, 388-391.

[53] Aspinall, H. C.; Bickley, J. F.; Greeves, N.; Kelly, R. V.; Smith, P. M. *Organometallics* **2005**, *24*, 3458–3467.

[54] Kepert, C. J.; Lu, W.; Skelton, B. W.; White, A. H. *Aust. J. Chem.* **1994**, *47*, 365-384.

[55] Berthet, J.-C.; Nierlich, M.; Miquel, Y.; Madic, C.; Ephritikhine, M. *Dalton Trans.* **2005**, 369-379.

[56] Berthet, J. -C.; Riviere, C.; Miquel, Y.; Nierlich, M.; Madic, C.; Ephritikhine, M. *Eur. J. Inorg. Chem.* **2002**, 1439-1446.

[57] Li, H. –X.; Xu, Q.- F.; Chen, J.- X.; Cheng, M.- L.; Zhang, Y.; Zhang, W.- H.; Lang, J.- P.; Shen, Q. *J. Organometallic. Chem.* **2004**, *689*, 3438-3448.

[58] (a) Lam, A. W. –H.; Wong, W. –T.; Gao, S.; Wen, G.; Zhang, X. –X. *Eur. J. Inorg. Chem.* **2003**, 149-163. (b) Singh, U. P.; Kumar, R. *J. Mol. Struc.* **2007**, *837*, 214-223.

[59] Berthet, J. –C.; Miquel, Y.; Iveson, P. B.; Nierlich, M.; Thuery, P.; Madic, C.; Ephritikhine, M. *J. Chem. Soc., Dalton Trans.* **2002**, *16*, 3265-3272.

[60] (a) Nakamoto, K. In *Infrared and Raman Spectra of Inorganic and Coordination Compounds. Part A. Theory and Applications in Inorganic Chemistry*. Wiley Interscience: New York, **1997**. (b) Nakamoto, K. In *Infrared and Raman Spectra of Inorganic and Coordination Compounds*. J. Wiley & Sons: New York, **1997**; 5th edition. Part B, pp 87-89.

[61] (a) Yang, C.; Wong, W. -T. *Chem. Lett.* **2004**, *33*, 856-857. (b) Yang, C.; Wong, W. T.; Chen, X.; Cui, Y.; Yansheng, Y. *Sci. China (B).* **2003**, *46*, 558-565. (c) Yang, C.; Wong, W. T. *J. Mater. Chem.* **2001**, *11*, 2898-2900. (c) Yang, C.; Chen, X. -M.; Cui, Y. –D.; Yang, Y. -S. *Chin. J. Chem.* **1999**, *17*, 411-414.

[62] (a) Beley, M.; Collin, J.-P.; Louis, R.; Metz, B.; Sauvage, J.-P. *J. Am. Chem. Soc.* **1991**, *113*, 8521-8522. (b) Yoshikawa, N.; Yamabe, S.; Kanehisa, N.; Kai, Y.; Takashima, H.; Tsukahara, K. *Eur. J. Inorg. Chem.* **2007**, *13*, 1911-1919. (c) Uma, V.; Vaidyanathan, V. G.; Nair, B.U. *Bull. Chem. Soc. Jpn.* **2005**, *78*, 845-850. (d) Zhou, X. –P.; Ni, W. –X.; Zhan, S. -Z.; Ni, J.; Li, D.; Yin, Y. –G. *Inorg. Chem.* **2007**, *46*, 2345-2347.

[63] (a) Yang, C.; Chen, X. –M.; Zhang, W. –H.; Chen, J.; Yang, Y. –S.; Gong, M. L. *J. Chem. Soc., Dalton Trans.* **1996**, *8*, 1767-1768. (b) Petoud, S.; Buenzli, J. -C. G.; Schenk, K. J.; Piguet, C. *Inorg. Chem.* **1997**, *36*, 1345-1353. (c) Nozary, H.; Piguet, C.; Tissot, P.; Bernardinelli, G.; Buenzli, J. -C. G.; Deschenaux, R.; Guillon, D. *J. Am. Chem. Soc.* **1998**, *120*, 12274-12288. (d) Ahrens, B.; Cotton, S. A.; Feeder, N.; Noy, O. E.; Raithby, P. R.; Teat, S. J. *J. Chem. Soc., Dalton Trans.* **2002**, *9*, 2027-2030.

[64] Binnemans, K. In *Handbook on the Physics and Chemistry of Rare Earths*.; Gschneidner, K. A. Jr.: Bünzli, J.-C.G.; Pecharsky, V. K., Eds.; Elsevier: Amsterdam, **2005**. Vol. 35, Ch. 225

[65] Zhou, X.; Yang, C.; Le, X.; Chen, S.; Liu, J.; Huang, Z. *J. Coord. Chem.* **2004**, *57*, 401-409.

[66] Bernadinelli, G.; Piguet, C.; Williams, A. F. *Angew. Chem., Int. Ed. Engl.* **1992**, *31*, 1622-1624.

[67] Li, Y.; Huffman, J. C.; Flood, A. H. *Chem. Comm.* **2007**, 2692-2694.

[68] Petoud, S.; Buenzli, J. -C. G.; Renaud, F.; Piguet, C.; Schenk, K. J.; Hopfgartner, G. *Inorg. Chem.* **1997**, *36*, 5750-5760.

[69] Wang, R.; Song, D.; Wang, S. *Chem. Commun.* **2002**, *4*, 368-369.

[70] (a) Yang, C.; Fu, L. -M.; Wang, Y.; Zhang, J. -P.; Wong, W. –T.; Ai, X. –C.; Qiao, Y. –F.; Zou, B. –S.; Gui, L. –L. *Angew. Chem., Int. Ed.* **2004**, *43*, 5010-5013; *Angew. Chem.* **2004**, *116*, 5120-5123. (b) Petoud, S.; Muller, G.; Moore, E. G.; Xu, J.; Sokolnicki, J.; Riehl, J. P.; Le, U. N.; Cohen, S. M.; Raymond, K. N. *J. Am. Chem. Soc.* **2007**, *129*, 77-83. (c) Coppo, P.; Duati, M.; Kozhevnikov, V. N.; Hofstraat, J. W.; Cola, L. D. *Angew. Chem., Int. Ed.* **2005**, *44*, 1806-1810.

[71] Jaradat, Q.; Akasheh, T. *Polyhedron* **1987**, *6*, 175-179.

[72] Brewer, D. G.; Wong, P. T. T.; Sears, M. C. *Can. J. Chemistry.* **1968**, *46*, 3137-3141.

[73] Katrizky, A. R. Chemistry. In *Methods in Heterocyclic chemistry.* Vol. 4, (Academic Press, New York) **1971,** P. 325.

[74] (a) Sutcliffe, V. F.; Young, G. B. *polyhedron* **1984**, *3*, 87-94. (b) Jaradat, Q.; Barqawi, K.; Akasheh, T. S. *Inorg. Chim. Acta.* **1986**, *116*, 63-73.

[75] (a) Paryzek, W. R.; Jankowska, E.; Luks, E. *Polyhedron* **1988**, *7*, 439-442. (b) Paryzek, W. R.; Jankowska, E. *Inorg. Chim. Acta.* **1987**, *134*, 179-183.

[76] Scholer, R. P.; Merbach, A. E. *Inorg. Chimica. Acta.* **1975**, *15*, 15-20.

[77] Bünzli, J. -C. G.; Wessner, D. *Inorg. Chim. Acta.* **1980**, *44*, L55-L58.

[78] Perlepes, S. P.; Galinos, A. G. *J. Less- Common Met.* **1984**, *96*, 69-77.

[79] Biju, S.; Raj, D. B. A.; Reddy, M. L. P.; Kariuki, B. M. *Inorg. Chem.* **2006**, *45*, 10651-10660.

[80] Aebischer, A.; Gumy, F.; Bünzli, J. –C. G. *Phys. Chem. Chem. Phys.* **2009**, *11*, 1346-1353.

[81] Zhang, H. -J.; Gou, R. –H.; Yan, L.; Yang, R. –D. *Spectrochim. Acta A.* **2007**, *66*, 289-294.

[82] Charbonniére, L. J.; Weibel, N.; Retailleau, P.; Ziessel, R. *Chem. Eur. J.* **2007**, *13*, 346-358.

[83] Chen, W. -H.; Reinheimer, E. W.; Dunbar, K. R.; Omary, M. A. *Inorg. Chem.* **2006**, *45*, 2770-2772.

[84] De Schryver, F. C.; Collart, P.; Vandendriessche, J.; Goedeweeck, R.; Swinnen, A. M.; Van der Auweraer, M. *Acc. Chem. Res.* **1987**, *20*, 159−166.

[85] (a) Deiters, E.; Song, B.; Chauvin, A. –S.; Vandevyver, C. D. B.; Bünzli, J. –C. G. *New J. Chem.* **2008**, *32*, 1140-1152. (b) Chauvin, A. –S.; Bünzli, J. –C. G.; Bochud, F.; Scopelliti, R.; Froidevaux, P.*Chem. Eur. J.* **2006**, *12*, 6852-6864. (c) Comby, S.; Imbert,

D.; Chauvin, A. –S.; Bünzli, J. –C. G.; Charbonniere, L. J.; Ziessel, R. F. *Inorg*. *Chem*. **2004**, *43*, 7369-7379. (d) Martin, N.; Bünzli, J. –C. G.; McKee, V.; Piguet, C.; Hopfgartner, G. *Inorg*. *Chem*. **1998**, *37*, 577-589.

[86] (a) Yang, C.; Messerschmidt, M.; Coppens, P.; Omary, M. A., *Inorg*. *Chem*. **2006**, *45*, 6592-6594. (b) Burress, C.; Elbjeirami, O.; Omary, M. A.; Gabbai, F. P. *J*. *Am*. *Chem*. *Soc*. **2005**, *127*, 12166-12167.

[87] Liu, Y. –F.; Rong, D. –F.; Xia, H. –T.; Wang, D. –Q.; Chen, Liang. *Journal of Coordination Chemistry.* **2009**, *62*, 1835-1845.

[88] Sinha, S. P. *J. Inorg*. *Nucl*. *Chem*. **1966**, *28*, 189-193.

[89] Lim, E. C. In *Excited States*, Academic Press: New York, **1982**.

[90] Blasse, G.; Dirksen, G. J.; Sabbatini, N.; Perathoner, S.; Lehn, J. M.; Alpha, B. *J*. *Phys*. *Chem*. **1988**, *92*, 2419-2422.

[91] Eliseeva, S. V.; Ryazanov, M.; Gumy, F.; Troyanov, S. I.; Lepney, L. S.; Bünzli, J.-C.G.; Kuzmina, N. P. *Eur*. *J*. *Inorg*. *Chem*. **2006**, 4809-4820.

[92] Pavithran, R.; Reddy, M. L. P.; Junior, S. A.; Freier, R. O.; Rocha, G. B.; Lima, P. P. *Eur. J. Inorg*. *Chem*. **2005**, 4129-4137.

[93] (a) Liang, H.; Wu, W.; Wang, Y.; Li, Z. *Spectrochim*. *Acta A*. **2005**, *61*, 2687-2690. (b) Wang, C.; Yan, B. *J*. *Non-Cryst*. *Solids* **2008**, *354*, 962-969.

[94] De Silva, C. R.; Maeyer, J. R.; Wang, R.; Nichol, G. S.; Zheng, Z. *Inorg*. *Chim*. *Acta*. **2007**, *360*, 3543-3552.

[95] Lenaerts, P.; Ryckebosch, E.; Driesen, K.; Deun, R. V.; Nockemann, P.; Walrand, C. G.; Binnemans, K. *J Lumin*. **2005**, *114*, 77-84.

[96] Klink, S. I.; Hebbink, G. A.; Grave, L.; Peters, F. G. A.; Van Veggel, F. C. J. M.; Reinhoudt, D. N.; Hofstraat, J. W. *Eur*. *J*. *Org*. *Chem*. **2000**, 1923-1931.

[97] Werts, M. H. V.; Jukes, R. T. F.; Verhoeven, J. W. *Phys*. *Chem. Chem*. *Phys*. **2002**, *4*, 1542-1548.

[98]. Braga, S. S.; Sá Ferreira, R. A.; Goncalves, I. S.; Pillinger, M.; Rocha, J.; Teixeira-Dias, J. J. C.; Carlos, L. D. *J*. *Phys*. *Chem*. *B*. **2002**, *106*, 11430-11437.

[99] (a) Sokolnicki, J.; Legendziewicz. J.; Muller, G.; Riehl, J. P. *Opt. Mater.* **2005**, *27*, 1529-1536. (b) Gawryszewska, P.; Jerzykiewicz, L.; Pietraszkiewicz, M.; Legendziewicz, J.; Riehl, J. P. *Inorg*. *Chem*. **2000**, *39*, 5365-5372. (c) Malta, O.L.; Legendziewicz, J.;

Huskowska, E.; Tyrk, T. I.; Albuquerque, R. Q.; de Silva, F. R. G.; de Mello, D. *J. Alloys Compd.* **2001**, *323-324*, 654-660. (d) Latva, M.; Takalo, H.; Mukkala, V. –M.; Matachescu, C.; Ubis, J. C. R.; Kankare. *J. Lumin*. **1997**, *75*, 149-169. (e) Sabbatini, N.; Guardigli, M.; Lehn, J. –M. *Coord. Chem. Rev*. **1993**, *123*, 201-228.

[100] Palsson, L. -O.; Monkman, A. P. *Adv* . *Mater*. **2002**, *14*, 757-758.

[101] (a) Bünzli, J.-C.G.; Piguet, C. *Chem. Soc. Rev.* **2005**, *34*, 1048–1077. (b) Bünzli, J.-C. G. *Acc. Chem. Res*. **2006**, *39*, 53-61. (b) Bünzli, J.-C. G. *Spectroscopic* Pr*operties of Rare Earths in Optical Materials.;* Liu, G.; Jacquier, B., Eds.; Springer Verlag: Berlin, **2003**.

[102] Riehl, J. P.; Muller, G. In *Handbook on the Physics and Chemistry of Rare Earths*.; Gschneidner, K. A., Jr.; Bünzli, J.-C.G.; Pecharsky, V. K., Eds.; North-Holland Publishing Company: Amsterdam, **2005**; Vol. 34, Chapter 220, pp. 289-357, see also references therein

[103] Carnall, W. T.; Fields, P. R.; Rajnak, K. *J. Chem. Phys*. **1968**, *49*, 4450-4455.

[104] Carnall, W. T.; Fields, P. R.; Rajnak, K. *J. Chem. Phys*. **1968**, *49*, 4447-4449.

[105] Sabbatini, N.; Guardigli, M.; Manet, I. In *Antenna Effect in encapsulation complexes of lanthanide ions. Handbook on the Physics and Chemistry of Rare Earths*.; Gschneidner, K. A.; Eyring, L., Eds.; Elsevier: Amsterdam, **1996**, 23, ch. 154

[106] Steemers, F. J.; Verboom, W.; Reinhoudt, D. N.; van der Tol, E. B.; Verhoeven, J. W. *J. Am. Chem. Soc*. **1995**, *117*, 9408-9414.

[107] (a) Yang, X.; Jones, R. A.; Wu, Q.; Oye, M. M.; Lo, W. –K.; Wong, W. –K.; Homes, A. L. *polyhedron* **2006**, *25*, 271-278. (b) Petoud, S.; Cohen, S. M.; Bunzli, J. –C. G.; Raymond, K. N. *J. Am. Chem. Soc*. **2003**, *125*, 13324-13325.

[108] Sun, L. -N.; Zhang, H. –J.; Peng, C. –Y.; Yu, J. –B.; Meng, Q. –G.; Fu, L.- S.; Liu, F. –Y.; Guo, X. –M. *J. Phys. Chem. B* **2006**, *110*, 7249-7258.

[109] (a) Bassett, A. P.; Magennis, S. W.; Glover, P. B.; Lewis, D. J.; Spencer, N.; Parsons, S.; Williams, R. M.; De Cola, L.; Pikramenou, Z. *J. Am. Chem. Soc*. **2004**, *126*, 9413-9424. (b) Hasegawa, Y.; Kimura, Y.; Murakoshi, K.; Wada, Y.; Kim, J. – H.; Nakashima, N.; Yamanaka, T.; Yanagida, S. *J. Phys. Chem*. **1996**, *100*, 10201-10205. (c) Roh, S. –G.; Kim, Y. H.; Beak, N. S.; Hong, K. –S.; Kim, H. K. *Mol. Cryst. Liq. Cryst*. **2006**, *446*, 295-304. (d) Shavaleev, N. M.; Scopelliti, R.; Gumy, F.; Bunzli, J. –C. G. *Inorg. Chem*. **2008**, *47*, 9055-9068. (d) Rizzo, F.; Destri, S.; Porzio, W.; Ottonelli, M.; Dellepiane, G.; Meinardi, F.; Monguzzi, A. *Mater. Sci. Eng., B.* **2008**, *146*, 45-49.

[110] Weber, M. J. *Phys. Rev*. **1968**, *171*, 283-291.

CHAPTER 3

PHOTOPHYSICS OF SILVER-AROMATIC COMPLEXES

3.1 Introduction

There has been increasing interest in cation-π interactions for the last two decades. This is because this kind of complex was involved in a variety of phenomena such as biochemical activity, molecular recognition, catalysis, chemistry in condensed phases etc.[1] There is significant work done in the area of alkali-metal-cation/π interactions.[2] Researchers have found that the Li^+-π interactions are short range whereas Ag^+-π interactions are long range interactions.[3] Zhu et al. have studied the cation-π interactions in aqueous solution.[4] They were studying the influence of different cations on the formation of cation-π interactions and their role in the environment. They found that the strong cation-π bonding observed between Ag^+ and aromatic hydrocarbons is attributed to covalent interactions between aromatic π electrons and the d orbitals of Ag^+, in addition to the normal electrostatic interactions. Upon interaction with an aromatic ligand the d- orbitals undergo splitting and polarization to optimally interact with the ligand orbitals.[5] Although soft base cations and soft transition metals (e.g., Cs^+; Ag^+) have weaker cation-π interactions they are stronger compared to hard base cations (e.g., Li^+; Na^+).

Many transition metal cations can accept π-electrons from unsaturated organic molecules and, thus, form very stable organometallic molecules. The Ag(I) cation is known to form comparatively weak interactions with aromatic molecules; hence,

measurements of association constants of Ag(I) with simple aromatic hydrocarbons lead to a conclusion that more extended conjugated electronic system is, the stronger the Ag(I)–π interaction.[4,6] The investigation of silver-aromatic compounds was first initiated by Hill in 1921.[7] Later in the 1950s, Mulliken and Dewar have formulated theoretical models for the bonding of silver perchlorate with benzene.[8] The first crystal structure of a complex of a silver perchlorate with benzene was published in 1950,[9] and later accurately refined in 1958.[10] From 1960s Amma et al. carried out a systematic investigation of the silver(I)-aromatic interactions. Several complexes of Ag(I) with aromatics are known in the literature from different stoichiometries and stereochemistry including benzene,[9,10,11] *m*-xylene,[12] *o*-xylene,[13] indene,[14] cyclohexylbenzene,[15] acenaphthene,[16] acenapthylene,[16] naphthalene,[17] anthracene.[17b,18] Several others also worked on the complexes of silver(I) with aromatics such as toluene,[19] paracyclophane,[20] cyclophane,[21] 9,10-diphenyl-anthracene,[22] rubrene[22] and stilbene.[23] Dargel et al. have calculated the binding energies for the Ag^+ interaction with the benzene.[24] They found that the Ag^+ binds to the benzene in a η^6 fashion with the metal ion being above the π plane of benzene.

Polycyclic aromatic hydrocarbons (PAHs) are a special class of organic molecules and their rich aromatic chemistry has aroused an interest in the study of the synthesis, coordination, property and theory for aromatic systems.[25] Many polycyclic aromatic hydrocarbons have been employed as exceptional donor molecules or as acceptor molecules in order to form donor-acceptor systems or else studied for charge transfer molecular systems because of their low ionization energy and extended delocalized π

system.[26] Polycyclic aromatic hydrocarbons have received considerable interest for their use in the construction of organic electronic devices for the past few decades.[27] Acenes are fused benzene rings in a rectilinear arrangement.[27c] These acenes are most commonly employed in two classes of electronic devices. Organic field effect transistors (OFETs, also called as organic thin-film transistors, OTFTs) and organic light-emitting diodes (OLEDs).[27b] The tuning of molecular properties such as solubility and stability are difficult with oligoacenes, which becomes a hurdle to take full advantage of organic electronics.[28] Incorporation of fluorine into acenes may contribute to the tuning of the electronic properties, and thus altering the π stacking in aryl-fluoroaryl interactions.[25i,28, 29] Larger acenes such as pentacene and graphene when doped with Ag^+ ions and its complexes could increase the mobility of their OTFT devices.

Several complexes of polycyclic aromatic hydrocarbons with metal ions with novel molecular architecture involving cation-π interactions have been received significant attention because of their electric and electrochemical properties.[9 -15a,16,17a,18-19,30] Budka et al. have found that infinite tubular assemblies based on preorganized π electron rich calix[4]arene cavities can be easily constructed using silver cation-π interactions in the solid state.[31] Munakata et al. have constructed a multidecker anthracene-silver(I) system using anthracene derivaties based on cation-π bonding and noncovalent aromatic stackings.[32] Munakata et al. have synthesized and characterized several organosilver compounds.[22,26,32] Most of these compounds were showing different architecture from double layer to multiple layer structures.[30a] The main interest was to synthesize and characterize these silver(I) coordination polymers of large

polycyclic aromatic hydrocarbons. Hill et al. have reported the formation of 1:1 complexes of silver with single ring aromatics.[33] Since then, PAHs are considered as potential donors for the formation of complexes with Ag(I).[34] Munakata et al. have written a review on the formation of Ag^+-PAH complexes in various phases.[30a] Lee et al. have demonstrated the fluorescence quenching of various PAHs by Ag^+, which can be used to quantify their Ag+ complexation constants.[35]

Despite the aforementioned strong interest that the cation-π (and Ag^+-π in particular) interaction concept has received; it is surprising that the associated photophysics have not been seriously investigated prior to this effort. It is well known that in aromatic molecules transition from singlet to triplet states are generally forbidden due to the orthogonality of the spin functions.[36] To be able to induce transitions between states of different spin multiplicity, spin-orbit perturbations are generally required. As the spin-orbit coupling is relatively small in these compounds because they contain light atoms of low Z (H=1, C=6), introduction of heavy atoms close to the fluorophore influences the spin-orbit coupling and increases the rate of intersystem crossing, ($S_0 \longrightarrow T_n$). This is due to the interactions between the orbital angular moment of the hydrocarbons and the spin angular moment of the heavy atom's nucleus. The incorporation of heavy atoms into molecular systems leads to changes in the photophysical parameters due to the enhancement intercombination transitions, which have come to be known as heavy atom effect. This effect was first discovered by Kasha.[36a] Here we report the characterization of several complexes of $AgClO_4$ with PAHs

such as naphthalene, pyrene, anthracene and perylene. Structures of the aromatics employed are shown below (Figure 3.1).

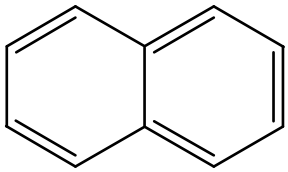

Naphthalene

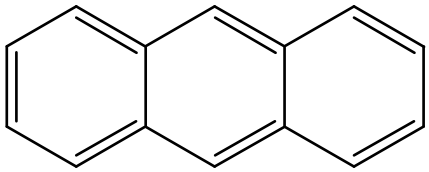

Anthracene

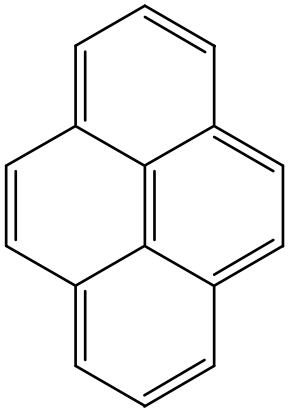

Pyrene

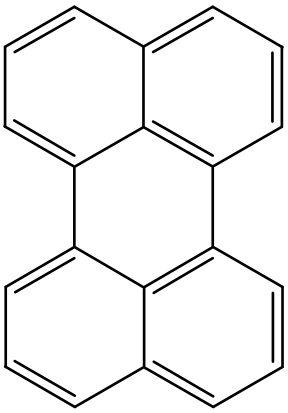

Perylene

Figure 3.1. Structure of various aromatics.

So far these complexes were synthesized and their single crystal X-ray diffraction studies were done. Their electronic properties have not been probed, however. We also studied the changes in the luminescence properties of aromatics upon coordination with silver(I) which quench fluorescence and leads to observance of phosphorescence characteristic of the aromatic ring in the solid state and also study the quenching mechanisms of fluorescence involved in the solution state.

3.2 Experimental Section

Silver perchlorate was obtained from Sigma-Aldrich and used as received. Naphthalene and anthracene were purchased from Lancaster. Pyrene and perylene were purchased from Aldrich. Naphthalene, anthracene, perylene and pyrene were sublimed before use. The solvents, toluene bought from Fox scientific and Hexane obtained from EMD chemicals, were distilled prior to use using standard procedure. The 2-methyl tetrahydrofuran solvent used in frozen studies was distilled and freeze pump thawed 3 cycles before use.

3.2.1 Synthesis

3.2.1.1 $\{[Ag_4(\text{tetra-}\eta^2\text{-naphthalene})][(ClO_4)_4]\}.H_2O$

This reaction was carried out as specified in the literature[17a] with little modification. Thus, 0.05 g (3.9×10^{-4} moles) of naphthalene was dissolved in minimum amount of distilled toluene. To this 0.3234g (1.56×10^{-3} moles) of $AgClO_4$ dissolved in minimum amount of distilled toluene was added. Later the reaction mixture was stirred at 0 °C for 2 hours under argon atmosphere. After that the reaction mixture was layered with distilled hexane and left in the refrigerator. After 2-3 days, crystals were obtained. M. P. = 120 °C (decomposed)

3.2.1.2 $\{[Ag_2(\text{tetra-}\eta^2\text{-pyrene})][(ClO_4)_2]\}$ and $\{[Ag_2(\text{tetra-}\eta^2\text{-perylene})][(ClO_4)_2]\}$

These reactions were done as per the procedure in the literature[37] with minor changes. Thus, 0.1g (3.96×10^{-4} moles) of perylene was dissolved in minimum amount of distilled toluene. To this 0.1643g (7.92×10^{-4} moles) of silver perchlorate was added

which was dissolved in minimum amount of distilled toluene. Later the solution mixture was stirred at 0 °C under argon atmosphere. After that it was layered with distilled hexane and left at refrigerator for crystal growth. Yellow brick red crystals were obtained. M.P. = 140 °C (decomposed).

To one mole of pyrene, 2 molar equivalents of $AgClO_4$ were added in distilled toluene. Layered with distilled pentane and pale yellow crystals were obtained.

3.2.1.3 $\{[(Ag)_4(\text{tetra-}\eta^2\text{-anthracene})][(ClO_4)_4]\}.H_2O$

The synthesis was carried out according to the procedure described in the literature[18] with little modification. Thus, 0.05g ($2.8x10^{-4}$ moles) of anthracene was dissolved in minimum amount of distilled toluene. To this 0.2326g ($1.12x10^{-3}$ moles) of silver perchlorate was added which was dissolved in minimum amount of distilled toluene. Later the solution mixture was stirred at 0 °C under argon atmosphere. The solution was then layered with distilled hexane and left in the refrigerator for crystal growth. Three days later crystals were obtained. M.P. = 150-160 °C (decomposed).

For all the compounds, crystal structures were confirmed by measuring the cell constants and compared with the literature.

3.3 Results and Discussion

3.3.1 Luminescence Data

The photoluminescence spectra of adducts of silver with naphthalene, anthracene, perylene and pyrene at 77 K is given in Figure 3.2. $\{[Ag_4(\text{tetra-}\eta^2\text{-naphthalene})][(ClO_4)_4]\}$, $\{[Ag_2(\text{tetra-}\eta^2\text{-pyrene})][(ClO_4)_2]\}$ and $[(Ag)_4(\text{tetra-}\eta^2\text{-}$

anthracene)][$(ClO_4)_4$] were exhibiting structured emission whereas the {[$(Ag)_4$(tetra-η^2-perylene)][$(ClO_4)_4$]} was showing the broad excimer like emission.

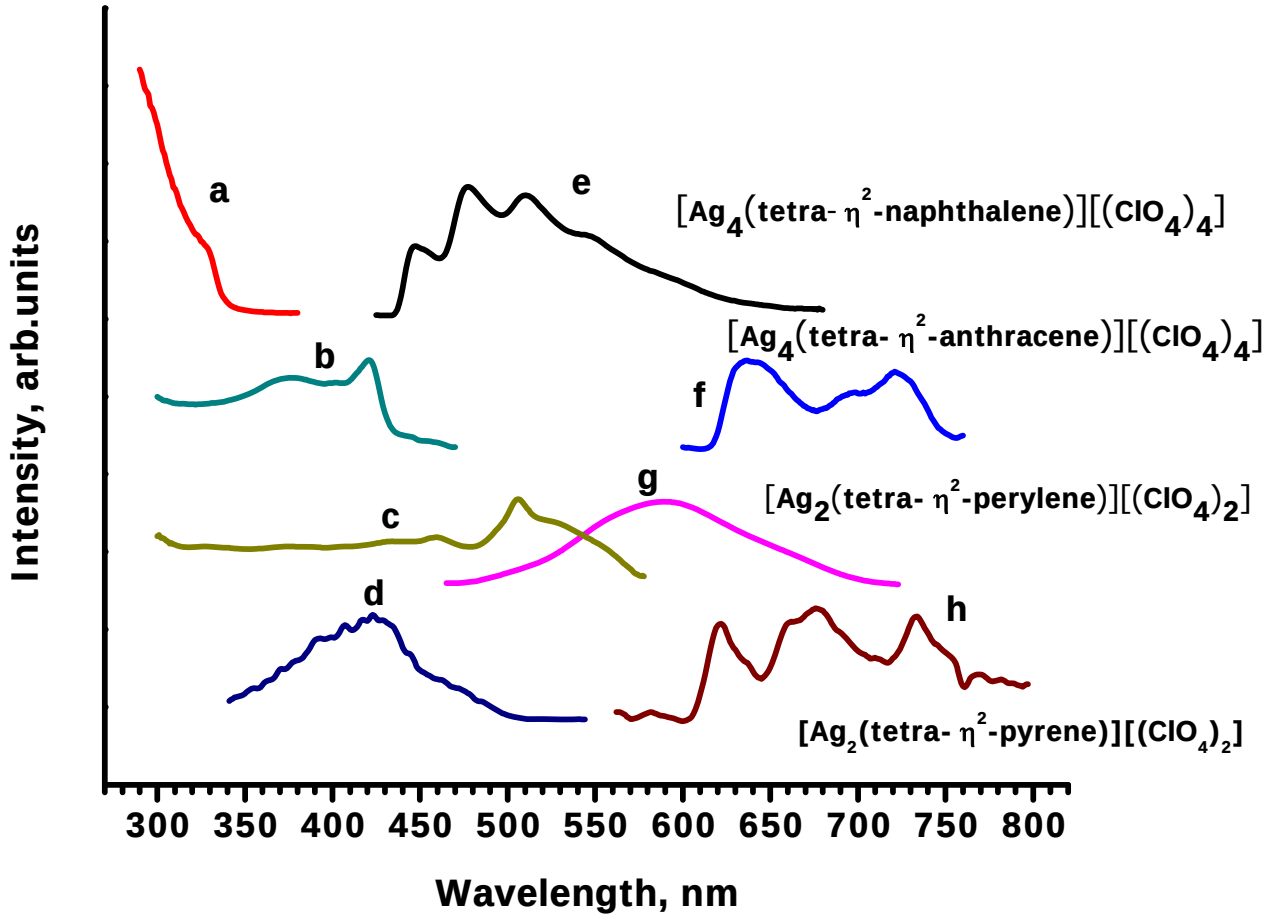

Figure 3.2 Excitation spectra (a-d) and emission spectra (e-h) of {[Ag_4(tetra-η^2-naphthalene)][$(ClO_4)_4$]}, [$(Ag)_4$(tetra-η^2-anthracene)][$(ClO_4)_4$], {[Ag_2(tetra-η^2-perylene)][$(ClO_4)_2$]} and {[Ag_2(tetra-η^2-pyrene)][$(ClO_4)_2$]} in the solid state at 77 K.

The spin-orbit perturbations of electronic states of molecules play an important role in the photophysics of molecules. In hydrocarbons, the excited triplet states are

nonemissive because of forbidden T_1-S_o transitions.[38] These triplet states can become phosphorescent upon presence of significant spin-orbit coupling due to a heavy atom. Heavy atom effect is internal or intramolecular and external, internal when the heavy atom is directly bonded to the fluorophore and external when the heavy atom is in the vicinity. For molecules containing heavy atoms, higher probability of intersystem crossing ($S_1 \longrightarrow T_1$) occurs. As a result, there will be quenching in the fluorescence (lower quantum yield) and sensitization in the phosphorescence (higher quantum yield). The internal heavy atom effect may be employed for experimentally probing the electronic structure of molecules. With this in mind, we can experimentally produce materials with predetermined properties. In order to establish the relationship between luminescence properties and the molecular structure, external heavy atom effect is also an important phenomenon.[39] Here we are probing the heavy atom effect of silver on the polyfused arenes such as naphthalene, anthracene, pyrene and perylene. These cation-π interactions bring significant changes on the photophysical properties of the aromatics. Pyrene shows monomer and excimer emissions. Monomer and excimer of pyrene exhibits fluorescence. Upon complexation with $AgClO_4$, monomer phosphorescence is observed. Pyrene monomer fluorescence is blue in color whereas the solid complex of pyrene with $AgClO_4$ that we have synthesized exhibit red phosphorescence. Pure naphthalene shows monomer fluorescence in the UV range. Upon complexation with $AgClO_4$, it exhibits enhanced green monomer phosphorescence. Figure 3.3 shows the excitation and emission spectra of the $\{[Ag_4(\text{tetra-}\eta^2\text{-naphthalene})][(ClO_4)_4]\}$ complex. The emission spectrum at 77 K is

more resolved than at RT. At RT, the emission spectrum is broad with a lifetime of 177 μs whereas at 77 K it is resolved into two peaks with a lifetime of 531 μs.

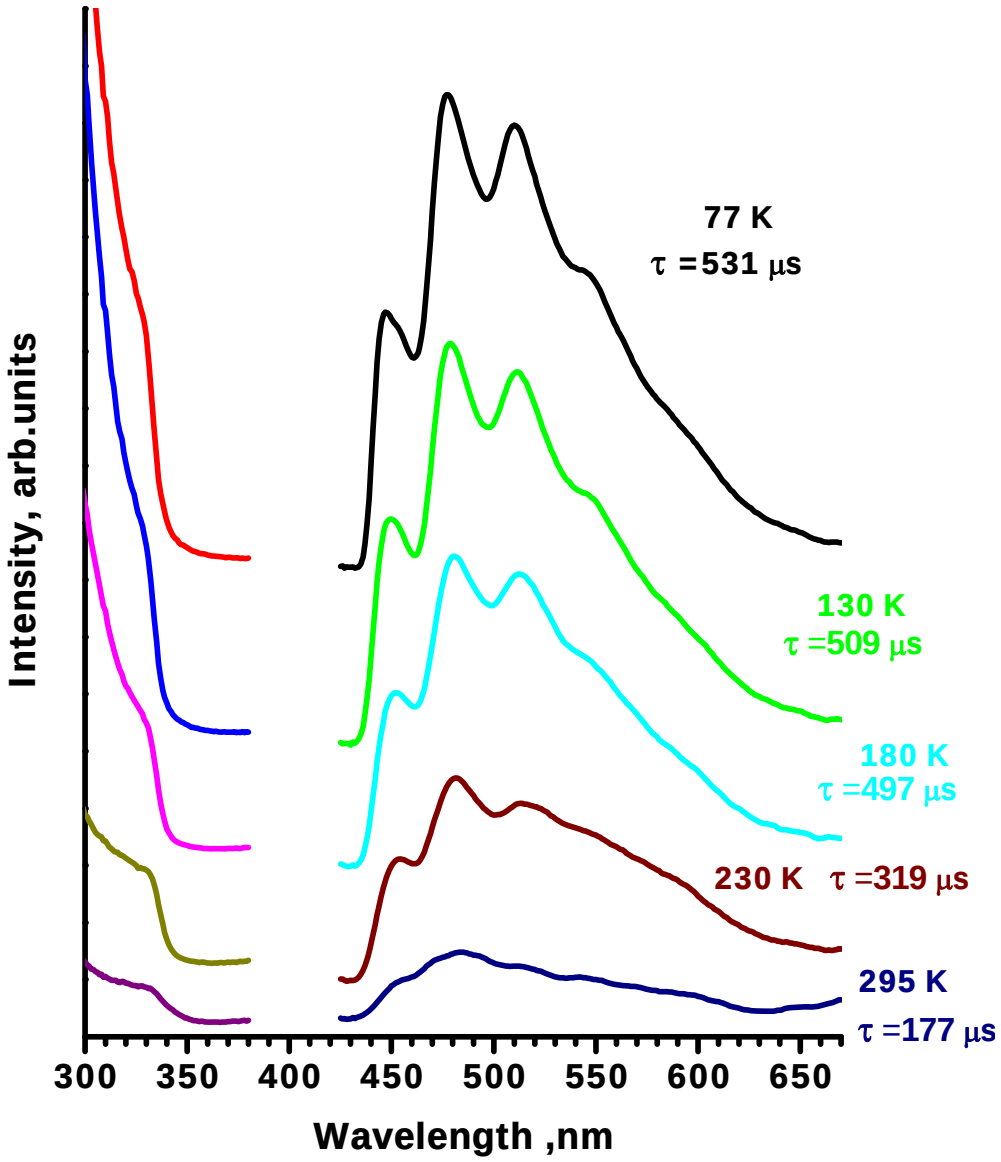

Figure 3.3. Photoluminescence spectra of {[Ag_4(tetra-η^2-naphthalene)][$(ClO_4)_4$]}.H_2O. λ_{exc} = 325 nm λ_{emi} = 475 nm.

In case of naphthalene and pyrene, no fluorescence emission is observed at all as the spectra are dominated by the phosphorescence emissions. The spin-orbit coupling due to the heavy atom (Silver) makes the forbidden singlet- triplet intersystem crossing allowable. Triplet states gain radiative character by spin-orbit coupling.[40] This intersystem crossing will be effective when the energy gap between the excited singlet to the excited triplet is small. This could be the reason why we could see strong phosphorescence signal in naphthalene (E_S-E_T= 10,500 cm^{-1})[41] and pyrene (E_S-E_T= 9,000 cm^{-1}).[41] In anthracene (E_S-E_T= 11700 cm^{-1}),[41] however very weak phosphorescence peak was observed. In perylene (E_S-E_T= 10,842 cm^{-1}), we could not see any phosphorescence peak at all. This energy difference is comparable to the energy difference in the case of naphthalene. According to Jin et al. any PAH whose triplet energy is below 14,000 cm^{-1} will be very hard to observe the phosphorescence signal[42] for this reasoning is consistent with our observations for the Ag^+ adducts of perylene and anthracence (T_1 = 12,600 cm^{-1} and 14,700 cm^{-1}, respectively).[43] The anthracene triplet energy is slightly above the threshold. This could be another reason why its phosphorescence is very weak. The triplet energies of naphthalene and pyrene are 20,980 cm^{-1} and 16,748 cm^{-1} respectively, which are significantly higher than the 14,000 cm^{-1} threshold. As a result, we are able to observe the phosphorescence peaks in both their Ag^+ adducts.

As with fluorescence, the most basic rule for polyaromatic hydrocarbon compounds involves the shift of the phosphorescence toward longer wavelengths with an increase in the ring size.[44] As a result the phosphorescence of anthracene (3 rings)

occurs at longer wavelengths than that of naphthalene (2 rings). For compounds having the same number of fused rings, the linear PAHs usually show phosphorescence at longer wavelengths than nonlinear (bent) PAHs.[45] As all the PAHs under study have π electrons, all the transitions are due to π-π*. The S_0-T_1 (π-π*) absorption of aromatic hydrocarbons is generally enhanced by spin-orbit perturbation due to the heavy atom, silver.[46] If the PAHs have n-π* absorptions as in ketones, they are insensitive to heavy atom perturbation.

The solid complex of perylene with silver perchlorate studied herein exhibits a broad structureless peak around 600 nm with a weak shoulder at about 510 nm (Figure 3.5). This indicates that the perylene molecules were held close to each other by the silver atoms showing the excimer emission. The shape of the emission peak did not change but the intensity decreases upon increasing the temperature. Figure 3.5 shows the excitation and emission spectra of {[Ag_2(tetra-η^2-perylene)][$(ClO_4)_2$]}. Even the lifetimes also decrease upon increasing the temperature from 77K to RT. This is due to the enhancement of radiationless relaxation processes at higher temperatures. The lifetime of the {[Ag_2(tetra-η^2-perylene)][$(ClO_4)_2$]} at 77K is 84.1 ns which is comparable to frozen solution of perylene in cyclohexane.[47,48]

Johnson et al. observed perylene excimer fluorescence upon freezing the solution with increasing pressure.[48] Sangster et al. has found perylene solid at 30 °C to exhibit excimer fluorescence at 579 nm.[49] Seko et al. studied perylene microcrystals showing excimer fluorescence.[50] Actually perylene exists in α and β forms.[51] The α form is dimeric and shows excimeric fluorescence while the β form exhibits structured

emission which is monomeric in nature like that of naphthalene[52] and anthracene.[46] The crystal structure {[Ag_2(tetra-η^2-perylene)][(ClO_4)$_2$]} was a 2-dimensional W type sandwich sheet of alternating perylene and $AgClO_4$ groups (Figure 3.4). These 2 D sheets are further connected by the superposed aromatic π-π sheets at an average distance of 3.31 Å. The perylene was coordinated with four Ag atoms in tetra-η^2 fashion forming W shaped sandwich sheet. There are no direct interactions of the cation, Ag^+ with the π electron cloud of perylene. The broad excimeric like emission as in α form of perylene in the {[Ag_2(tetra-η^2-perylene)][(ClO_4)$_2$]} is due to the interaction of perylene rings with each other (Figure 3.4). The emission peak of the {[Ag_2(tetra-η^2-perylene)][(ClO_4)$_2$]} complex is red shifted by 20 nm when compared to that of pure perylene by itself. This is caused by the coordination of silver with the perylene. But this interaction is not very strong for the spin orbit coupling which allows the appearance of phosphorescence of perylene which shows about 795 nm.

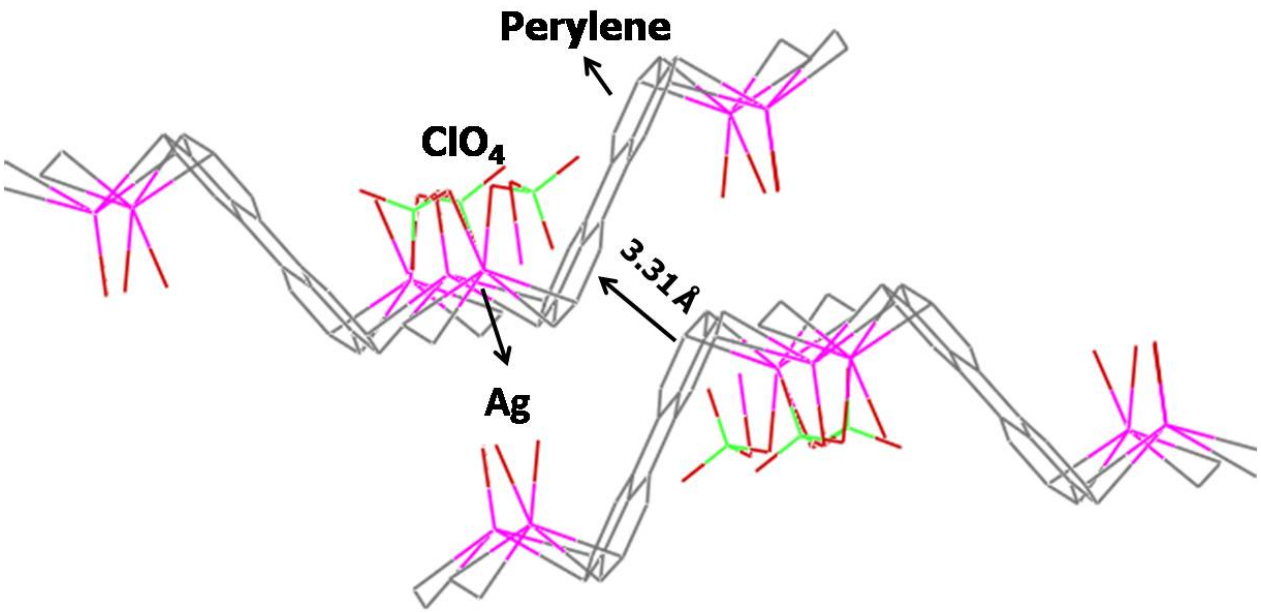

Figure 3.4 Crystal structure of {[Ag_2(tetra-η^2-perylene)][$(ClO_4)_2$]}.[37]

Another interesting feature is observed with the luminescence of the {[Ag_2(tetra-η^2-perylene)][$(ClO_4)_2$]} complex. There was a single very broad peak with weak shoulder seen in the steady state emission (Figure 3.5). But when time-resolved measurements were carried out, two emission peaks were resolved. Figure 3.6 shows the time-resolved emission spectra of {[Ag_2(tetra-η^2-perylene)][$(ClO_4)_2$]} at 77 K.

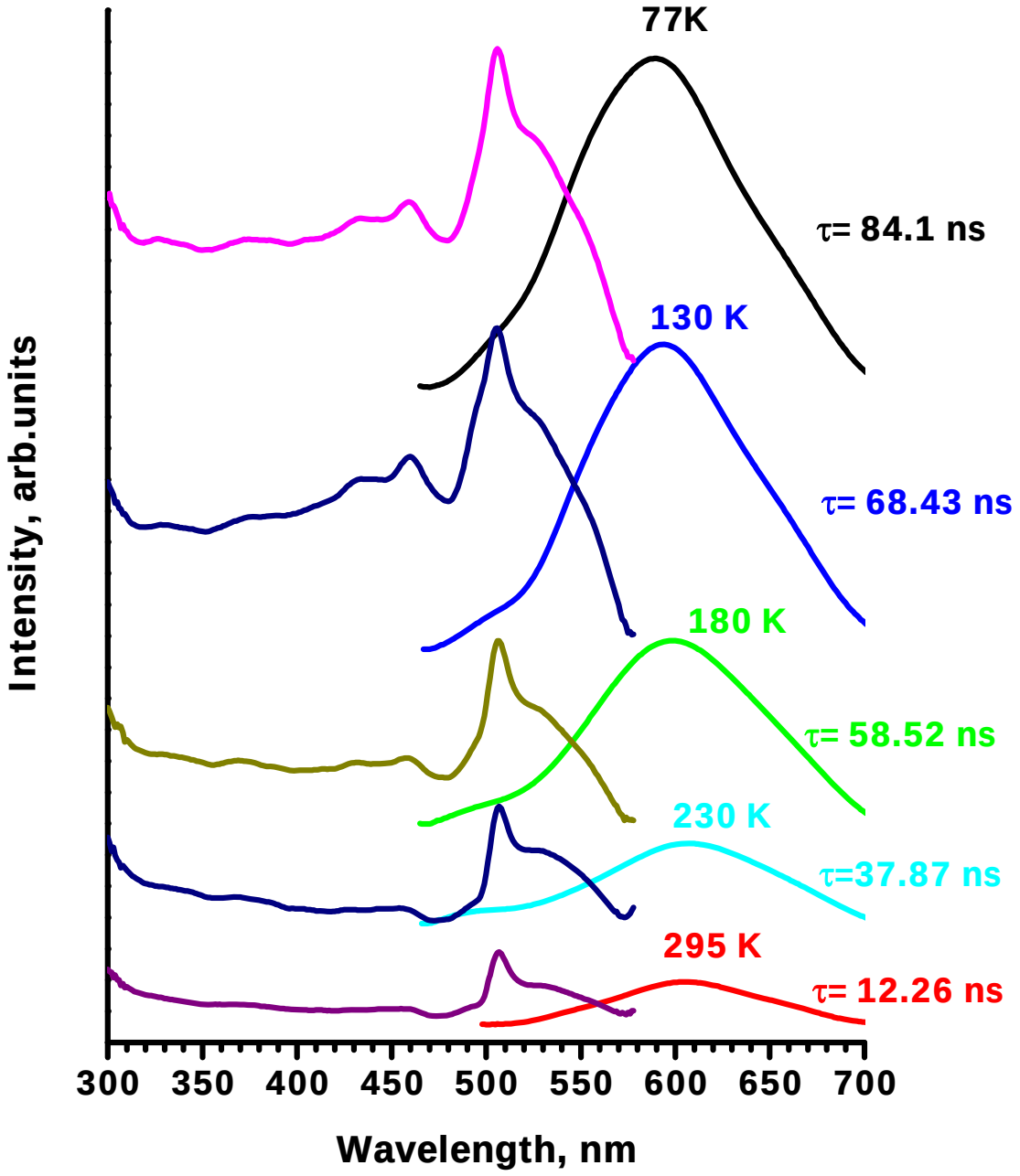

Figure 3.5. Excitation and emission spectra of {[Ag_2(tetra-η^2-perylene)][(ClO_4)$_2$]}. λ_{exc} = 450 nm λ_{emi} = 620 nm.

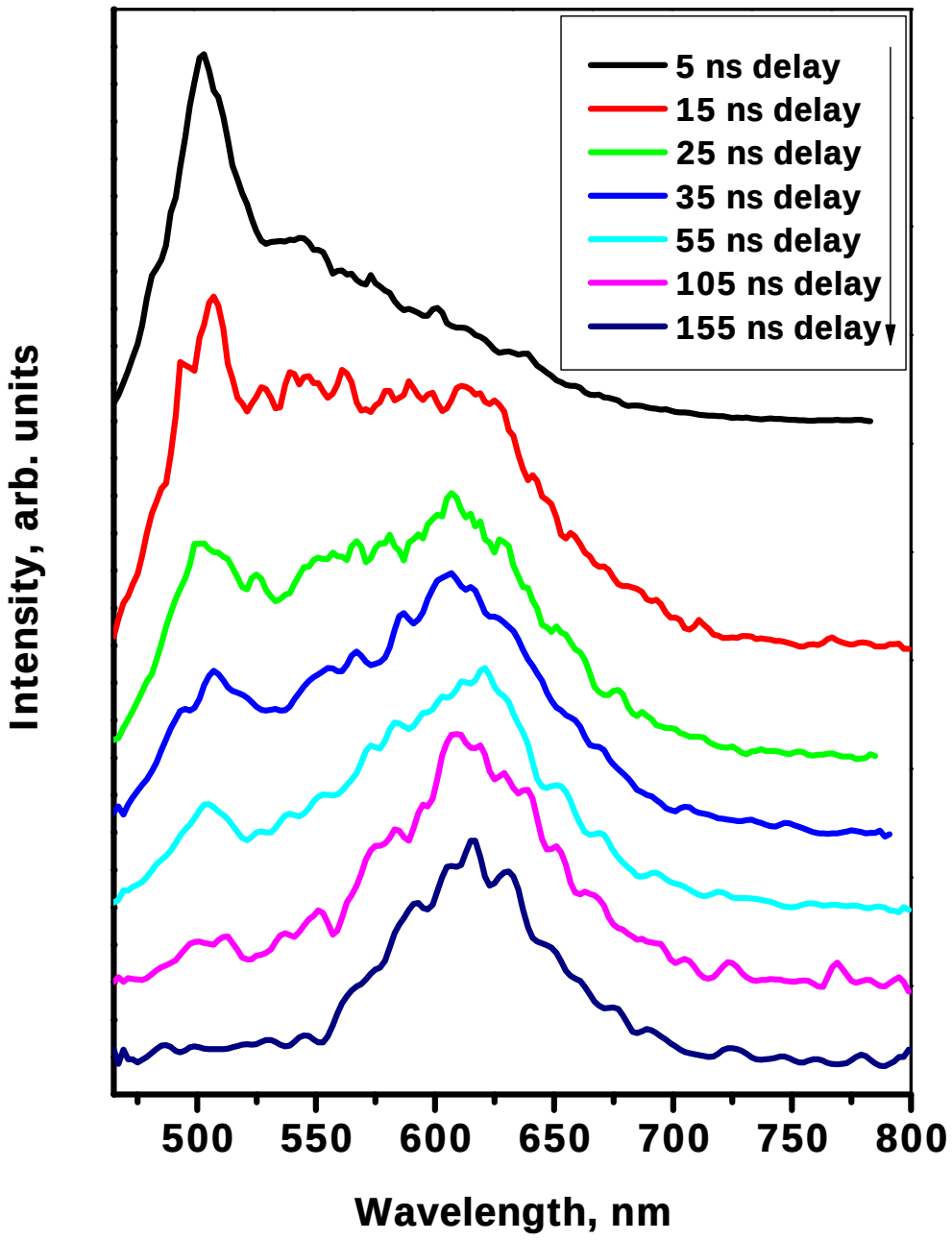

Figure 3.6 Time resolved spectra of {[Ag_2(tetra-η^2-perylene)][$(ClO_4)_2$]} at 77 K.

At 5 ns delay, a peak with maximum at about 500 nm appears along with its shoulder extending up to 650 nm. This peak at 500 nm with 5 ns delay corresponds to the weak shoulder as observed in the emission spectra of the {[Ag_2(tetra-η^2-perylene)][$(ClO_4)_2$]} (Figure 3.5). At 155 ns delay, this peak at 500 nm disappears completely and a broad peak centered about 630 nm becomes dominant which was the major peak in steady state emision. At 5 ns delay, the compound exhibits the features of β perylene and by 105 ns it was exhibiting emission similar to α perylene. The perylene rings of the 2 D sheets of {[Ag_2(tetra-η^2-perylene)][$(ClO_4)_2$]} are weakly overlapping at a distance of 3.31 Å with each other resulting in the excimer emission similar to the α perylene. Phase changes from β to α occurred to the perylene by changes in temperature[51a] and pressure.[51b]

Naphthalene complex with Ag, {[Ag_4(tetra-η^2-naphthalene)][$(ClO_4)_4$]} was exhibiting green emission. This emission is ascribed to monomer phosphorescence based on the structured profile of the emission. According to Chandra and Lim, excimer triplet state is unstable with respect to dissociation into monomer triplet and a monomer ground state.[53] This emission from the complex cannot be triplet excimer because naphthalene excimer triplet was broad as observed by Langelaar et al.[54] Takemura also obtained naphthalene triplet excimer in isooctane at 293 K in the same region as observed by Langelaar.[55] So the emission observed is from the naphthalene monomer and not excimer. This is also confirmed by the crystal structure where excimer formation is inhibited by the presence of silver atom between two different naphthalene rings. A chem draw of the structure is given in the Figure 3.7. The

naphthalene T_1 state emission is enhanced in the presence of silver due to the spin-orbit coupling. The phosphorescence spectrum of the complex is similar to the profile of naphthalene T_1 state. The intensity and vibronic resolution increased as we lowered the temperature from RT to 77 K, which is expected as the inhibition of nonradiative depopulation of T_1 state upon cooling. Figure 3.3 shows the excitation and emission spectra of the {[Ag_4(tetra-η^2-napthalene)][$(ClO_4)_4$]}. The excitation band is red shifted compared to the absorption peak of naphthalene[56] suggesting that this could be due to the charge transfer excitation route as known in the literature for Au_3, Ag_3 and Hg_3 heavy atom sensitizers.[38,57,58] There is charge transfer from the π electrons of the naphthalene ring to the Ag^+.

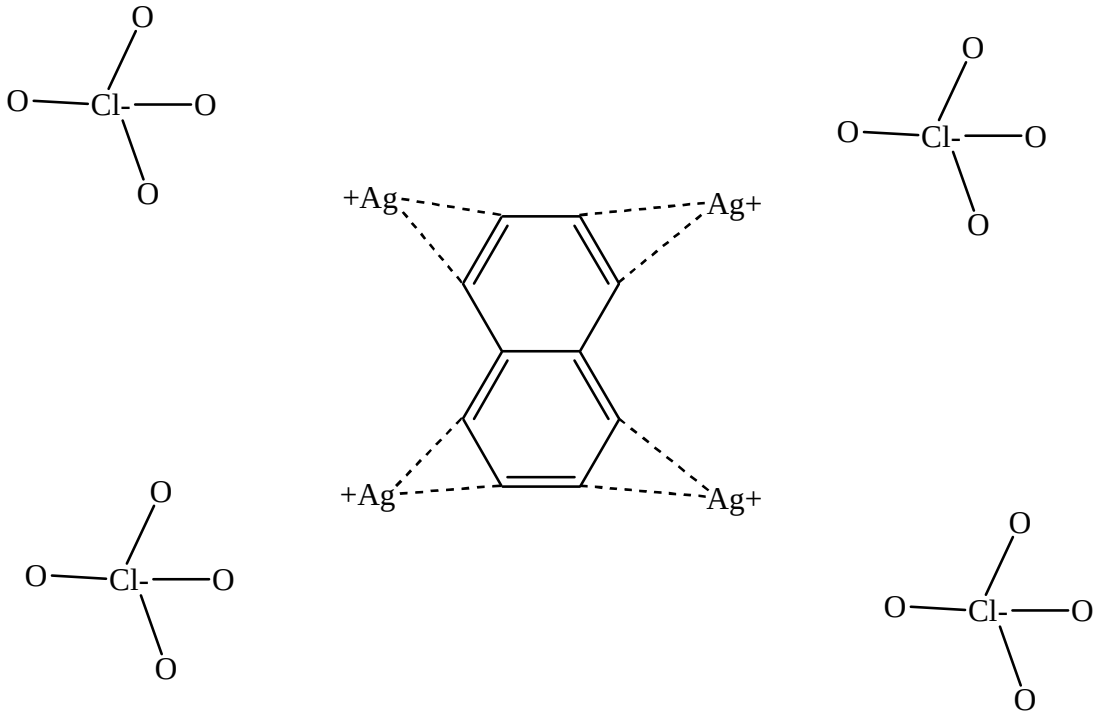

Figure 3.7 Crystal structure diagram of {[Ag_4(tetra-η^2-naphthalene)][$(ClO_4)_4$]}.

The external heavy atom effect of silver is further assessed by lifetime measurements. The phosphorescent lifetime of the complex at 295 K, 230 K, 180 K, 130 K and 77 K are 177, 319, 497, 509 and 531 μs, respectively. These lifetimes are much shorter than the lifetime of naphthalene monomer phosphorescence reported in the literature in EPA glass and in frozen CH_2Cl_2 solution.[39,59] A similar situation was noticed by Omary and co workers with silver trimer pyrazolate complex with naphthalene.[58] Gabbaï et al. have found that mercury trimer complex, $[Hg(o\text{-}C_6F_4)]_3$ upon π complexation with polycyclic aromatic compounds shown an intense T_1-S_0 monomer phosphorescence with reduction in triplet lifetimes by upto 5 orders of magnitude.[59]

Anthracene complex with silver, $\{[(Ag)_4(\text{tetra-}\eta^2\text{-anthracene})][(ClO_4)_4]\}$ showing very weak phosphorescence peaks in the 600-780 nm region along with monomer fluorescence emission of anthracene (Figure 3.10). The crystal structure shown is a chem draw picture (Figure 3.8). Even in this complex as in the naphthalene complex, there is no interaction between two anthracene rings. As a result there is no possibility of excimer formation. Each anthracene molecule is bonded to four silver atoms at 1, 4, 5 and 8 positions. There are no metal-carbon bonds to the 9 and 10 positions of the anthracene which is where generally the bonding is expected based on free valence and atom polarizabiltiy.[60]

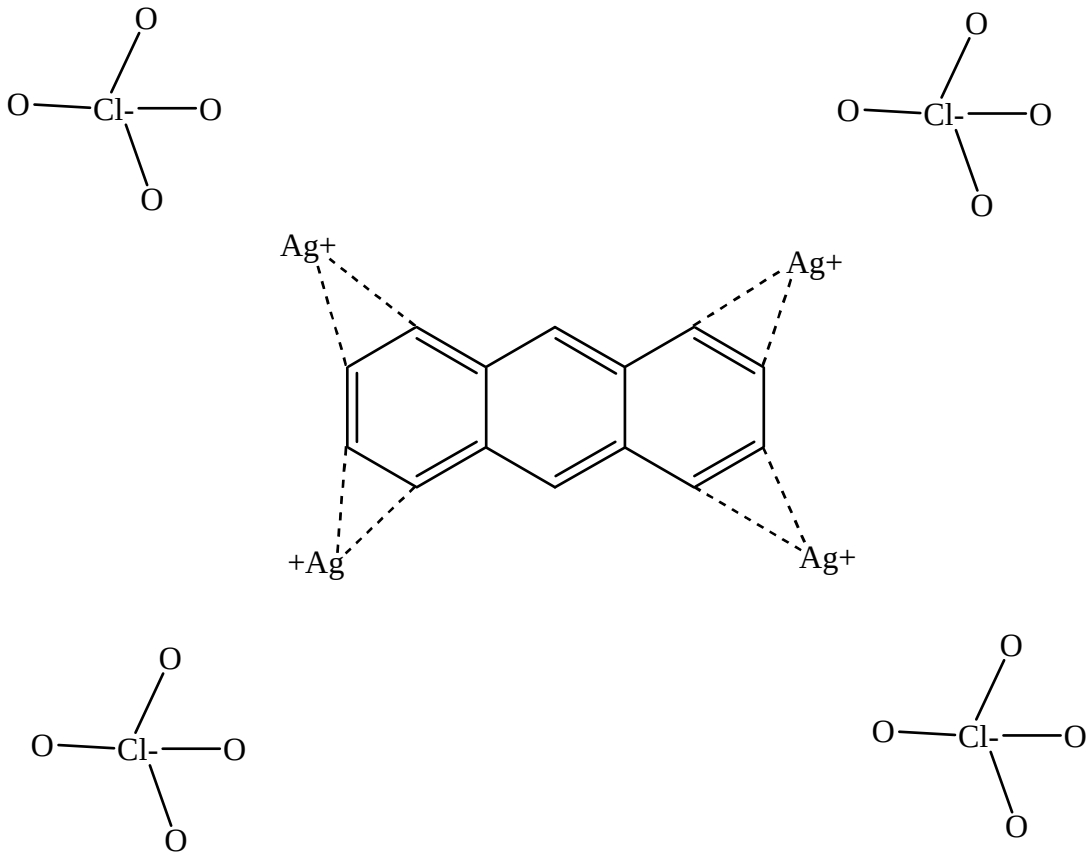

Figure 3.8 Crystal structure diagram of {[$(Ag)_4$(tetra-η^2-anthracene)][$(ClO_4)_4$]}.

The monomer fluorescence emission is stronger than the weak phosphorescence peaks. When excited with 320 nm, both monomer fluorescence and phosphorescence peaks were observed. The excitation spectra exhibits one peak at about 415 nm when monitored at 450 nm emission whereas it has two peaks (375 nm and 415 nm) when monitored at 640 nm. The phosphorescence spectrum of this complex is less resolved when compared to the free anthracene phosphorescence spectrum.[61] Not only less resolved but also they are blue shifted compared to free anthracene. But the profile of the spectrum resembles to that of free anthracene. The 0-0 peak of anthracene appears

at 14,927 cm^{-1} whereas in the complex it is at 15,698 cm^{-1}. Bathochromic shift of 0-0 peak of anthracene was observed in chlorinated compounds of anthracene[61] and in 9-nitroanthracene.[62] The emission peak at 637 nm was dominant at 77K whereas the peak at 721nm was dominant at RT. Figure 3.9 is the solid state photoluminescence of $\{[(Ag)_4(\text{tetra-}\eta^2\text{-anthracene})][(ClO_4)_4]\}$. These phosphorescence emission peaks of the complex are assigned to $T_1 \rightarrow S_0$ transitions which are in the range with anthracene peaks.[46] The lifetime at RT is almost half when compared to 77 K which is due to the competitive nonradiative decay as we increase the temperature from 77 K to RT.

The excitation peaks in the $\{[(Ag)_4(\text{tetra-}\eta^2\text{-anthracene})][(ClO_4)_4]\}$ complex are due to $S_0 \rightarrow S_1$ transitions as the $S_0 \rightarrow T_1$ transitions of anthracene are in the region of 500-650 nm. These observations are in accordance with the literature.[44,46]

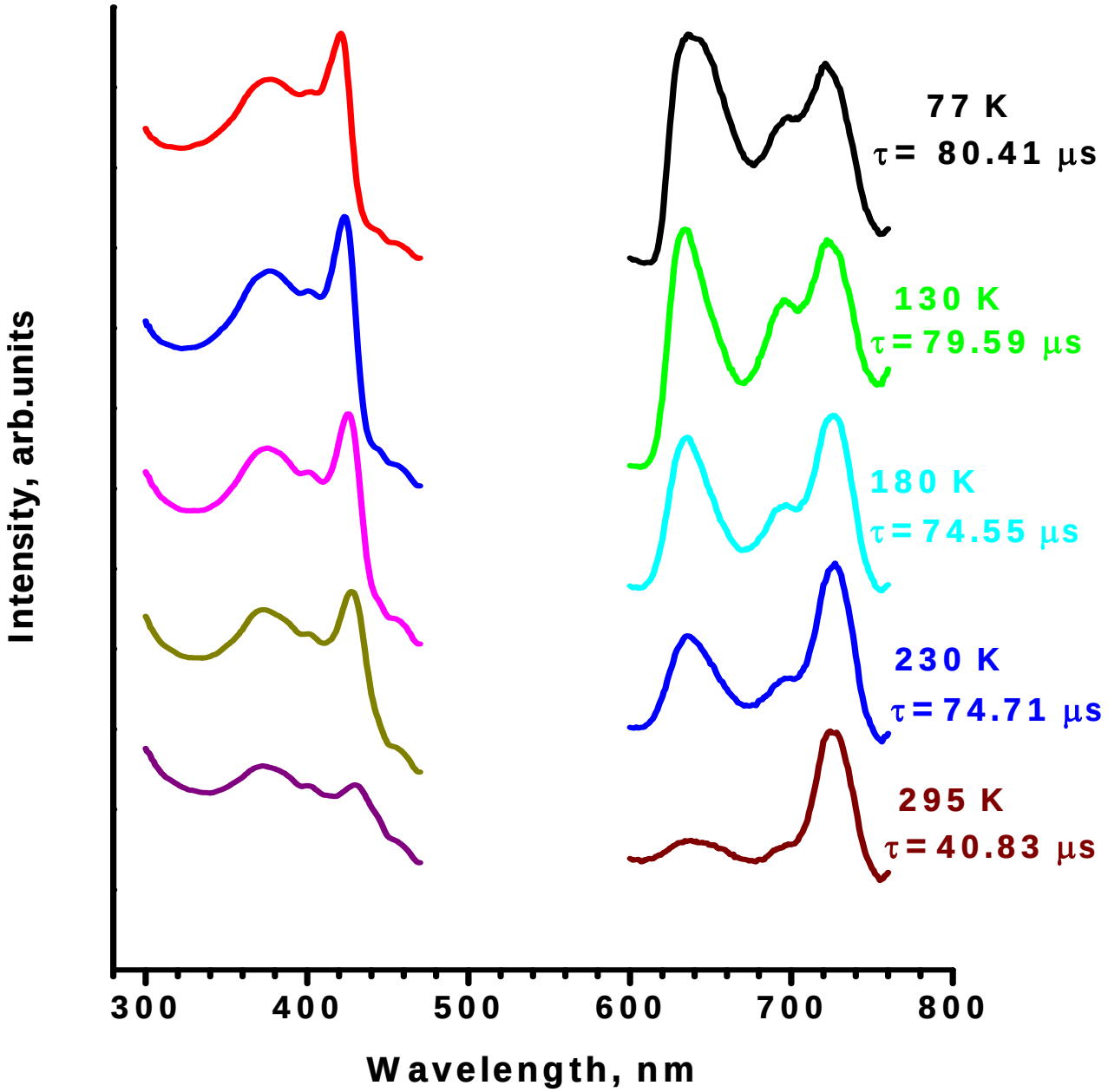

Figure 3.9. Solid state photoluminescence of $\{[(Ag)_4(\text{tetra-}\eta^2\text{-anthracene})][(ClO_4)_4]\}$. λ_{exc} = 420 nm λ_{emi} = 640 nm.

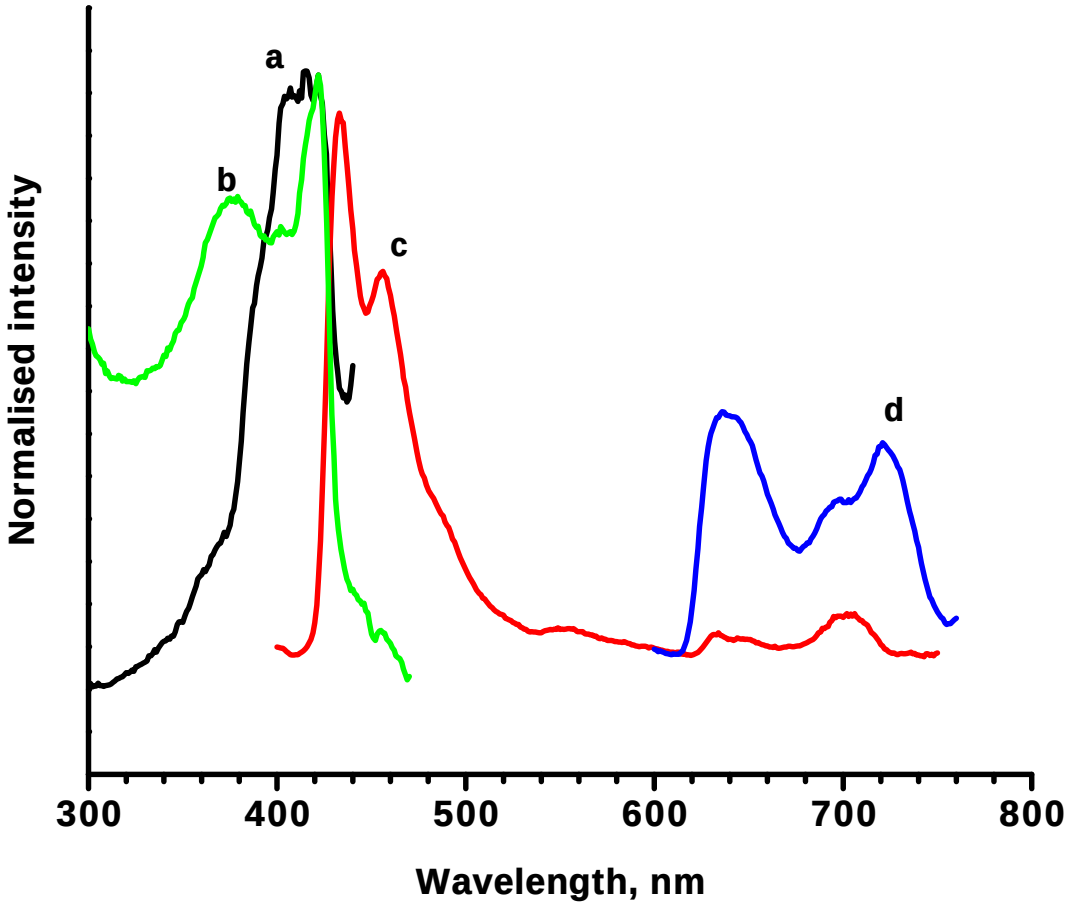

Figure 3.10. Photoluminescence spectra of {[$(Ag)_4$(tetra-η^2-anthracene)][$(ClO_4)_4$]} solid at 77 K. a. excitation spectra with λ_{emi} = 450 nm b. excitation spectra with λ_{emi} = 640 nm c. emission spectra with λ_{exc} = 320 nm d. emission spectra with λ_{exc} = 420 nm.

3.3.2 Fluorescence Quenching Studies

Quenching is a radiationless process involving two molecules, the fluorophore and the quencher. Fluorophore is the one which upon excitation emits fluorescence and the quencher is the chemical species which reduces the observed fluorescence of the fluorophore. Fluorescence quenching can be defined as any process which decreases

the observed fluorescence intensity of any sample.[63] The trivial phenomena such as primary and secondary absorption as well as light scattering due to changes in refractive index and turbidity of the solution are included in the above definition. The phenomenon of fluorescence quenching provides a kinetic method for detection and determination of quencher molecules.[64] It is also useful in the estimation of diffusion coefficient of oxygen in swollen polymers.[65] Eftink and Ghiron showed the successful use of fluorescence quenching techniques to study protein dynamics.[66]

In fluorescence quenching, it is important to know the type of molecular process and the nature of inner mechanism involved in the quenching.[67] The quenching phenomenon can be explained by two different processes.[56] One is the static quenching, where the fluorophore and quencher interact with each other in the ground state and form a ground-state complex that does not emit in the excited state. Such a complex is called as dark complex.[68] The ground state complex differs in its spectral properties from the uncomplexed fluorophore. Equation 1 describes the static quenching:

$$F_0/F = 1 + K_s [Q] \qquad (1)$$

F_o is the intensity of fluorophore in the absence of quencher

F is the intensity of the fluorophore in the presence of quencher

K_s is the association constant

[Q] is the quencher concentration

The second phenomenon by which quenching takes place is dynamic quenching that occurs in the excited state. In dynamic quenching, the fluorophore in its excited state and the quencher diffuse towards each other to form the encounter complex and subsequently energy transfer or electron transfer takes place. As this process occurs due to collision, it is also called as collisional quenching. The excited-state complex dissociates upon radiative or nonradiative deactivation. This makes both the fluorophore and the quencher to be in their respective ground state. There will be neither spectral shift nor observation of new band in the absorption spectra as the dynamic quenching takes place in the excited state. The Stern-Volmer equation can describe this kind of quenching. This is given by equation 2.

$$F_0/F = 1 + k_q\tau_o [Q] = 1 + K_D [Q] \qquad (2)$$

F_o and F and [Q] are same as in static quenching

k_q is the bimolecular quenching constant

τ_o is the lifetime of the fluorophore in the absence of quencher

$K_D = k_q\tau_o$ is the Stern-Volmer quenching constant.

A plot of F_o/F versus [Q] is expected to be linearly dependent upon the concentration of quencher. The slope of the plot gives the Stern-Volmer constant K_D. The higher the value of K_D, the more efficient is the quenching. An observation of linear Stern-Volmer plot does not prove whether the quenching is due to static or dynamic quenching. The lifetimes or the temperature and viscosity dependence of quenching can be used to distinguish static and dynamic quenching. For static quenching $\tau_o/\tau=1$,

as complexed fluorophores are nonluminescent and the remaining uncomplexed fluorophore's lifetime is τ_o. For dynamic quenching $F_0/F= \tau_o/\tau$.

Dynamic quenching becomes more effective at higher temperatures due to increased rate of diffusion while static quenching will be less prominent due to thermal dissociation of complex at elevated temperatures.[69] In dynamic quenching, charge transfer occurs and the fluorescence will be quenched when the electron acceptor collides with the excited fluorophore. As a result, no changes in the absorption spectra will occur as the collision between the quencher and the fluorophore occurs in the excited state. On the contrary, perturbation of absorption spectra will be observed in static quenching as the complex between the fluorophore and the quencher forms in the ground state.

The fluorescence quenching of organic fluorophores by heavy atoms can be achieved by two different pathways. In the first one, a heavy atom is present in the fluorophore itself, which is called "internal heavy atom effect." In the second one, it is a different molecule (the quencher) that contains a heavy atom, termed as "external heavy atom effect." The external heavy-atom quenching is usually treated as a bimolecular process with a rate constant dependent on the nature of the quencher. Here we study the external heavy atom effect. The fluorophores used in quenching studies are the light polyaromatic compounds, such as naphthalene and anthracene, and heavy polyaromatic compounds, such as pyrene and perylene, which are used to study the complexes of these compounds with silver perchlorate (Figure 3.11). The quenchers employed are the heavier metal salts, such as silver perchlorate ($AgClO_4$)

and thallium hexafluorophosphate ($TlPF_6$), and the lighter metal salt potassium tertiary butoxide (KO^tBu). As silver has a closed-shell electronic configuration and its lowest energy excitation is higher than that of the fluorophores studied here, any quenching due to paramagenetic interaction and/or energy transfer is excluded.[70] The quenching by heavy atoms such as silver and thallium solely operates by collisional mechanism. The counter ions perchlorate,[71] hexafluorophosphate and tertiary butoxide does not have any significant effect on the quenching.[70] Hashimoto has studied the mechanism of fluorescence quenching of pyrene with purines in polar media.[72] Both dynamic and static quenching was observed in aqueous solution where there is appreciable formation of ground-state complex between pyrene and the purine. Only dynamic quenching was observed in acetonitrile.

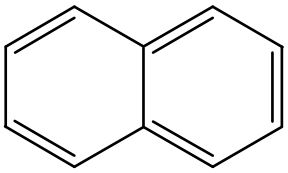

Naphthalene, ϕ_F = 0.20*

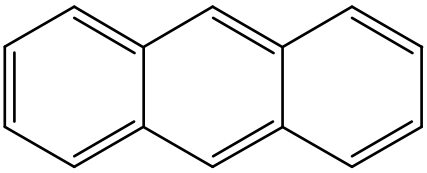

Anthracene, ϕ_F = 0.40*

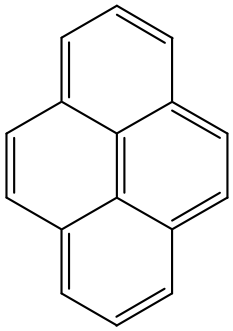

Pyrene, ϕ_F = 0.7*

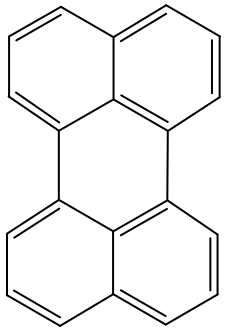

Perylene, ϕ_F =1.0* * = Ref 45

Figure 3.11 Aromatics with their fluorescence quantum yield.

The fluorescence intensity of the aromatics such as pyrene, naphthalene anthracene and perylene falls off in a regular way when the quenchers $AgClO_4$, $TlPF_6$ and KO^tBu are added gradually (Figures 3.12, 3.14, 3.16, 3.18, 3.20, 3.22, 3.24, 3.26, 3.28, 3.31). Also, the decrease of fluorescence intensity in all of the aromatics upon addition of quenchers is not accompanied by appearance of new bands. This discards the possibility of luminescent exciplex formation. A similar observation was found in the quenching of some aromatics with nitroxide radicals.[73] For the same compounds, no changes in the absorption spectra were observed. So the static quenching due to nonfluorescent complex in the ground state is ignored and only dynamic quenching is considered as the dominant phenomenon for quenching. Similar observations are also seen by Saito et al. in the fluorescence quenching of aromatic hydrocarbons by the silver ion.[70] It is also confirmed by the S-V plot of lifetimes vs quencher concentrations where the τ_o/τ is not equal to 1 (Figures 3.13, 3.15, 3.17, 3.19, 3.21, 3.23, 3.25, 3.27).

Naphthalene molecule is rigid with a molecular configuration planar leading to high fluorescence efficiency.[74] The Stern-Volmer quenching constant of pyrene is larger than that of perylene (Table 3.1). This difference can be attributed to the molecular structure of perylene which is not a typical large conjugated system and is less coplanar configuration than pyrene.[75] This is similar to the fluorescence quenching of pyrene and perylene by dimethyl terephthalate (DMTP) and N,N-dimethylaniline (DMA) as observed by Chen et al.[75] They found that the K_{SV} values of pyrene are greater than the perylene. For pyrene, only monomer emission is considered in our studies. This is due to the fact that the excimer emission is less sensitive to the quenching action of quenchers.[67] The

S-V constants of pyrene with $AgClO_4$ and also with $TlPF_6$ are higher than the anthracene and perylene (Table 3.1). There are four fused aromatic rings in pyrene which makes it more fluorescent efficient and more prone to quenching when compared to anthracene, which has three fused rings. Perylene is not a typical large conjugated system and is less coplanar compared to pyrene, which makes it less prone to quenching. This situation is similar to the quenching of these systems by nitromethane in acetonitrile, 90 Wt.% glycerol in water and 1-butyl-3-methylimidazolium hexafluorophosphare (BMIM PF_6).[76] They found that the K_{SV} of pyrene (39.6 M^{-1}) is larger compared to anthracene (2.4 M^{-1}) followed by perylene (2.2 M^{-1}) in $BMIMPF_6$. The fluorescence of perylene in fluid solution is not readily quenched by heavy-atom induced intersystem crossing (ISC) in contrast to most other polycylic aromatic hydrocarbons.[71] This was attributed to the difference in the energy gaps between S_1 and the accepting triplet state which is assumed to be T_1 in the case of perylene and a higher state T_n in most other cases. (Napthalene T_1 = 21,300 cm^{-1},[77] Anthracene T_1= 14,700 cm^{-1},[78] Pyrene T_1 = 16,900 cm^{-1} and Perylene T_1 = 12,600 cm^{-1}.[42])

The K_{SV} constant of pyrene with $TlPF_6$ (141 M^{-1}) is higher when compared to S-V constant of pyrene with $AgClO_4$ (52.4 M^{-1}). This is due to the fact that thallium is heavier than the silver.[79] But the same phenomenon was not observed with other aromatics. This may be due to a better size match, however, the reasoning has to be investigated further. For anthracene with $TlPF_6$ in 2 MTHF, the K_{SV} obtained was 27.6 M^{-1} but a higher value (61 M^{-1}) was obtained for the same combination in acetonitrile by Giaimucciuo et al.[79] This is likely because of the polarity of the solvents employed.

Acetonitrile is more polar compared to the non polar 2 methyl THF. A bimolecular quenching constant in the range of $1x10^{10}$ $M^{-1}s^{-1}$ is very common and near the limit for diffusion controlled processes.[79,80] A higher quenching constant means greater diffusion and collision between the fluorophore and quencher and higher the quenching. The bimolecular quenching constants are given in Table 3.2. The quenching is small with potassium when compared to silver and thallium. This is because potassium is a lighter metal compared to silver and thallium. This can be observed from the S-V constants and also from bimolecular quenching constants, where their values are much higher for silver and thallium. Fluorescence quenching with K^+ was studied only with naphthalene and anthracene for illustration purpose. The possibility of electronic energy transfer is discarded as there is no or little overlap between the fluorescence spectra of fluorophore and the absorption spectra of the quencher. As there is no new band observed in the florescence spectra, no luminescent exciplex is formed. Although no exciplex band is observed, the fact that the quenching was found to be dynamic suggests that the formation of a charge transfer encounter complex in the excited state (i.e., a non-luminescent exciplex). This is observed with all the aromatics with silver and thallium as quenchers. A similar phenomenon was observed in the quenching of polycylic aromatic hydrocarbons with various anilines as quenchers.[81] With potassium, on the other hand, the quenching is due to the non fluorescent complex formation in the ground state. This is clearly seen from the Stern- Volmer plot where $\tau_o/\tau = 1$ (Figures 3.30 and 3.32).

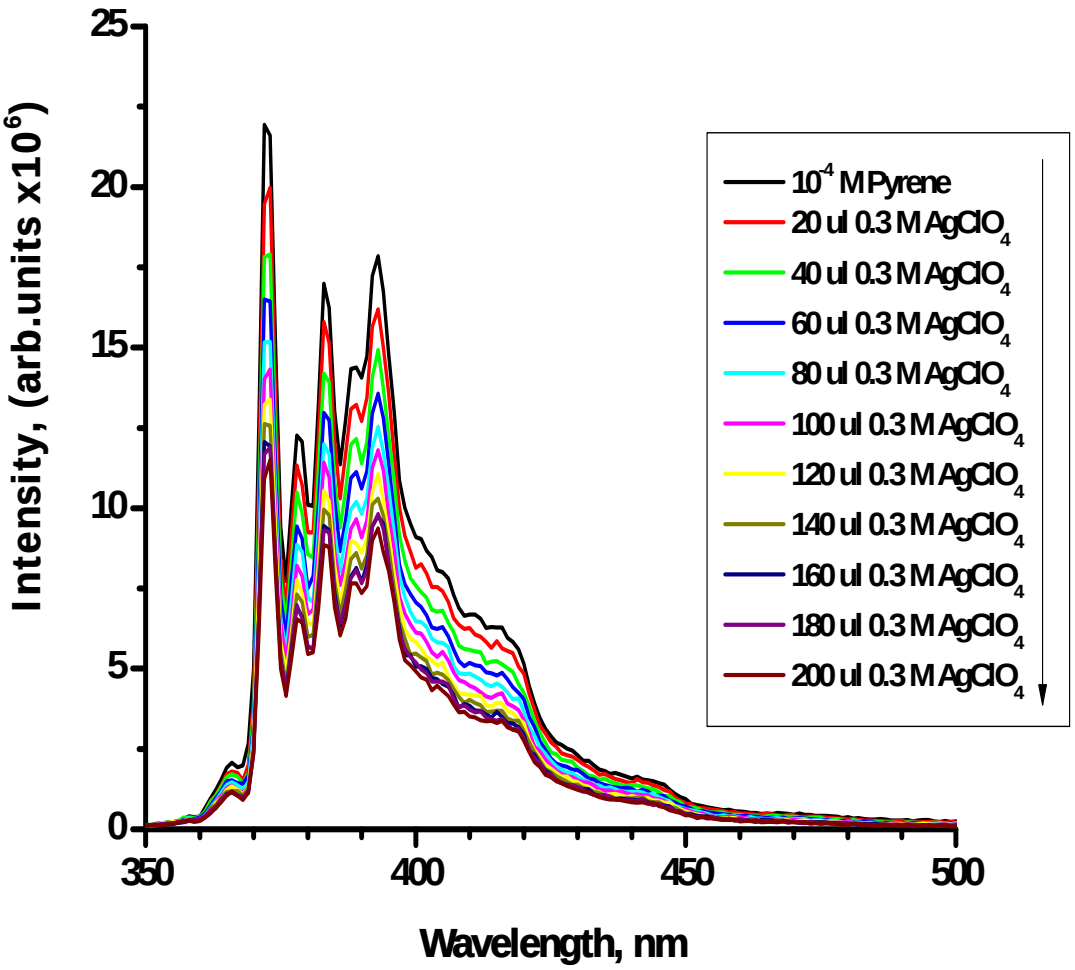

Figure 3.12. 10^{-4} M Pyrene with 20 µl increments increments of 0.3 M $AgClO_4$.

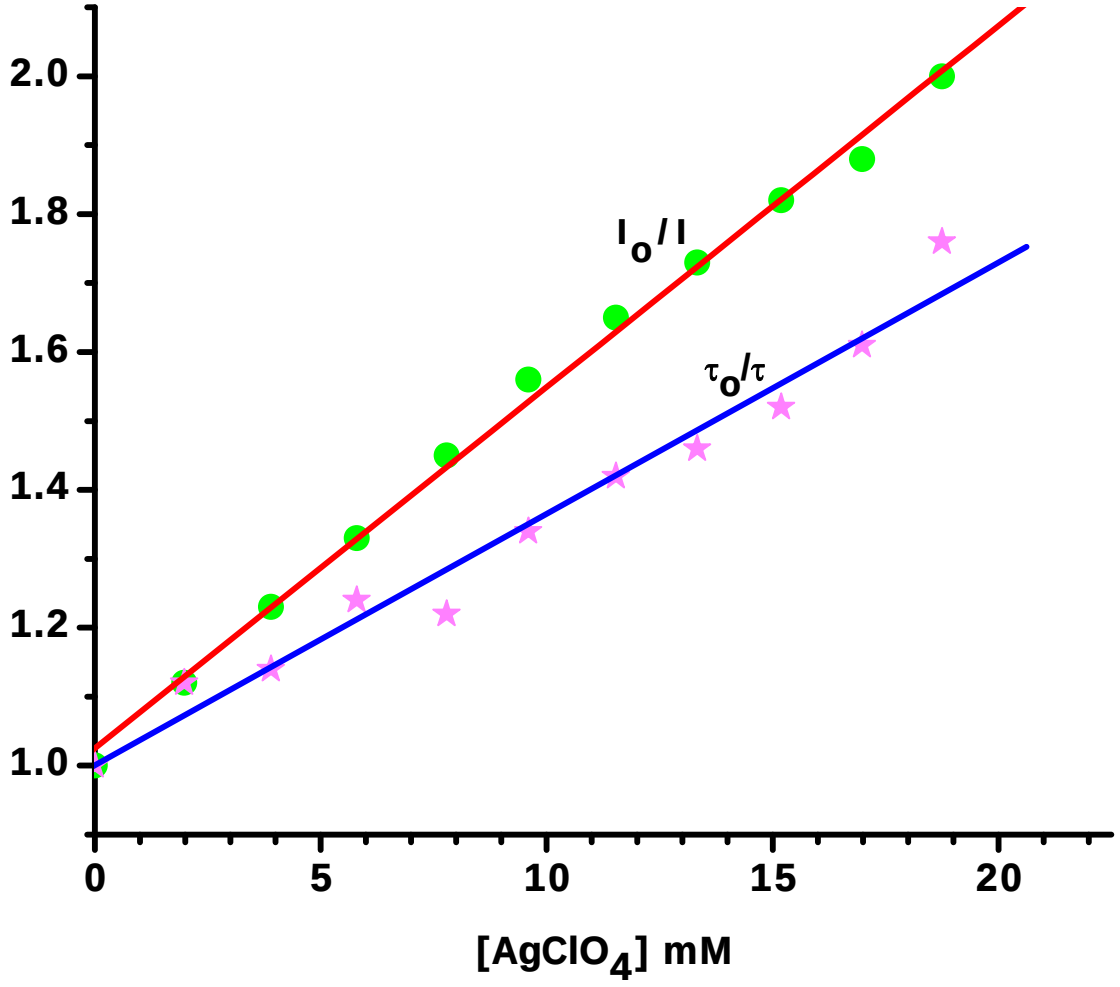

Figure 3.13 Stern-Volmer plot of 10^{-4} M Pyrene with 20 µl increments of 0.3 M $AgClO_4$.

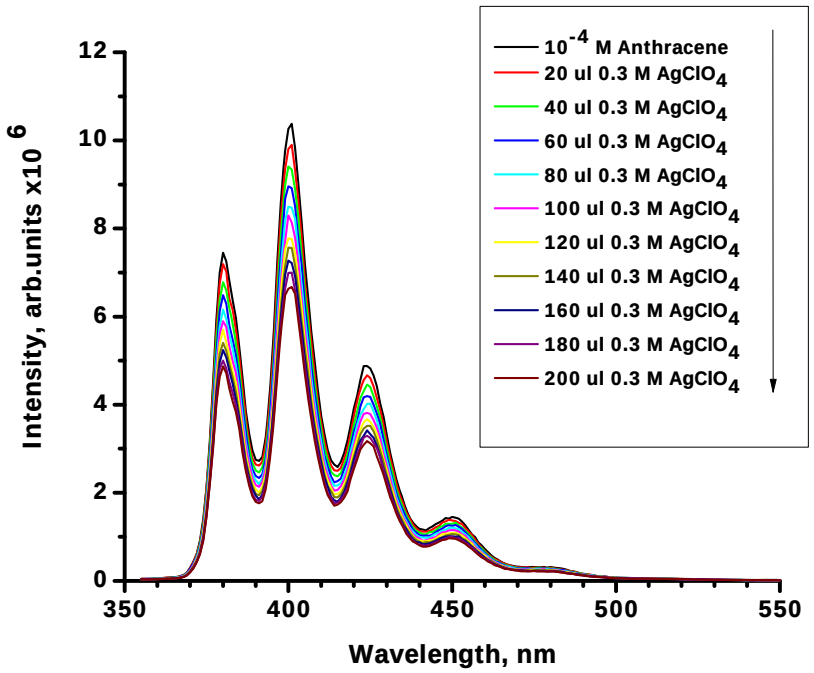

Figure 3.14. Steady state quenching of 10^{-4} M Anthracene with 20 µl increments of 0.3 M $AgClO_4$.

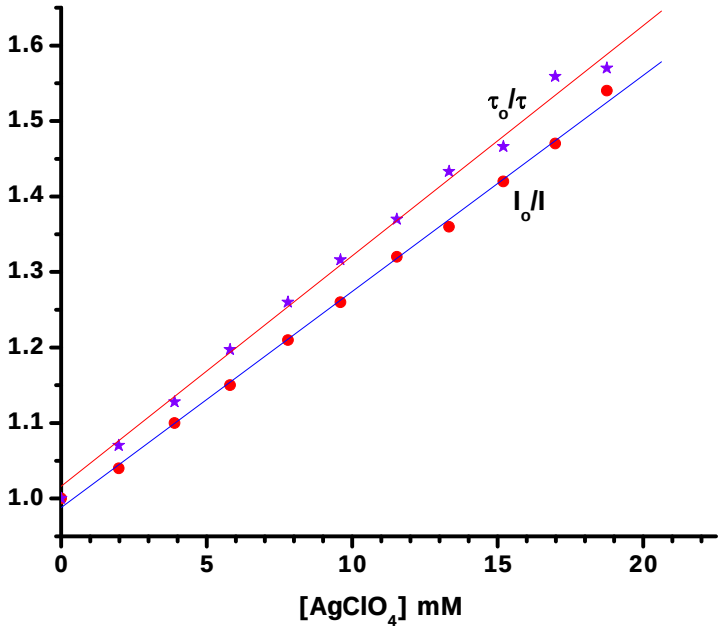

Figure 3.15. S-V plot of 10^{-4} M Anthracene with 20 µl increments of 0.3 M $AgClO_4$.

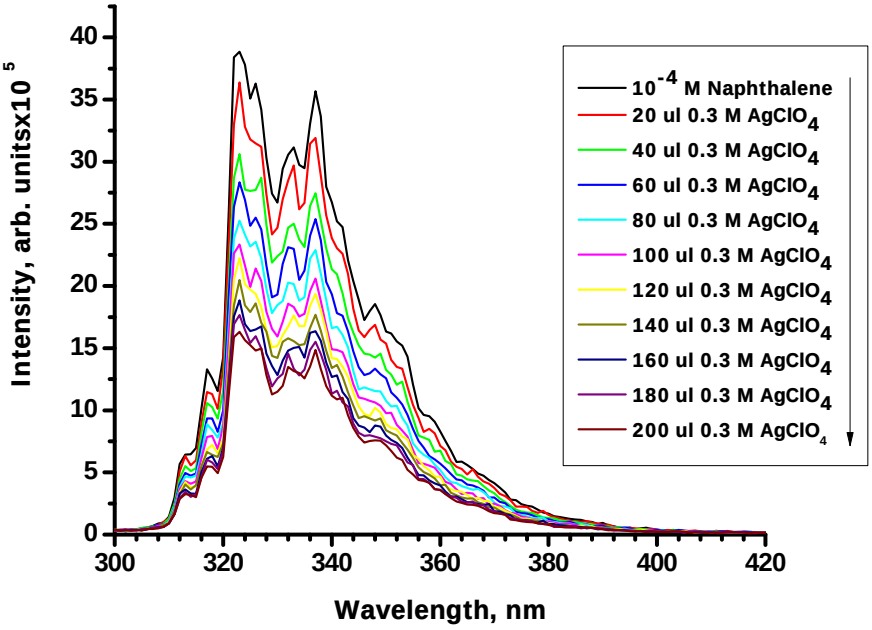

Figure 3.16. Steady state quenching of 10^{-4} M Naphthalene with 20 µl increments of 0.3 M $AgClO_4$.

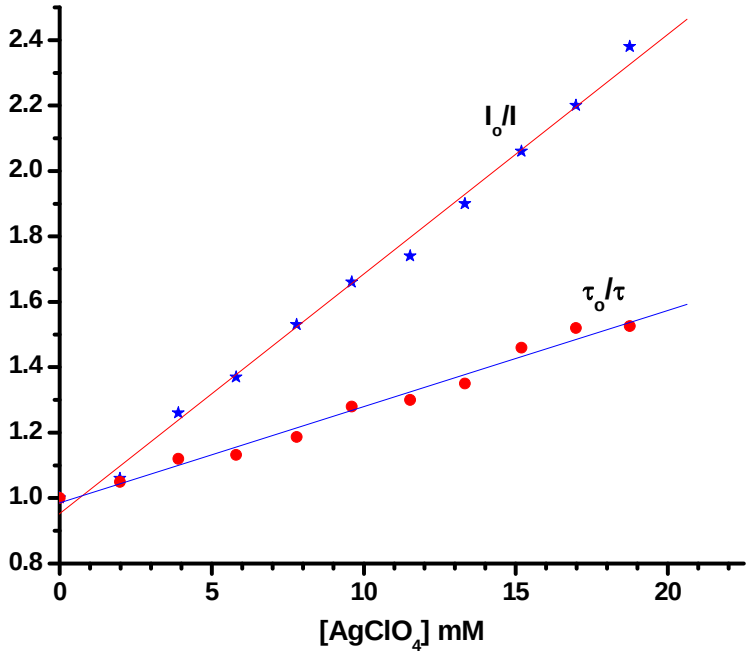

Figure 3.17. S-V plot of 10^{-4} M Naphthalene with 20 µl increments of 0.3 M $AgClO_4$.

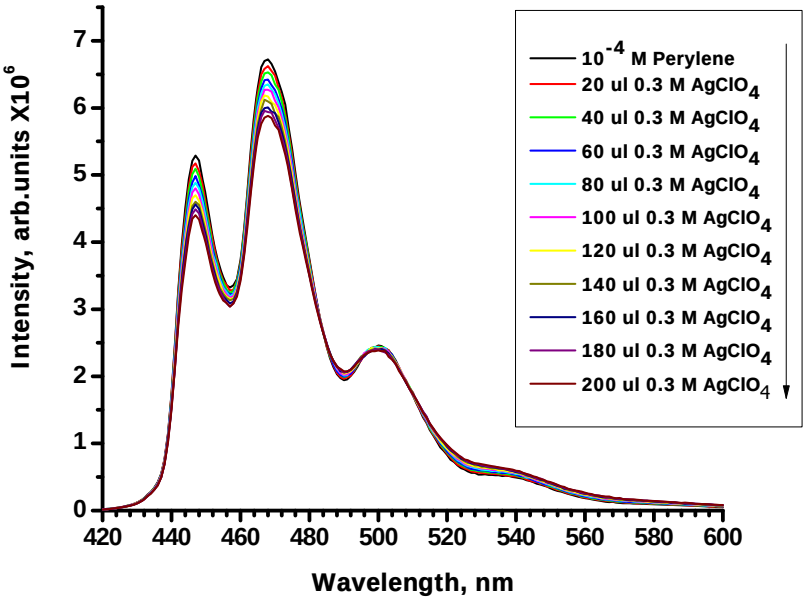

Figure 3.18. Steady state quenching of 10^{-4} M Perylene with 20 µl increments of 0.3 M $AgClO_4$.

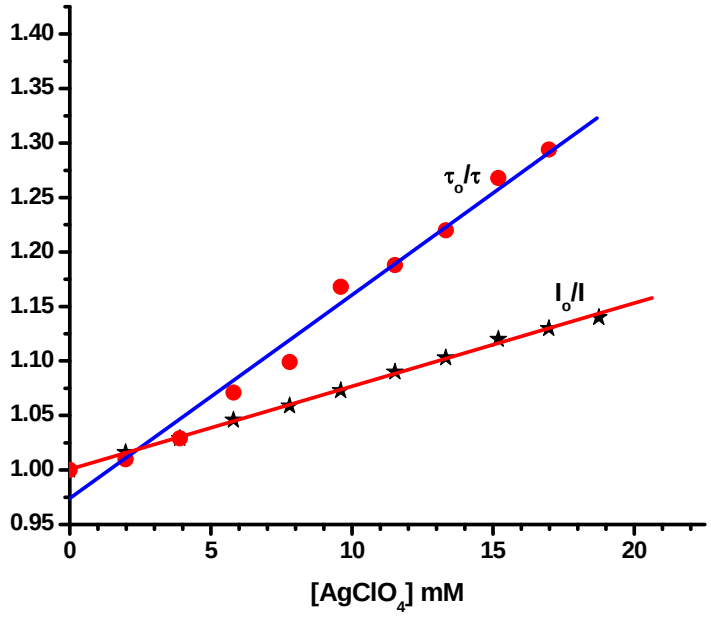

Figure 3.19. S-V plot of 10^{-4} M Perylene with 20 µl increments of 0.3 M $AgClO_4$.

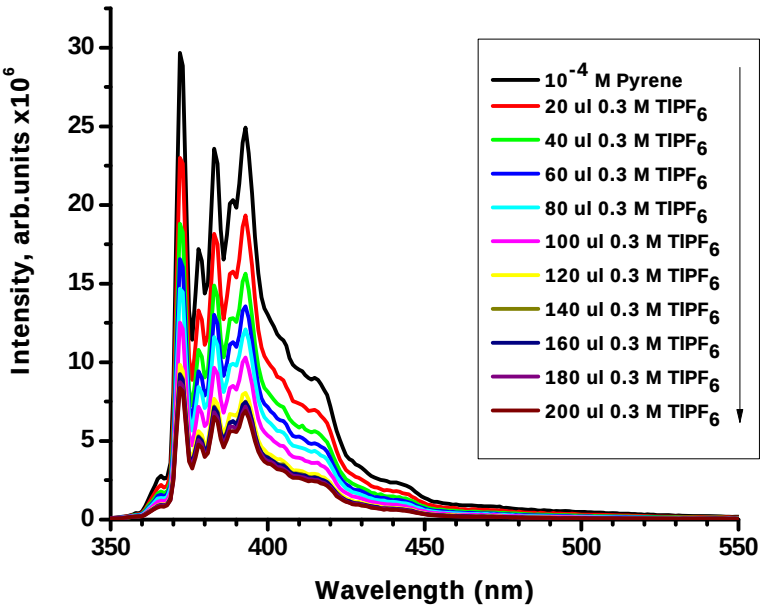

Figure 3.20. Steady state quenching of 10^{-4} M Pyrene with 20 µl increments of 0.3 M $TlPF_6$.

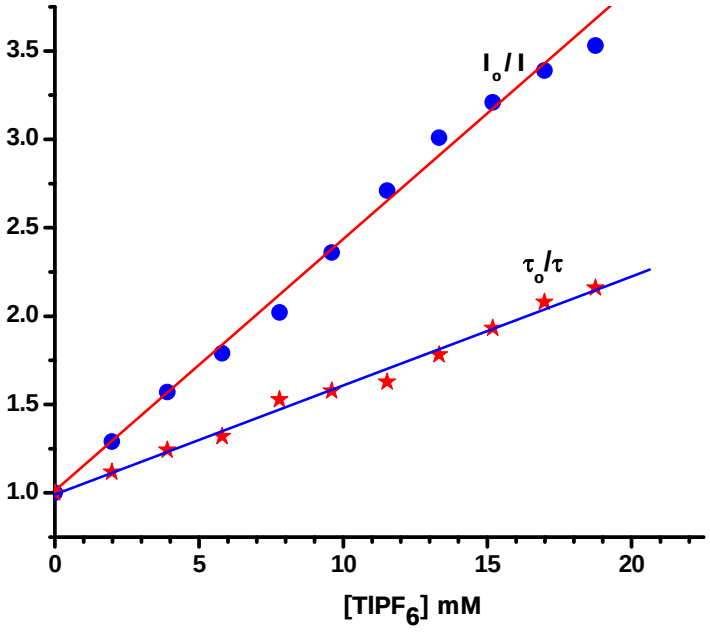

Figure 3.21. S-V plot of 10^{-4} M Pyrene with 20 µl increments of 0.3 M $TlPF_6$.

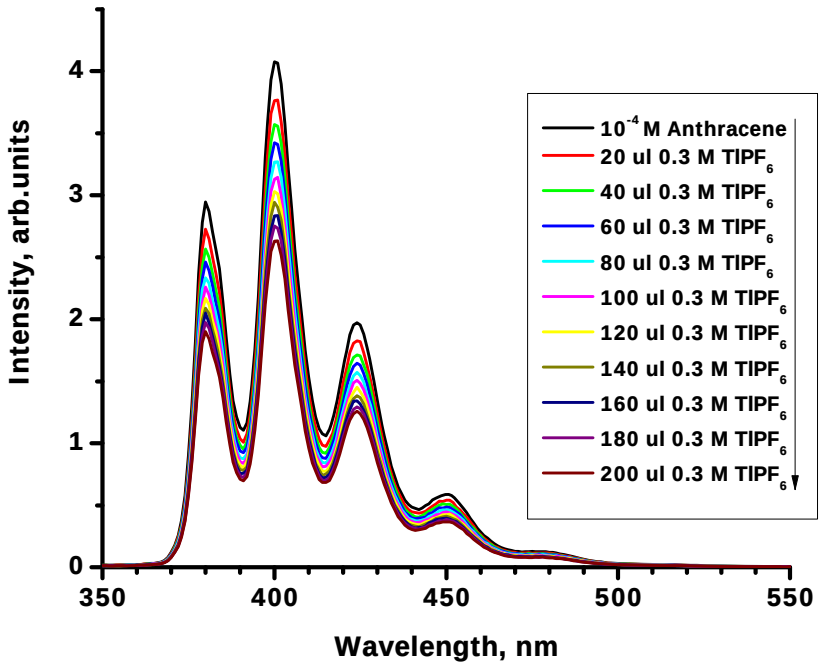

Figure 3.22. Steady state quenching of 10^{-4} M Anthracene with 20 µl increments of 0.3 M $TlPF_6$.

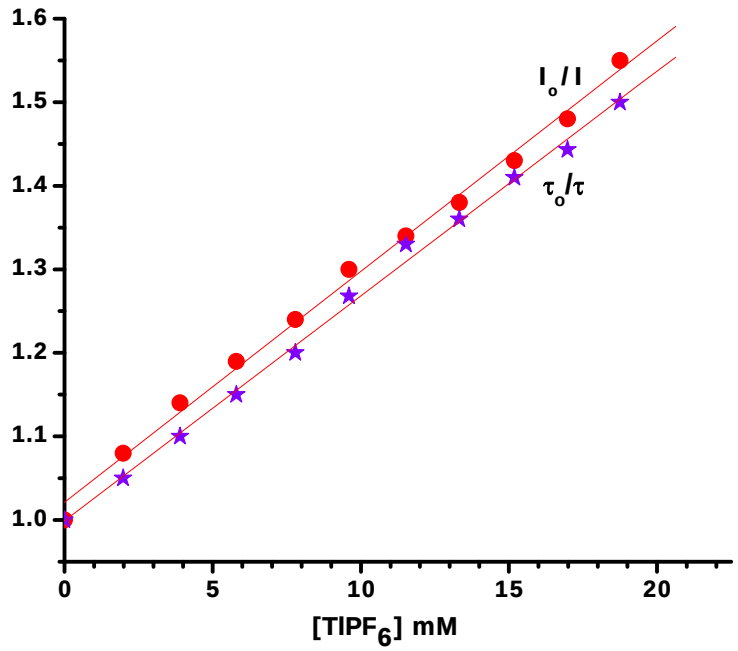

Figure 3.23. S-V plot of 10^{-4} M Anthracene with 20 µl increments of 0.3 M $TlPF_6$.

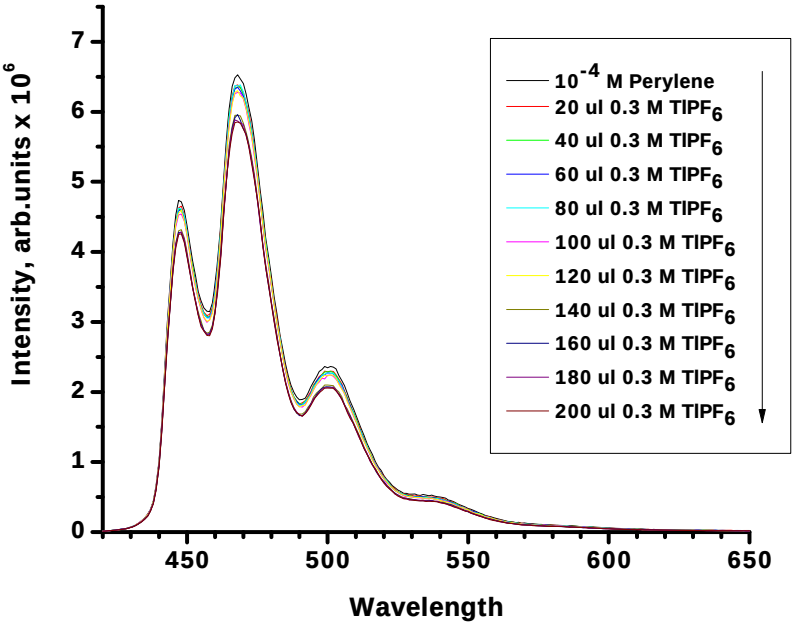

Figure 3.24. Steady state quenching of 10^{-4} M Perylene with 20 µl increments of 0.3 M $TlPF_6$.

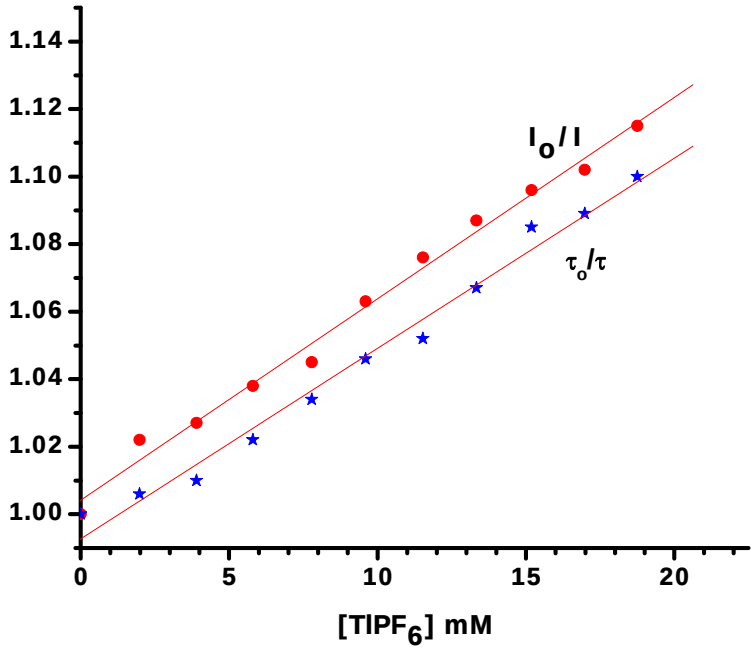

Figure 3.25. S-V plot of 10^{-4} M Perylene with 20 µl increments of 0.3 M $TlPF_6$.

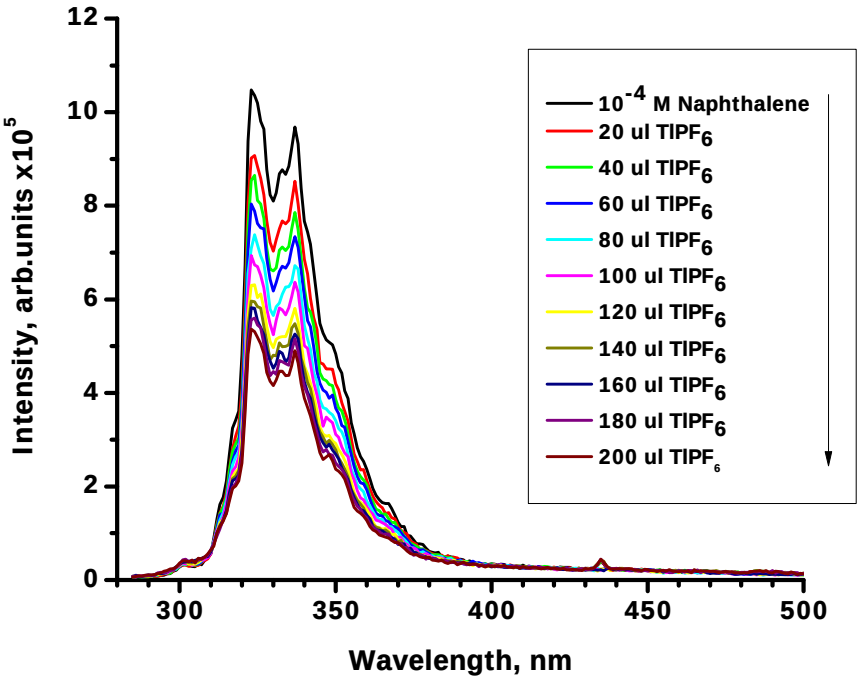

Figure 3.26. Steady state quenching of 10^{-4} M Naphthalene with 20 µl increments of 0.3 M $TlPF_6$.

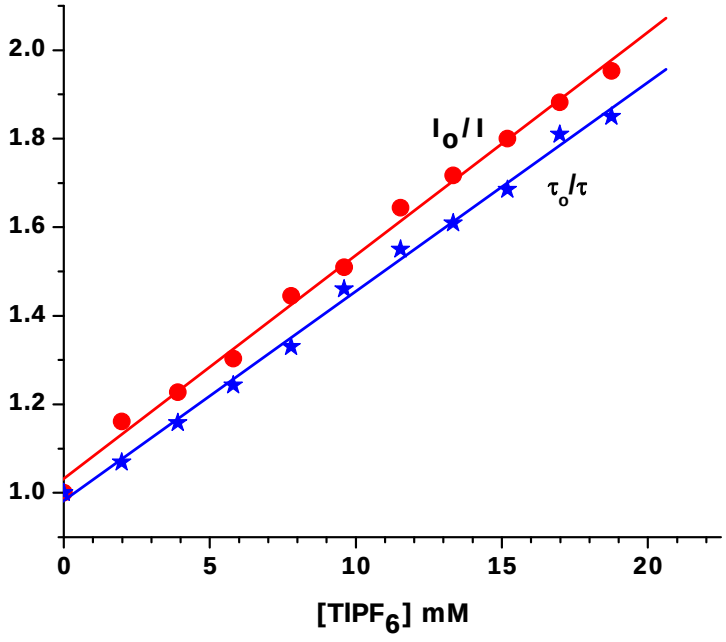

Figure 3.27. S-V plot of 10^{-4} M Naphthalene with 20 µl increments of 0.3 M $TlPF_6$.

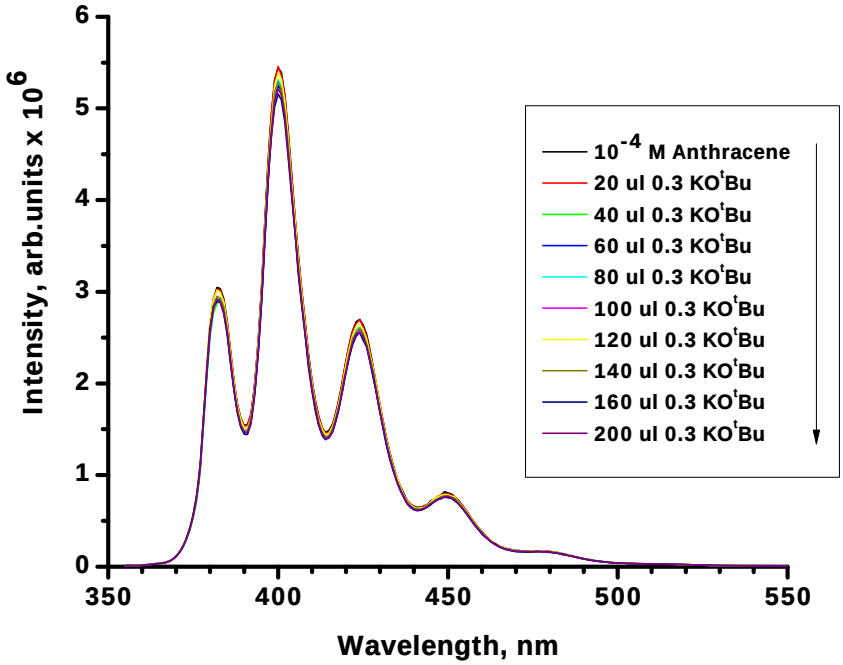

Figure 3.28. Steady state quenching of 10^{-4} M Anthracene with 20 µl increments of 0.3 M KO^tBu.

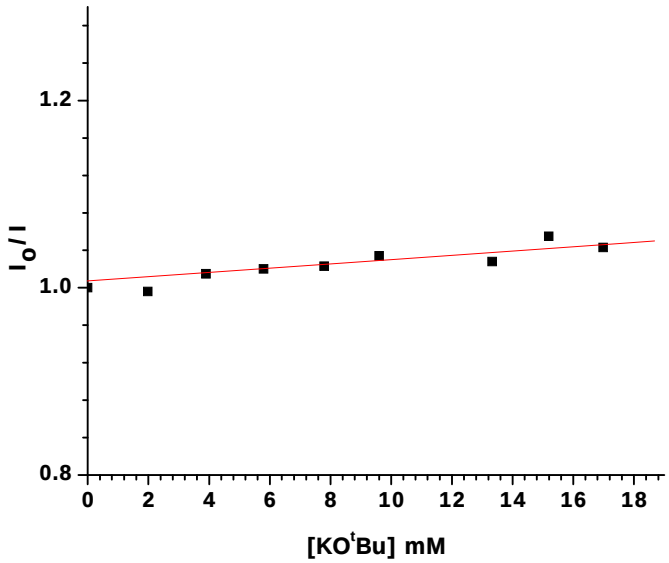

Figure 3.29. S-V plot of intensities of 10^{-4} M Anthracene with 20 µl increments of 0.3 M KO^tBu.

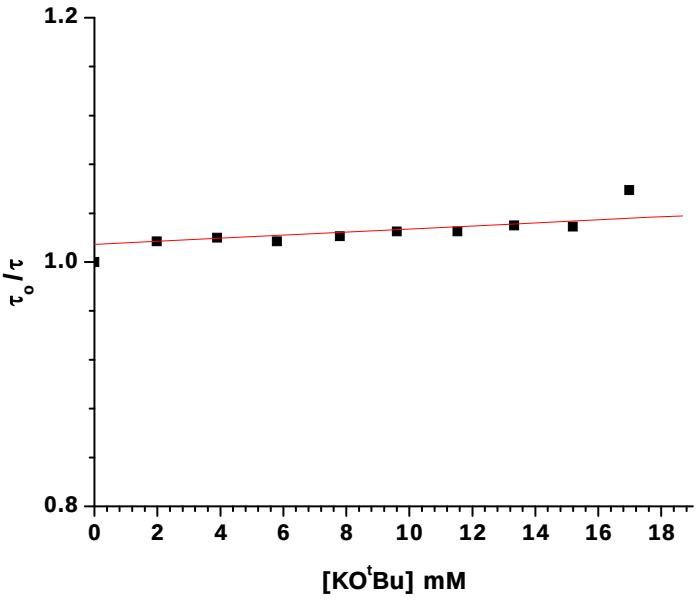

Figure 3.30. S-V plot of lifetimes of 10^{-4} M Anthracene with 20 µl increments of 0.3 M KO^{t}Bu.

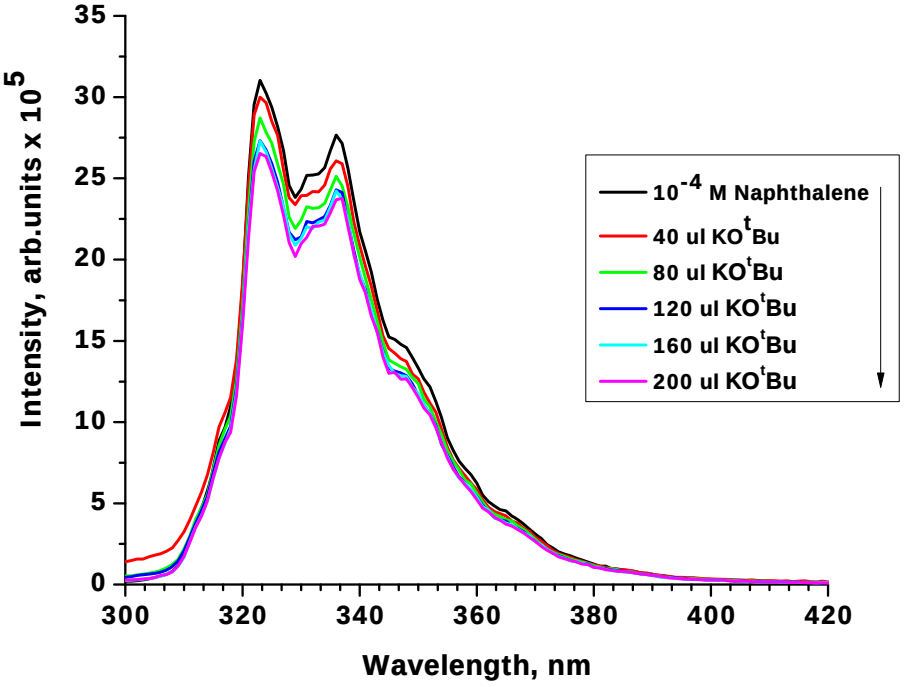

Figure 3.31. Steady state quenching of 10^{-4} M Naphthalene with 40 µl increments of 0.3 M KO^{t}Bu.

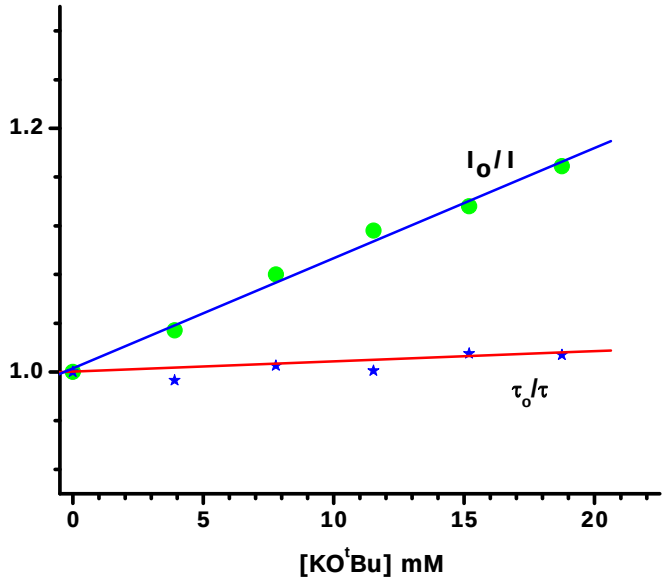

Figure 3.32. S-V plot of 10^{-4} M Naphthalene with 40 ul increments of 0.3 M KO^{t}Bu.

Table 3.1 Stern-Volmer constants for the quenching of aromatics studied by $AgClO_4$, $TlPF_6$ and KO^{t}Bu.

	$AgClO_4$, M^{-1}	$TlPF_6$, M^{-1}	KO^{t}Bu , M^{-1}
Napthalene	73.2	50.3	9.05
Pyrene	52.4	141	-
Anthracene	28.6	27.6	5.69
Perylene	7.63	5.97	-

Table 3.2 Bimolecular quenching constants.

	$AgClO_4$, $M^{-1}s^{-1}$	$TlPF_6$, $M^{-1}s^{-1}$	KO^{t}Bu, $M^{-1}s^{-1}$
Napthalene	$1x10^{10}$	$7.42x10^{9}$	$7.93x10^{8}$
Pyrene	$3.23x10^{9}$	$7.19x10^{9}$	-
Anthracene	$6.13x10^{9}$	$6.95x10^{9}$	$1.43x10^{9}$
Perylene	$1.55x10^{9}$	$1.08x10^{9}$	-

3.3.3 Frozen Solution Studies

To gain insight into the phosphorescence enhancement by the heavy atoms, frozen solution studies were carried out. To the pure naphthalene solution in 2-MTHF, four equivalents of $AgClO_4$, $TlPF_6$ and KO^tBu were added. To one mole of pyrene, two moles of each $AgClO_4$, $TlPF_6$ and KO^tBu are added in 2-MTHF. The peaks in the range of 550-800 nm of pyrene with $AgclO_4$ are attributed to monomer of the pyrene due to its structured profile and it is phosphorescence based on its lifetime of 1.5 ms (Figure. 3.37)

Figure 3.33 compares the excitation spectra of naphthalene monitored at fluorescence and phosphorescence peaks of naphthalene. It has also UV-Vis absorption spectra too. Figure 3.35 shows emission spectra of naphthalene with various metals. It also displays the monomer fluorescence and monomer phosphorescence of the naphthalene. Huge enhancement in the phosphorescence of naphthalene was observed with $AgClO_4$ but not with $TlPF_6$ eventhough Tl is also a heavy atom (Figure. 3.35). The phosphorescence lifetime of naphthalene in frozen solution is 2.48 s and it was lowered to 419.9 ms with the addition of $TlPF_6$ and then to 264.7 ms with addition of silver perchlorate. With KO^tBu, the lifetime remained the same as naphthalene phosphorescence without quencher addition. With Ag^+, there is greater interaction between naphthalene and the silver and so greater decrease in its lifetime due to the heavy atom effect. Eventhough thallium is heavier than silver, the lifetime decrease is small, which can be attributed to less interaction between thallium and naphthalene. Attempts to make the complexes of thallium with naphthalene and pryene were

unsuccessful also supports no or less interactions. Another reason for the lower interaction of Tl^+ compared to Ag^+ due to its larger ionic radius. The ionic radius of Tl^+ is 1.54 Å while for Ag^+ it is 1.27 Å.[82] With K^+ (1.44 Å), which is a lighter element, there is no effect and the lifetime remained same. There is less interaction between the hard acid cation such as K^+ when compared to soft acid cation Ag^+ with naphthalene. The monomer fluorescence lifetime upon addition of $AgClO_4$ was the same as for pure naphthalene solution but it went up with addition of $TlPF_6$ and then further with KO^tBu.

Similar observations are seen for the pyrene interaction with $AgClO_4$ and also $TlPF_6$. Ag^+ forms a strong cation-π bonding which is due to covalent interactions between aromatic π electrons and the d orbitals of Ag^+, in addition to the normal electrostatic interactions. Upon interaction with an aromatic ligand, the d- orbitals undergo splitting and polarization to optimally interact with the ligand orbitals.[5] It is very difficult for the outer pair electrons on Tl^+ for removal or to participate in covalent bond formation or hydrogen bonding due to inert pair effect as Tl(I) being the post transition metal.[83] In literature lot of cyclopentadienyl complexes of thallium were known but not many Tl-arene complexes were known.[84] There are few thallium-arene complexes in which the arene was a free molecule and not a part of the metal-ligand system. This indicates that the Tl(I) does not form complexes with arenes such as naphthalene and pyrene and so we did not observe enhanced phosphorescence in frozen solution studies. Murayama et al. have synthesized 3 complexes of potassium with calix[6]arene.[85] They have found that K^+ was interacting with the aromatic rings along with usual K^+ with O bonding.

The monomer fluorescence intensity of pyrene was also quenched by $AgClO_4$ much more than $TlPF_6$. Consequently, the fluorescence lifetime was also lowered by three orders of magnitude with $AgClO_4$. The fluorescence intensity and lifetime lowering with enhancement of monomer phosphorescence of pyrene with $AgClO_4$ interaction shows the heavy atom effect of silver. The excitation spectrum of the frozen solution of pyrene with $AgClO_4$ indicates a red shift compared to pyrene and it is less structured (Figure. 3.36). This is due to charge transfer from the pyrene to the Ag^+.

Overall, the monomer fluorescence intensity of naphthalene was decreased upon addition of $AgClO_4$ and more with $TlPF_6$ but less with KO^tBu. This indicates that the heavier the metal, the greater the quenching of fluorescence intensity. The monomer phosphorescence was enhanced several times with the addition of $AgClO_4$ but not with $TlPF_6$ or else KO^tBu.

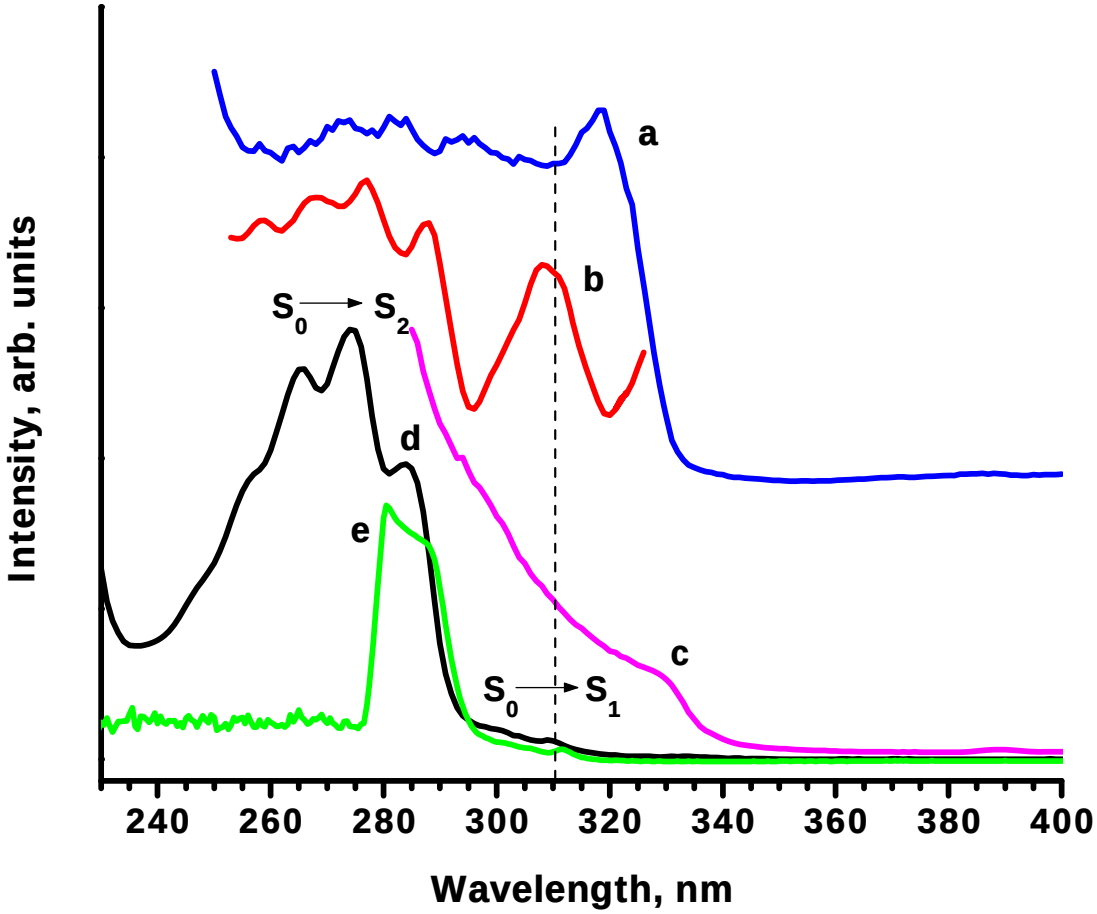

Figure 3.33. Excitation and absorption spectra. (a) 1:4 Naphthalene-$AgClO_4$ excitation spectra. λ_{emi} = 495 nm in 2-MTHF (b) 1:4 Naphthalene-$AgClO_4$ excitation spectra. λ_{emi} = 340 nm in 2-MTHF. (c) Excitation spectra of solid {[Ag_4(tetra-η^2-naphthalene)][$(ClO_4)_4$]} at 77 K. λ_{emi} = 475 nm. (d) UV-Vis absorption of 10^{-5} M Naphthalene in 2-MTHF (e) UV-Vis absorption of 1:4 Naphthalene:$AgClO_4$ in 2-MTHF.

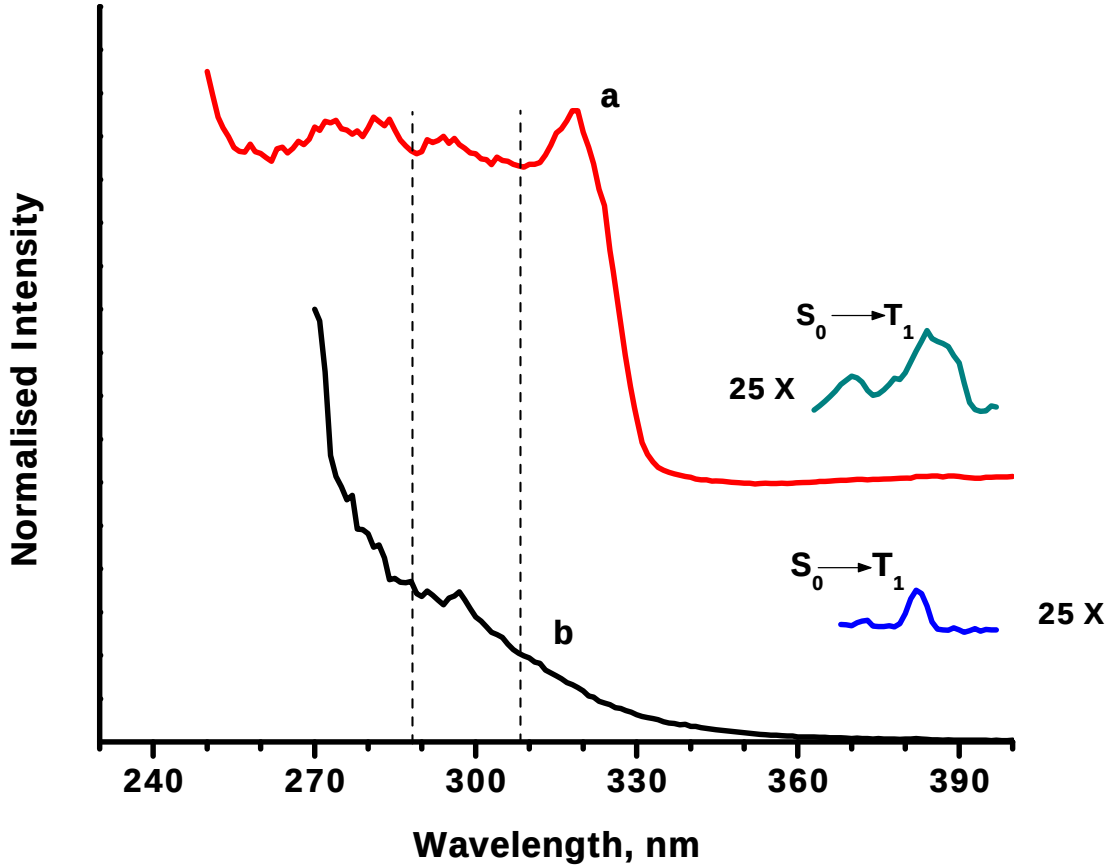

Figure 3.34. Luminescence excitation spectra for naphthalene with $AgClO_4$ (a) and naphthalene (b) monitoring the phosphorescence emission peak at 470 nm. Dashed lines indicate the positions for S_0-S_1 and S_0-S_2 known for naphthalene. The S_0-T_1 peaks are weak and are magnified by 25 times for clarity.

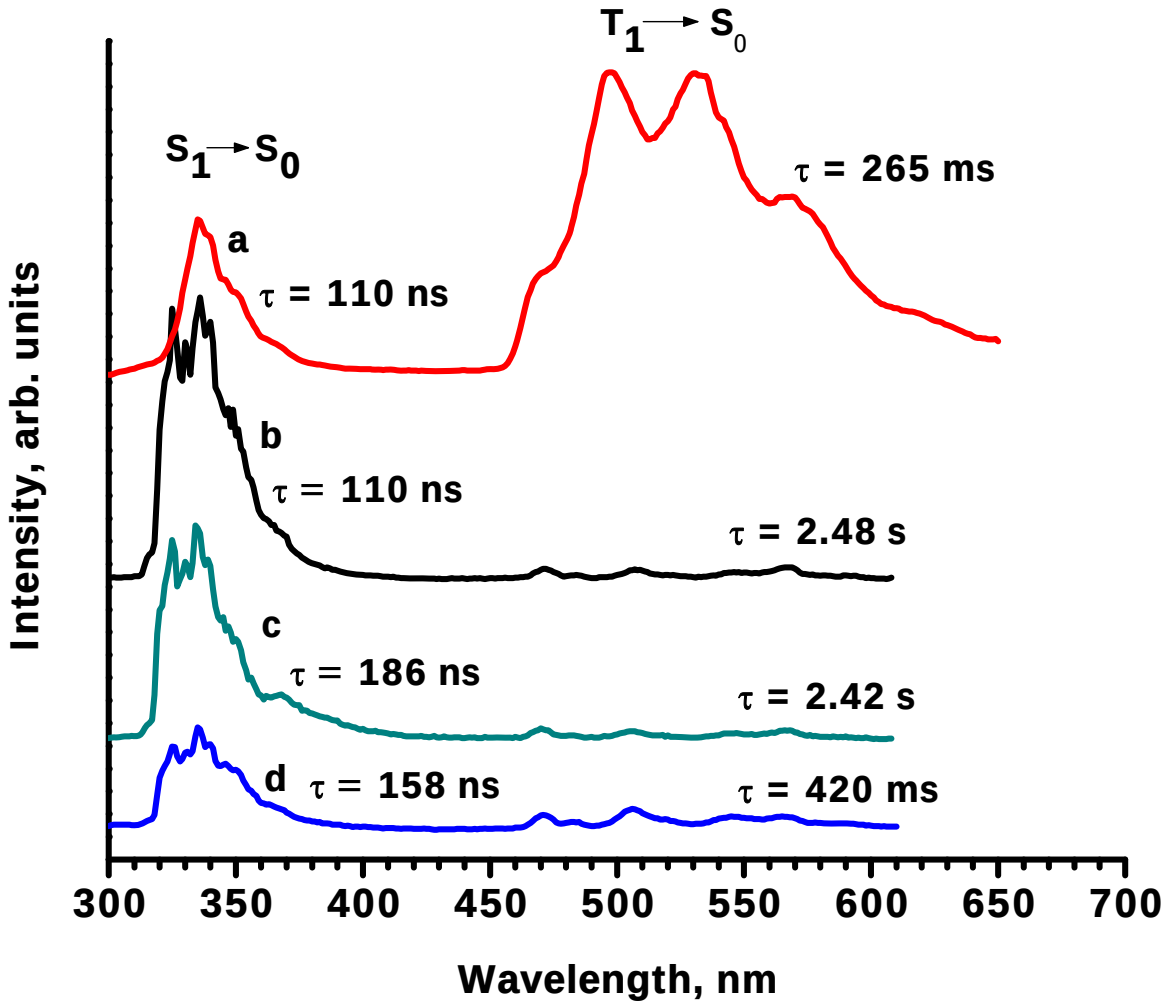

Figure 3.35. Emission spectra in 2-MTHF at 77 K along with lifetimes. (a) 1:4 Naphthalene:$AgClO_4$, λ_{exc} = 280 nm (b) 0.6 M Naphthalene, λ_{exc} = 280 nm (c) 1:4 Naphthalene:KO^tBu, λ_{exc} = 280 nm (d) 1:4 Naphthalene:$TlPF_6$, λ_{exc} = 280 nm.

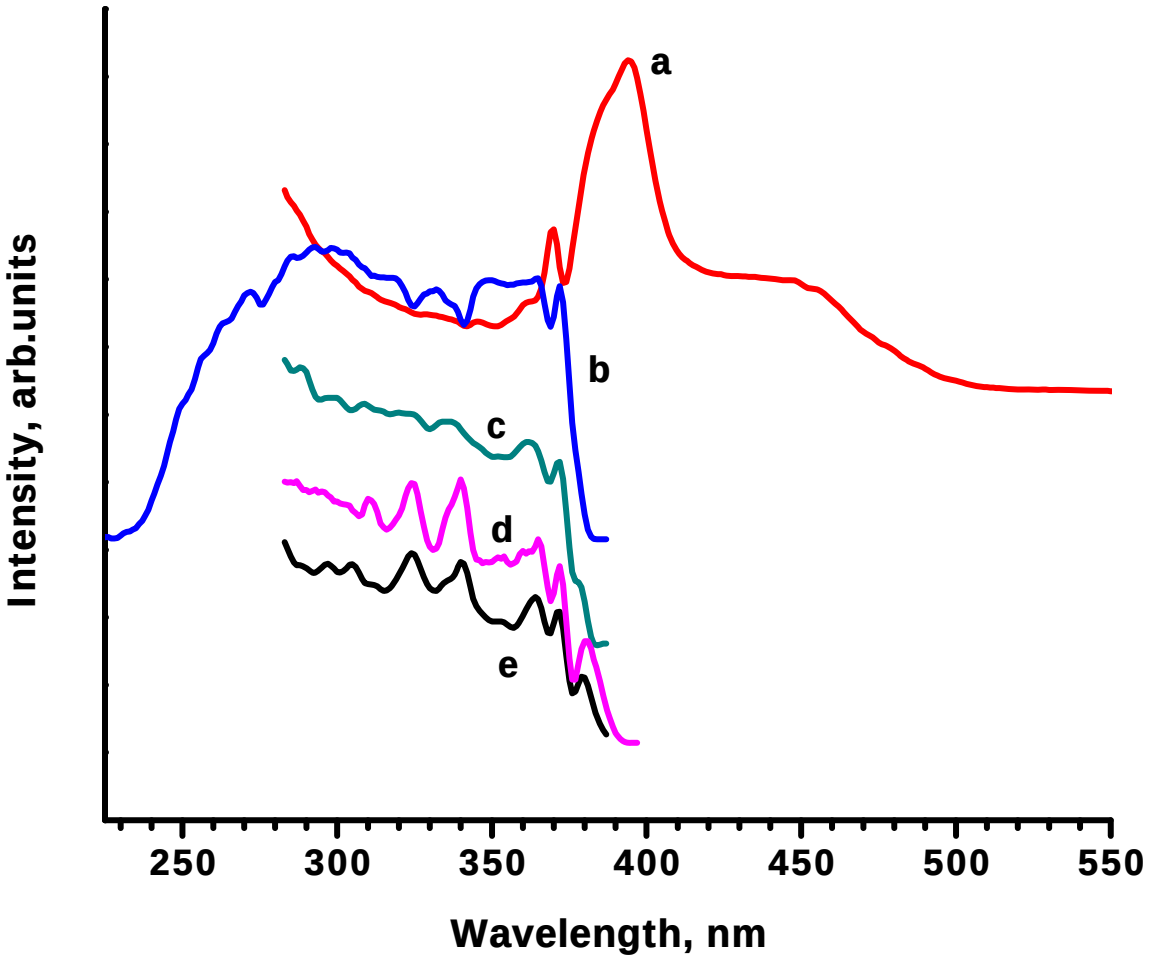

Figure 3.36. Excitation spectra in 2-MTHF at 77 K. (a) 1:2 Pyrene:$AgClO_4$, λ_{emi} = 610 nm (b) 0.6 M Pyrene, λ_{emi} = 400 nm (c) 1:2 Pyrene:KO^tBu, λ_{emi} = 400 nm (d) 1:2 Pyrene:$AgClO_4$, λ_{emi} = 420 nm (e) 1:2 Pyrene:$TlPF_6$, λ_{emi} = 420 nm.

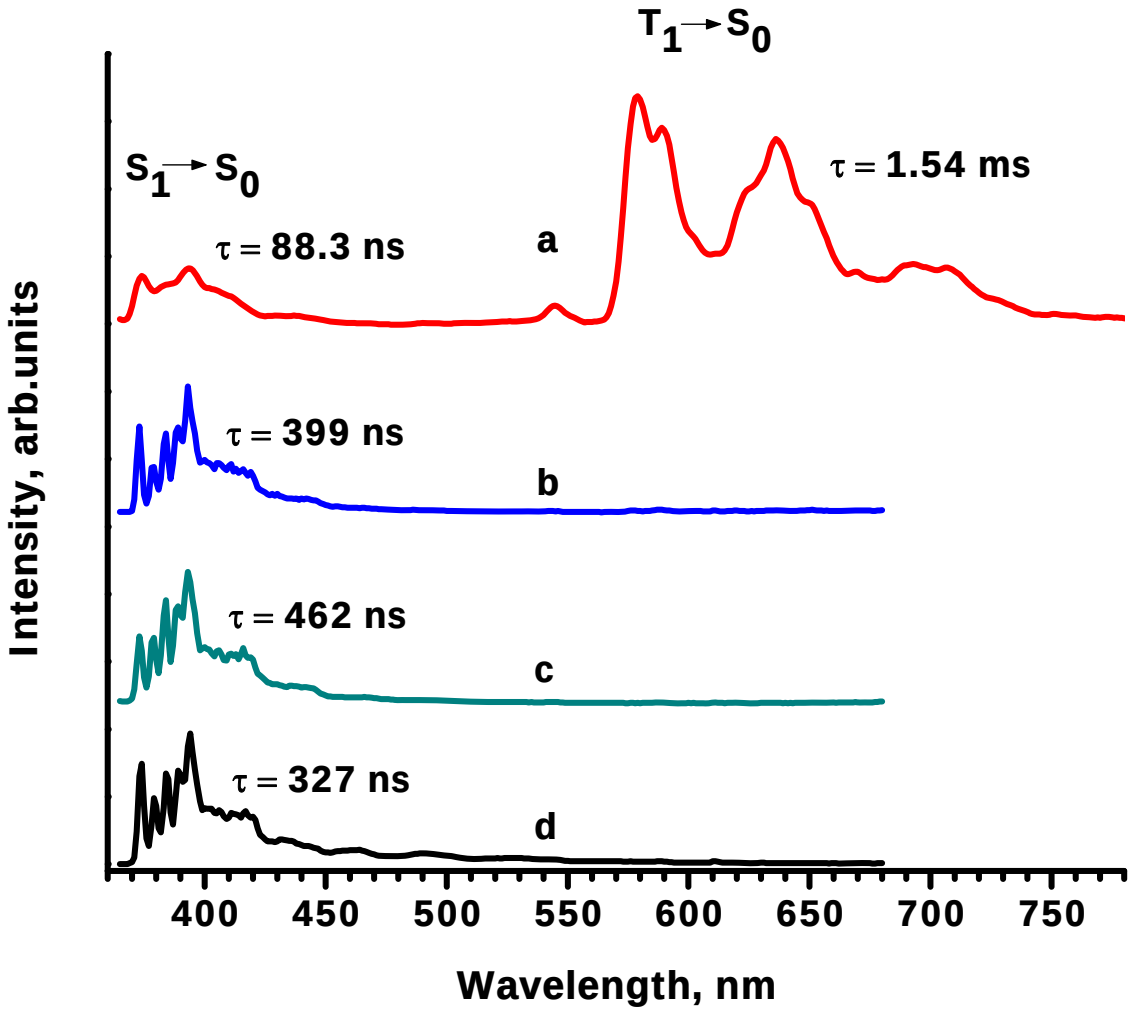

Figure 3.37. Emission spectra in 2-MTHF at 77 K along with their lifetimes. (a) 1:2 Pyrene:$AgClO_4$, λ_{exc} = 350 nm (b) 1:2 Pyrene:$TlPF_6$, λ_{exc} = 350 nm (c) 1:2 Pyrene: KO^tBu, λ_{exc} = 350 nm (d) 0.6 M Pyrene, λ_{exc} = 350 nm.

3.4 Photophysical Pathway

To understand the mechanism by which the enhancement of phosphorescence occurring in the complexes, the excitation spectra of the naphthalene with $AgClO_4$ is compared to the excitation spectra of naphthalene in frozen solution (Figure 3.34). The excitation spectra are also compared to the absorption spectra of pure naphthalene and naphthalene with $AgClO_4$ (Figure 3.33). The excitation spectra of the frozen solution of naphthalene with $AgClO_4$ at about 310 nm correlates with the absorption spectra of napthalene which is due $S_0 \longrightarrow S_1$ transition (π,π^*).[86] The $S_0 \longrightarrow S_1$ transitions are lower in energy and less intense than the $S_0 \longrightarrow S_2$ transitions.[46] In Figure 3.33, the red shifted peak at about 320 nm for the naphthalene-$AgClO_4$ is assigned to charge transfer spectra. This charge transfer band is slightly further red shifted in the solid state. This is reasonable as the charge transfer from the naphthalene ring to the silver, which is electrophilic in nature, occurs.

Further analysis of the excitation spectra of naphthalene with $AgClO_4$ and naphthalene by itself in frozen solution revealed the weak direct $S_0 \longrightarrow T_1$ absorptions (Figure. 3.34). Observation of these weak absorptions compared to the strong CT band clearly indicates that the $S_0 \longrightarrow T_1$ transition has minor effect on the excitation route in the $\{[Ag_4(\text{tetra-}\eta^2\text{-naphthalene})][(ClO_4)_4]\}$ complex.

Based on the above observations, sensitized phosphorescence in all the silver adducts with aromatics studied herein, is due to direct excitation to the charge transfer state and then nonradiatively to the T_1 state of the aromatic as depicted in the energy

level diagram (Figure 3.38 (Left)). The energy levels shown in the Figure 3.38 are obtained from the various transitions observed in Figure 3.33 and Figure 3.34.

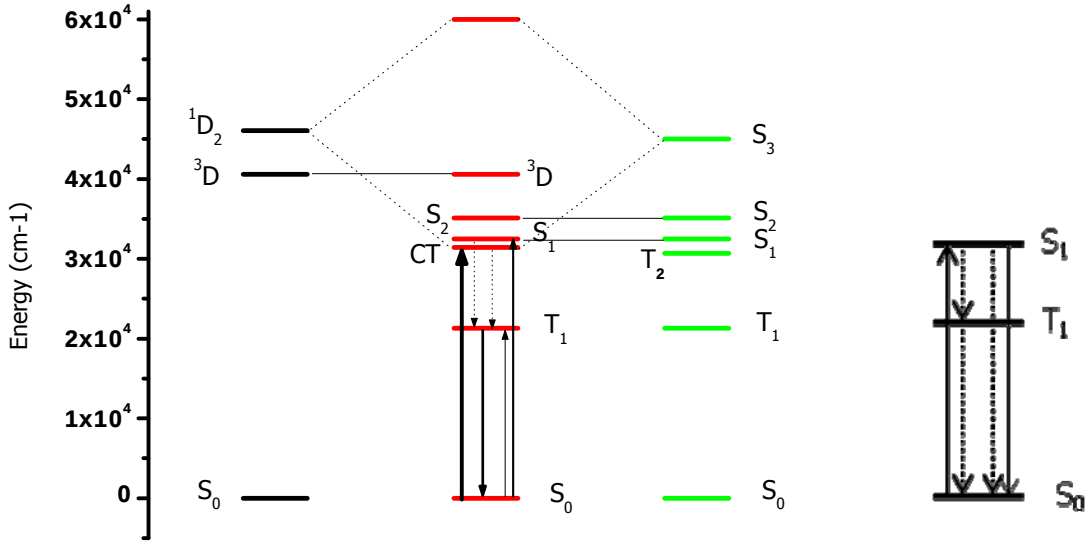

Figure 3.38. Energy level diagram showing the formation of charge transfer state in the naphthalene-$AgClO_4$ (left) and naphthalene-Tl^+/K^+ (right). The energy levels of various states are based on the spectra shown in Figures 3.33 and 3.34. Solid and dashed lines indicate radiative and nonradiative processes.

The T_1 state of pure naphthalene is unperturbed in the adduct as a result of complexation between naphthalene and $AgClO_4$. This is clearly seen from the excitation spectra in Figure 3.34 and the charge transfer state is higher in energy than the T_1 state. Figure 3.38 shows the charge transfer state is formed as a result of the interaction of the S_3 state of naphthalene with the ^1D state of silver. The S_1, S_2 and T_1 state essentially remains nonbonding in nature. Excitation through the charge transfer state due to an external heavy atom effect is not known for organic compounds to

sensitize the phosphorescence. Here such phenomenon is observed similar to those observed in literature.[38,57a]

In the case of naphthalene with Tl^+ or K^+, no such charge transfer state is formed and no enhancement in the phosphorescence was observed. Same is the case with the pyrene. Figure 3.38 on the right depicts this phenomenon.

3.5 Conclusions

The compounds of silver perchlorate with aromatics such as naphthalene, perylene and anthracene were synthesized and their crystal structures were confirmed. Spin-orbit coupling effects of heavy atom, silver was most manifest owing to a combined effect of strong cation-π interaction and electronic factor. Enhancement of monomer phosphorescence of naphthalene and anthracene was observed in solid state. With perylene, α form of perylene emission was red shifted by about 20 nm was seen.

The frozen solution studies of naphthalene and pyrene with $AgClO_4$, $TlPF_6$ and KO^tBu have shown interesting results. Enhancement of monomer phosphorescence of naphthalene (green) and pyrene (red) were observed with $AgClO_4$. The frozen solution of naphthalene and pyrene with $AgClO_4$ has shown huge enhancement of monomer phosphorescence. However, with $TlPF_6$, only modest changes were seen despite the fact that Tl^+ is much heavier than Ag^+. Monomer fluorescence intensity and lifetimes are lowered with $AgClO_4$ addition. Also the monomer phosphorescence lifetimes of free naphthalene and pyrene were in seconds whereas their frozen solutions with $AgClO_4$ were reduced to milliseconds. The lighter metal, potassium (KO^tBu) did not show any significant effect.

Stern-Volmer studies of the aromatics with $AgClO_4$, $TlPF_6$ and KO^tBu were also studied. The quenching of fluorescence was large with $AgClO_4$ and $TlPF_6$ and very weak with KO^tBu. This is because silver and thallium are heavy metals whereas potassium is a lighter metal. The quenching of perylene with these metals is weak, which can be attributed to more number of aromatic rings compared to other aromatics employed

here. Formation of charge transfer state was responsible for the sensitization of phosphorescence in the naphthalene and pyrene adduct with $AgClO_4$.

3.6 References

[1] Gal, J. –F.; Maria, P. –C.; Decouzon, M.; Mo, O.; Yañez, M.; Abboud, J. L. M. *J. Am. Chem. Soc.* **2003**, *125*, 10394-10401.

[2] (a) Larrivee, M. L.; Allison, J. *J. Am. Chem. Soc.* **1990**, *112*, 7134- 7140. (b) Goldfuss, B.; Scheleyer, P. V. R.; Hampel, F. *J. Am. Chem. Soc.* **1997**, *119*, 1072-1080. (c) Ma, J. C.; Dougherty, D. A. *Chem. Rev.* **1997**, *97*, 1303-1324. (d) Wu, J.; Polce, M. J; Wesdemiotis, C. *J. Am. Chem. Soc.* **2000**, *122,* 12786-12794. (e) Siu, F. M.; Ma, N. L.; Tsang, C. W. *J. Chem. Phys.* **2001**, *114,* 7045-7051.

[3] Mascal, M.; Kerdelhue, J. –L.; Blake, A. J.; Cooke, P. A.; Mortimer, R. J.; Teat, S. J. *Eur. J. Inorg. Chem.* **2000**, 485-490.

[4] Zhu, D.; Herbert, B. E.; Schlautman, M. A.; Carraway, E. R. *J. Environ. Qual.* **2004**, *33*, 276-284.

[5] Ruan, C.; Yang, Z.; Rodgers, M. T. *Phys. Chem. Chem. Phys.* **2007**, *9*, 5902-5918.

[6] Khlobystov, A. N.; Blake, A. J.; Champness, N. R.; Lemenovskii, D. A.; Majouga, A. G.; Zyk, N. V.; Schröder, M.; *Coord. Chem. Rev.* **2001**, *222*, 155-192.

[7] Hill, A. E. *J. Am. Chem. Soc.* **1921**, *43*, 254-268.

[8] (a) Mulliken, R. S. *J. Am. Chem. Soc.* **1952**, *56*, 811-824. (b) Dewar, M. J. S. *Bull. Soc, Chim. Fr.* **1951**, C71-79.

[9] Rundle, R. E.; Goring, J. H. *J. Am. Chem. Soc.* **1950**, *72*, 5337-5337.

[10] Smith, H. G.; Rundle, R. E. *J. Am. Chem. Soc.* **1958**, *80*, 5075-5080.

[11] Turner, R. W.; Amma, E. L. *J. Am. Chem. Soc.* **1960**, *88*, 3243-3247.

[12] Taylor, I. F., Jr.; Hall, E. A.; Amma, E. L. *J. Am. Chem. Soc.* **1969**, *91*, 5745-5749.

[13] Amma, E. L.; Taylor, I. F., Jr.; *J. Chem. Soc.* Chem. Commun. **1970**, *21*, 1442-1443.

[14] Rodesiler, P. F.; Griffith, E. A. H.; Amma, B. L. *J. Am. Chem. Soc.* **1972**, *94*, 761-766.

[15] (a) Amma, E. L.; Griffith, E. A. H. *J. Am. Chem. Soc.* **1971**, *93*, 3167-3172 (b) Hall, E. A.; Amma, E. L. *J. Chem. Soc. Chem. Commun.* **1968,** *11*, 622-624.

[16] Rodesiler, P. F.; Amma, E. L.; *Inorg. Chem.* **1972**, *11*, 388-395.

[17] (a) Griffith, E. A. H.; Amma, E. L. *J. Am. Chem. Soc.* **1974**, *96*, 743-749. (b) Hall, E. A.; Amma, E. L. *J. Am. Chem. Soc.* **1969**, *91*, 6538-6540.

[18] Griffith, E. A. H.; Amma, E. L. *J. Am. Chem. Soc.* **1974**, *96*, 5407-5413.

[19] Strauss, S. H.; Noirot, M. D.; Anderson, O. P. *Inorg. Chem.* **1985**, *24*, 4307-4311.

[20] Schmidbaur, H.; Bublak, W.; Huber, B.; Reber, G.; Mueller, G. *Angew. Chem. Int. Ed. Engl.* **1986**, *98*, 1108-1109.

[21] Kang, H. C.; Hanson, A. W.; Eaton, B.; Boekelheide, V. *J. Am. Chem. Soc.* **1985**, *107*, 1979-1985.

[22] Munakata, M.; Wu, L. P.; Kuroda-Sowa, T.; Maekawa, M.; Suenaga, Y.; Ning, G. L.; Kojima, T. *J. Am. Chem. Soc.* **1998**, *120*, 8610-8618.

[23] Gano, J. E.; Subramaniam, G.; Birnbaum, R. *J. Org. Chem.* **1990**, *55*, 4760-4763.

[24] Dargel, T. K.; Hertwig, R. H.; Koch, W. *Mol. Phys.* **1999**, *96*, 583-591.

[25] (a) Harvey, R. G. *Polycyclic Aromatic Hydrocarbons*: **1997,** Wiley-VCH: Weinheim, Germany, (b) Clar, E. *Polycyclic hydrocarbons.* **1964.** Academic press: New York. Vols 1 and 2. (c) Cioslowski, J.; Liu, G.; Martinov, M.; Piskorz, P.; Moncrieff, D. *J. Am. Chem. Soc.* **1996**, *118*, 5261-5264. (d) Debad, J. D.; Morris, J. C.; Lynch, V.; Magnus, P.; Bard, A. J. *J. Am. Chem. Soc.* **1996**, *118*, 2374-2379. (e) Iuliucci, R. J.; Phung, C. G.; Facelli, J. C.; Grant, D. M. *J. Am. Chem. Soc.* **1996**, *118*, 4880-4888. (f) Schulman, J. M.; Disch, R. L. *J. Am. Chem. Soc.* **1996**, *118*, 8470-8474. (g) Langhoff, S. R.; Bauschlicher, C. W., Jr.; Hudgins, D. M.; Sandford, S. A.; Allamandola, L. J. *J. Pjys. Chem. A* **1998**, *102*, 1632-1646. (h) Hagihara, S.; Gremaud, L.; Bollot, G.; Mareda, J.; Matile, S. *J. Am. Chem. Soc.* **2008**, *130*, 4347-4351. (i) Sugi, Y.; Maekawa, H.; Hasegawa, Y.; Naiki, H.; Komura, K.; Kubota, Y. *Catal. Today.* **2008**, *132*, 27-37. (j) Kim, J.; Morozumi, T.; Kurumatani, N.; Nakamura, H. *Tetrahedron Lett.* **2008**, *49*, 1984-1987. (k) Kollár, J.; Hrdlovič, P.; Chmela, Š. *J. photochem. Photobiol. A. Chem.* **2008**, *195*, 64-71. (l) Li, S.; Xiang, J.; Mei, X.; Xu, C. *Tetrahedron Lett.* **2008**, *49*, 1690-1693.

[26] Zhong, J. C.; Munakata, M.; Kuroda, T. S.; Maekawa, M.; Suenaga, Y.; Konaka, H. *Inorg. Chem.* **2001**, *40*, 3191-3199.

[27] (a) Bendikov, M.; Wudi, F. *Chem. Rev.* **2004**, *104*, 4891-4945. (b) Anthony, J. E. *Chem. Rev.* **2006**, *106*, 5028-5048. (c) Pascal, R. A., Jr. *Chem. Rev.* **2006**, *106*, 4809-4819.

[28] Chen, Z.; Muller, P.; Swager, T. M. *Org. Lett.* **2006**, *8*, 273-276.

[29] (a) Wang, Z.; Wang, C.; Xi, Z. *Tetrahedron Lett.* **2006**, *47*, 4157-4160. (b) Tannaci, J. F.; Noji, M.; McBee, J.; Tilley, T. D. *J. Org. Chem.* **2007**, *72*, 5567-5573.

[30] (a) Munakata, M.; Wu, L. P.; Ning, G. L. *Coord. Chem. Rev.* **2000**, *198*, 171-203. (b) Porter, L. C.; Polam, J. R.; Mahmoud, J. *Organometallics.* **1994**, *13*, 2092-2096. (c) Suravajjala, S.; Polam, J. P.; Porter, L. C. *Organometallics.* **1994**, *13,* 37-42.

[31] Budka, J.; Lhoták, P.; Stibor, I.; Sýkora, J.; Cisaŕová, I. *Supramol. Chem.* **2003**, *15*, 353-357.

[32] Munakata, M.; Wu, L. P.; Kuroda-Sowa, T.; Maekawa, M.; Suenaga, Y.; Ohta, T.; Konaka, H. *Inorg. Chem.* **2003**, *42*, 2553-2558.

[33](a) Hill, A. E. *J. Am. Chem. Soc.* **1921**, *43*, 254-268. (b) Hill, A. E. *J. Am. Chem. Soc.* **1922**, *44*, 1163-1193. (c) Hill, A. E.; Miller, F. W., Jr. *J. Am. Chem. Soc.* **1925**, *47*, 2702-2712.

[34] (a) Andrews, L. J.; Keefer, R. M. *J. Am. Chem. Soc.* **1949**, *71*, 3644-3647. (b) Nosaka, Y.; Kira, A.; Imamura, M. *J. Phys. Chem.* **1981**, *85*, 1353-1358. (c) Ogimachi, N.; Andrews, L. J.; Keefer, R. M. *J. Am. Chem. Soc.* **1956**, *78*, 2210-2213. (d) Masuhara, H.; Shioyama, H.; Saito, T.; Hamada, K.; Yasoshima, S.; Mataga, N. *J. Phys. Chem.* **1984**, *88*, 5868-5873.

[35] Lee, J. H.; Schlautman, M. A.; Carraway, E. R.; Yim, S.; Herbert, B. E. *J. Photochem. Photobiol., A* **2004**, *163*, 165-170.

[36] (a) Kasha, M. *J. Chem. Phys.* **1952**, *20*, 71-74. (b) McClure, D. S. *J. Chem. Phys.* **17**, 905-913.

[37] Munakata, M.; Wu, L. P.; Kuroda-Sowa, T.; Maekawa, M.; Suenaga, Y.; Sugimoto, K. *Inorg. Chem.* **1997**, *36*, 4903-4905.

[38] Elbjeirami, O.; Burress, C. N.; Gabbaï, F. P.; Omary, M. O. *J. Phys. Chem. C* **2007**, *111*, 9522-9529.

[39] Solovyov, K. N.; Borisevich, E. A. *Phys. Usp.* **2005**, *48*, 231-253.
[40] Samanta, S.; Roy, M. B.; Chatterjee, M.; Ghosh, S. *J. Lumin.* **2007**, *126*, 230-238.

[41] Horrocks, A. R.; Wilkinson, F. *Proc. R. Soc. London, Sect. A 1968*, *306,* 257-273.

[42] Jin, W.; Liu, C. *Anal. Chem.* **1993**, *65*, 863-865.

[43] Porter, G.; Windsor, M. W. *Proc. Roy. Soc. (London),* **1958**, *A245,* 238-258.

[44] Birks, J. B. *Photophysics of Aromatic Molecules.* J. Wiley and Sons, New York. Chapter 4. **1970.**

[45] Vo-Dinh, T. *Room Temperature Phosphorimetry for Chemical Analysis.* J. Wiley and sons, New York. Chapter 1. **1984.**

[46] Turro, N. J. *Modern Molecular Photochemistry.* University science books, California. Chapter 5. **1991.**

[47] Mataga, N.; Torihashi, Y.; Ota, Y. *Chem. Phys. Lett.* **1967**, *1*, 385-387.

[48] Johnson, P. C.; Offen, H. W. *Chem. Phys. Lett.* **1973**, *18*, 258-260.

[49] Sangster, R. C.; Irvine, J. W., Jr. *J. Chem. Phys.* **1956**, *24*, 670-715.

[50] Seko, T.; Ogura, K.; Kawakami, Y.; Sugino, H.; Toyotama, H.; Tanaka, J. *Chem. Phys. Lett.* **1998**, *291*, 438-444.

[51] (a) Tanaka, J. *Bull. Chem. Soc. Jpn.* **1963**, *36*, 1237-1249. (b) Offen, H. W.; Beardslee, R. A. *J. Chem. Phys.* **1968**, *48*, 3584-3587.

[52] Uy, J.O.; Lim, E. C. *Chem*. *Phys*. *Lett*. **1970**, *7*, 306-310.

[53] Chandra, A. K.; Lim, E. C. *J. Chem. Phys.* **1968**, *49*, 5066-5072.

[54] (a) Langelaar, J.; Rettschnick, R. P. H.; Lambooy, A. M. F.; Hoytink, G. J. *Chem. Phys. Lett.* **1968**, *1*, 609-612.

[55] Takemura, T.; Aikawa, M.; Baba, H. *J. Lumin.* **1976**, *12-13*, 819-823.

[56] Lakowicz, J. R. *Principles of Fluorescence Spectroscopy.* Plenum press: New York. **1999.**

[57] (a) Mohamed, A. A.; Rawashdeh-Omary, M. A.; Omary, M. A.; Fackler, J. P., Jr. D*alton Trans.* **2005**, 2597-2602. (b) Omary, M. A.; Mohamed, A. A.; Rawashdeh-Omary, M. A.; Fackler, J. P. *Coord. Chem. Rev.* **2005**, *249*, 1372-1381.

[58] Omary, M. A.; Elbjeirami, O.; Gamage, C. S. P.; Sherman, K. M.; Dias, H. V. R. *Inorg. Chem.* **2009**, *48*, 1784-1786.

[59] (a) Omary, M. A.; Kassab, R. M.; Haneline, M. R.; Elbjeirami, O.; Gabbaï, F. P. *Inorg. Chem.* **2003**, *42*, 2176-2178. (b) Buress, C.; Elbjeirami, O.; Gabbaï, F. P.; Omary, M. A.

J. Am. Chem. Soc. **2005**, *127*, 12166-12167. (c) Burress, C. N.; Bodine, M. I.; Elbjeirami, O.; Reibenspies, J. H.; Omary, M. A.; Gabbaï, F. P. *Inorg. Chem.* **2007**, *46*, 1388-1395.

[60] Streitwieser, A., Jr. *Molecular orbital Theory for Organic Chemists*. **1959,** Wiley, New York, P 330.

[61] Padhye, M. R.; McGlynn, S. P.; Kasha, M. *J. Chem. Phys.* **1956**, *24*, 588-594.

[62] Hirayama, S.; Kajiwara, Y.; Nakayama, T.; Hamanoue, K.; Teranishi, H. *J. Phys. Chem.* **1985**, *89*, 1945-1947.

[63] Goodpaster, J. V.; McGuffin, V. L. *Anal. Chem.* **2000**, *72*, 1072-1077.

[64] Guilbault. G. G., *Practical Fluorescence-Theory, Methods, and Techniques,* Marcel Dekker. New York, **1973**.

[65] Danko, M.; Hrdlovič, P.; Borsig, E. *Eur. Polym. J.* **2003**, *39*, 2175-2182.

[66] Eftink, M. R.; Ghiron, C. A. *Anal. Biochem.* **1981**, *114*, 199-227.

[67] Nakajima, A.; Akamatu, H. *Bull. Chem. Soc. Jpn.* **1968**, *41*, 1961-1963.

[68] Zakrzewski, J.; Giannotti, C.; Delaire, J. *Inorg. Chem.* **2001**, *40*, 831-835.

[69] Wang, J.; Wang, D.; Moses, D.; Heeger, A. J. *J. Appl. Polym. Sci.* **2001**, *82*, 2553-2557.

[70] Saito, T.; Yasoshima, S.; Masuhara, H.; Mataga, N. *Chem. Phys. Lett.* **1978**, *59*, 193-196.

[71] Dreeskamp, H.; Laufer, A.; Zander, M. *Chem. Phys. Lett.* **1984**, *112*, 479-482.

[72] Hashimoto, S. *J. Phys. Chem.* **1993**, *97*, 3662-3667.

[73] Fayed, T. A.; Grampp, G.; Landgraf, S. *Int. J. Photoenergy.* **1999**, *1*, 173-176.

[74] Li, L.; Zhao, Y.; Wu, Y.; Tong, A. *Talanta* **1998**, *46*, 1147-1154.

[75] Chen, Z.; Zhang, Z.; Yuan, X.; Zhang, G.; Bai, F. *Guang pu xue guang pu fen xi= Guang pu.* **2001**, *21*, 362-365.

[76] Fletcher, K. A.; Pandey, S.; Storey, I. K.; Hendricks, A. E.; Pandey, S. *Anal. Chim. Acta.* **2002**, *453*, 89-96.

[77] Locke, R. J.; Lim, E. C. *Chem. Phys. Lett.* **1987**, *138*, 489-493.

[78] Lewis, G. N.; Kasha, M. *J. Am. Chem. Soc.* **1944**, *66*, 2100-2116.

[79] Giaimuccio, J. M.; Rowley, J. G.; Meyer, G. J.; Wang, D.; Galoppini, E. *Chem. Phys.* **2007**, *339*, 146-153.

[80] Mallik, G. K.; Pal, T. K.; Ganguly, T.; Banerjee, S. B. *Bull. Chem. Soc. Jpn.* **1988**, *61*, 3673-3680.

[81] Tong, L.; Weixiao, C.; Xinde, F. *Polym. Commun.* **1985**, *4*, 341-349**.**

[82] Cotton, F. A.; Wilkinson, G.; Murillo, C. A.; Bochmann, M. *Advanced Inorganic Chemistry.* J. Wiley and sons. New York. Sixth edition. **2003**

[83] Akhbari, K.; Morsali, A. *J. Organomet. Chem.* **2007**, *692*, 5109-5112.

[84] Janiak, C. *Coord. Chem. Rev.* **1997**, *163*, 107-216.

[85] Murayama, K.; Aoki, K. *Inorg .Chim. Acta.* **1998**, *281*, 36-42.

[86] Ermolaev, V. L.; Svitashev, K. K. *Opt. Spectrosc. USSR*, **1959**, *7*, 664-667.

CHAPTER 4

STRUCTURE-LUMINESCENCE RELATIONSHIPS IN BIS(THIOCYANATO) GOLD(I) COMPLEXES*

4.1 Introduction

Gold(I) complexes have been among the most prominent luminescent transition-metal coordination compounds. The luminescence in most Au(I) compounds is attributed to the d^{10}-d^{10} closed shell "aurophilic bonding" interactions,[1] though ligand-centered emissions and Au-centered emissions in monomeric mononuclear complexes are also known.[2] The aurophilic interactions between Au(I) centers are usually considered significant when the Au-Au distance is less than 3.6 Å.[3,4] These interactions between closed-shell Au(I) play an important role in determining the solid-state structural arrangement of Au(I) compounds.[5,6] The luminescence exhibited by Au(I) compounds is useful in a variety of applications such as detection of volatile organic compounds,[7] ion sensors,[8] oxygen sensors,[9] and molecular light emitting devices.[10] Several interesting luminescence phenomena associated with the alteration of Au-Au interactions in Au(I) complexes have been reported, such as solvoluminescence,[11] polymorph-selective luminescence,[12] luminescence tribochromism,[13] and exciplex tuning.[14] Solvoluminescence has been reported by Balch group for colorless crystals of $[Au(CH_3N{=}COCH_3)_3]$ previously irradiated with near UV light that exhibit solvent-stimulated spontaneous phosphorescence.[11] The same group reported a few examples

* This work is published. Arvapally, R.K.; Sinha, P.; Hettiarachchi, S.; Coker, N. L.; Bedel, C. E.; Patterson, H. H.; Elder, R. C.; Wilson, A. K.; Omary, M. A. *J. Phys. Chem. C.* **2007**, *111*, 10689-10699.

of polymorph-selective luminescence, including a recent report in which [μ_3-$S(AuCNC_7H_{13})_3$](SbF_6) undergoes a reversible phase change from orthorhombic to monoclinic upon cooling, affecting both the luminescence and aurophilic interactions.[12] Luminescence tribochromism has been reported by the Eisenberg group for gold(I) thiouracilate complexes that exhibit bright blue or cyan emissions upon grinding.[13] Similar observations have been reported earlier by Fackler and co-workers for $[(TPA)_2Au][Au(CN)_2]$ (TPA = 1,3,5-Triaza-7-phosphaadamantane).[15] Rawashdeh-Omary et al. have shown that dicyano complexes of both Ag(I) and Au(I) exhibit multiple excimeric emissions that can be tuned across the UV and visible regions by wavelength-selective excitation, temperature, varying the concentration in solution or the solid state (alkali halide hosts), and/or controlled laser irradiation that leads to reversible "write/read/erase" changes.[14]

Despite the great attention given to luminescent Au(I) compounds over the past few decades, as illustrated above, establishing a clear structure-luminescence relationship remains an elusive goal in this area. What has been clearly established is the need to have intramolecular or intermolecular aurophilic bonding to observe Au-centered luminescence in two-coordinate complexes while three-coordinate complexes do not require such interactions.[2] The difficulty lies in trying to relate the luminescence energy to the crystallographic Au-Au ground state distances as situations wherein direct correlation,[16] inverse correlation,[17,18] and even absence of correlation[19] were reported to exist between the luminescence energy and the Au-Au distance. This is in contrast to the situation in luminescent systems of other metals that were studied earlier, such as

the tetracyanoplatinates(II) in which a clear correlation has long been established between the luminescence energy and the Pt-Pt distance;[20] other recent reports reinforce this trend for other types of Pt(II) complexes that exhibit Pt-Pt interactions.[21] In this work, we examine the structure-luminescence relationship in an intriguing class of Au(I) complexes, $[Au(SCN)_2]^-$, in which varying the counterion leads to interesting and unexpected changes in both the supramolecular structure and the luminescence energy. We are reporting a detailed photophysical study of $M[Au(SCN)_2]$ compounds (M= K^+, Na^+, nBu_4N^+, Rb^+, and Cs^+) to assess the factors important for establishing structure-luminescence relationships. A better understanding of these factors will aid in design of tunable solid-state systems based on two coordinate Au(I) complexes for photonic applications in which phosphorescent materials are of much current interest.[22, 23]

4.2 Experimental Details

4.2.1 Syntheses

A solution of 0.0735g ($6.8x10^{-4}$ moles) of KSCN in acetonitrile was added to another solution composed of 0.0966g ($3.3x10^{-4}$ moles) of $Au(Me_2S)Cl$ in acetonitrile. The resultant solution was stirred for about 4 hours. The white precipitate (potassium chloride) formed was filtered out, and the filtrate was subjected to evaporation under reduced pressure. The yield obtained was 89%. The obtained product was white in color.

4.3 Results and Discussion

4.3.1 Solid State Luminescence Behavior

When excited with UV light, colorless crystalline samples of the potassium salt of gold(I) thiocyanate show bright green emission at room temperature. As shown in Figure 4.1, temperature dependent photoluminescence studies carried out from 4 to 295 K show two emission bands: an intense lower-energy (LE) green band at 535 nm and a weaker higher-energy (HE) blue band at 443 nm, which appears as a shoulder in the steady-state spectra. No significant changes in the peak maxima are observed upon decreasing the temperature from 295 to 4 K. However, the HE shoulder becomes more distinct, and its relative intensity increases at lower temperatures. Figure 4.2 shows the steady-state emission and excitation spectra of $K[Au(SCN)_2]$ at 77 K. The luminescence excitation spectra for crystalline $K[Au(SCN)_2]$ monitoring either the HE or LE emission bands give a similar profile. Two excitation bands are obtained: one at 315 nm and the other at 365 nm. Both excitation peaks likely represent oligomeric species because they are significantly red shifted from the solution absorption bands, which occur at very short wavelengths below 300 nm.[17]

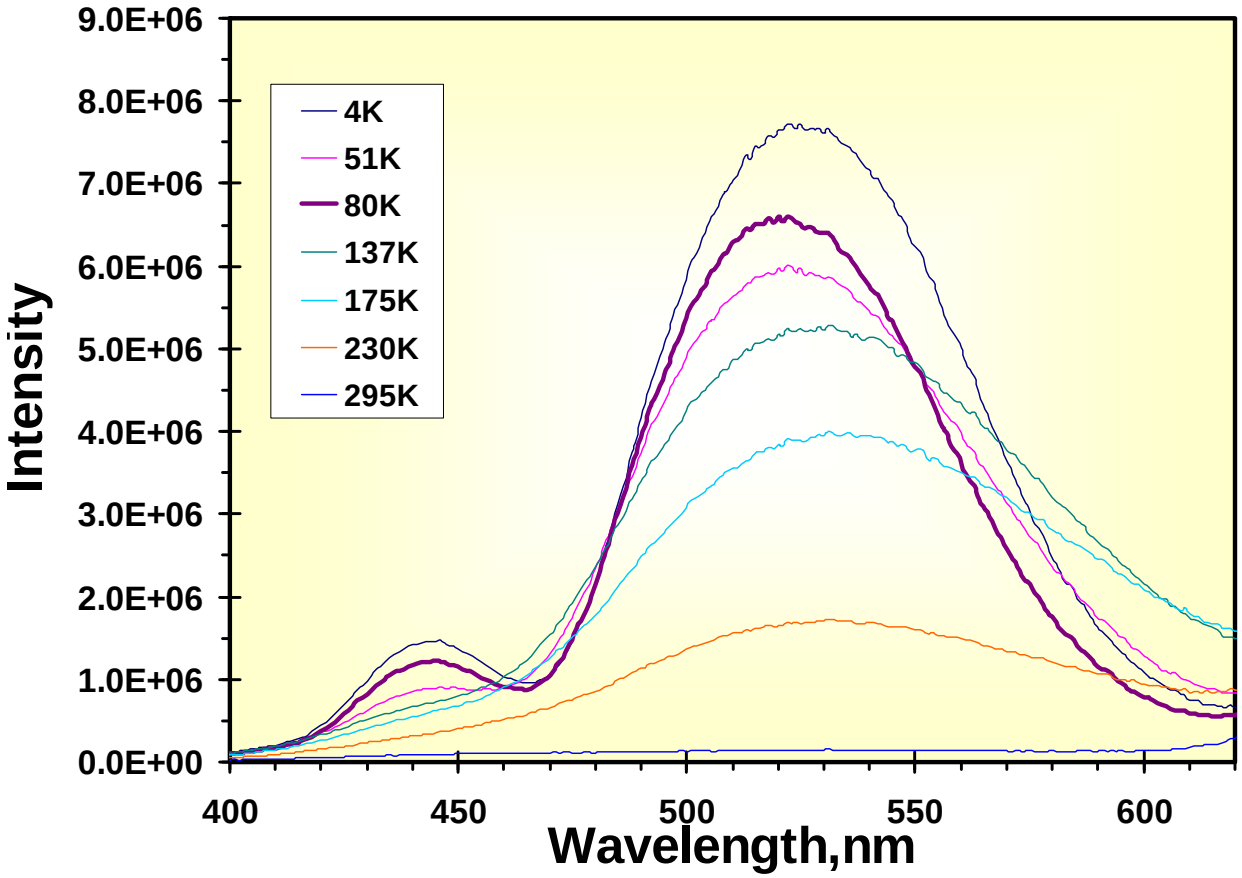

Figure 4.1. Temperature-dependent photoluminescence spectra for crystalline $K[Au(SCN)_2]$ using 365 nm excitation.

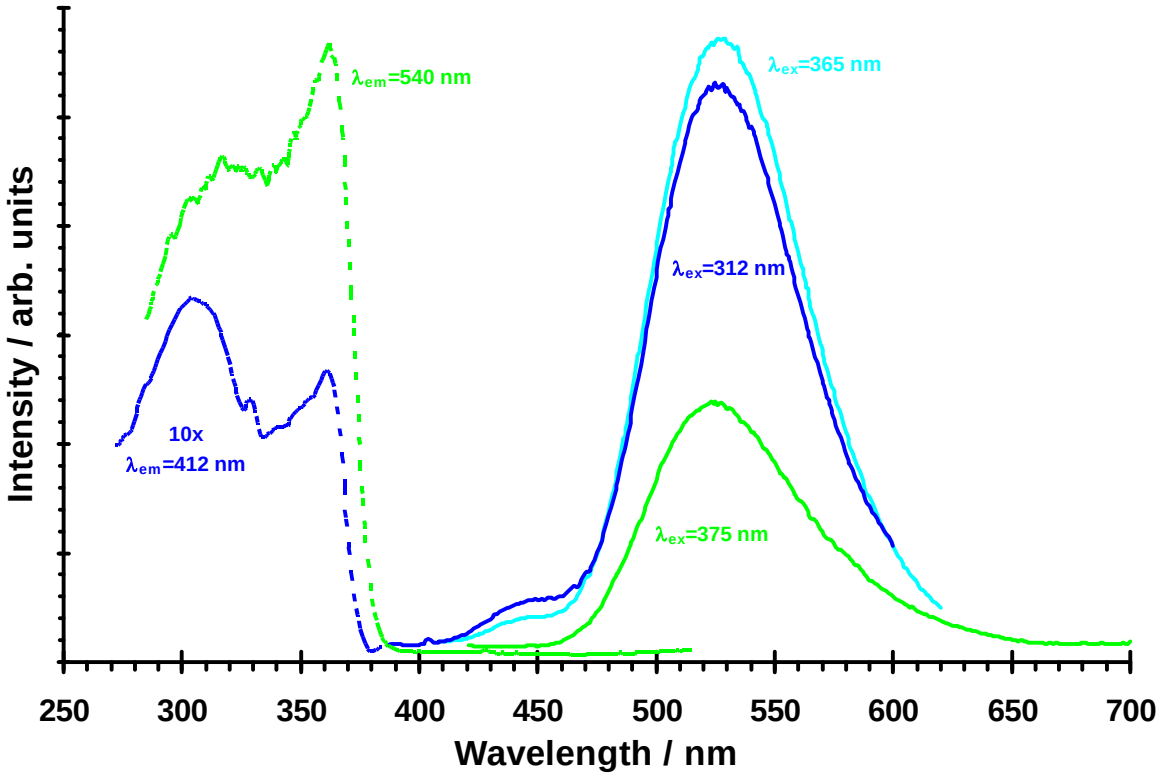

Figure 4.2. Photoluminescence spectra of crystalline $K[Au(SCN)_2]$ at 77K.

As shown in Figure 4.3, use of time resolved luminescence spectra for crystalline $K[Au(SCN)_2]$ at 77 K allows the HE band to be fully resolved and separated from the more dominant LE green band. The lifetime data show that the HE emission represents fluorescence with a lifetime of 24.4 ns, while the LE emission represents phosphorescence with a lifetime of 45.4 μs. Thus, the blue and green emissions are assignable to radiative transitions that are formally $S_1 \rightarrow S_0$ and $T_1 \rightarrow S_0$ of oligomeric $\{K[Au(SCN)_2]\}_n$ species.[24] This is somewhat unusual because the presence of the gold heavy atom is associated with rather strong spin-orbit coupling (ξ_{5d} = 5.1 x 10^3 cm^{-1}),[25] which usually leads to unity intersystem crossing and thus observation of only phosphorescence band in Au(I) compounds.[2] However, a precedent wherein both fluorescence and phosphorescence are exhibited simultaneously in an Au(I) complex

has been reported by Eisenberg and co-workers for dimeric dithiophosphate complexes.[26] Given the assignment of the HE and LE emissions in $K[Au(SCN)_2]$ to fluorescence and phosphorescence, respectively, we now assign the corresponding excitation feature near 315 nm to $S_0 \rightarrow S_1$ transition while the feature near 365 nm to an $S_0 \rightarrow T_1$ transition.

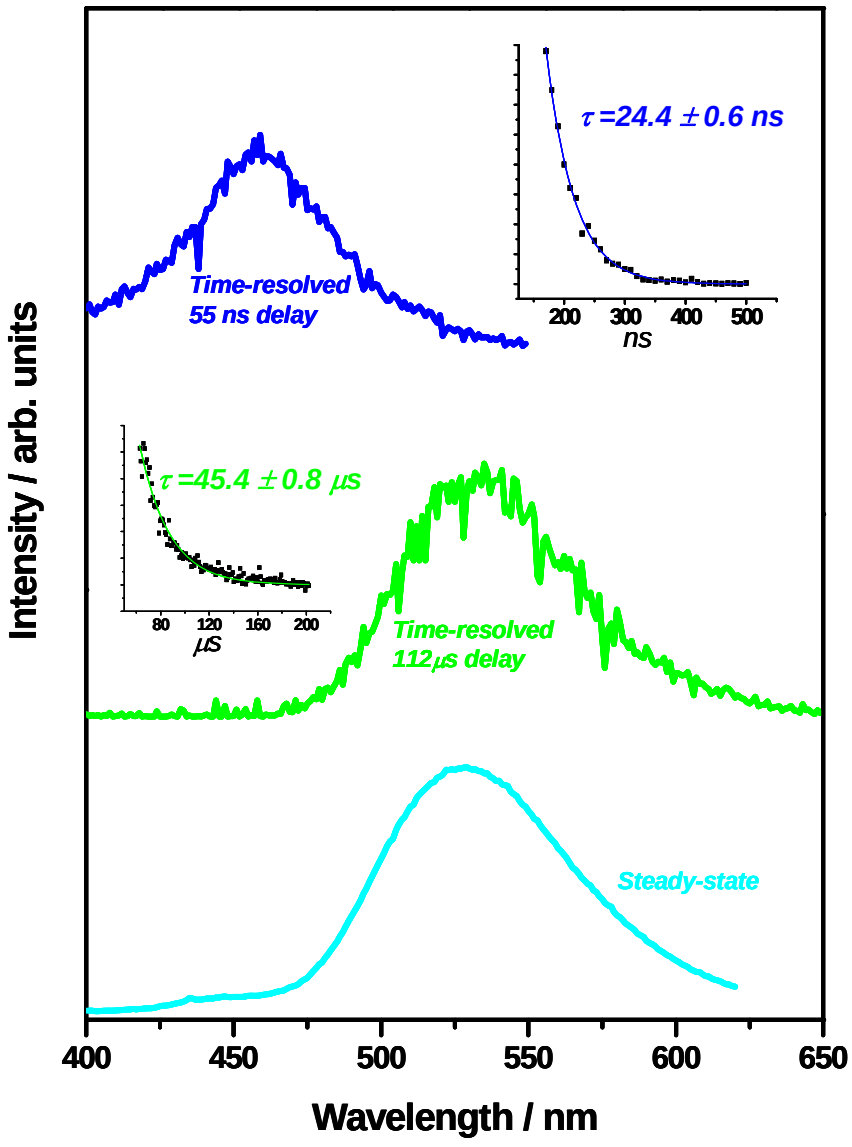

Figure 4.3. Time-resolved spectra showing the resolution of the fluorescence and phosphorescence bands for crystalline $K[Au(SCN)_2]$.

Photoluminescence spectra for other gold(I) salts are shown in Figure 4.4, illustrating the tuning of the emission energy across the visible region by changing the counterion. To represent non alkali metal salts, we have selected (n-Bu_4)N[$Au(SCN)_2$] to carry out detailed luminescence studies similar to the above ones for the potassium salt. Similar to the potassium salt, two luminescence bands are observed. The LE band appears in the green region and is more intense than the HE blue band. No significant change in peak maximum is observed in either band upon decreasing the temperature from 295 to 4 K. However, the notable changes from the luminescence results for the potassium salt are (1) a greater reduction in the relative intensity of the LE band upon heating and (2) a more structured profile in the emission spectra. The phosphorescence bands in K[$Au(SCN)_2$] and (n-Bu_4)N[$Au(SCN)_2$] upon increasing the temperature from 4 K to 295 K is due to multiphonon relaxation processes to the ground state, leading to faster nonradiative decay at higher temperatures. It is not unusual for this decay to be different for multiple emission bands in the same material or for different materials.

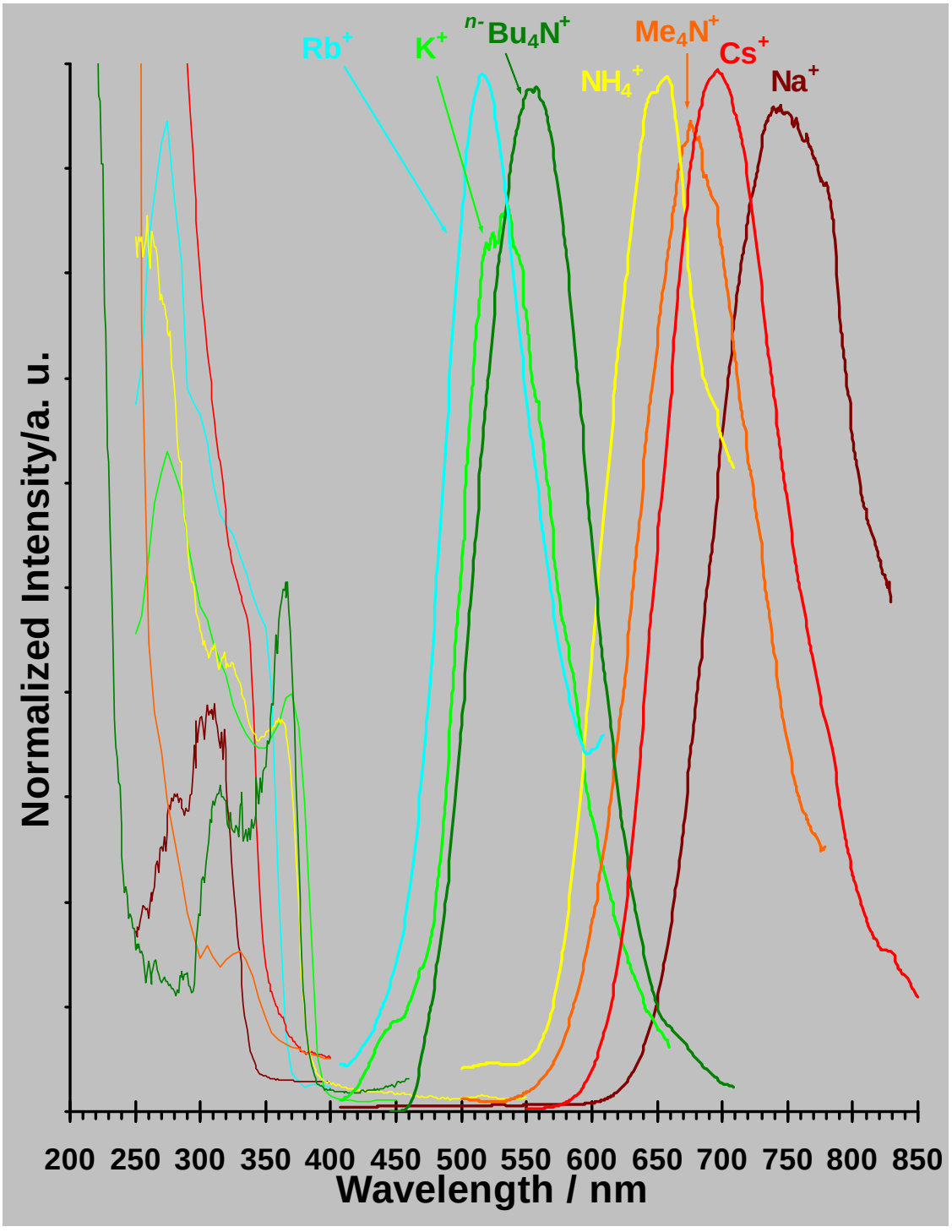

Figure 4.4. Photoluminescence spectra at 77 K for crystalline samples of various $[Au(SCN)_2]^-$ salts, as identified by the counter ion. Emission and excitation spectra are indicated by thick and thin lines, respectively.

The above luminescence data illustrate broad emission bands and large energy gaps between the emission and excitation maxima for all compounds examined. These are typical characteristics of Au-centered emissions in associating Au(I) complexes. The solid state luminescence data for various $[Au(SCN)_2]^-$ salts examined herein are consistent with what has been established in literature, in that two coordinate Au(I) complexes exhibit Au-centered emissions only in the presence of aurophilic bonding between adjacent complexes.[2] The $R_4P[Au(SCN)_2]$ salts are the only samples that do not exhibit such emissions, which is consistent with the lack of Au-Au interactions only in these phosphonium salts. Crystals of all other salts exhibit Au-Au interactions and thus Au-centered emissions. It is interesting to note that the observation of luminescence and Au-Au interactions in $R_4N[Au(SCN)_2]$ crystals is dissimilar to the situation for the analogous dicyano complexes, wherein $[Au(CN)_2]^-$ units are essentially isolated from one another in salts such as (n-Bu_4)$N[Au(CN)_2]$,[27] for which no Au-Au centered emissions have been reported.

4.3.2 Structure-Luminescence Correlation

Computational calculations have been carried out by my colleague Pankaj Sinha. Table 4.1 summarizes the calculated $T_1 \rightarrow S_0$ phosphorescence and $S_0 \rightarrow T_1$ excitation energies for the dimeric complexes. The experimental data in Figure 4.4 clearly show that each complex luminesce in the visible region. However, calculations for the dimeric models give rise to luminescence in the near-IR region even when using theoretical treatments that have been validated. Indeed, these treatments give rise to a reasonable agreement with the experimental data for the excitation energies.

Table 4.1. Emission and excitation wavelengths along with stokes shift.

M^+	λ_{emi}/nm[c]	λ_{exc}/nm[d]	SS/cm^{-1} [e]	d_{Au-Au} (T1)/Å
none[a]	1229	348	20585	2.745
none[a]	1241	361	19642	2.743
K^+ [a]	1389	398	17942	2.667
Rb^+ [a]	1222	395	17133	2.698
Cs^+ [a]	1158	391	16940	2.701

[a] Method/basis: B3PW91/aug-cc-pVDZ-PP - Au, aug-cc-pV(d+D)Z - S, aug-cc-pVDZ – C, N, and LANL2DZ – counterion. [b] Method/basis: B3PW91/aug-cc-pVTZ-PP – Au, aug-cc-pV(d+T)Z – S, and aug-cc-pVTZ- C, N. [c] $T_1 \rightarrow S_0$ excitation at the experimental geometry of a dimeric unit from the structure of $K[Au(SCN)_2]$. [d] $S_0 \rightarrow T_1$ at the T_1 optimized geometry. [e] Stokes' shift based on the computed λ_{emi} and λ_{ex} values listed.

Table 4.1 shows that the vertical excitations for dimeric models at their experimental crystallographic geometries give rise to wavelengths that are well within the 350-400 nm experimental range when correlation consistent basis sets are used in conjuction with B3PW91. Because monomeric models give rise to significantly higher $S_0 \rightarrow T_1$ excitation energies while dimeric models are sufficient to shift these excitation energies to the experimentally observed range, this identifies dimeric clusters to be responsible for the luminescence in $M[Au(SCN)_2]$ solids. The fully optimized geometries

of dimeric models in their T_1 state give rise to drastically red-shifted phosphorescence energies compared to experimental values. This is surprising particularly because literature work suggests that Au-Au excimer formation in dimeric Au(I) complexes leads to UV phosphorescence while Patterson and co-workers have shown that $*[Au(CN)_2]_2^{2-}$ excimers and even trimeric analogues emit in the UV region,[14a] Che and co-workers have shown that intramolecular excimer formation in dinuclear Au(I) phosphine complexes leads to UV phosphorescence that is shifted to the visible region only upon exciplex formation with a counterion or solvent molecule.[28] Fully optimizations by a computational treatment that has been validated to attain accurate transition energies give rise to NIR phosphorescence and huge Stokes' shifts as in Table 4.1. Thus, we conclude that these energies are related to the fact that the solid-state lattice does not allow for the drastic rearrangements in the excimeric T_1 states. Thus, the constrained environment in the crystalline solid state would not allow such distortions to the extent predicted by gas-phase calculations for dimeric models in vacuum, which lack matrix effects. A similar conclusion was reached by Coppens and co-workers by time-resolved X-ray diffraction studies that experimentally determined the crystal structures of phosphorescent molecular states. In an effort to provide experimental evidence of the aforementioned hypothesis that the predicted NIR emissions are due to lack of matrix effects, we have performed frozen solution studies for $K[Au(SCN)_2]$ in acetonitrile. Figure 4.5 shows that these solutions exhibit phosphorescence (τ_{77K} = 55 ± 2 μs) in the yellow-orange region, significantly red shifted from the bluish-green phosphorescence exhibited by the solid compound. For example, the 10^{-3} M frozen solution exhibits an

emission maximum of 582 nm and a Stokes' shift of 14.2 x 10^3 cm^{-1}, compared to analogous values of 525 nm and 8.6 x 10^3 cm^{-1} for the crystals. The 10^{-2} M frozen solution exhibits a Stokes' shift of 13.5 x10^3 cm^{-1}, slightly lower than that for the more dilute 10^{-3} M solution but still significantly higher than that for the crystals. These trends clearly support the aforementioned hypothesis since the frozen solution matrix is less constrained and thus allows for a greater distortion in the phosphorescent state of dimeric units compared to the solid-state environment.

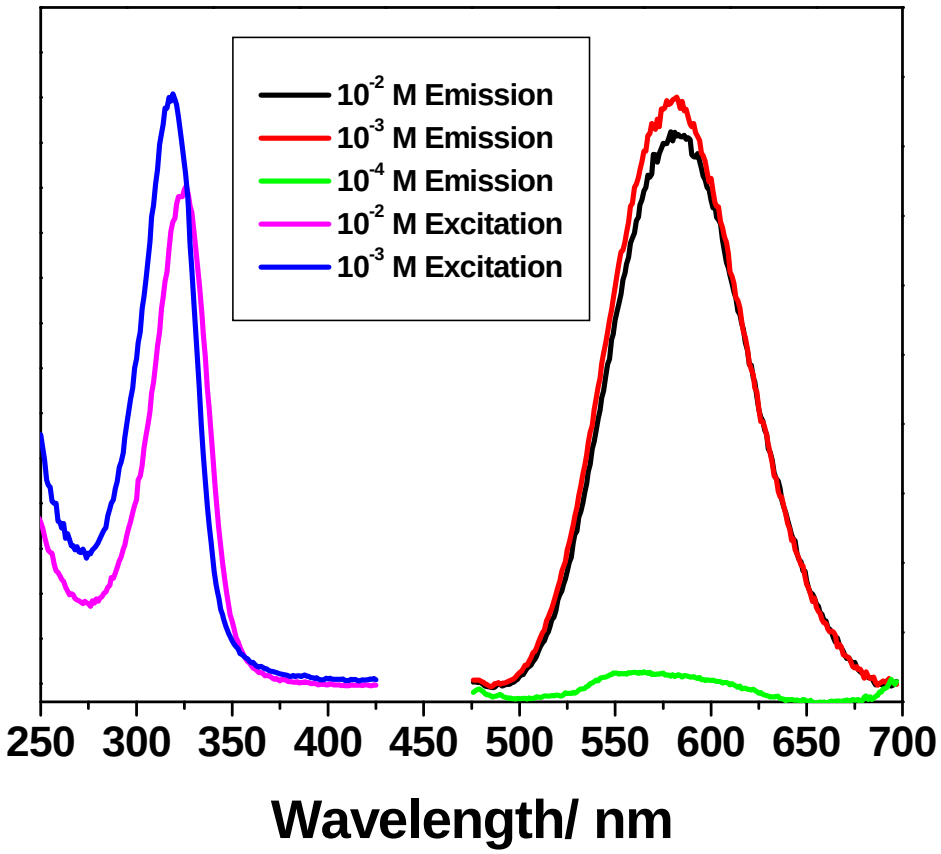

Figure 4.5. Luminescence spectra of $K[Au(SCN)_2]$ in acetonitrile frozen glassy solutions (77 K) at different concentrations.

The puzzling trend of the emission energy with different counterions is explained as follows. There is a general counterintuitive correlation between the emission energy (as well as the Stokes' shift) and the Au-Au distance in different salts whereby blue instead of red shifts are observed for Au-centered emissions in salts with shorter aurophilic bonds. Compounds that have lower emission energies, such as red-emitting Cs^+ salt (λ_{max} = 688 nm; Stokes's shift = 15.7x 10^3 cm^{-1}), exhibit significantly longer Au-

Au distances as well as longer cation-complex distances than those in compounds that exhibit much higher emission energies, such as the blue-green emitting Rb^+ (λ_{max} = 513 nm; Stokes' shift = 9.5 x 10^3 cm^{-1}) and K^+ salts (λ_{max} = 525 nm; Stokes' shift = 8.6 x 10^3 cm^{-1}). The shortest Au-Au distances in the Cs^+ salt are 3.213 and 3.240 Å, much longer than the analogous distances in the Rb^+ salt (3.082 and 3.114 Å) or the K^+ salt (3.006 and 3.043 Å) . Likewise, the shortest counterion-N (thiocyanate) distances in the Cs^+ salt (3.214, 3.179, 3.210, and 3.219 Å) are much longer than the analogous distances in the Rb^+ salt (2.958, 3.011, 3.014, and 3.056 Å) or the K^+ salt (2.832, 2.863, 2.866, 2.889 Å) . These crystallographic distances are consistent with the aforementioned structure of the emitting exciton because there is more freedom for photoinduced rearrangement in the lattices of crystals exhibiting long Au-Au and counterion-complex separations such that the geometry of the emitting exciton becomes closer to the predicted distortion of the excimeric T_1 state. Thus, such compounds will emit at lower energies compared to compounds whose lattices allow for significantly smaller excited-state distortions and thus smaller Stokes' shifts and higher emission energies. In contrast, the excitation energies in different salts lead to an intuitive correlation with the aurophilic distances. This is because the excitation process occurs at the crystallographic geometry at which shorter Au-Au distances lead to smaller HOMO-LUMO gaps and lower transition energies, as is indeed observed.

There is a contrast between photophysical behavior suggested for $M[Au(SCN)_2]$ species with that of haloisonitrilegold (I) complexes. It has been suggested that the contrast in the Au-centered phosphorescence energies of these RNCAuX neutral

complexes is based on the association mode so that extended-chain structures with longer Au-Au distances emit at lower energies and exhibit larger Stokes' shift than those in crystals whose structures entail crossed dimers with shorter Au-Au distances.[18,19] This is not the case here for $M[Au(SCN)_2]$ crystals because the emitting species is a dimeric unit (vide supra) even for crystals in which the complexes pack in infinite chains, such as the three alkali metals whose structures exhibit extended chains according to ref 17. Thus, it is possible that crystals in which complexes pack as dimers or oligomers emit at lower energies than those for crystals in which complexes stack as extended chains. Consistent with this argument is that both ammonium salts exhibit a lesser extent of clustering of their aurophilically interacting bis(thiocyanato)-gold(I) complexes (dimers and loosely connected trimers for the *n*-Bu_4N^+ and MeN_4^+ salts, respectively); yet both, emit at lower energies than the K^+ and Rb^+ salts in which the complexes stack as chains. Compression of extended structures of interacting d^{10} complexes into dimeric units, like suggested here, is not reasonable. Indeed, a recent study by Coppens and co-workers has shown that a trinuclear Cu(I) pyrazolate complex whose molecules stack in zigzag infinite chains in the ground state exhibits discrete excimeric units in its phosphorescent state.[29] While a drastic contraction by 0.58 Å of the intermolecular Cu-Cu distances takes place within the excimer, the excimeric units are well separated from one another (d_{Cu-Cu} = 4.33 Å, further separated by 0.55Å from the ground-state structure).

4.4 Conclusions

The photophysics of ground state Au-Au aurophilic bonding and excited state Au-Au excimeric bonding have been studied. A rare phenomenon of simultaneous existence of fluorescence and phosphorescence is observed in these complexes, and the two components have been resolved in the $K[Au(SCN)_2]$ salt by the time-resolved luminescence spectroscopy. Unstructured emission bands with large Stokes's shifts are exhibited by all five compounds whose crystal structures show Au-Au interactions, including salts of some bulky counterions such as n-Bu_4N^+, while this luminescence is undetectable in the one structurally characterized salt that does not exhibit any Au-Au interactions. The luminescence from these gold complexes is assigned to gold-centered emissions in which excimeric Au-Au bonding plays a major role but ligand rearrangement also takes place. The anomalous trend in the emission energies in which higher-energy phosphorescence is obtained in crystals that exhibit shorter Au-Au interactions has been related to a more constrained photoinduced rearrangement in matrices that do not allow freedom for a drastic structural change in the two complexes comprising the excimer. This has been substantiated by observing significantly red shifted phosphorescence and larger Stokes' shifts in frozen solutions of $K[Au(SCN)_2]$ compared to crystals.

4.5 References

[1] For reviews, see: (a) Pyykko, P. *Chem. Rev*. **1997**, *97*, 597-636. (b) Pyykko, P. *Angew. Chem. Int. Ed*. **2004**, 43, 4412-4456. (c) Pyykko, P. *Inorg. Chim. Acta* **2005**, *358*, 4113-4130.

[2] For a review, see: Forward, J. M.; Fackler, J. P., Jr.; Assefa, Z. Photophysical and Photochemical Properties of Gold (I) Complexes. *In Optpelectronic Properties of Inorganic Compounds*; Roundhill, D. M., Fackler, J. P., Jr., Eds.; plenum: New York **1999** Chapter 6.

[3] Schmidbaur, H. *Gold*: *Progress in Chemistry*, *Biochemistry and Technology;* Wiley; New York, **1999**.

[4] Grohman, A.; Schmidbaur, H. *In Comprehensive Organometallic Chemistry II;* Abel, E. W., Stone, F. G. A., Wilkinson, G., Eds.; Elsevier: Oxford, **1995**.

[5] Jones, P. G. *Gold Bull.* **1986**, *19*, 46-54; **1983**, *16*, 114-120; **1981**, *14*, 159-168; **1981**, *14*, 102-118.

[6] Patheneni, S. S.; Desiraju, G. R. *J. Chem. Soc., Dalton Trans.* **1993**, 319-322.

[7] Mansour, M. A.; Connick, W. B.; Lachicotte, R. J.; Gysling, H. J.; Eisenberg, R. *J. Am. Chem. Soc.* **1998**, *120*, 1329-1330.

[8] Yam, V. W. –W.; Li, C. –K.; Chan, C. –L. *Angew. Chem. Int. Ed.* **1998**, *37*, 2857-2859.

[9] Mills, A.; Lepre, A.; Theobald, B. R. C.; Slade, E.; Murrer, B. A. *Anal. Chem.* **1997**, *69*, 2842-2847.

[10] a) Ma, Y.; Zhou, X.; Shen, J.; Chao, H. –Y.; Che, C. –M. *App. Phys. Lett.* **1999**, *74*, 1361-1363. (b) Ma, Y.; Che, C. –M.; Chao, H. –Y.; Zhou, X.; Chan, W. –H.; Shen, J. *Adv. Mater.* **1999**, *11*, 852-857. (c) Yam, V. W. –W.; Chan, C. –L.; Choi, S. W. –K.; Wong, K. M. –C.; Cheng, E. C. –C.; Yu, S. –C.; Ng, P. –K.; Chan. W, -K.; Cheung, K. –K. *Chem. Commun.* **2000**, *1*, 53-54. (d) Lai, S. –W.; Che, C. –M. *Top. Curr. Chem.* **2004**, *241*, 27-63.

[11] (a) Fung, E. Y.; Olmstead, M. M.; Vickery, J. C.; Balch, A. L. *Coord. Chem. Rev.* **1998**, *171*, 151-159. (b) Vickery, J. C.; Olmstead, M. M.; Fung, E. Y.; Balch, A. L. *Angew. Chem. Int. Ed.* **1997**, *36*, 1179-1181.

[12] Gussenhoven, E. M.; Fettinger, J. C.; Pharm, D. M.; Malwitz, M. M.; Balch, A. L. *J. Am. Chem. Soc.* **2005**, *127*, 10838-10839.

[13] Lee, Y. –A.: Eisenberg, R. *J. Am. Chem. Soc.* **2003**, *125*, 7778-7779.

[14] (a) Rawashdeh-Omary, M. A.; Omary, M. A.; Patterson, H. H.; Fackler, J. P., Jr. *J. Am. Chem. Soc.* **2001**, *123*, 11237-11247. (b) Omary, M. A.; Patterson, H. H. *J. Am. Chem. Soc.* **1998**, *120*, 7696-7705. (c) Omary, M. A.; Hall, D. R.; Shankle, G. E.; Siemiarczuck, A.; Patterson, H. H. *J. Phys. Chem. B* **1999**, *103*, 3845-3853. (d) Rawashdeh-Omary, M. A.; Omary, M. A.; Shankle, G. E.; Patterson, H. H. *J. Phys. Chem. B* **2000**, *104*, 6143-6151. (e) Hettiarachchi, S. R.; Rawashdeh-Omary, M. A.; Kanan, S. M.; Omary, M. A.; Patterson, H. H.; Tripp, C. P. *J. Phys. Chem. B* **2002**, *106*, 10058**-**10064. (f) Hettiarachchi, S. R.; Patterson, H. H.; Omary, M. A. *J. Phys. Chem. B* **2003**, *107*, 14249-14254. (g) Omary, M. A.; Colis, J. C. F.; Larochelle, C.L.; Patterson, H. H. *Inorg. Chem.* **2007**, *46*, 3798-3800.

[15] Assefa, Z.; Omary, M. A.; McBurnett, B. G.; Mohamed, A. A.; Patterson, H. H.; Staples, R. J.; Fackler, J. P., Jr. *Inorg. Chem.* **2002**, *41,* 6274-6280.

[16] Assefa, Z.; McBurnett, B. G.; Staples, R. J.; Fackler, J. P., Jr.; Assmann, B.; Angermaier, K.; Schmidbaur, H. *Inorg. Chem.* **1995**, *34*, 75-83.

[17] (a) Coker, N. L.; Krause Bauer, J. A.; Elder, R. C. *J. Am. Chem. Soc.* **2004**, *126*, 12-13. (b) Coker, N. L.; Bedel, C. E.; Krause, J. A.; Elder, R. C. *Acta. Crystallogr., Sect E: Struct. Rep. Online* **2006**, *E62,* m319-m321.

[18] Elbjeirami, O.; Omary, M. A.; Stender, M.; Balch, A. L. *Dalton Trans.* **2004**, *20*, 3173-3175.

[19] Morris, R. L. W.; Olmstead, M. M.; Balch, A. L.; Omary, M. A.; Elbjeirami, O. *Inorg. Chem.* **2003**, *42*, 6741-6748.

[20] (a) Gliemann, G.; Yersin, H. *Struct. Bond.* **1985**, *62,* 87-153. (b) Yersin, H.; Gliemann, G. *Ann. N. Y. Acad. Sci.* **1973**, 313, *539*-559.

[21] (a) Ma, B.; Li, J.; Djurovich, P. I.; Yousuffuddin, M.; Bau, R.; Thompson, M. E. *J. Am. Chem. Soc.* **2005**, *127,* 28-29. (b) Lu, W.; Chan, M. C. W.; Zhu, N.; Che, C. –M.; Li, C.; Hui, Z. *J. Am .Chem. Soc.* **2004**, *126*, 7639-7651.

[22] Representative examples include: (a) Lamansky, S.; Djurovich, P.; Murphy, D.; Abdel-Razzaq, F.; Lee, H.; Adachi, C.; Burrows, P. E.; Forrest, S. R.; Thompson, M. E. *J. Am. Chem. Soc.* **2001**, *123*, 4304-4312. (b) Adachi, C.; Baldo, M. A.; Forrest, S. R. *J. Appl. Phys.* **2000**, *87*, 8049-8055. (c) Baldo, M. A.; O'Brien, D. F.; You, Y.; Shoustikov. A.; Sibley, S.; Thompson, M. E.; Forrest, S. R. *Nature* **1998**, *395*, 151-154. (d) Grushin, V. V.; Herron, N.; LeCloux, D. D.; Marshall, W. J.; Petrov, V. A.; Wang, Y. *Chem. Commun.* **2001**, *16*, 1494-1495. (e) van Dijken, A.; Bastiaansen, J. J. A. M.; Kiggen, N. M. M.; Langeveld, B. M. W.; Rothe, C.; Monkman, A.; Bach, I.; Stossel, P.; Brunner, K. *J. Am. Chem. Soc.* **2004**, *126*, 7718-7727. (f) Brunner, K.; van Dijken, A.; Borner, H.; Bastiaansen, J. J. A. M.; Kiggen, N. M. M.; Langeveld, B. M. W. *J. Am. Chem. Soc.* **2004**, *126*, 6035-6042. (g) Zhang, J.; Kan, S.; Ma, Y.; Shen, J.; Chan, W.; Che, C. *Synth. Met.* **2001**, *121*, 1723-1724. (h) Ma, Y.; Che, C. –M.; Chao, H. -Y.; Zhou, X.;

Chan, W. –H.; Shen, J. *Adv. Mater.* **1999**, *11*, 852-857. (i) Sinha, P.; Wilson, A. K.; Omary, M. A. *J. Am. Chem. Soc.* **2005**, *127*, 12488-12489. (j) Burress, C.; Elbjeirami, O.; Omary, M. A.; Gabbai, F. P. *J. Am. Chem. Soc.* **2005**, *127*, *12166*-12167.

[23] For reviews, See: (a) Sibley, S.; Thompson, M. E.; Burrows, P. E.; Forrest, S. R. Electroluminescence in Molecular Materials. In *Optoelectronic properties of Inorganic Compounds;* Roundhill, D. M., Fackler, J. P., Jr., Eds.; Plenum: New York, **1999**; Chapter 5. (b) Yersin, H. *Top. Curr. Chem.* **2004**, *241,* 1-26.

[24] This is an approximate description because spin-orbit coupling affords significant mixing of the pure singlet and triplet states in Au(I) species.

[25] Griffith, J. S. *Theory of Transition Metal Ions:* Cambridge University Press: Cambridge, **1964**.

[26] Lee, Y. A.; McGarrah, J. E.; Lachicotte, R. J.; Eisenberg R. *J. Am. Chem. Soc.* **2002**, *124*, 10662-10663.

[27] Schubert, R. J.; Range, k. –J. *Z. Naturforsch., B: Chem. Sci.* **1990**, *45*, 1118-1122.

[28] (a) Fu, W. –F.; Chan, K. –C.; Miskowski, V. M.; Che, C. –M, *Angew. Chem. Int. Ed.* **1999**, *38*, 2783-2785. (b) Zhang, H. –X.; Che, C. –M. *Chem. Eur. J.* **2001**, *7*, 4887-4893. (c) Philips, D. L.; Che, C. –M.; Leung, K. H.; Mao, Z.; Tse, M. –C. *Coord. Chem. Rev.* **2005**, *249*, 1476-1490.

[29] Vorontsov, I. I,; Kovalevsky, A. Y.; Chen, Y. –S.; Graber, T.; Novozhilova, I. V.; Omary, M. A.; Coppens, P. *Phys. Rev. Lett.* **2005**, *94*, 193003/1-193003/4.

CHAPTER 5

CONCLUSIONS AND FUTURE DIRECTION

Phosphorescence sensitization in lanthanides via energy transfer mechanism from the ligand, 4′-*p*-tolyl-[2,2′;6′,2″]-terpyridine and in organic fluorophores such as naphthalene, anthracene, pyrene, and perylene via heavy atom was carried out. Sensitization of room temperature phosphorescence in the organic fluorophores in the solid state was obtained through external heavy atom effect. The following is the summary and major results of this dissertation (Section 5.1) and the future work to be pursued based on this research (Secion 5.2).

5.1 Conclusions

5.1.1 Bright Luminescence from Lanthanide-4′-*p*-tolyl-[2,2′;6′,2″]-terpyridine Complexes

Complexes of lanthanides such as europium, terbium, erbium and neodymium with the ligand, ttrpy (4′-*p*-tolyl-[2,2′;6′,2″]-terpyridine) were synthesized and characterized. Infrared spectra clearly indicated the formation of the compounds. The crystal structures of all the compounds were obtained. Lanthanides have the ability of high coordination due to their f orbitals. As a result most of the lanthanide complexes synthesized showed a coordination number of 8 and above. Sensitized luminescence was observed in europium and terbium compounds as the ligand was acting as antennae which transferred their energy in the excited state to the lanthanides. Bright red and green emissions were observed in europium and terbium complexes, respectively. The excitation spectra of the complexes showed ligand absorption and not

the direct absorption from the lanthanides. Even the electronic absorption spectra did not show direct absorption from the lanthanides. The sensitized luminescence was very weak in the case of $Tb(hfa)_3(L)$. This is due to the back energy transfer from the terbium emitting level to the triplet level of the donor. Quantum yield (QY) measurements were studied and the solid state $Eu(hfa)_3(ttrpy)$ exhibited highest QY.

5.1.2 Enhancement of Phosphorescence in Aromatics with Complexation of Silver Perchlorate

The compounds of silver perchlorate with aromatics such as naphthalene, anthracene and perylene were synthesized and their crystal structures were characterized. The influence of external heavy atom effect of silver was observed to be manifested by the spin-orbit coupling which enhanced the monomer phosphorescence of the aromatics was noticed. The complex of silver perchlorate with naphthalene showed enhanced monomer phosphorescence whereas with anthracene, weak monomer phosphorescence was observed. No such phenomenon was seen with perylene due to its triplet energy level which is below the threshold of 12,000 cm^{-1} but emission due to the α perylene which displayed a bathochromic shift of 575 cm^{-1} was observed.

To corroborate the enhancement of monomer phosphorescence in the solid state, frozen solution studies of naphthalene and pyrene with $AgClO_4$, $TlPF_6$ and KO^tBu were done. Enhancement of monomer phosphorescence of naphthalene (green) and pyrene (red) were observed with $AgClO_4$. Huge enhancement in the monomer phosphorescence of naphthalene and pyrene was witnessed with $AgClO_4$ but with $TlPF_6$,

it is very weak. Monomer fluorescence intensity was quenched with the addition of heavy metal, silver in the form of silver perchlorate. Perchlorate ion did not have any effect on the quenching process. The lighter metal, potassium (KO^tBu) did not show any significant effect with enhancement of phosphorescence. Lifetimes of monomer phosphorescence of naphthalene and pyrene were in milliseconds with $AgClO_4$ while the free naphthalene and pyrene have lifetimes that are generally in the range of seconds.

To understand the phenomenon of fluorescence quenching, Stern-Volmer studies of the aromatics with $AgClO_4$, $TlPF_6$ and KO^tBu were also studied. The quenching of fluorescence was large with $AgClO_4$ and $TlPF_6$ and very weak with KO^tBu. This is attributed to the heavy atom effect of silver and thallium. The effect of potassium is insignificant because it is a light metal. The quenching was attributed to the dynamic process. As perylene has more number of aromatic rings, the fluorescence quenching effect of these metals was very weak. The heavier the metal cation, $Tl^+ > Ag^+ > K^+$, greater was the quenching observed.

5.1.3 Structure Luminescence Relationship in Gold(I) Thiocyanate Complexes

Several gold thiocyanate complexes with different counterions were studied. The photophysics of ground state Au-Au aurophilic bonding and excited state Au-Au excimeric bonding have been studied. A rare phenomenon of simultaneous existence of fluorescence and phosphorescence is observed in these complexes. The fluorescence and phosphorescence components have been resolved in the $K[Au(SCN)_2]$ salt by the time-resolved luminescence spectroscopy. Unstructured emission bands with large Stokes's shifts are exhibited by all five compounds whose crystal structures show Au-Au

interactions, including salts of some bulky counterions such as *n*-Bu_4N^+, while this luminescence is undetectable in the one structurally characterized salt that does not exhibit any Au-Au interactions. The luminescence from these gold complexes is attributed to gold-centered emissions which are due to excimeric Au-Au bonding but ligand rearrangement also takes place. The observation of higher energy phosphorescence in crystals that exhibit shorter Au- Au interactions is attributed to the more constrained photoinduced rearrangement in solid state matrices which does not allow for any freedom for movement. This is manifested by observing significantly red shifted phosphorescence and larger Stokes' shifts in frozen solutions of $K[Au(SCN)_2]$ compared to crystals.

5.2 Future Direction

5.2.1 Development of Gold(I) Thiocyanate in Biomedicine

Gold drugs such as solganol, myochyrsine, allochrysine and aurofin are commonly used for the treatment of rheumatoid arthritis. Auranocyanide anion, $Au(CN)_2^-$, is a human metabolite of these drugs. A major effect of $Au(CN)_2^-$ is that it inhibits the oxidative burst of polymorphonuclear leukocytes and the proliferation of lymphocytes in vitro. Both these cells are responsible for the development and maintenance of inflammatory processes of rheumatoid arthritis.[1] This $Au(CN)_2^-$ acts by delaying the oxidative burst of these cells. Use of the above drugs generally considered as toxic because of their after effects.[2] $Au(SCN)_2^-$ will be a safer alternative to the $Au(CN)_2^-$ as $Au(SCN)_2^-$ will not transform into cyanide.

Gold based drugs are not only used for rheumatoid arthritis but also as antitumor agents. Auranofin and triethylphosphine gold(I) chloride (Et_3PAuCl) are both monomeric linear gold(I) complexes that are used as antitumour agents.[3] (Et_3PAuCl) is known for its cytotoxic effect on the mitochondria of the rat hepatocytes rather than on the DNA. Biological studies can be performed using gold thiocyanates for chrysotherapy, use of gold drugs for rheumatoid arthritis and also for their antitumor activity. These gold thiocyanate salts can also be employed in singlet O_2 generation in biological media.

5.2.2 Data Storage

Molecular materials that can exhibit reversible changes in their optical, electrical and/or magnetic properties upon the application of external stimuli are very valuable in many applications such as data storage, which exhibit write/read/erase properties[4] and for transition metal clusters whose magnetic moments reverse sign by slight changes in the applied field strength.[5] The d^{10} compounds of metal ions, such as Au^+ and Ag^+ show an interesting phenomenon known as optical memory. For example, $Pb[Au(CN)_2]_2$, laser excitation at 377 nm for Pb(II) salt at 78 K decreases the luminescence intensity which is reversed by heating to 300 K in dark and then cooling back to 78 K.[6] No such studies were performed on the thiocyanate compounds. These $[Au(SCN)_2]^-$ salts of potassium and sodium are excellent candidates to study the optical memory effect on their luminescence.

Apart from data storage, the gold(I) thiocyanate salts can also be used as linkers for building blocks of porous materials for storage of H_2 and other gases.

5.2.3 Gold Nanoparticles

The chemistry community has enthusiastically embraced nanomaterials. At the nanoscale, materials display unique electronic properties. These unique electronic properties translate into unique optical properties. There is an increased interest in the design of molecular assemblies to provide function at the nanoscale – the concept of creating molecular switches that can function as a diagnostic technology at the single molecule (assembly) level. Aggregation of gold nanoparticles in solid phase assays allows the colorimetric detection of DNA[7,8] and RNA.[9] They possess catalytic activity, and hence can be used for water gas shift reactions and selective oxidation of CO.[10] They can also be used in the field of sensors,[11] DNA labels,[12,13] and in medicine.[14] In the literature, gold nanoparticles are commonly synthesized by reduction of chloroauric acid, $HAuCl_4$ by sodium citrate in which the oxidation of gold is Au(III).[15] There are no incidences of using Au(I) complexes to produce stable gold nanoparticles besides pioneering work by our group on isonitrile and carbonyl complexes.[16] Gold(I) thiocyanate complexes can be employed to produce the gold nanoparticles as a function of concentration, counter ion and/or stabilizer in organic and aqueous media.

5.2.4 Sensitization of Lanthanides by Means of Inorganic Sensitizers

The lanthanide complexes of europium (Eu) and terbium (Tb) with 4'-*p*-tolyl-[2,2';6',2"]-terpyridine (ttrpy) ligand utilized the organic ligand as the antennae or sensor in which it transferred the absorbed energy in the excited state and resulted in sensitized luminescence. The literature has lot of examples of this kind of organic ligands employed for sensitization.[17] Another way to sensitize these lanthanides is to

use the $[M(SCN)_2]^-$ or else $[M'(SCN)_4]^{2-}$ anions. This way we can utilize the inorganic ligands as sensitizers, analogous to previous successful utilization of their cyano congeners.[18]

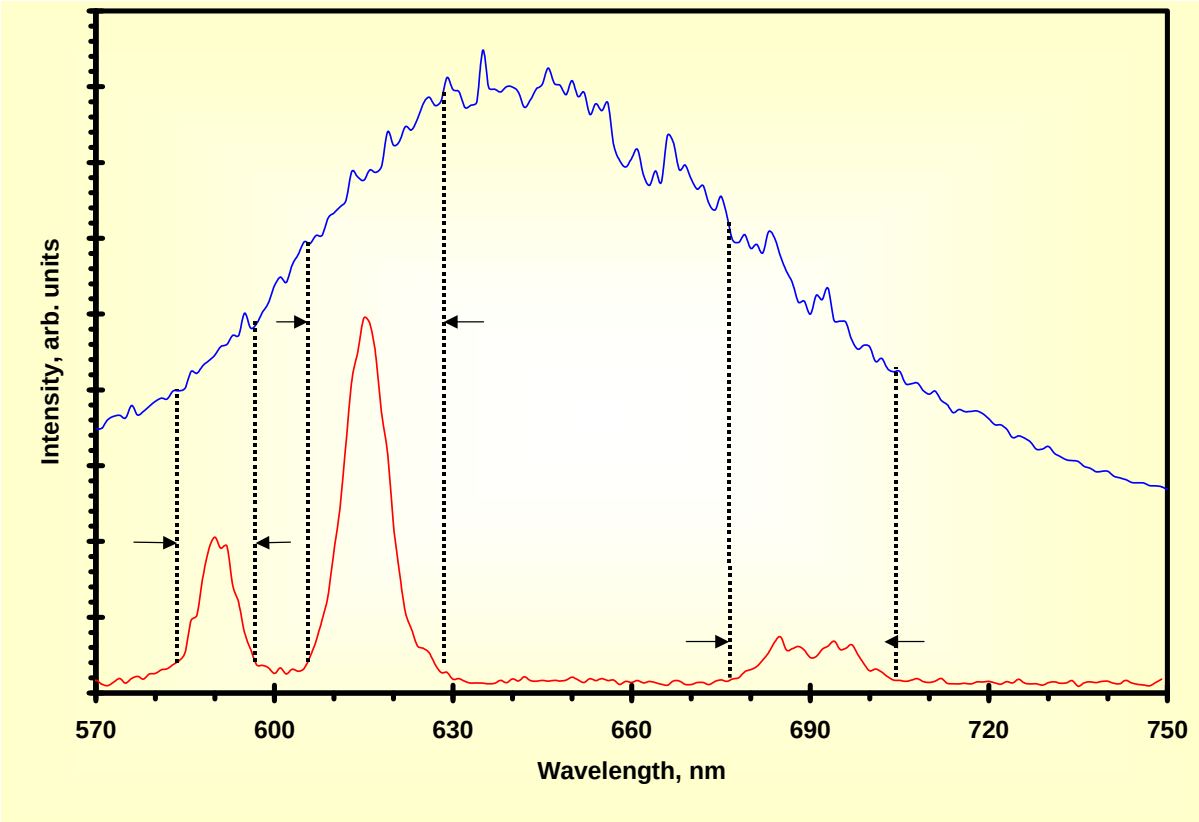

Figure 5.1 Spectral overlap between $K_2[Pt(SCN)_2]$ donor emission (top) and Eu^{3+} (bottom) absorption.

With good spectral overlap between the donor emission and acceptor absorption the greater sensitization of the emission of the acceptor. Figure 5.1 shows the spectral overlap between $K_2[Pt(SCN)_2]$ donor emission and the f-f absorptions of Eu^{3+}. The broad emission from the $K_2[Pt(SCN)_2]$ completely overlaps with the f-f transitions of Eu^{3+}, so the complexation of $[Pt(SCN)_2]^{2-}$ should theoretically produce full sensitization and therefore greatly enhance the emission from the Eu^{3+}. Figure 5.2 shows the

spectral overlap between donor $[Au(SCN)_2^-]_n$ emission with the acceptor levels of terbium and europium. There is some spectral overlap between donor emission and acceptor levels of terbium and europium but majority of the terbium absorptions is in the UV range. As a result the $[Au(SCN)_2^-]_n$ cannot act as good inorganic sensitizer. Table 5.1 lists the energy levels of various metals. Comparison of energy levels of metals with the terbium and europium energy acceptor levels, silver is a suitable metal to be used as inorganic sensitizer either in the form of $[Ag(SCN)_2]^-$ or $[Ag(CN)_2]^-$.

The perchlorate as couterions on the lanthanide-ttrpy complexes can be replaced by silver thiocyante or silver cyanate and can utilize these as inorganic sensitizer along with the ttrpy as the organic sensitizer. By using both organic and inorganic sensitizers, quantum yield of the lanthanide complexes can be increased which is useful in photonic applications[19] such as OLEDs (Organic light emitting diodes), sensors.[20] One of the neutral complex of $Eu(hfa)_3(ttrpy)$ was used in the fabrication of OLED which is discussed in section 5.2.5 These materials can also be used as porous metal organic frameworks (MOF). These MOFs are very useful in several applications such as ion exchange, catalysis, adsorption, electro-optical and luminescent probes.[21] These MOFs can be used in emerging technologies such as molecular electronics, miniature fuel cells and materials with hybrid properties.[22] TCNQ (7,7,8,8-tetracyanoquinodimethane), an organocyanide ligand has interesting magnetic[23] and electronic properties.[24] It has the ability to from 0-D complexes, 1-D chains and 2-D net.[25] This TCNQ can be complexed with the lanthanides and use as MOF material.

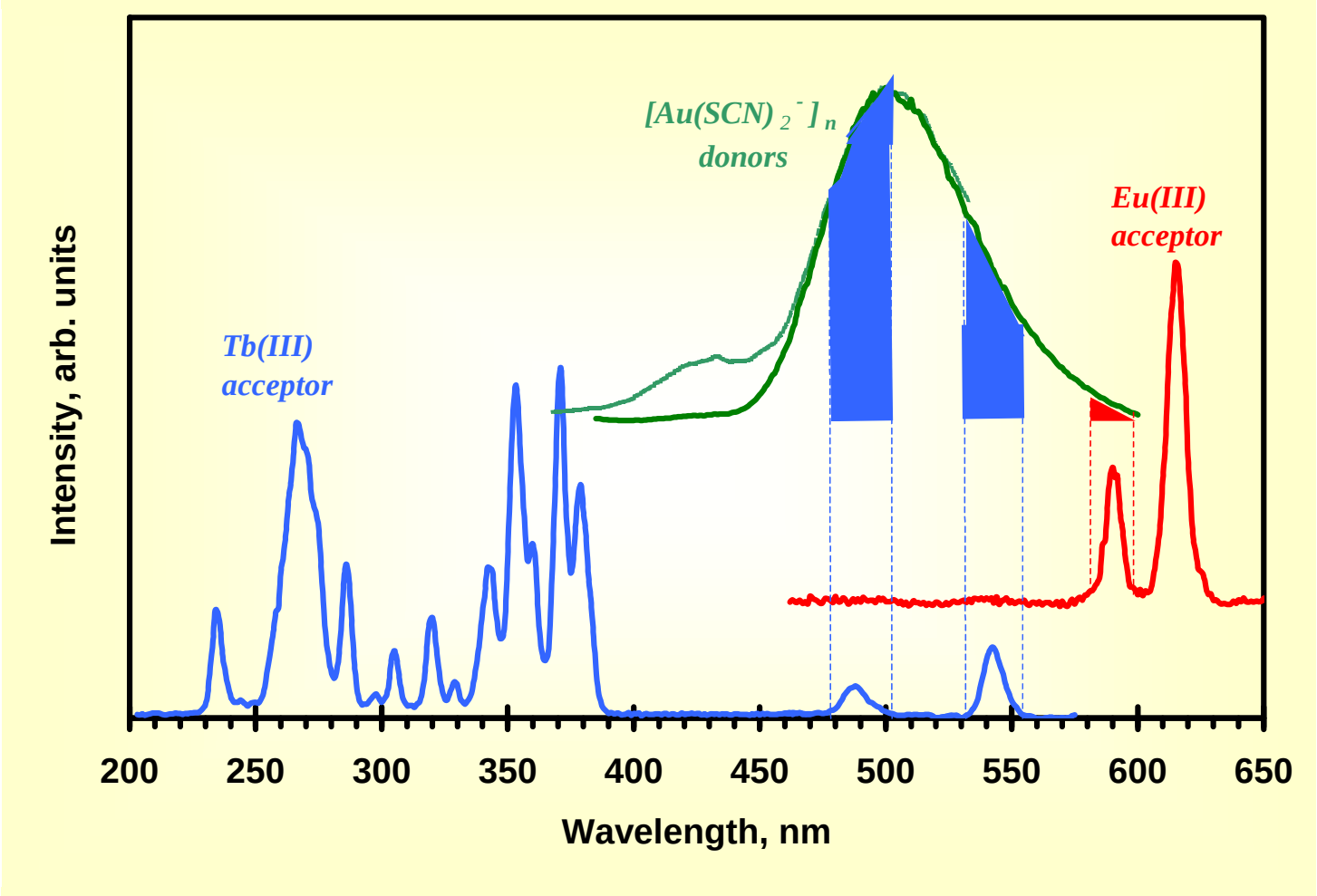

Figure 5.2 Spectral overlap between donor $[Au(SCN)_2]^-$ emission and terbium and europium acceptor levels.

Table 5.1. Energy levels of the various metals.[26]

$^{2S+1}L_J$	Cu(I), cm-1 (nm)	Ag(I), cm^{-1} (nm)	Au(I), cm^{-1} (nm)	Ni(II), cm^{-1} (nm)	Pd(II), cm^{-1} (nm)
$^1S_0$	0	0	0		
^3D_J J=3,2,1	22,600 (441)	40,600 (246)	18,400 (542)		
$^1D_2$	26,300(380)	46,000 (217)	29,600 (337)		
^3F_J J=4,3,2				9,900 (1006)	21,900 (455)
^3P_J J=2,1,0				16,800 (595)	

5.2.5 Fabrication of OLEDs using Lanthanide Complexes

In the past two decades significant research was focused on the photophysical properties of organic materials for the photonic devices.[19] The photonic devices include development of organic electroluminescent devices which can be used for displays and offer potential applications for the novel lighting sources to replace inefficient and expensive incandescent and fluorescent light sources. Liquid crystal displays (LCDs) were a breakthrough in 1980. LCDs reigning role has been over taken by organic light emitting diodes (OLEDs). The lighting of OLEDs has more advantages over LCDs such as low driving voltage, high light efficiency and low power consumption, environmental friendliness, tunability of emitting color and cheap to produce. Polymer light emitting diodes (PLEDs) are another form of OLEDs which employ polymers.

OLEDs device structure consists of thin organic film or metal-organic film sandwiched between cathode, usually a low work function metal and the anode, usually a transparent layer of indium tin oxide (ITO) as shown in the Figure 5.3.[27] When a voltage is applied, electrons from the cathode and holes from the anode join together in the emitting material i.e thin organic film. Electron transport layer (ETL) often oxidizole derivates such as 8-hyroxy quinoline aluminum salts or 2,9 dimethyl-4,7 diphenyl-1, 10-phenanthroline, abbreviated as BCP, is used to inject electron with low drive voltage. Hole transport layer (HTL) usually comprises tertiary amine such as N, N'-biphenyl-N,N'-bis (3-methylphenyl)1-1 biphenyl-4,4' diamine abbreviated as TPD will confine the holes efficiently in the emitting layer. The light is emitted upon the radiative relaxation of recombination of electrons and the holes (exciton) in the emitting layer.

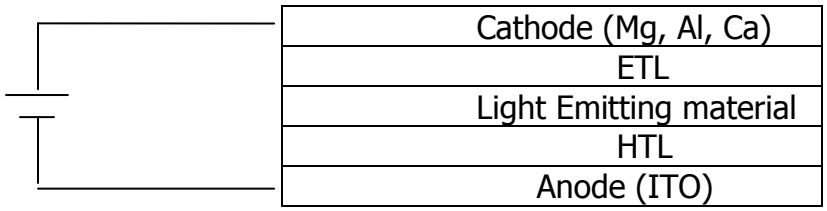

Figure 5.3. Schematic drawing of OLED device.

In collaboration with Dr. Shepherd group at Material science department at UNT, an OLED device similar to the schematic diagram 5.3 utilizing the $Eu(hfa)_3(ttrpy)$ (ttrpy= 4'-(*p*-tolyl)-2,2":6',2"-terpyridine) complex as the light emitting material was made. This complex was selected due to its neutral charge state, and consequent compatibility with sublimation. Figure 5.4 shows the electroluminescence device using the 4.5 % $Eu(hfa)_3(ttrpy)$ as dopant with CBP as the host at low and high voltages. At low voltage (7 V) only red emission from the europium complex was dominant whereas at higher voltages contributions from CBP, NPB and Alq3 were evident causing white electroluminescence from the device. The observation of emission from CBP could be due to the impartial or incomplete energy transfer from CBP to the dopant, $Eu(hfa)_3(ttrpy)$. The long phosphorescence lifetimes of Eu(III) facilitate exciton diffusion to the HTL (NPB) and ETL (Alq3) for blue and green emissions, with Alq3 (green) emission as prominent due its lower energy absorption overlapping with the host emission.

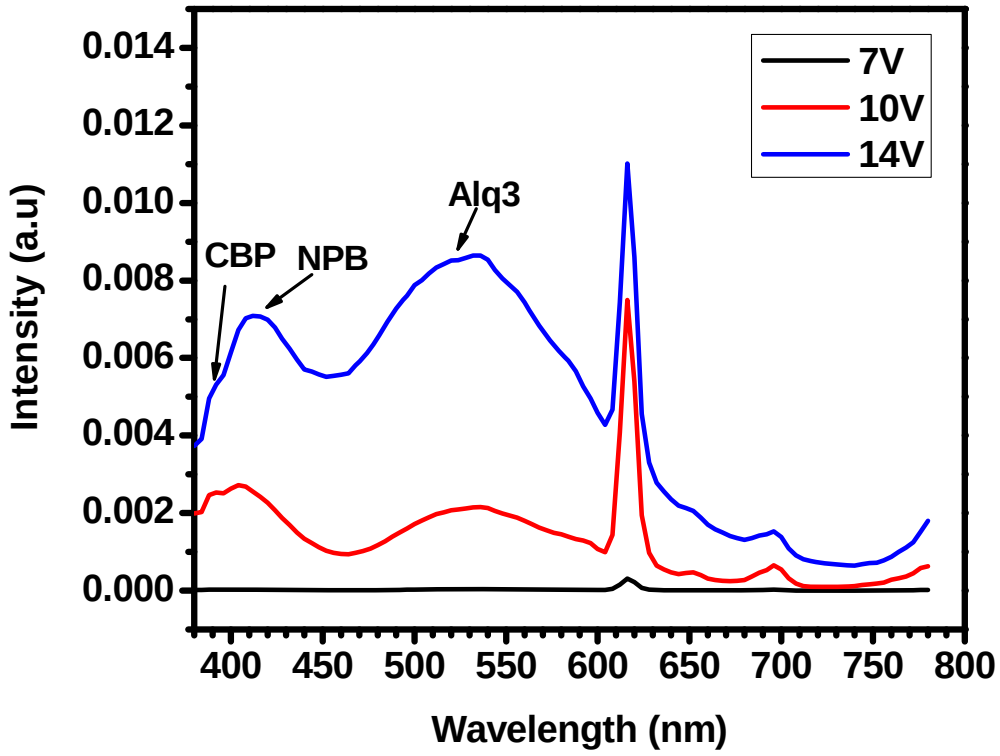

Figure 5.4. Electroluminescence spectrum of an OLED device (glass/ITO/NPB(50 nm) /4.5% Eu(hfa)3(ttrpy):CBP (30nm)/TPBI(30nm)/Alq3(25nm)/Mg:Ag).

Figure 5.5 is the electroluminescence device made of 4.5% $Eu(hfa)_3(ttrpy)$ as dopant in the CDBP host. No contribution from CDBP and little contributions from the NBP and Alq3 were observed only at higher voltages. This device was exbiting red electroluminescence. This electroluminescence data (Figures 5.4 and 5.5) suggests that the energy transfer is more efficient from CDBP host to the ttrpy ligand which in turn sensitizes the europium emission. CDBP acts as a better host for UV absorbers i.e $Eu(hfa)_3(ttrpy)$, because of good overlap between CDBP emission and absorption of the dopant, $Eu(hfa)_3(ttrpy)$. The luminous and power efficiencies obtained for these non-optimized devices were typically around 1.09 Cd/A and 0.53 lm/W respectively.

Luminance was ~500 cd/m^2 at 12-14 V. Device optimization still needed and that will be the future direction.

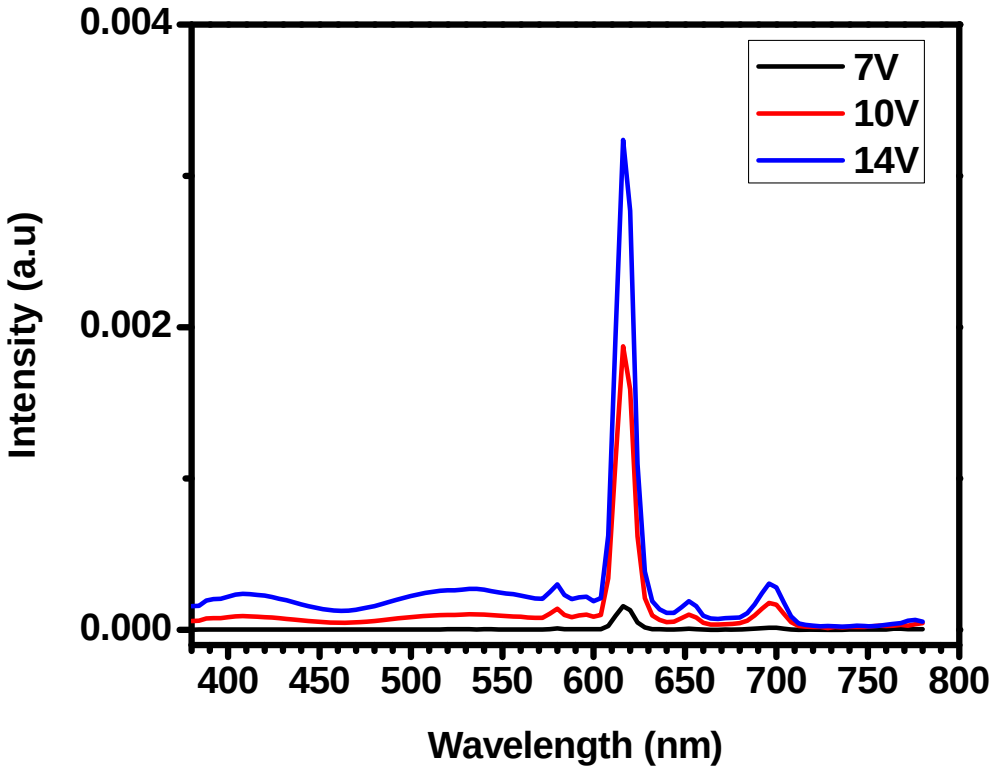

Figure 5.5. Electroluminescence spectrum of an OLED device. (glass/ITO/NPB(50 nm) /4.5% Eu(hfa)3(ttrpy):CDBP (30nm)/TPBI(30nm)/Alq3(25nm)/Mg:Ag).

Synthesizing compounds of lanthanides such as $Eu(hfa)_3$ (hfa = hexafluoroacetyl aceonato) with 2 moles of ttrpy ligand replacing the hfa's with ttrpy and then reacting with coordinating polymers such as polyvinylpyridine should result in neutral metallopolymers. This might allow use of solution-based polymer light emitting diodes (PLEDs). PLEDs can take advantage of both neutral and ionic compounds, so the strategy can be employed for ionic precursors as well. The high luminescence efficiency and color purity of Ln^{3+} and their dispersion in hosts with large energy gaps allows the

combination of energy transfer (of the excitons formed in the host) with charge trapping at the Ln^{3+} sites and direct recombination at these sites, leading to the amplification of the metal emission. Collaboration with the Rawashdeh-Omary and Gnade group has been formed based on this idea.[28]

The materials proposed above can be potentially used in sensor applications. Park et al. have prepared periodic mesoporous organosilica (PMO) doped with Eu^{3+}, Tb^{3+} and Tm^{3+} and developed potential applicants with red, green and blue UV sensors respectively.[20] They employed chlorides of Eu, Tb and Tm, however, use of materials such as $[Eu(L)_2Cl_2]Cl$, $Tb[(L)_2Cl_2]Cl$ or the nitrate and perchlorate complexes of Eu, Tb and fabricate red and green UV sensors, respectively. These complexes are better candidates than pure lanthanide chlorides, lanthanide nitrates or lanthanide perchlorates as they have high molar extinction coefficients because of the organic ligand as sensitizer than the direct excitation of the lanthanides alone. The neodymium and erbium complexes with ttrpy have to be studied for their NIR luminescence properties. These complexes have shown that the absorption spectra resemble that of the ligand. No direct absorption due to the erbium and neodymium has been observed.

5.2.6 Enhancement of Monomer Phosphorescence of Large Arenes with Silver

The Silver pyrene complex will be synthesized and its monomer phosphorescence will be studied. This compound like naphthalene should enhance the pyrene monomer phosphorescence and exhibit red luminescence as the frozen solution of pyrene with $AgClO_4$ was exhibiting. Other complexes of silver with aromatics such as tetracene, pentacene, cyclophane, rubrene, stilbene, 9, 10-diphenyl anthracene and graphene

have to be synthesized and their electronic properties can be studied. So far the complexes are synthesized with perchlorate as the counterion. As these complexes were not stable for long time, changing the counterion from ClO_4^- to BF_4^-, PF_6^-, and/or coordinating ligands may improve their stabilities. The fluorescence will appear at longer wavelength as the number of benzene rings increase. For example, the emission of anthracene (3 rings) occurs at longer wavelength than naphthalene (2 rings) and the tetracene (4 rings) fluorescence should occur longer than anthracene. As a result the tetracene monomer phosphorescence should occur in the NIR region as its monomer fluorescence ranges from 450-630 nm.[29] NIR emitters are novel for optical telecommunications, night vision and other applications such as luminescence bioassays.[21b] Large arenes such as pentacene and graphene can be used as organic semiconductors. Doping of pentacene and graphene with Ag^+ ions or its complexes could increase the mobility of their organic thin film transistor (OTFTs) devices.

5.2.7 Substituent Effects on Monomer Phosphorescence of Aromatics

Complexes of unsubstituted aromatics (naphthalene, perylene and anthracene) with $AgClO_4$ were studied. The next step is to study the effect of addition of substituents to the aromatic rings. Addition of electron donating, such as amine or n-alkyl groups should enhance the availability of π electrons of the aromatics to the cation, Ag^+, or Ag(I) complexes . We can study the effect of substituents on the intensity of monomer fluorescence versus monomer phosphorescence and their lifetimes.

5.5 References

[1] Graham, G. G.; Whitehouse, M. W.; Bushell, G. R. *Inflammopharmacol.* **2008,** *16,* 126-132.

[2] Sigel, A.; Sigel, H. *Metal Ions in Biological Systems.* Vol 41, **2004,** Marcel and Dekker, New York. Chapter 9.

[3] McKeage, M. J.; Maharaj, L.; Berners-Price, S. J. *Coord. Chem. Rev.* **2002,** *232,* 127-135.

[4] Kim, K. Y.; Hassenzahl, J. D.; Selby, T. D.; Szulczewski, G. J.; Blackstock, S. C. *Chem. Mater.* **2002**, *14*, 1691-1694.

[5] Zhao, H.; Cle´rac, R.; Sun, J.-S.; Ouyang, X.; Clemente-Juan, J. M.; Gomez-Garcia, C. J.; Coronado, E.; Dunbar, K. R. *J. Solid State Chem.* **2001**, *159*, 281-292.

[6] Patterson, H. H.; Bourassa, J.; Shankle, G. *Inorg. Chim. Acta.* **1994,** *226,* 345-348.

[7] Taton, T. A.; Mirkin, C. A.; Letsinger, R. A. *Science* **2000**, *289,* 1757-1760.

[8] Alexandre, I.; Hamels, S.; Dufour, S.; Collet, J.; Zammatteo, N.; De Longueville, F.; Gala, J.-L.; Remacle, J. *Anal. Biochem*. **2001**, *295*, 1-8.

[9] Liang, R. –Q.; Li, W.; Li, Y.; Tan, C.-Y.; Li, J. –X.; Jin, Y. –X.; Ruan, K. –C. *Nucleic Acids Res*. **2005,** *33,* e17, 1-18.

[10] (a) Andreeva, D. *Gold Bull.* **2002***, 35,* 82–88 (b) Grisel, R.; Weststrate, K, -J.; Gluhoi, A.; Nieuwenhuys, B. E.; *Gold Bull.* **2002***, 35*, 39–45 (c) Hutchings, G, J.; Haruta, M. *Appl Cata.,l A.* **2005,** *291*, 2–5.

[11] (a) Yanez-Sedeno, P.; Pingarron, J, M. *Anal. Bioanal. Chem.* **2005**, *382*, 884–886. (b) Liu, J.; Lu, Y. *J Fluoresc.* **2004**, *14***,** 343–354.

[12] Groning, R.; Breitkreutz J.; Baroth, V, Muller, R, S. *Pharmazie* **2001***, 56,* 790–792.

[13] Tang, D.; Yuan, R.; Chai, Y. *Biotechnol Bioeng.* **2006,** *94,* 996–1004.

[14] Paciotti, G, F.; Myer, L.; Weinreich, D.; Goia, D.; Pavel, N.; McLaughlin, R, E. *Drug Deliv.* **2004**, *11,* 169–183.

[15] Shan, J.; Tenhu, H. *Chem. Commun.* **2007**, *44*, 4580-4598 and the articles referenced in that.

[16] Elbjeirami, O.; Omary, M. A. *J. Am. Chem. Soc.* **2007**, *129*, 11384-11393.

[17] (a) Durham, D.A.; Frost, G. H.; Hart, F. A. *J. Inorg. Nucl. Chem.* **1969,** *31,* 833-838. (b) Chapman, R. D.; Loda, R. T.; Riehl, J. P.; Schwartz, R. W. *Inorg. Chem.* **1984,** *23,* 1652-1657 (c) Semenova, L. I.; White, A. H. *Aust. J. Chem.* **1999**, *34,* 3520-3527 (d) Semenova, L. I.; Sobolev, A. N.; Skelton, B. W.; White, A. H. *Aust. J. Chem.* **1999**, *52*, 519–529. (e) Drew, M. G. B.; Iveson, P. B.; Hudson, M. J.; Liljenzin, J. O.; Spjuth, L.; Cordier, P.-Y.; Enarsson, A.; Hill, C.; Madic, C. *J. Chem. Soc., Dalton Trans.* **2000**, 821–830. (f) Mürner, H.-R.; Chassat, E.; Thummel, R. P.; Bünzli, J.-C. G. *J. Chem. Soc., Dalton Trans.* **2000**, 2809–2816.

[18] (a) Rawashdeh-Omary, M. A.; Larochelle, C. L.; Patterson, H. H. *Inorg*. *Chem*. **2000**, *39*, 4527-4534. (b) Olken, M. M.; Verschoor, C. M.; Ellis, A. B. *Inorg*. *Chem*. **1986**, *25*, 80-82. (c) Yersin, H. *J*. *Chem*. *Phys*. **1978**, *68*, 4707-4713. (c) Assefa, Z.; Shankle, G.; Patterson, H. H.; Reynolds, R. *Inorg*. *Chem*. **1994**, *33*, 2187-2195. (d) Assefa, Z.; Patterson, H. H. *Inorg*. *Chem*. **1994**, *33*, 6194-6200 (e) Yersin, H.; Truemback, D.; Strasser, J.; Patterson, H. H.; Assefa, Z. *Inorg*. *Chem*. **1998**, *37*, 3209-3216.

[19] Mori, T.; Masumato, Y.; Itoh, T. *J. Photopolym. Sci. Technol.* **2008,** *21,* 173-180.

[20] Park, S. S.; An, B.; Ha, C, -S. *Microporous Mesoporous Mater*. **2008,** *111,* 367-378.

[21] (a) Peng, G.; Qiu, Y. -C.; Liu, Z. –H. Li, Y. –H.; Liu, B.; Deng, H. *Inorg*. *Chem*. *Commun*. **2008**, *11*, 1409-1411. (b) Li, X.; Xie, Z.; Lin, J.; Cao, R. *J*. *Solid State Chem*. **2009**, *182*, 2290-2297.

[22] Yaghi, O. M.; Keeffe, M. O.; Ockwig, N. W.; Chae, H. K.; Eddaoudi, M.; Kim, J. *Nature*. **2003**, *423*, 705-714.

[23] (a) Clerac, R.; O'Kane, S.; Cowen, J.; Ouyang, X.; Heintz, R.; Zhao, H.; Bazile, M. J. Jr.; Dunbar, K. R. *Chem*. *Mater*. **2003**, *15*, 1840-1850. (b) Vickers, E. B.; Giles, I. D.; Miller, J. S. *Chem*. *Mater*. **2005**, *17*, 1667-1672.

[24] (a) Potember, R. S.; Poehler, T. O.; Cowan, D. O. *Appl*. *Phys*. *Lett*., **1979**, *34*, 405-407.(b) Heintz, R.A.; Zhao, H.; Grandinetti, O. G.; Cowen, J.; Dunbar, K. R. *Inorg*. *Chem*. **1999**, *38*, 144-156.

[25] Lopez, N.; Zhao, H.; Prosvirin, A. V.; Chouai, A.; Shatruk, M.; Dunbar, K. R. *Chem*. *Commun*., **2007**, 4611-4613.

[26] Moore, C. E. *Atomic Energy Levels*; United States Dept. of Commerce, National Bureau of Standards: Washington, D. C.; 1971; vol I, II, III.

[27] Kalinowski, J. *J. Non-Cryst. Solids* **2008,** *354,* 4170-4175.

[28] (a) Rawashdeh-Omary, M. A.; Lopez-de-Luzuriaga, J. M.; Rashdan, M. D.; Elbjeirami, O.; Monge, M.; Rodriguez-Castillo, M.; Laguna, A. *J. Am. Chem. Soc.* **2009**, *131*, 3824-3825. (b) Chen, X.- Y.; Yang, X.; Holliday, B. J. *J. Am. Chem. Soc.* **2008**, *130*, 1546-1547. (c) Sudhakar, M.; Djurovich, P. I.; Hogen-Esch, T. E.; Thompson, M. E. *J. Am. Chem. Soc.* **2003**, 125, 7796-7797. (d) Furuta, P. T.; Deng, L.; Garon, S.; Thompson, M. E.; Fretchet, J. M. *J. Am. Chem. Soc.* **2004**, *126*, 15388-15389.

[29] Müller, A. M.; Avlasevich, Y. S.; Müllen, K.; Bardeen, C. J. *Chem. Phys. Lett.* **2006,** *421,* 518-522.